NASA CR-54230

GA-5750

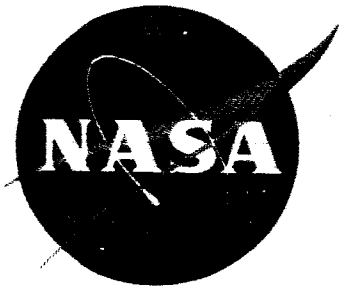

MEASUREMENT OF NEUTRON SPECTRA IN LIQUID HYDROGEN

by

G. D. Trimble, G. K. Houghton, and J. H. Audas

prepared for

NATIONAL AERONAUTICS AND SPACE ADMINISTRATION

Contract NAS 3-4214

GENERAL ATOMIC

DIVISION OF

GENERAL DYNAMICS

JOHN JAY HOPKINS LABORATORY FOR PURE AND APPLIED SCIENCE

P.O. BOX 608 SAN DIEGO 12, CALIFORNIA

NOTICE

This report was prepared as an account of Government sponsored work. Neither the United States, nor the National Aeronautics and Space Administration (NASA), nor any person acting on behalf of NASA:

A.) Makes any warranty or representation, expressed or implied, with respect to the accuracy, completeness, or usefulness of the information contained in this report, or that the use of any information, apparatus, method, or process disclosed in this report may not infringe privately owned rights; or

B.) Assumes any liabilities with respect to the use of, or for damages resulting from the use of any information, apparatus, method or process disclosed in this report.

As used above, "persons acting on behalf of NASA" includes any employee or contractor of NASA, or employee of such contractor, to the extent that such employee or contractor of NASA, or employee of such contractor prepares, disseminates, or provides access to, any information pursuant to his employment or contract with NASA, or his employment with such contractor.

Request for copies of this report should be referred to:

National Aeronautics and Space Administration
Office of Scientific and Technical Information
Washington, D.C.
Attention: AFSS-A

GENERAL ATOMIC

DIVISION OF

GENERAL DYNAMICS

JOHN JAY HOPKINS LABORATORY FOR PURE AND APPLIED SCIENCE

P.O. BOX 608, SAN DIEGO, CALIFORNIA 92112

NASA CR-54230

GA-5750

FINAL REPORT

MEASUREMENT OF NEUTRON SPECTRA IN LIQUID HYDROGEN

Work Done by:

G. D. Trimble
G. K. Houghton
J. H. Audas
K. L. Crosbie
J. C. Sayer
J. H. Diaz
J. R. Beyster

Report Written by:

G. D. Trimble
G. K. Houghton
J. H. Audas

prepared for

NATIONAL AERONAUTICS AND SPACE ADMINISTRATION

September 30, 1964

Contract Nas 3-4214

Technical Management
NASA-Lewis Research Center
Advanced Development and Evaluation Division
Michael J. Kolar

LIST OF SYMBOLS

MeV	=	million electron volts
LH_2	=	liquid hydrogen
LN_2	=	liquid nitrogen
(γ, n)	=	photonuclear reaction
(γ, f)	=	photofission reaction
E_c	=	energy of the Compton peak or the maximum single-collision energy transfer.
G(E)	=	energy dependent efficiency of the fast neutron detector.
T(E)	=	energy dependent transmission of the neutron flight path.
S(E)	=	energy dependent sensitivity of the fast neutron detector; $S(E) = G(E)\ T(E)$.
N(E)	=	number of neutrons per unit energy interval
N_i	=	atom density for the i^{th} element.
n_i	=	number of counts for the i^{th} time channel
ℓ	=	number of Linac beam pulses
E	=	energy
m	=	mass of the neutron
v	=	velocity of the neutron
x	=	flight path of the neutron
t	=	time
t_o	=	fiducial time point or zero time reference
$m_o c^2$	=	electron rest energy
RL	=	radiation length

TABLE OF CONTENTS

TABLE OF FIGURES

ABSTRACT

19701

Differential fast neutron spectra are presented for the neutron energy range 0.5 to 15 MeV in both water and liquid hydrogen as a function of space and angle. Measurements were made for 13.0, 10.5, 7.0, 4.5, and 2.5 inches of liquid hydrogen, at angles of 0, 15, 37, 53, and 78°; water measurements were made for 1.5 and 6.4 inches at the same angles.

A description of the liquid hydrogen experimental facility is given, including design considerations. Also included is a discussion of the development of the isotropic fast neutron source and differential neutron spectra taken with this source.

I. INTRODUCTION

This Final Report describes the measurements of fast neutron spectra in liquid hydrogen which were performed under Contract NAS 3-4214 issued by the Advanced Development and Evaluation Division, NASA-Lewis Research Center.

Differential fast neutron spectra were measured from 0.5 to 15 MeV neutron energy as a function of space and angle. These clean-geometry measurements are designed for comparison with the predictions of both the Transport Theory and Monte Carlo numerical methods so that the calculational procedures may be verified. This is the only known program conducted to date in which high-precision experimental differential neutron spectra have been measured for comparison with the results of advanced calculational methods. However, fast neutron fluxes in liquid hydrogen have been made using threshold detectors.[1] Since the experimental results presented here do not consist of dose measurements or studies of spectral indices, one does not encounter the usual ambiguities of interpretation, and, therefore, clear-cut comparisons of experimental data with theory under clean conditions are possible.

Even the most elegant methods (Transport, Monte Carlo, and energy dependent removal theory) give surprisingly different answers. Therefore, the objectives of this program were to develop reliable experimental tie points or experimental standards for comparison with any realistic theoretical technique. Differential spectral measurements, in appropriate geometries designed specifically for code validation, can

---

1. Hens, W. A., and G. E. Miller, Measured and Calculated Radiation Distributions in Liquid Hydrogen, March, 1964, NASA CR-54003, FZK-182.

serve to establish these standards before the codes are used in neutronic design problem areas such as neutron energy deposition analysis, secondary gamma production, and fast neutron transport problems.

This report has been organized using the following guidelines: Section II is a description of the electron linear accelerator and facility within which the liquid hydrogen experimental facility is located; Section III is a detailed description of the design problems and the final design of the liquid hydrogen experimental facility; Section IV is a description of the water mockup facility used to anticipate experimental problems which might be encountered during the liquid hydrogen experiments; Section V is a discussion of the fast neutron isotropic target, fast neutron detector, time-of-flight electronics, source monitor and background studies; Section VI is a discussion of the reduction of the data from the time-of-flight to the finished spectrum; Section VII is a discussion of the results and a graphical and tabular presentation of the differential fast neutron spectra in water and liquid hydrogen; Appendix A is a presentation of neutron heating calculations in liquid hydrogen; Appendix B considers possible heat leaks which could change the density or create voids in the liquid hydrogen; Appendix C presents the check off list and operational and emergency procedures for the liquid hydrogen experiments; Appendix D is a topical report entitled, "Calculation of Slow Neutron Scattering Cross Sections of Molecular Hydrogen and Deuterium," by James A. Young and Juan U. Koppel.

II. LINEAR ACCELERATOR FACILITY DESCRIPTION AND MODIFICATIONS

2.1 LINEAR ACCELERATOR FACILITY

The General Atomic linear accelerator is a three-section, high current, L-band machine manufactured by the Applied Radiation Corporation and installed in 1961. During the first part of the LH_2 preliminary experiments, the machine was capable of delivering a beam current of approximately 1 amp on a target at a pulse width of 20 nanoseconds and a pulse rate of 360 pulses per second, with an average electron energy of 27 $\pm$1 MeV. This corresponds roughly to a neutron flux (from U^{238}) of 3.6×10^9 neutrons per pulse or an average intensity of 1.3×10^{12} neutrons per second. In the spring of 1964, improvements were made in the Linac which raised the delivered current capability to as much as 1.6 amps at a pulse width of 20 nanoseconds. This gave 2.1×10^{12} neutrons per second and increased the intensity for large angle deep-penetration studies in liquid hydrogen. More Linac improvements are planned for the near future in order to increase both the available electron energy and the delivered current and to raise the maximum power point. Many of our low count rate experiments will be improved, and many more made feasible, by these Linac modifications.

For the LH_2 experiment, one Linac operator was selected to handle the initial tuning procedure; this operator was one who had a great deal of

experience tuning for a particular energy with a small spread in electron energy of $\pm$ 1 MeV. The machine parameters were more critical than usual for this experiment because of the dependence of the source spectrum and isotropy upon the Linac electron energy spectrum, the necessity of bending the beam at various angles to strike the source properly, and the difficulty of operating the machine at a narrow pulse width and high pulse rate. Several of the LH_2 experimenters assisted the regular Linac operators, both in practice tuning and steering operations and during the LH_2 experiments source study and associated experiments, with the rather complex operations of tuning, beam bending, focusing, and steering, so as to provide a consistently shaped and located beam spot. The importance of the beam steering and quality requirements is discussed in the section on source design.

Since a large linear accelerator is a very complex combination of electronic, electrical, and mechanical components, only a very great effort in maintenance and repair and constant checking will allow any degree of reliability. The maximum possible reliability was required of the linear accelerator to allow maximum utilization of the scheduled experiment time since the facility was already operating on a twenty-four hour day basis. Part of this reliability was provided by intensive checkout

and maintenance operations on the Linac by the operating crew immediately prior to the actual LH_2 experiment; part was provided by careful experimental design to allow the Linac to be operated continually during a given experimental period, without shutdown, so that waveguide temperature changes and other important tuning parameters would not necessitate time-wasting retuning and resteering of the beam. The result of this effort was 70% of the total machine time was used for the LH_2 experiments. Our previous experience indicates that, considering the fact that six initial tune-ups were required, this is an excellent reliability record.

2.2 FACILITY MODIFICATIONS

Many modifications were made to the General Atomic linear accelerator facility experimental areas to accommodate the equipment and piping systems associated with the liquid hydrogen experiment. The final facility configuration is shown in Fig. 1. One of the first and most important facility changes was the splitting of the large experimental room into two smaller rooms; this change allowed experiments on the Linac side of the three foot thick lead and heavy cement shield wall to be operated at their normal Linac beam power rates while setup crews worked on experiments on the other side of the wall. The Linac facility is geared to run experiments for all but sixteen of the 168 hours in the week. Therefore, setup time is at a premium and any additional setup time that can be gained will obviously greatly speed up any experimental program. Because of the size and complexity of the liquid hydrogen experiment, a great deal larger ratio

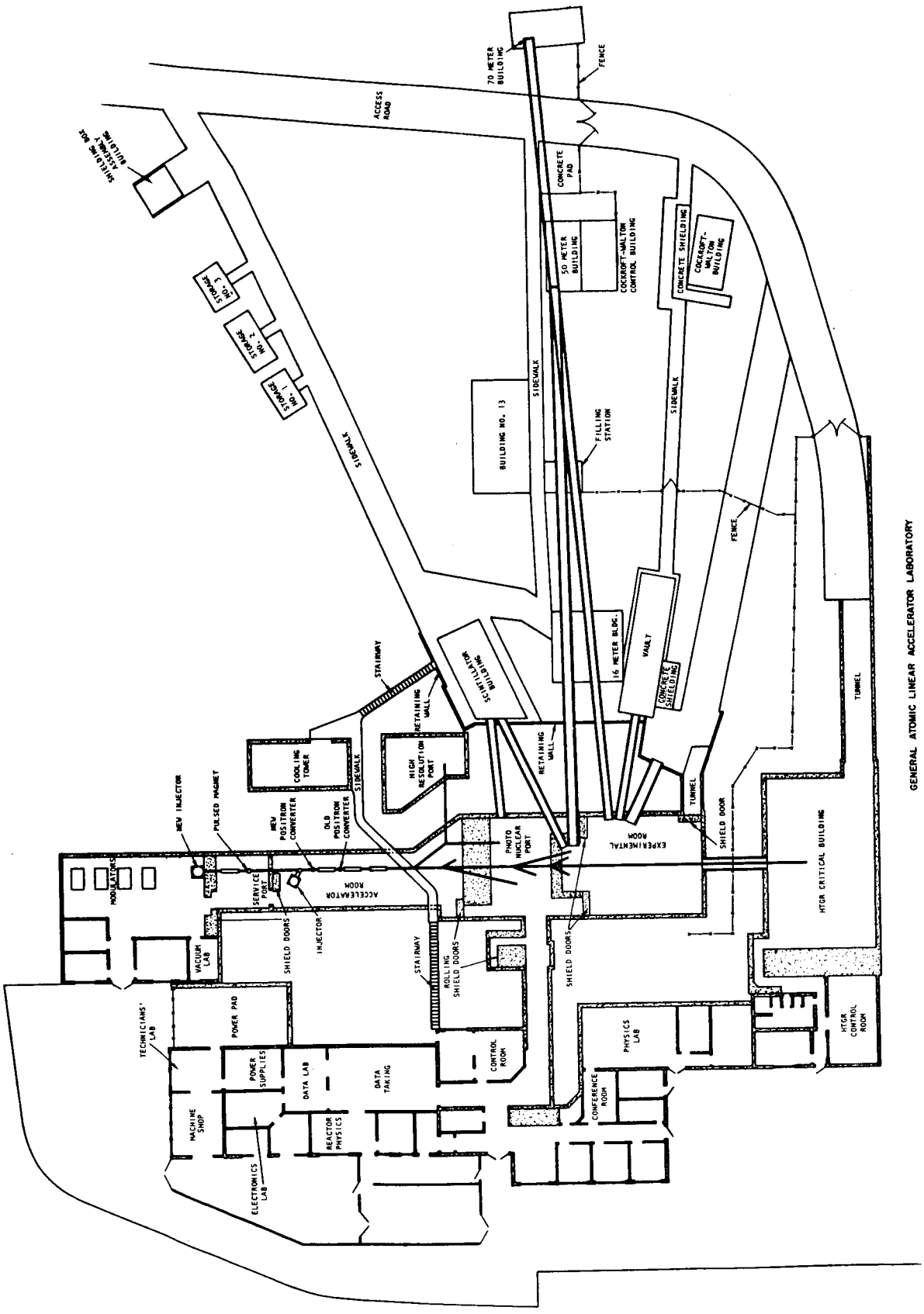

Fig. 1 -- Linear accelerator facility layout

of setup time to experimental time than usual was required. The new shield wall allowed us approximately twenty-four additional hours a week in the experimental area for construction, setup, and testing purposes, without which we would have had an impossible task in the time allotted.

Since the only entrance to the new experimental area behind the shield wall was through another experimental area in which we expected the Linac to be running, it was necessary to construct a new entrance through the concrete and dirt shielding at the rear corner of the building. A large concrete pad and three 9-ft high retaining walls were also poured at this time, forming a relatively protected area for storage and temporary parking of experimental gear; a concrete/steel roof was added later for weather protection. To shield the outside of the rear entrance and storage area, we built a 7-ft high by 10-ft long by 4-ft thick rolling concrete door weighing about sixteen tons. This door attenuates the very high fields inside the experimental room enough to allow work immediately outside the door at the maximum available Linac power conditions.

The construction of the three-foot-thick shield wall necessitated the demolition of a concrete low-background cave structure in the middle of the experimental room and fairly extensive modifications to the floor and the ventilation and electrical systems. An existing room exhaust blower was relocated at the outer end of a lengthened duct and reversed to act as a room pressurizer. The necessity of running the liquid hydrogen vent and dump lines out through the roof - which consists of six inches of concrete

covered with nine feet of dirt for radiation shielding purposes - caused us to construct an 18-inch diameter vertical tunnel through the ceiling. A new explosion proof room exhaust fan and ducting were attached to the upper end of this tunnel with provisions for the vent and dump lines and some of the electrical and electronics cables to pass out through the ducting. The steel and boral floor in the old cave area was removed, some of the water piping and electrical conduits in the floor were relocated, and a new floor was poured. Several new electrical service circuits were run into the new experimental area and a portion of the ceiling lighting system was removed to make room for the LH_2 valve package and dewar; these lights were replaced with explosion proof lights on a separate circuit for use during the actual LH_2 experiment.

Our data-taking area is of necessity located remotely from the experimental areas. Almost 250 linear feet of wire are required for each run between the two areas and thirty new cables - a total of 185 conductors - were run, in addition to about seventy existing cables which we used. A separate control console area was set up in the data-taking area, complete with all the required experimental control, warning, readout, and condition indicating devices. The data readout and storage functions utilized the existing electronics located in this area on a share basis with the other experimenters who were using the Linac during the same period, so it was generally impossible to leave the time-of-flight and monitoring electronics set up past our experiment time which meant that it had to be completely

set up from scratch for each preliminary experiment period; we were, however, able to leave the experimental electronics set up during the week of the actual LH_2 experiment.

Because of the hazards associated with both liquid and gaseous hydrogen mixed with air, we felt it necessary to put the outlets of the vent and dump stacks at least thirty feet above ground level. Wind and climatic conditions in this area made it imperative that a strongly constructed tower be installed at the top of the 18-inch diameter roof tunnel to support these stacks. A triangular cross-section lightweight tubular steel antenna tower was purchased and installed into a poured foundation and securely guyed (see Figs. 2 and 3). This tower and the attachments for holding the stacks have since been observed to be completely stable in all kinds of typical local weather conditions.

Operation of the LH_2 experiment required that a very large number of nitrogen and helium bottles and associated piping be installed in the vicinity of the new rear entrance. A pad was poured for this purpose with "hitching rails" for the bottles and support structures for the required valves and piping. When fifty-two additional feet of vacuum-jacketed LH_2 transfer line became available through the courtesy of General Dynamics/ Astronautics, the LH_2 storage trailer was moved from its original location in the rear entrance storage area to a safer and more open area in the driveway, and new supports were constructed for the additional transfer line which was carried high off the ground. This area is shown in Fig. 4.

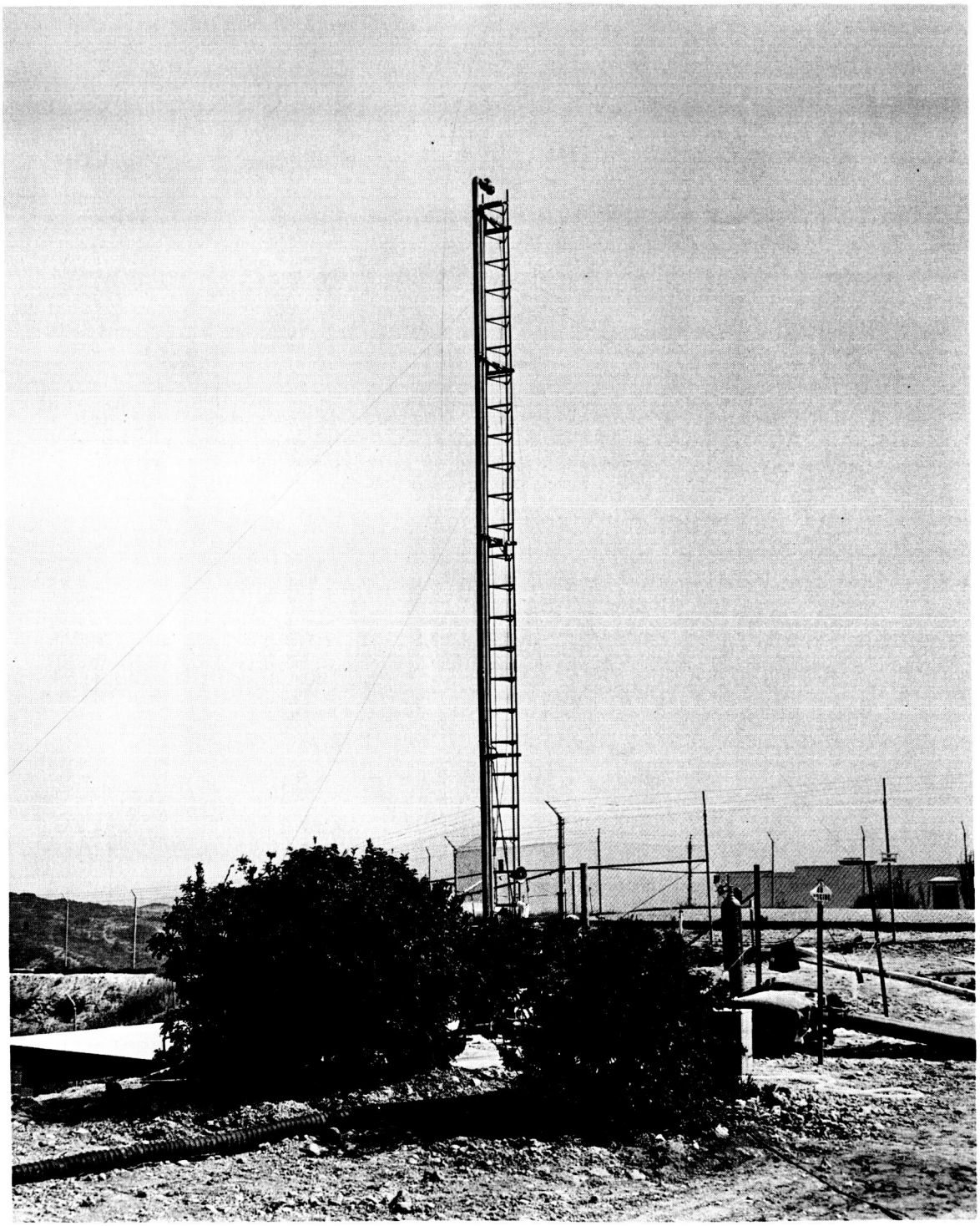

Fig. 2 -- LH_2 vent/dump stack support tower area

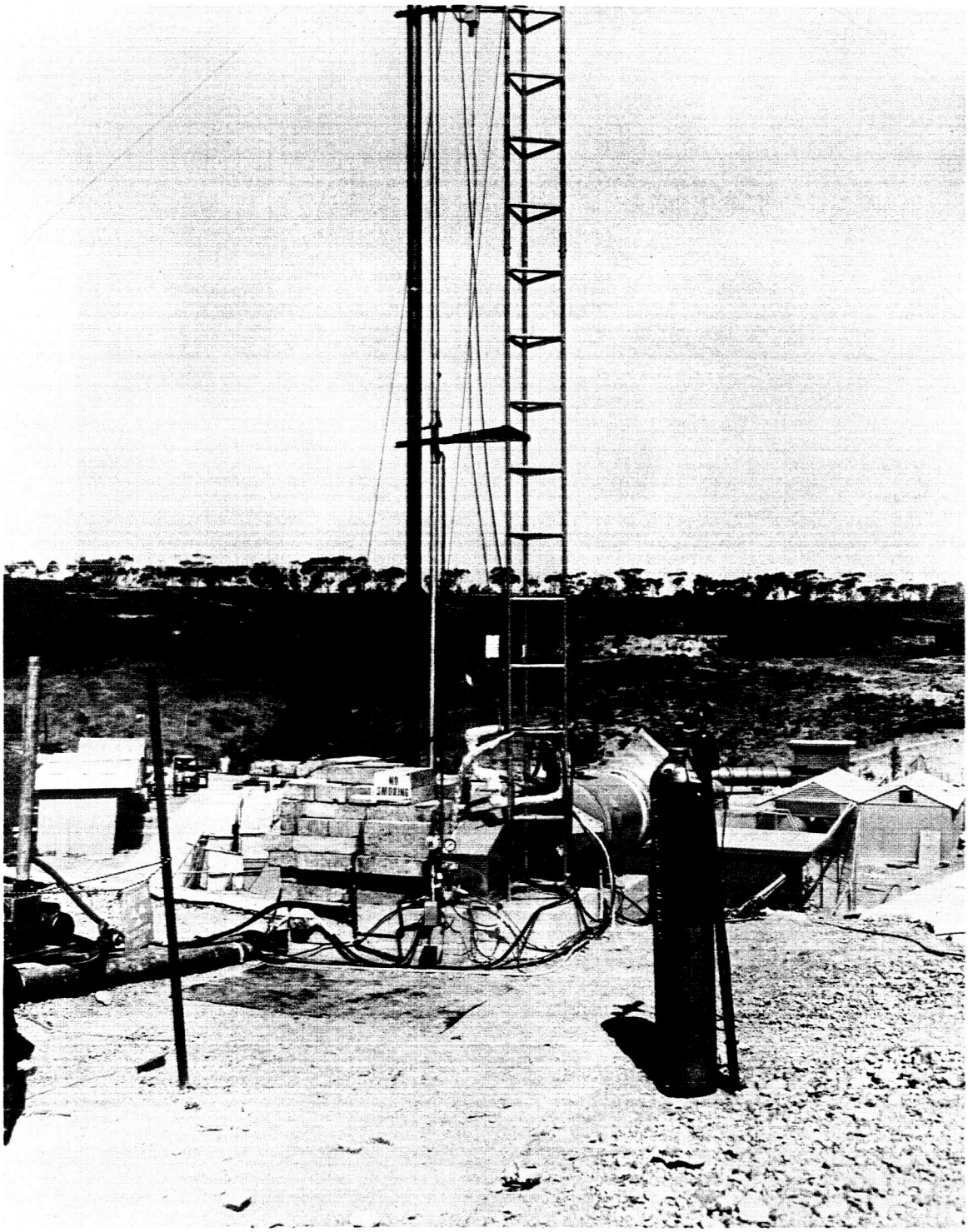

Fig. 3 -- LH_2 vent/dump stack support tower area

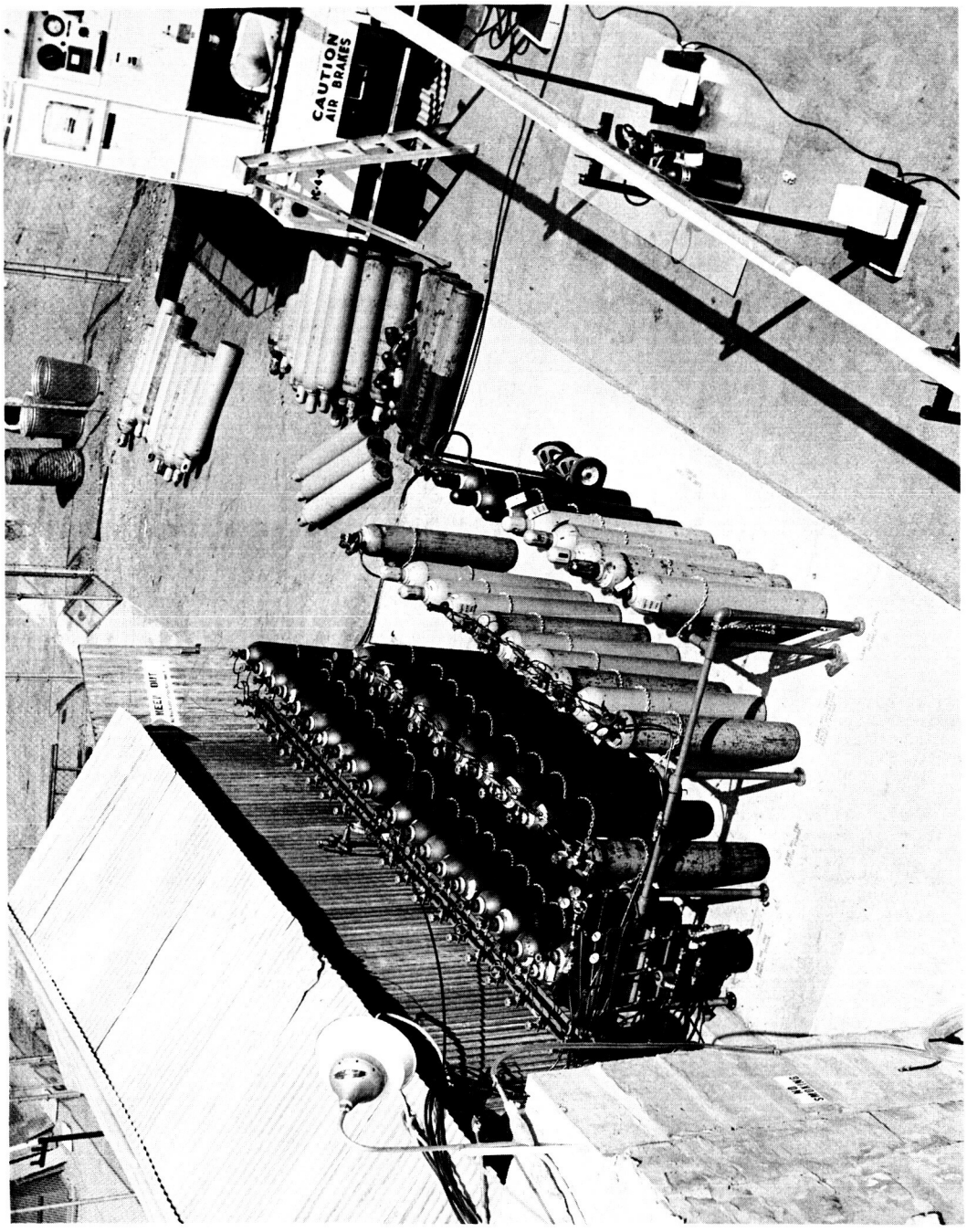

Fig. 4 -- Gas bottle farm and LH_2 storage dewar area

2.3 VARIABLE ANGLE BEAM BENDING SYSTEM

Many changes to the Linac's beam-piping system were necessitated by the physical demands of the LH_2 experiment. Several new beam-bending boxes were required to pierce the new 3 ft. thick wall dividing the experimental room, with much research and experimentation being required to adequately shield the openings in the wall through which the beam passes. A new evacuation station was built and several large beam bending magnets and their accompanying water and electrical systems were moved to allow the installation of the LH_2 experiment's bending magnet and beam tube system. A new form of beam bending envelope was developed especially for this experiment. This system, shown in Fig. 5, consists of a guided bellows section in the beam tube which passes between the pole pieces of the bending magnet. The bellows allows the beam tube to be bent, using the center of the pole pieces as the center of rotation, from -15° to $+60^{\circ}$ in an infinitely variable manner. Previous Linac beam bending envelopes consisted of welded stainless steel boxes with fixed angle beam exiting tubes. The nature of the LH_2 experiment required a large number of bends, not necessarily very different from each other, which made a normal beam box completely impractical. No difficulty of any kind was encountered with any part of the new beam piping system.

2.4 70-METER FLIGHT PATH

At the time work on the LH_2 experiment was started, the

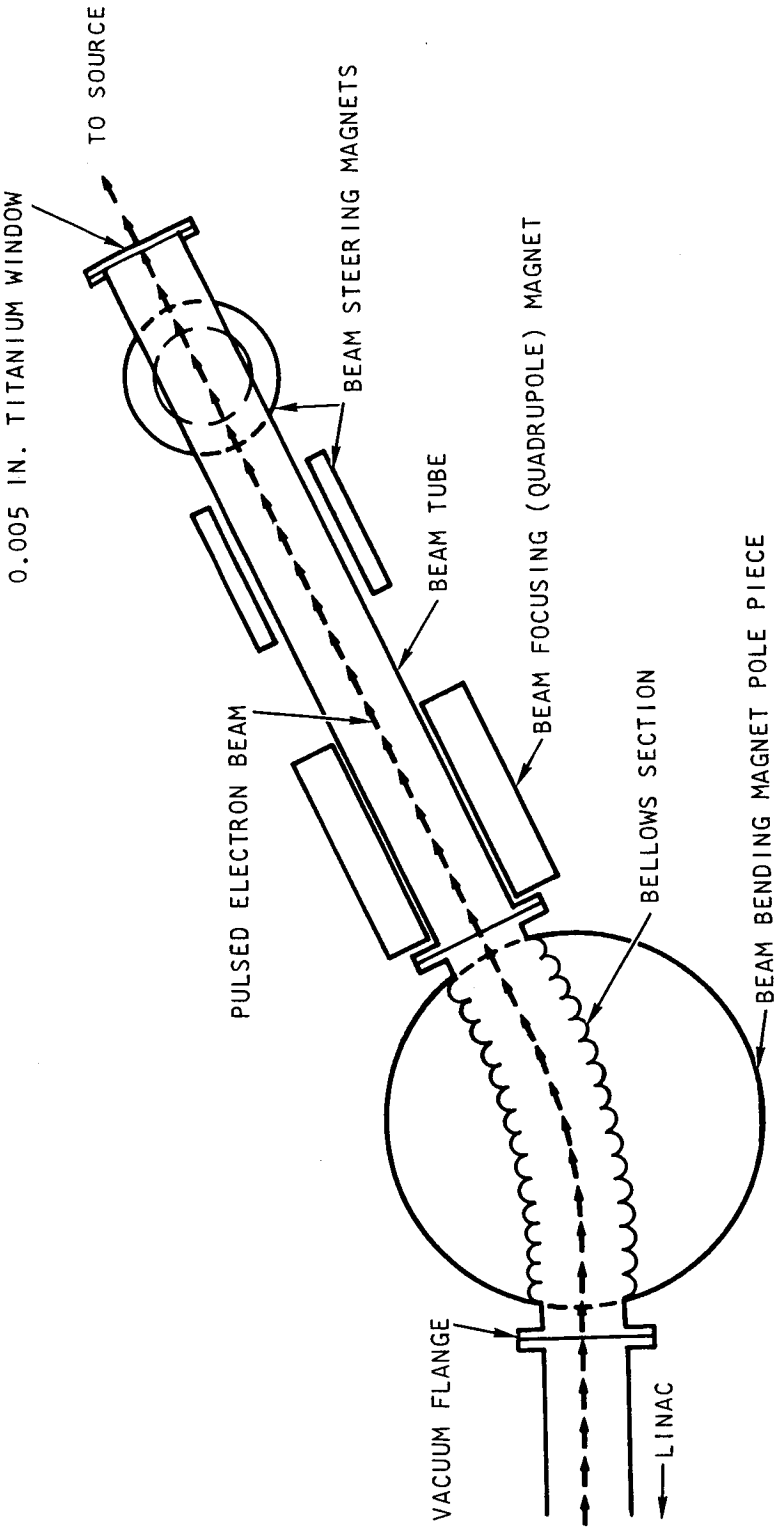

Fig. 5 -- Schematic of variable angle beam bending system

General Atomic Linac facility did not have a long flight path expressly designed for high-energy neutron work. An existing 50 meter flight path (comprised of a 16 meter evacuated section and two helium or argon filled rubberized fabric bags totaling 34 meters in length, with a final diameter of 36 inches) had been used to some extent for high-energy neutron studies, but the shielding and collimation were designed for use in thermal neutron studies. Since much of the work at the linear accelerator laboratory is in the thermal neutron field, a new flight path was required with shielding and collimation for fast neutrons to handle the fast neutron work load without disrupting the scheduling of the thermal neutron group, and at the same time eliminate the bothersome helium/argon filled flight bags and make the outer end of the new flight path serve for both the thermal and fast neutron flight paths. A schematic diagram of the flight paths can be seen in Fig. 1. This new outer section was designed as a two-piece evacuated steel tube. The end closest to the experimental area translates on rails between the flight paths, while the outer tube pivots about the cross-over point of the flight paths. Two additional evacuated steel tubes were built to extend the fast neutron flight path to seventy meters, but the seventy meter portion was not finished and checked out in time to be used on the LH_2 experiment; at present both flight paths are completed, tested, and have been extensively used at fifty meters.

One rather useful feature of both flight paths is a break in the

vacuum space at sixteen meters. Most of the thermal neutron experiments have been run at this station since the thermal neutron flight times are sufficiently great to give good energy resolution even at this short distance. The sixteen meter portion of the new flight path is very similar to the older flight path's first section, with the exception of the collimation and shielding, which are intended for fast neutron work.

While the evacuation of the new outer sections caused some additional difficulty, the end result was more than worth all the added effort. The vacuum eliminates the former need for hourly checks and repressurizations of the flight bags. The evacuation of the flight path gave a fairly large increase in intensity, as well as eliminated the spectral distortions due to the argon or helium.

Details of the fast neutron flight path are shown in Fig. 6. The collimation and shielding were designed to give the lowest possible Linac-associated background to allow low flux-intensity experiments to provide valid results; the types, locations, and materials used in the collimators and shields have proven very satisfactory in giving a good signal-to-background ratio even with liquid hydrogen, which is an excellent neutron attenuator and an extremely poor gamma shield. Design of the iris system was based on the elimination of neutrons scattered from the inner walls of the first section, with more than two bounces being required for a neutron entering the flight path in any direction other than the beam path to leave the outer end of the first

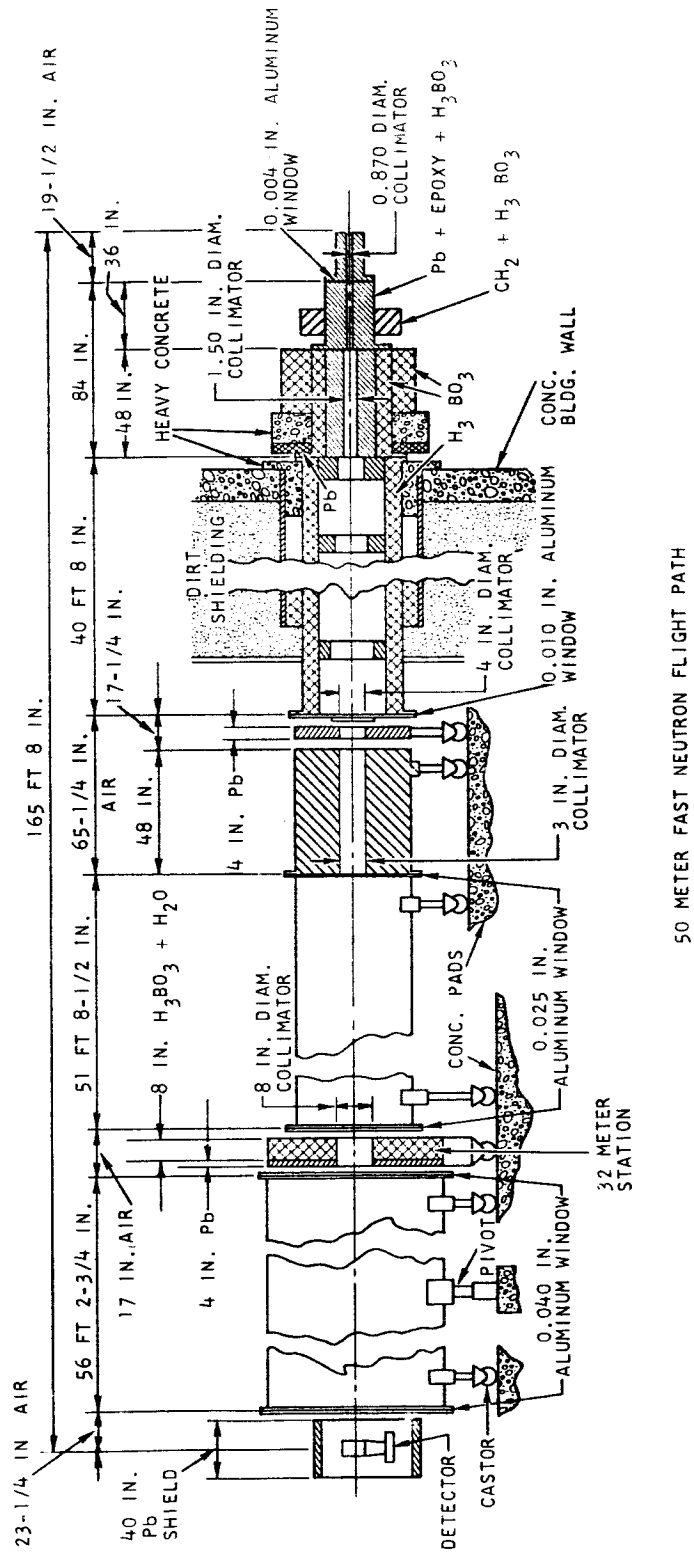

50 METER FAST NEUTRON FLIGHT PATH

Fig. 6 -- Fifty meter fast neutron flight path

section. The collimation system was designed to allow the edge of the precollimator nearest the experimental assembly and the 3.0 inch I.D. water tank collimator at sixteen meters to define the viewed spot size at the assembly and the beam spot size at the detector. With a given assembly dewar probe tube inner diameter of 1.125 inch at a distance of about 28 inches from the precollimator, a .870 inch I.D. precollimator gave a viewed spot diameter on the probe tube window of about 1.03 inches; this allowed a misalignment tolerance of 0.095 inch which was well within our capability. The beam spot diameter produced by this system (at the detector in the 50 meter position) was 10.62 inches. A Geiger counter check of the gamma flux beam diameter at the detector position gave almost exactly this figure. One additional postcollimator was added at the 32 meter position to eliminate stray background-producing gamma rays and high energy neutrons from reaching the detector. It appears that, in high energy neutron studies at least, one must use a very large amount of shielding around the flight path near the radiation source, and continue to shield heavily around the flight path at frequent intervals, but not adjacent to the detector, in order to make sure that the only information the detector receives is that carried directly in the beam. Shielding close to the detector which extends into the well-defined beam, however, can create capture gamma rays which may be seen as spurious signals by the detector.

Very heavy collimators were required near the experimental

assembly to reduce the tendency for fast neutrons to be scattered in the collimators themselves and be seen by the detector. The 0.870 inch diameter portion of the precollimator is 67.5 inches long and is backed up by a 48 inch long by 1.50 inch diameter collimator. These collimators were constructed from a special mixture of H_3BO_3, lead powder and epoxy. Additional heavy concrete block and lead shielding was used around the flight path at the point where it enters the experimental room wall to help reduce the transmission of gamma rays and fast neutrons into the the first portion of the flight path.

III. LIQUID HYDROGEN EXPERIMENTAL FACILITY

3.1 DESIGN CONSIDERATIONS

At the beginning of the experiment's design phase, the primary objective of the LH_2 neutron heating experiment was to measure the fast (0.5 to 15 MeV) neutron flux at various penetrations in the LH_2, but only in the 0^o direction; that is, only with the source, re-entrant tube axis, and flight path and detector in line. Our solution to this problem was to make a portion of the dewar probe tube out of a long welded-diaphragm type stainless steel bellows which could be extended and compressed over a 13-inch range to vary the thickness of LH_2 layer within the tank. This design of the experimental tank was considerably simpler than later designs, and the number of individual experiments needed to satisfy the information requirements was much lower and with much less difficulty of operation. Before the original design was finalized, however, a decision was made to transfer emphasis from the planned 0^o fast neutron flux measurements, which were to some extent just transmission studies as a function of energy and space, to differential neutron spectrum measurements as a function of space and angle.

The new experiments almost completely nullified the original design concepts and brought up a great many new and much more difficult problems in almost all design phases of the experiment. In addition, the actual

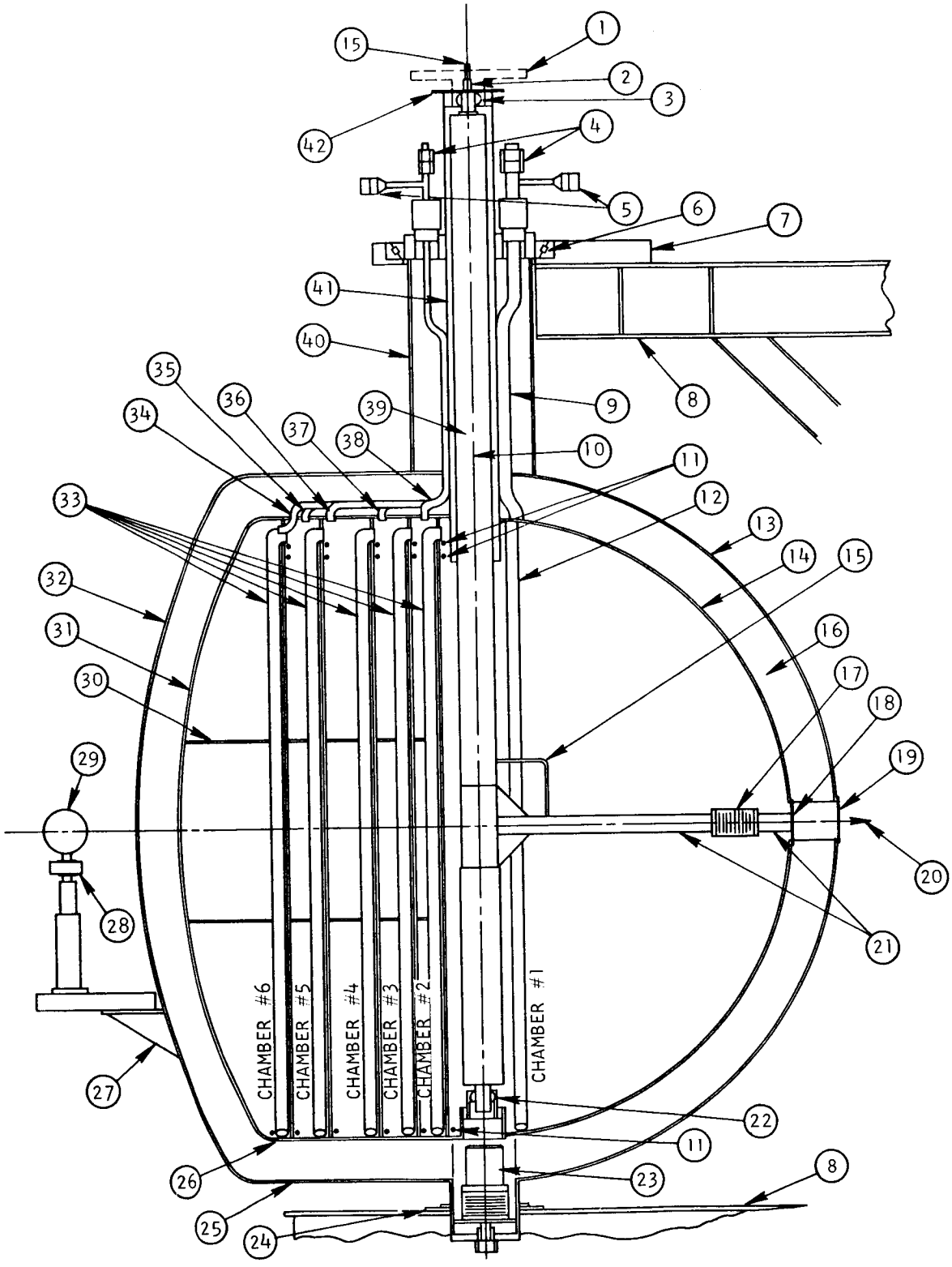

Fig. 7 -- LH_2 dewar design details

FIGURE 7 LEGEND

1. Alignment plate
2. Alignment plate bearing surface
3. Upper probe pivot spherical bearing
4. Vent line fittings
5. Liquid level sensor fittings
6. Dewar rotation tapered roller bearing
7. Yoke bearing seat
8. Yoke arm
9. No. 1 vent tube
10. Probe pivot axis
11. Liquid level sensors
12. Fill/dump tube
13. Outer hemispherical head
14. Inner hemispherical head
15. Probe evacuation tube
16. Super insulation and vacuum space
17. Probe tube bellows
18. Inner head window
19. Outer head window
20. Neutron flight path axis
21. Probe tube
22. Lower probe pivot spherical bearing
23. Retractable transportation stabilizer
24. Guide plate
25. Outer shell cylinder
26. Inner shell cylinder
27. Source location bracket
28. Source/Linac beam tube guide
29. Fast neutron source
30. Baffle stay rod
31. Inner torospherical head
32. Outer torospherical head
33. Chamber-to-chamber LH_2 transfer tubes
34. No. 6 vent tube
35. No. 5 vent tube
36. No. 4 vent tube
37. No. 3 vent tube
38. No. 2 vent tube
39. Invar probe pivot tube
40. Outer neck tube
41. Inner neck tube
42. Angle indication scale

operation of the experiment was greatly affected by this change, as neutron source intensity, detector sensitivity, run-to-run monitoring, collimation and shielding, and experimental running time all became much more critical. Several of the cryogenic equipment manufacturers with whom we had been discussing proposed designs refused to consider the problem, as the technical difficulties of design and construction seemed almost insurmountable. Finally, after several weeks of intensive study, some preliminary answers to the main problem areas were evolved. Cryogenic Engineering Company was awarded the system design and construction contract with six no-bid replies coming from the other manufacturers contacted. The Cryenco personnel which were acquainted with the program and its goals expressed many doubts about the techniques and methods that would be required to accomplish the design objectives, but, operating in close coordination with the General Atomic physicists and engineers assigned to the project, the Cryenco designers eventually developed the liquid hydrogen experimental dewar shown in detail in Figs. 7, 8, and 9. A plan view of the liquid hydrogen facility is shown in Fig. 10.

The following is a discussion of the experimental design parameters and the methods and techniques used to meet all the design parameters. Some of the problems remained incompletely solved until after installation and trial operation; however, the solutions finally adopted are the only ones discussed.

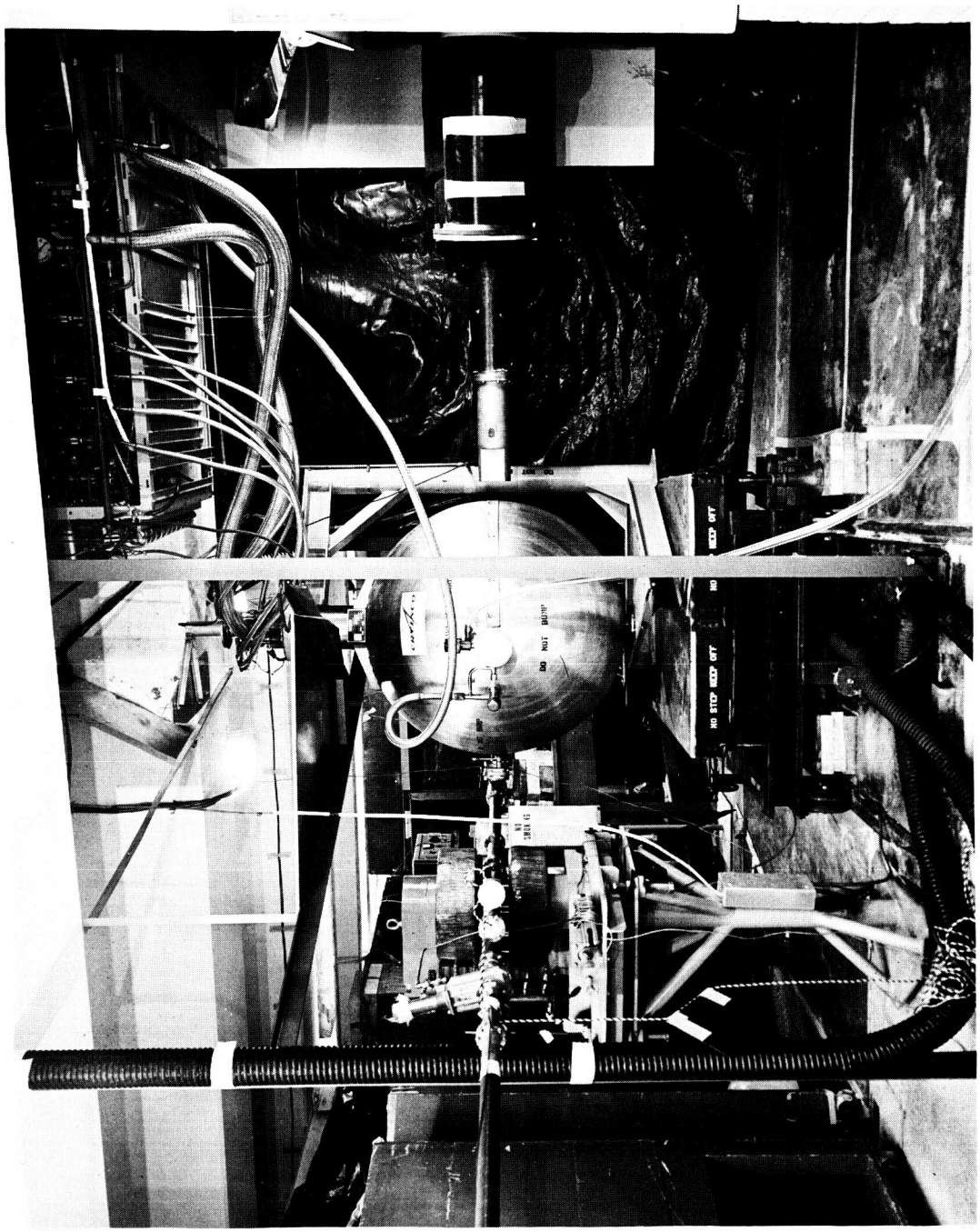

Fig. 8 -- LH_2 dewar and experimental area

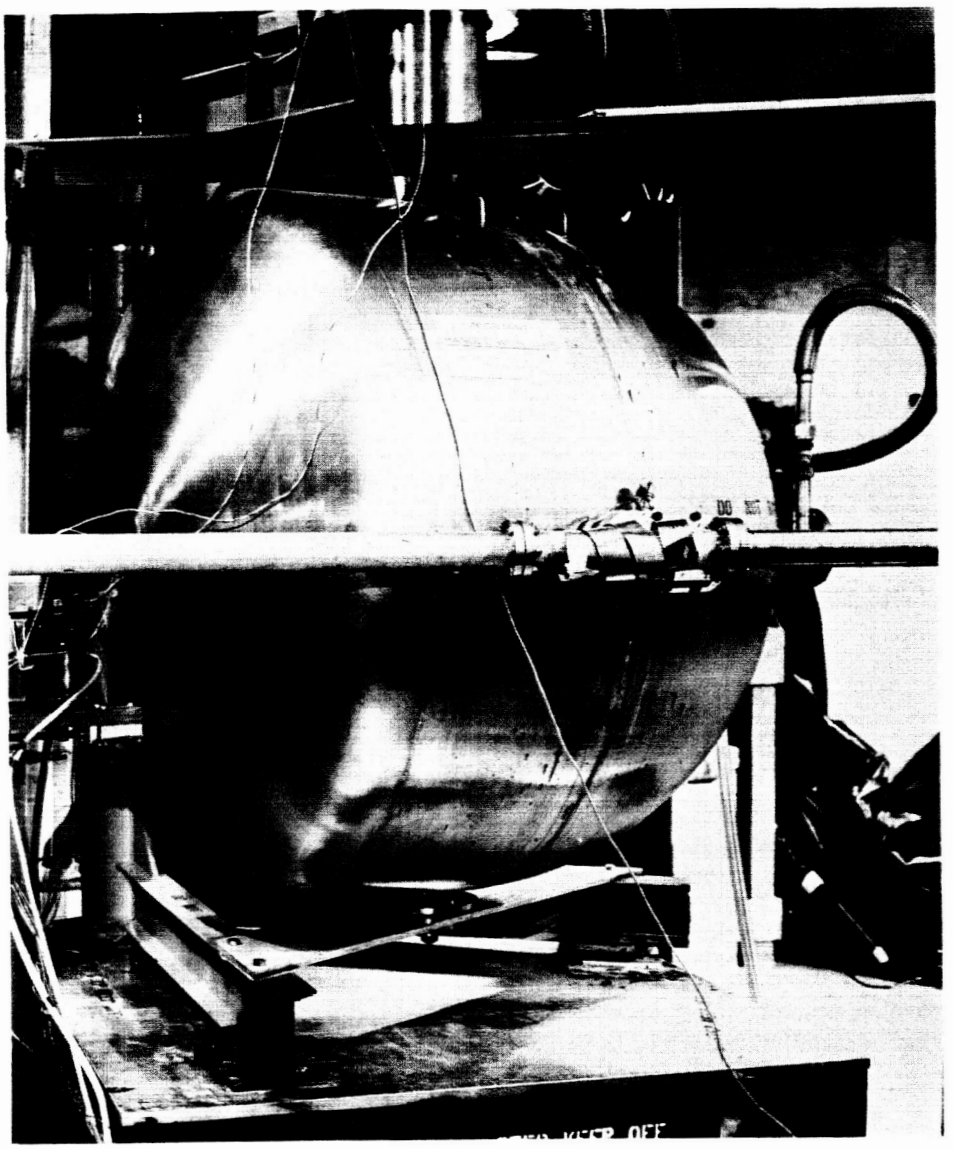

Fig. 9 -- LH_2 dewar

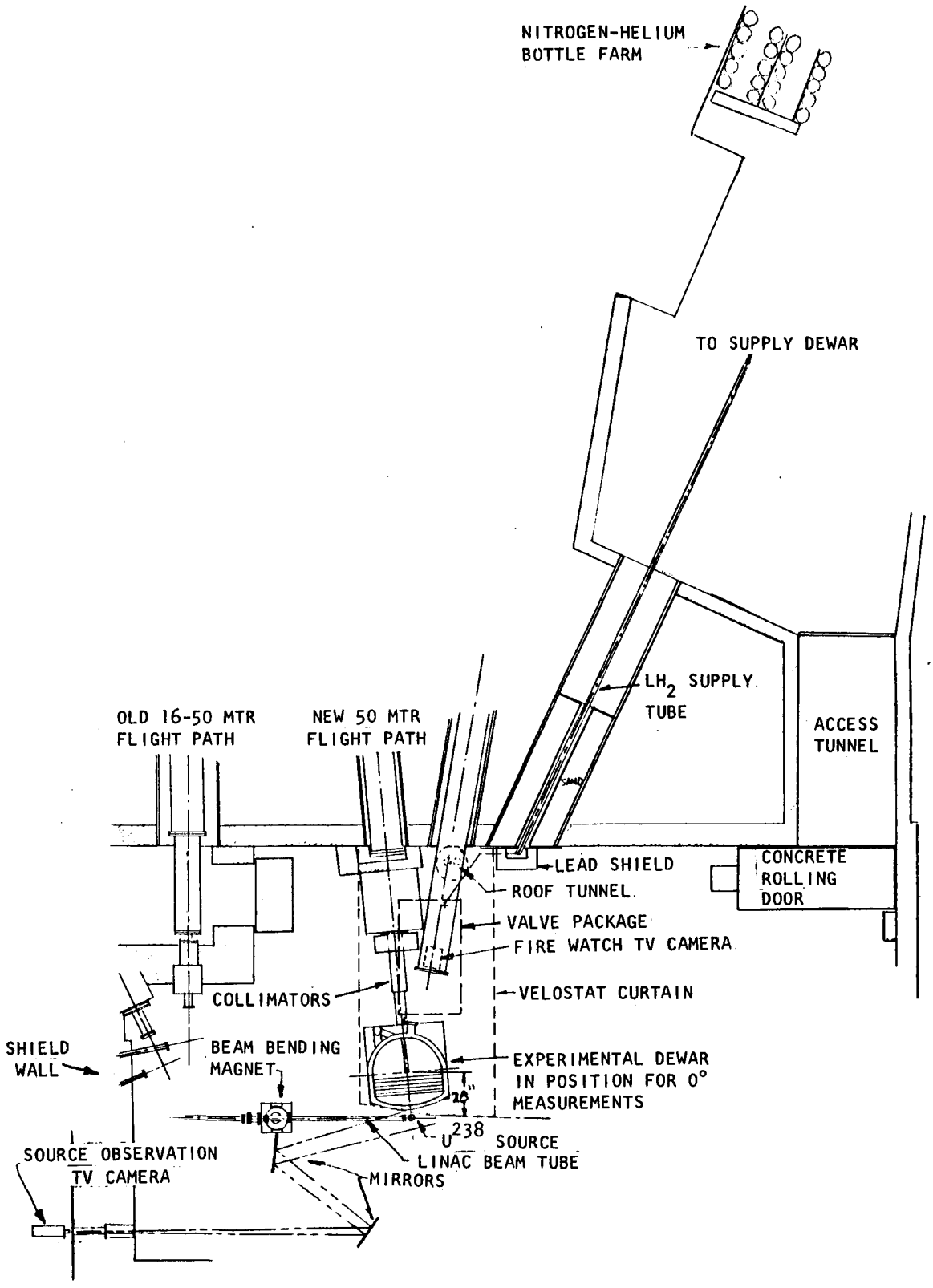

Fig. 10 -- Plan view of the liquid hydrogen facility

3.1.1 Geometry of Liquid Hydrogen Dewar

The shape of the hydrogen envelope had to be compatible with the input requirements characteristic of the computer codes which were expected to be used in conjunction with the experimental results; these include the Monte Carlo and transport theory type codes. The source should be located on the extension of the geometrical axis and should be isotropic.

Code compatibility was resolved by making the LH_2 inner dewar shell in the form of a 42 inch I. D. horizontal right circular cylinder from the point of measurement (the inner face of the probe tube) to the face of the dewar nearest the fast neutron source, with the axis of the cylinder, the re-entrant probe tube, and the source center coincident.

3.1.2 Infinite Medium

The diameter of the liquid hydrogen dewar had to be large enough so that the proper equilibrium neutron spectrum could be established at each axial position. The spectra could not be changed in shape or intensity by the addition of material to the outside of the cylindrical hydrogen surface. Obviously, with the exception of the source configuration, what was desirable was to calculate essentially a one-dimensional geometry. From the experimental standpoint, infinite-medium conditions were desirable in the radial direction since one could then ignore neutron room wall return, support scattering, and dewar

scattering in calculating the axial flux.

A mockup of the dewar geometry was made using polyethylene sheets (18 x 18 x 1/8 in.) rolled into a right circular cylinder with the axis of the cylinder horizontal. Between each 1/8 in. thickness of polyethylene was a 1/2 in. air gap, thus providing a 5 to 1 ratio. This ratio of air to polyethylene reduces the effective density of the polyethylene and gives an equivalent macroscopic transport cross section equal to that for liquid hydrogen at about 5 MeV. This assembly also maintained the same angular properties of the fast neutron source as were used to measure fast neutron spectra in liquid hydrogen. The experimental set-up for these measurements is shown in Fig. 11.

The infinite medium experiment consisted of measuring the change in the magnitude of the neutron flux as the diameter of the assembly was changed from 34 to 50 in. The fast neutron detector views a spot (see Fig. 11) through the 0.92 in. diameter lead precollimator at a 12-3/8 in. penetration into the polyethylene roll. The fast neutron source was placed off axis at a small angle since if it were on axis with the precollimator any effect due to the size of the assembly would be partially masked by the transmission of the fast neutrons through the polyethylene. These neutron spectra are shown in Fig. 12. It can be seen in Fig. 12 that little spectral perturbation occurred for the effective diameter range of 34 to 50 in. A final inside diameter of the hydrogen dewar of 42 in. was chosen to completely minimize this effect.

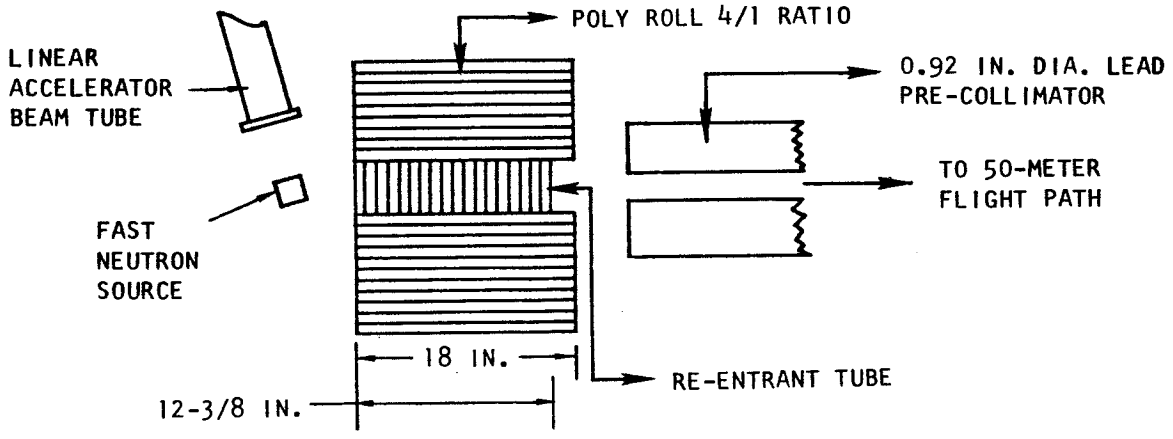

Fig. 11 -- Infinite medium studies mockup diagram

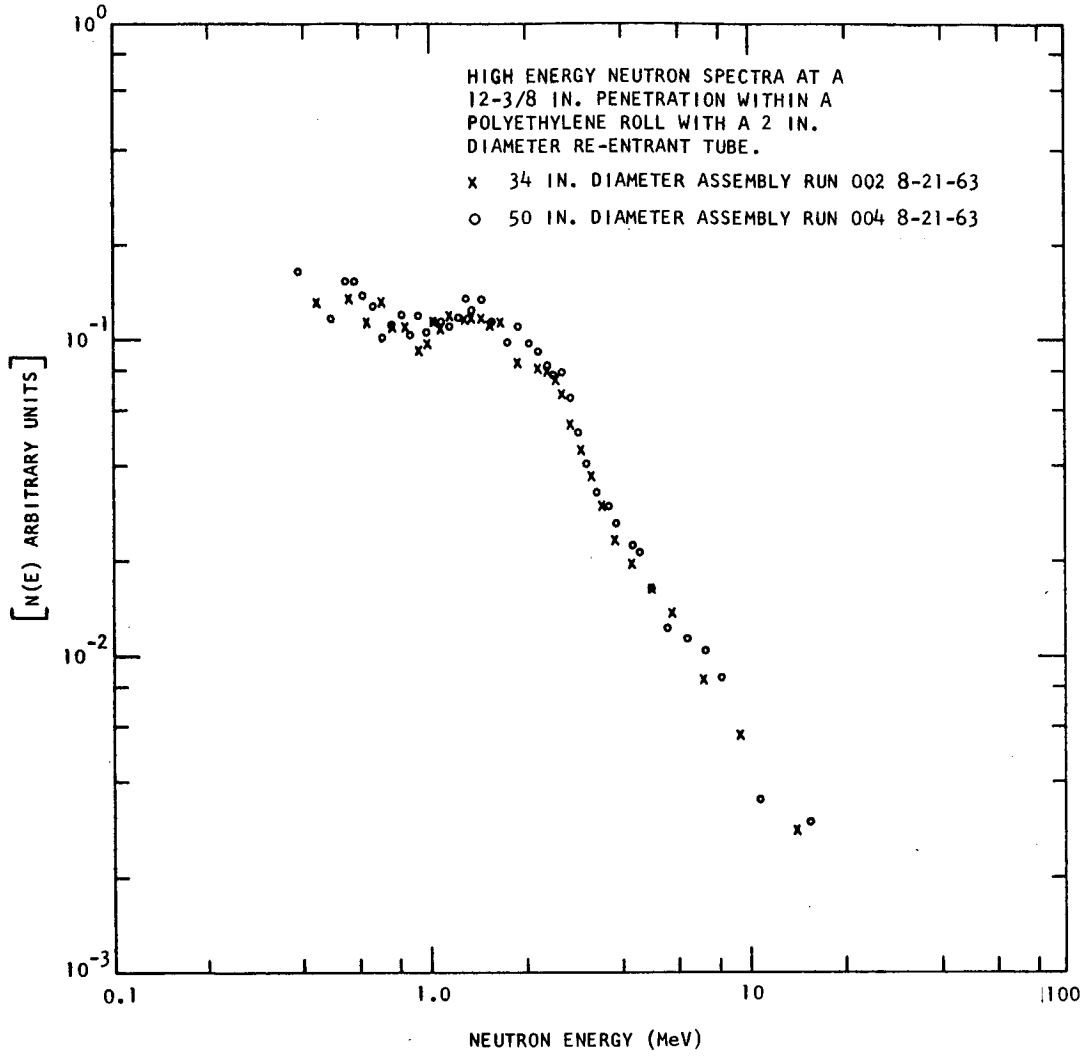

Fig. 12 -- Infinite medium studies neutron spectra

3.1.3 Re-entrant Tube Perturbations

Another question which naturally arises in the interpretation of neutron spectral data is whether the measurement technique has perturbed the spectrum being measured. This perturbation occurs for foil or spectral flux mappings when the foil may cause characteristic adsorption or scattering foreign to the medium. It also occurs for chopper and pulsed time-of-flight measurements where probe tubes must penetrate the assembly under study for beam extraction. The question of the possibility of perturbations caused by probe tubes thus comes up in the liquid hydrogen experiment. How do we know or how can we tell whether the angular flux will be perturbed by the probe tubes?

The best method of checking the importance of this effect was to use the polyethylene mock-up and measure the spectral dependence on re-entrant tube size. These measurements were made in the polyethylene mock-up of the geometry described in the previous section. Fast neutron spectra were measured for re-entrant tube diameters of 2 in. and 1.25 in. The results of these spectral measurements, shown in Fig. 14, indicate that within the statistical error of $\pm 5\%$ there are no spectral perturbations due to the re-entrant tube. Thus, the perturbation at high neutron energies is small and probably less than that experienced at the lower (thermal) energies.

Other measurements made by General Atomic also have indicated that the perturbation is less at higher energies. This was especially

well demonstrated in a previous program of lithium hydride shielding measurements. A top view of the setup for these measurements is shown in Fig. 13.

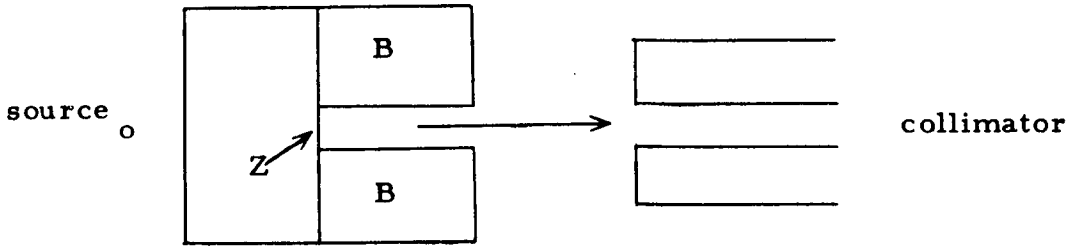

Fig. 13 -- Probe tube perturbation studies setup

The spectra were measured at point Z with and without shield B in place. The neutron energy range above 0.5 MeV was studied. For the lithium hydride shield the spectral shape and intensity were not influenced noticeably by the removal of shield B. This was an even more severe test than that illustrated in Fig. 14.

On the basis of the above arguments it was believed that the 1-1/4 in. probe tube used for the spectral studies in the liquid hydrogen dewar did not perturb the true neutron spectrum present.

3.1.4 Variable Angle

The design of the dewar was such that a neutron flux could be extracted from the measurement point at any given angle from 0^{o} (on the cylinder-source axis) to 90^{o}, with a minimum of difficult changes and special handling problems associated with the angle change and location.

The angular measurement problem, which was certainly one of the most difficult, was solved by the method shown in Fig. 15. The end

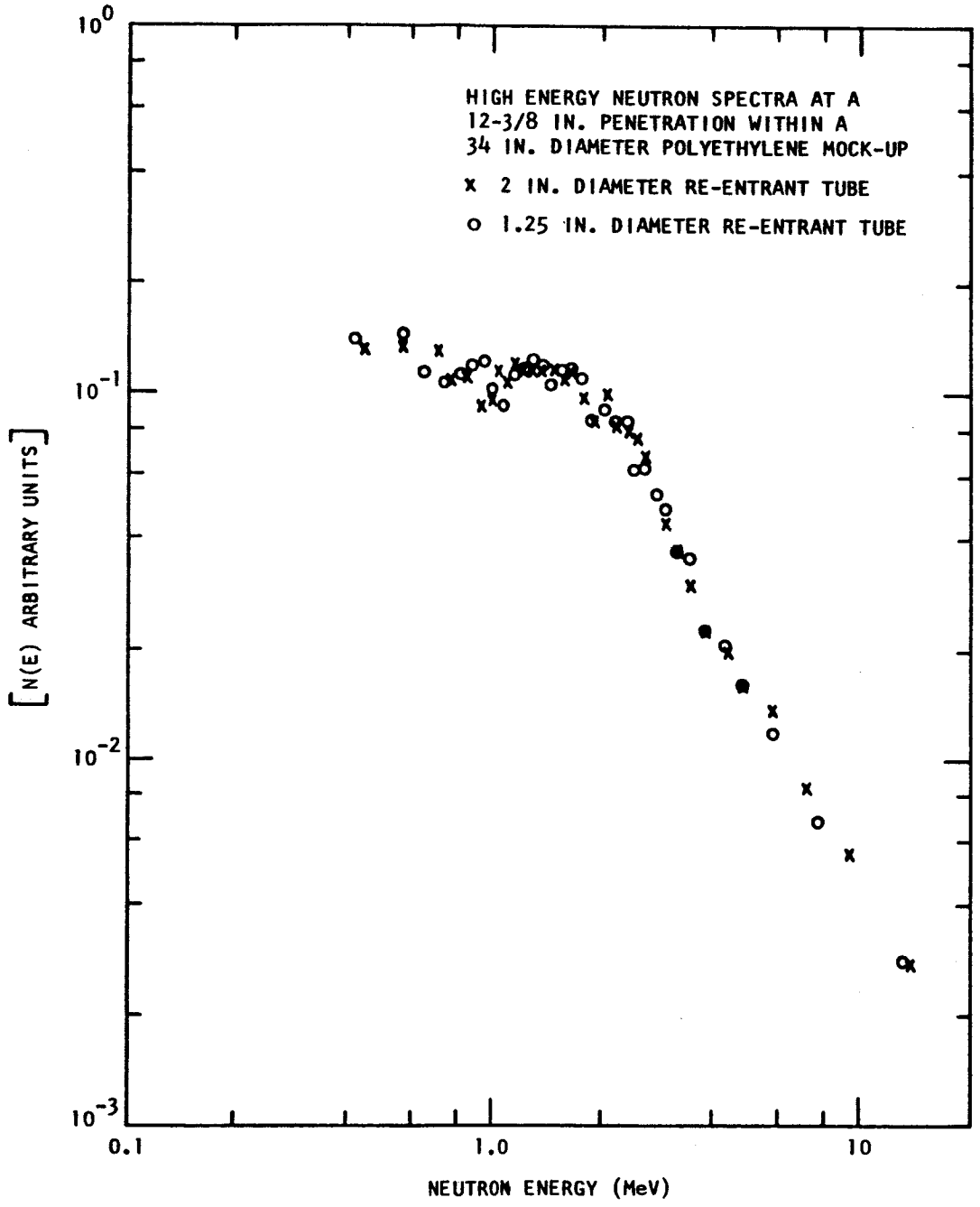

Fig. 14 -- Probe tube perturbation studies neutron spectra

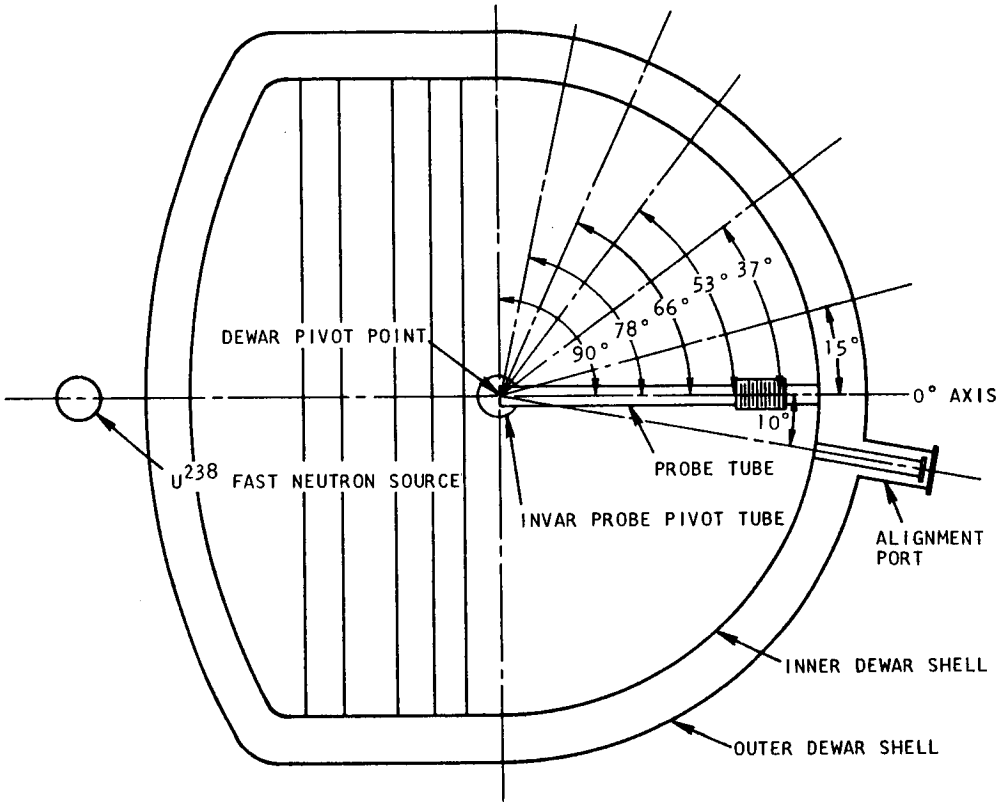

Fig. 15 -- LH_2 dewar angular flux extraction

of the dewar located away from the neutron source was formed by hemispherical stainless steel heads; the probe tube was attached to a large-diameter thin-walled invar tube, with its inner (measurement) face at the geometric center of the hemisphere. Spherical bearings were located at both ends of the vertical invar probe support tube, the axis of the tube being exactly vertical and parallel with the bearing seats located in the dewar shell so that a true horizontal plane was formed by rotation of the probe tube. A fitting at the top extends the invar pivot tube's axis outside the outer dewar so that the position and attitude of the probe tube could be known exactly. The outer face of the probe tube was on a window welded into a slot cut into the inner hemispherical head at the belt line. A guided bellows in the probe tube permitted the length of the probe tube to be varied by varying its internal pressure. Evacuation of the tube allowed it to shorten and rotate without rubbing on the shell window, while pressurization forced the probe tube outer face tightly against the shell window to eliminate all but about a 0.005 inch layer of LH_2 from the flight path. In practice the measurement of neutron spectra at various angles was accomplished by fixing the probe tube, via the invar tube extension, with respect to the position of the flight path; the dewar was then rotated about the axis of the probe support tube to the proper angle. Since the fast neutron source remained fixed with respect to the dewar, spectrum measurements could be made at any angle of interest between 0° and 90° --the design limit angles.

3.1.5 Variable Thickness

In the original design considerations a variable thickness of liquid hydrogen could have been measured by means of a stainless steel bellows which could be extended and compressed as described above. However, this was prohibited by cost in the variable angle version due to the complexity of such a mechanism. Therefore, an alternate method was used which allowed the hydrogen layer thickness between the fast neutron source and the measurement end of the probe tube to vary in five integral steps. Baffles defined the limits of the chambers, with LH_2 being transferred progressively out of the chambers to reduce the layer thickness. The values of the layer thicknesses were chosen using the criteria and calculations shown in the neutron heating calculations in Appendix A of this report.

3.1.6 Minimal Material in Neutron Beam

The neutron information beam had to pass through an absolute minimum of material, especially LH_2, consistent with structural strength and safety.

Material through which the neutrons from the probe tube inner face must pass was minimized as much as possible, by slotting the hemispherical inner and outer heads and welding stainless steel windows, sized according to the ASME pressure vessel code for low temperature pressure vessels, over the openings. In addition, all insulation was eliminated from the region traversed by the probe tube, and the faces on

the probe tube itself were designed to the minimum thickness allowed by the ASME low temperature pressure vessel code. During the actual LH_2 experiment, helium at a 5 psig positive pressure was applied to the probe tube to insure positive seating at the hemispherical head window.

3.1.7 Liquid Hydrogen Density Variations

The LH_2 container had to be designed so that the density and quality of the LH_2 in the central portion of the container did not vary and perturb the measurements. Thus, the temperature had to remain constant and no violent boiling or bubbling could occur, for any reason, in the central region; this required that the insulation and the design of supporting structures, etc., follow the best cryogenic practice for minimum heat leak.

Our need for a good cryogenic design to eliminate perceptible density variations and agitation was met by the Cryenco design group. Very careful attention was given to the problem of heat leaks in the region of the measurement face of the probe tube. No high heat transfer rate materials were allowed to extend into the central portion of the dewar from any warm region, and the insulation of the dewar itself was multilayered which allowed the lowest heat leak of any known insulation material.

Film boiling tendencies in the central region were also considered, but calculations by heat transfer specialists, R. K. Livett and H. F. Poppendick of Geoscience Limited, presented in Appendix B,

indicated that all the heat leaks into the dewar were really negligible in terms of producing significant density variations.

3.1.8 Probe Tube Alignment

Probe tube alignment with the flight path system had to be done externally with little margin for error, so some positive external indication of probe tube attitude and position had to be provided. Also, an alignment port for the initial transit alignment of the probe tube had to be provided to allow a very exact initial placement and alignment to be accomplished, and to check for potential misalignment due to unequal filling of the tank and other external factors.

Probe tube alignment with the flight path system proved to be our most difficult and serious problem. A positive and reliable alignment method was not perfected until shortly before the start of the LH_2 experiment; this method is illustrated in Fig. 16 and shown in a photograph in Fig. 17. The alignment plate is the key to the method; it was machined at the Cryenco plant during assembly of the inner dewar so that its flat surface was exactly perpendicular to the centerline of the probe pivot tube. A close-tolerance bore in the center of the plate fits tightly over a bearing surface concentrically machined at the top of the probe pivot tube during the pivot bearing machining operation. Since this alignment plate bearing surface protrudes from the top of the outer dewar, and since the probe tube was carefully welded to the invar pivot tube with its centerline perpendicular to the pivot tube's centerline

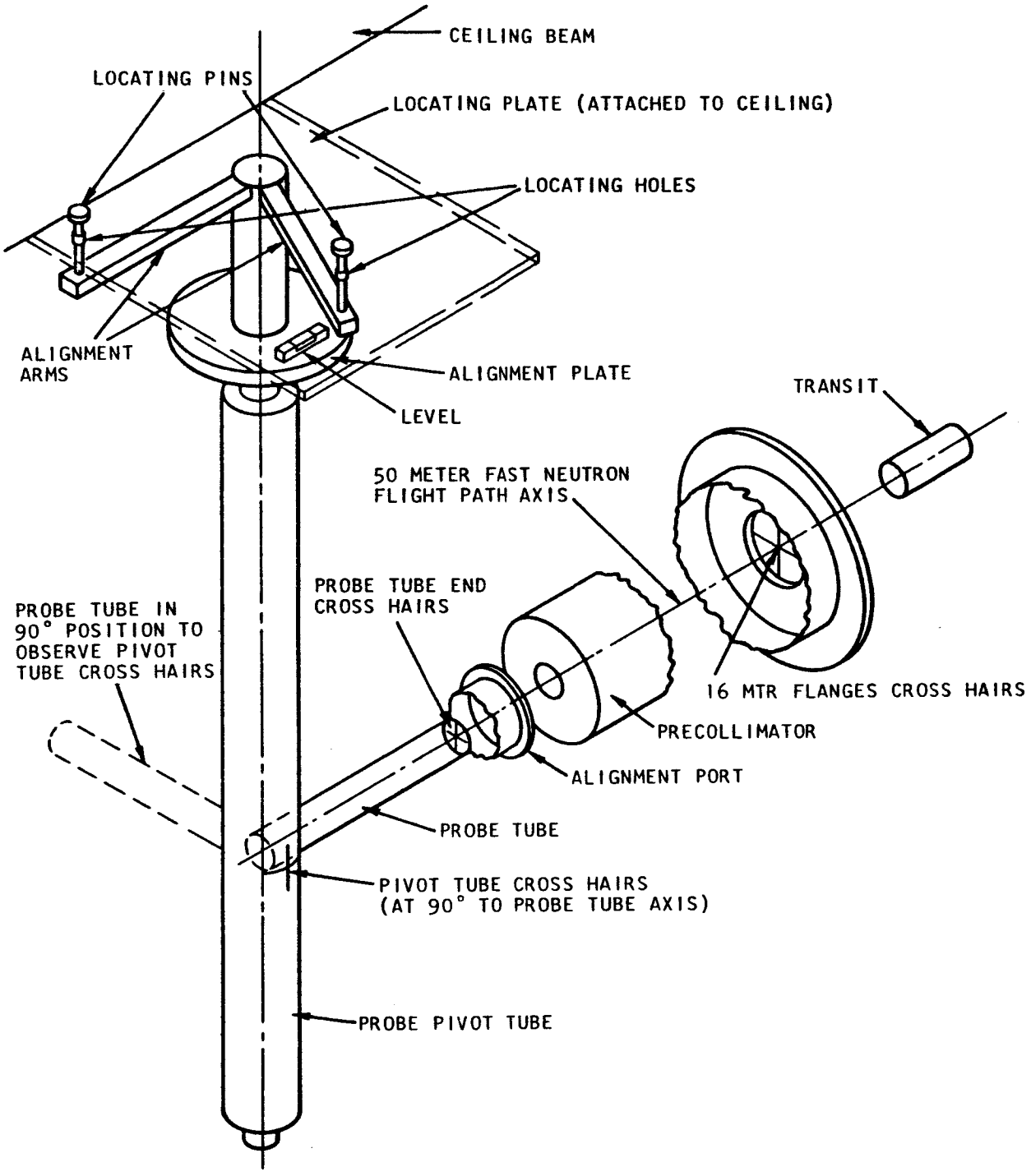

Fig. 16 -- Details of dewar alignment and locating method

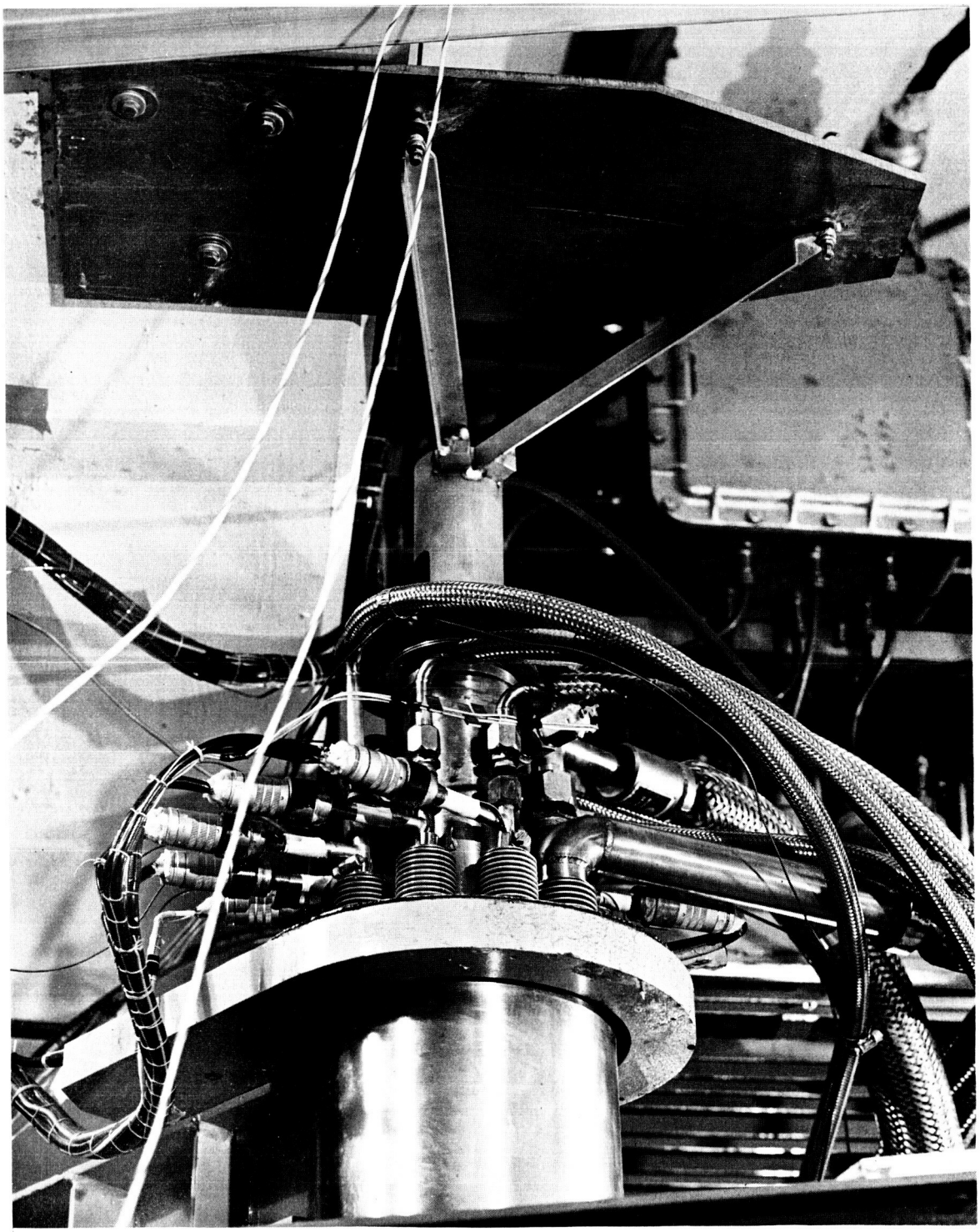

Fig. 17 -- Top of LH_2 dewar showing alignment arms

within 0.005 inch over the probe tube's 21 inch length, we therefore had a positive method of knowing the attitude of the probe tube's centerline in relation to the horizontal. During our alignment procedure, the initial step was the adjustment, by means of leveling jacks, of the outer dewar so that a precision level placed on the machined surface of the alignment would indicate dead horizontal at two positions 90^{o} apart.

A much more difficult problem arose in trying to externally align the probe tube centerline with the flight path centerline. Our solution was to provide two-point location at the top of the pivot tube, with two horizontal 16 inch arms attached to the alignment plate system 45^{o} apart. Holes in the ends of these arms had to line up with holes bored in a plate fixed to the ceiling of the experimental room; fairly tight fitting pins which connect the arms to the plate ensured that the holes really did line up properly. Since the alignment arms are fixed with relation to the probe tube centerline and since the ceiling plate could be fixed with relation to the flight path centerline, it followed that a careful initial transit alignment of the probe tube with the flight path would allow an accurate placement of the ceiling plate so that future realignments could be confidently made externally. This is an important feature since transit alignment involved two relatively difficult and time-consuming disruptions of the experimental setup: first, the dewar, which may be at an extremely low temperature, had to be opened at the alignment port; besides the difficulty of seeing through the resulting

fog, a cold dewar, unless strongly flushed with nitrogen or helium gas, would condense and freeze water in the LH_2 space. Water or ice inside the dewar is a dangerous condition, and the dewar had to be warmed and dried before it could be refilled with LH_2. Second, looking through the flight path with a transit involves removal of the flight path windows with the accompanying loss of vacuum and re-evacuation problems.

External probe tube centerline height alignment is not generally necessary after the initial alignment because of the extremely rigid nature of the dewar supports. Eight ton house movers' screw jacks were used at each corner of the dewar support table for leveling and height adjustment. External transit-located height marks were made on the outer dewar shell and a height check with relation to the flight path centerline could easily be made at any time.

At the conclusion of the LH_2 experiments, the dewar was opened at the alignment port and the alignment checked with a transit. A lateral displacement of about 0.060 inch and a vertical displacement of about 0.060 inch was found, both of which were still within the misalignment tolerance of 0.095 inch. Before final adoption of the aforementioned alignment system several very exhaustive checks had been made of its accuracy and repeatability, and we felt sure that the method could be counted upon to keep the alignment well within tolerance. A strong tendency for the dewar to move in its supports when filled with relatively heavy liquid nitrogen prompted us to very carefully check for mislocation

tendencies when the dewar was loaded with weights approximating the distribution and mass of liquid hydrogen. Absolutely no motion or misalignment was noted during these tests, so we felt that no loading misalignment could have occurred during the LH_2 experiments.

3.1.9 Ease of Operation

The entire LH_2 containment structure had to be competently and carefully designed by someone familiar with cryogenic pressure vessels and their applications to ensure a maximum of safety, efficiency, and ease of handling and operation. The nature of the experiment and the facility scheduling made it mandatory for each part of the experiment to be of long duration; since the personnel who were scheduled to operate the system could be expected to be suffering from fatigue, especially during the latter phases of the experiment, ease of handling and operation and a fail-safe type design greatly contributed to the margin of safety for the experiment, the facility, and the personnel involved.

As previously mentioned, the experimental dewar was designed by the Cryenco design engineers, who have an extensive background in LH_2 storage vessel design, in adherence to the ASME low temperature pressure vessel code. Much thought and effort was put into designing the functions and operations of the dewar and associated systems for ease, accuracy, and reliability. Hydrostatic pressure tests were performed at 1-1/2 times the design pressure of 35 psig to insure the maximum possible confidence in vessel integrity.

3.1.10 Geometry - Source Considerations

Because of the limitations of source heat capacity, Linac power output capability, and the low neutron intensity for large-angle neutron spectrum measurements, maximum use had to be made of the source neutrons. This could only be accomplished by placing the first LH_2 surface very near to the neutron source, thus presenting a large solid angle to the source. Further, the foreign material comprising the source end of the LH_2 envelope and the insulation had to be kept as thin and of as low a neutron attenuation coefficient as possible to reduce the source loss.

Because of the pressure vessel nature of the dewar, it was necessary to increase the minimum source-to-LH_2 distance somewhat over the distance which would have been possible by using a flat plate at the source end of the dewar. To contain the expected pressure, a 42-inch diameter flat plate would have been required to be over one inch thick, even if made of 304 stainless steel. A standard pressure vessel torospherical type head, on the other hand, could be less than one-eighth inch in thickness but would increase the separation distance by about eight inches. About three inches of insulation were required, followed by the outer shell torospherical head. Both heads were specified to be 0.125 inch thick 304 stainless steel. Our final source-center to nearest-hydrogen-surface distance, with a full dewar, proved to be 14-7/8 inches, giving a fractional solid angle of 0.21. Thus, 21 percent

of the isotropic source's neutrons would strike the first LH_2 surface, ignoring transmission losses.

3.1.11 Liquid Level Indication

Some method of liquid level indication had to be provided to ensure that the correct experimental conditions were met for each phase of the program.

Three liquid level indicators, positioned as shown in Fig. 18, were provided in each chamber with the exception of chamber six which had only a bottom indicator. Each liquid level indicator was backed by two more liquid level indicators in case of failure. The liquid level sensors were 1000 ohm, 1/4 watt resistors. The normal resistance at LN_2 temperature was 1400 ohms and at LH_2 temperature it was 2800 ohms. The instrumentation for the readout of the sensors was built by Apogee Products Inc., Boulder, Colorado. After an initial period of adjustment and familiarization, these level sensors proved to be reasonably sensitive indicators of the fluid level and condition.

3.2 VALVES, PIPING, AND TRANSFER SYSTEM

A complete liquid and gas transfer system was designed by General Atomic and Cryenco to handle the various functions required for liquid hydrogen, gaseous hydrogen, purge gas, vacuum, and fire extinguishing gas transfer. Our basic design philosophy governing all decisions required in this design was to have a fail-safe system; that is, one which would remove the liquid hydrogen from the experimental

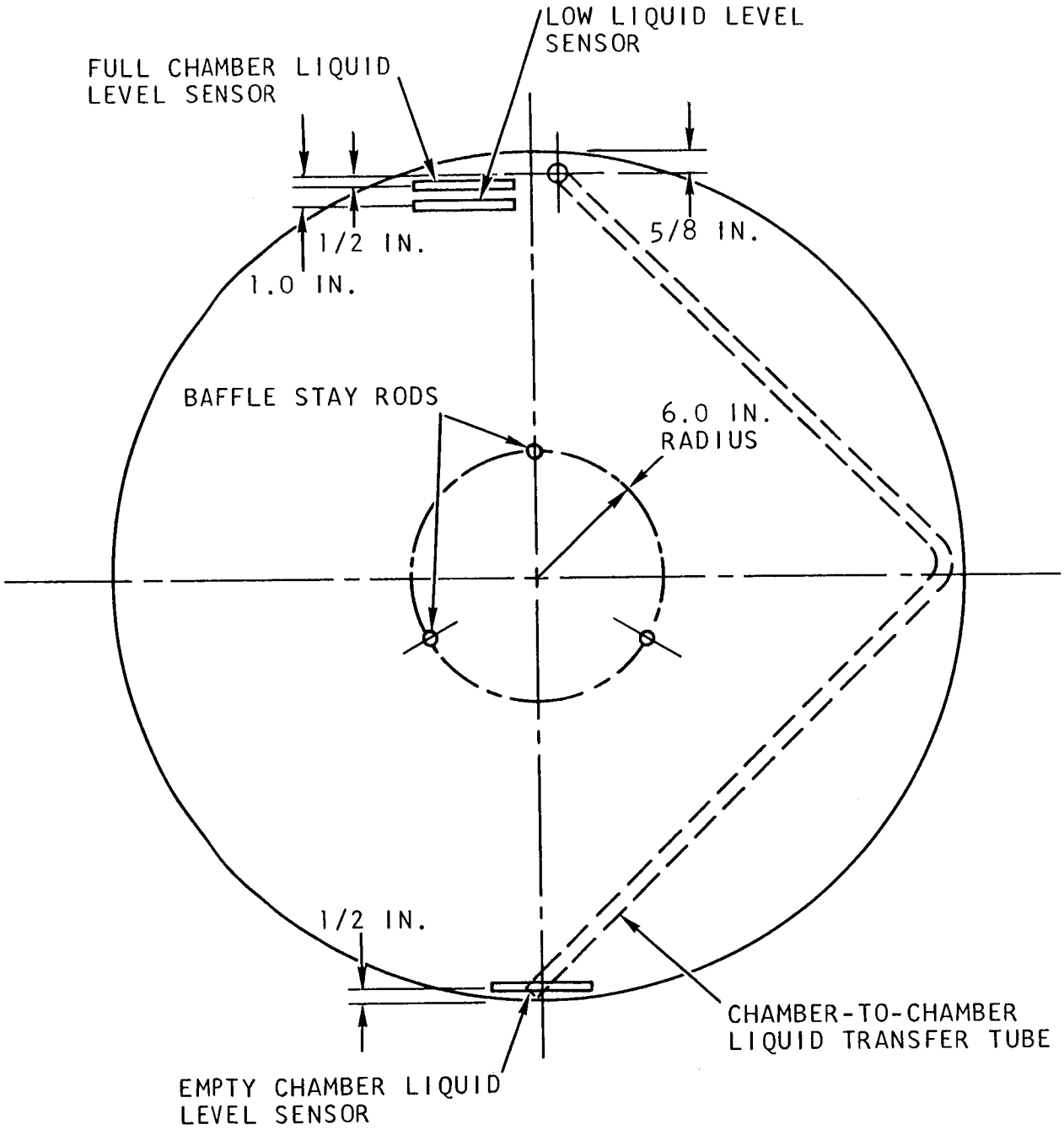

Fig. 18 -- Details of typical baffle showing location of liquid level sensors

dewar if an electrical or pneumatic failure was experienced in the control system. It was our opinion that the best place for the liquid hydrogen to go under these conditions was out the dump stack. Therefore, the normal positions of all the remote operated valves in the system were chosen to perform this function in the event of failure. In addition, a manual emergency dump switch was included in the control circuit so that any situation calling for an emergency dump, followed by a rapid personnel evacuation of the area, could be handled very quickly. A subsequent emergency procedures study caused some modification in our thinking and the emergency dump concept has been pretty much dropped as possibly more dangerous than the alternates. The emergency procedures written for the LH_2 experiments are included in Appendix C of this report.

A schematic of the final piping system used for the LH_2 experiments is shown in Fig. 19. All the valves seeing liquid hydrogen or cold gas are electro-pneumatic remote-operated extended stem valves, with the fill valve and dump valve vacuum jacketed. The cryogenic valves were made by Black, Sivalls, and Bryson, Inc. of Kansas City, Missouri, and are of the metal-to-metal seal variety; some leaking was experienced in several of these valves but it apparently was stopped after a minor adjustment in stem length and a large increase in operator pressure. Additional remote-operated solenoid warm gas valves were provided for control of purge and fire-extinguishing gas, and throttleable hand

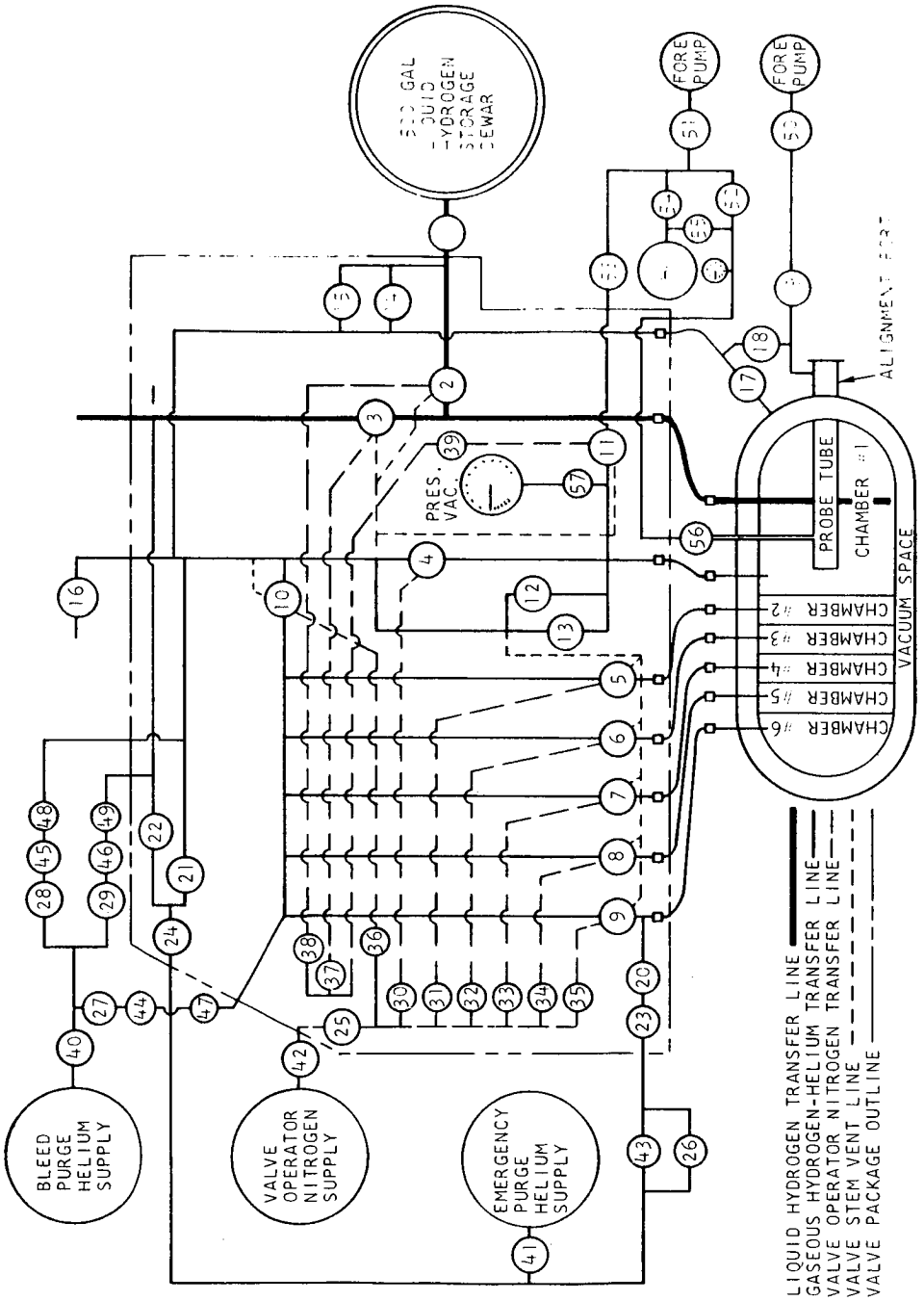

Fig. 19 -- Valve and piping system schematic

LEGEND FOR FIGURE 19

Number	Normal Position	Valve
1		Storage dewar hand valve
2	NC	Dewar fill valve - BS&B vacuum jacketed 3/4" pneumatic valve
3	NO	Dewar dump valve - BS&B vacuum jacketed 3/4" pneumatic valve
4	NC	Chamber No. 1 vent valve - BS&B extended stem 2" pneumatic valve
5	NC	Chamber No. 2 vent valve - BS&B extended stem 3/8" pneumatic valve
6	NC	Chamber No. 3 vent valve - BS&B extended stem 3/8" pneumatic valve
7	NC	Chamber No. 4 vent valve - BS&B extended stem 3/8" pneumatic valve
8	NC	Chamber No. 5 vent valve - BS&B extended stem 3/8" pneumatic valve
9	NC	Chamber No. 6 vent valve - BS&B extended stem 3/8" pneumatic valve
10	NC	Chamber No. 2 - No. 6 isolation valve - BS&B extended stem 3/4" pneumatic valve
11	NC	Vacuum purge valve - BS&B extended stem 3/4" pneumatic valve
12		Rupture disk - BS&B 2" - set at 60 psig
13		Blowoff valve - Farris 2" - set at 40 psig
14		Blowoff valve - Farris 1/2" - set at 100 psig
15		Rupture disk - BS&B 1/2" - set at 150 psig

Legend for Figure 19 (Cont'd)

Number	Normal Position	Valve
16		Vent line flapper valve
17		Cryenco dewar vacuum space relief valve
18		Cryenco alignment port vacuum space relief valve
19		Alignment port evacuation hand valve
20	NO	Dewar purge valve - 1/2" Skinner solenoid valve
21	NO	Vent line purge valve - 1/2" Skinner solenoid valve
22	NO	Dump line purge valve - 1/2" Skinner solenoid valve
23		Dewar purge line regulator - Fisher 1/2" valve set at 35 psig
24		Vent-dump purge line regulator - Fisher 1/2" valve set at 35 psig
25		Valve operator line relief valve - Kunkle 1/2" valve set at 68 psig
26	NO	Transfer bypass solenoid valve
27	NC	Dewar micropurge solenoid valve
28	NC	Vent line micropurge solenoid valve
29	NC	Dump line micropurge solenoid valve
30	NC	No. 1 vent operator solenoid valve
31	NC	No. 2 vent operator solenoid valve
32	NC	No. 3 vent operator solenoid valve
33	NC	No. 4 vent operator solenoid valve
34	NC	No. 5 vent operator solenoid valve
35	NC	No. 6 vent operator solenoid valve

Legend for Figure 19 (Cont'd)

Number	Normal Position	Valve
36	NC	No. 2 - No. 6 isolation operator solenoid valve
37	NC	Dump operator solenoid valve
38	NC	Fill operator solenoid valve
39	NC	Vacuum purge operator solenoid valve
40		Bleed purge regulator valve - set at 35 psig
41		Emergency purge regulator valve - set at 35 psig
42		Operator regulator valve - set at 65 psig
43		Liquid transfer regulator valve - set at 5-8 psig
44		Dewar micropurge hand flow rate valve
45		Vent line micropurge hand flow rate valve
46		Dump line micropurge hand flow rate valve
47		Dewar micropurge flowmeter
48		Vent line micropurge flowmeter
49		Dump line micropurge flowmeter
50		Alignment port hand vacuum pump shutoff valve
51		Tower hand vacuum pump shutoff valve
52		Probe tube vacuum hand valve
53		Dewar vacuum hand valve
54		Helium vacuum pump relief hand valve
55		Helium probe tube hand valve
56		Probe tube hand shutoff valve
57		Vacuum-pressure gauge hand shutoff valve.

operated valves located at the bottle farm were included to allow precise control of constant purge flow rates and low LH_2 transfer rate pressurization. Manual vacuum valves were installed at the tower for control of dewar purge evacuation and probe tube evacuation, together with helium control hand valves to fill the evacuation lines when not in use and to pressurize the probe tube; the evacuation lines were run down through the 18 inch diameter roof tunnel together with the vent and dump lines.

Nitrogen gas at 68 psig was used to operate the electropneumatic valves, eliminating the moisture and occasionally unstable supply problems associated with using air from the Linac's compressors. During practice runs with liquid nitrogen, nitrogen gas was used as the pressurizing medium and as a line purge, because of the large cost difference between nitrogen and helium. However, the lower temperatures associated with the use of liquid hydrogen required the use of either hydrogen or helium gas, and since helium is much safer, helium was used for all pressurizing and purging operations. A great deal of helium gas was required to run this experiment because of the need for a constant purge in the vent and dump stacks to prevent back-diffusion of moisture and air, and because of the temperature-volume relationship of a gas, i.e., its volume at a temperature of 20° K is one-fifteenth its volume at 300° K, for equal pressures. Pressurization of the dewar to 15 psig at 20° K, as during purging or liquid transfer operations, decreased this factor to one-thirtieth the original volume. At the conclusion of each portion of

the LH_2 experiment, our safety procedures required us to raise the dewar internal temperature to a point above the liquefication temperature of oxygen after dumping the LH_2. This process required a great deal of helium gas, although only thirty minutes of helium purging were usually required to raise the internal temperature to about 100° K. A total of about 34, 080 cubic feet of helium were used during the eight days the LH_2 experiment was activated.

All transfer lines which could be expected to carry liquid hydrogen were of a double-wall vacuum insulated construction, while the vent and evacuation lines were uninsulated. The fill/dump line and the chamber vent lines between the dewar and the valve package were flexible to allow dewar rotation. A photograph of the valve package and the flexible vent and fill/dump lines are shown in Fig. 20. Initially, ferrule type fittings were used at each end of the flexible vent lines but it was so difficult to stop the leaks at these connections that the fittings were replaced with flared fittings using copper inserts manufactured by the Del Manufacturing Company in Los Angeles, California. After the installation of these fittings, no further leak problems were encountered. All connections in the vacuum jacketed liquid transfer lines were by bayonet fittings, with no difficulty arising at any time from leaks in these connections.

One of the procedures followed prior to filling the experimental dewar with liquid hydrogen consisted of evacuating the dewar and as much of the dewar piping system as possible to check the leak tightness. It was

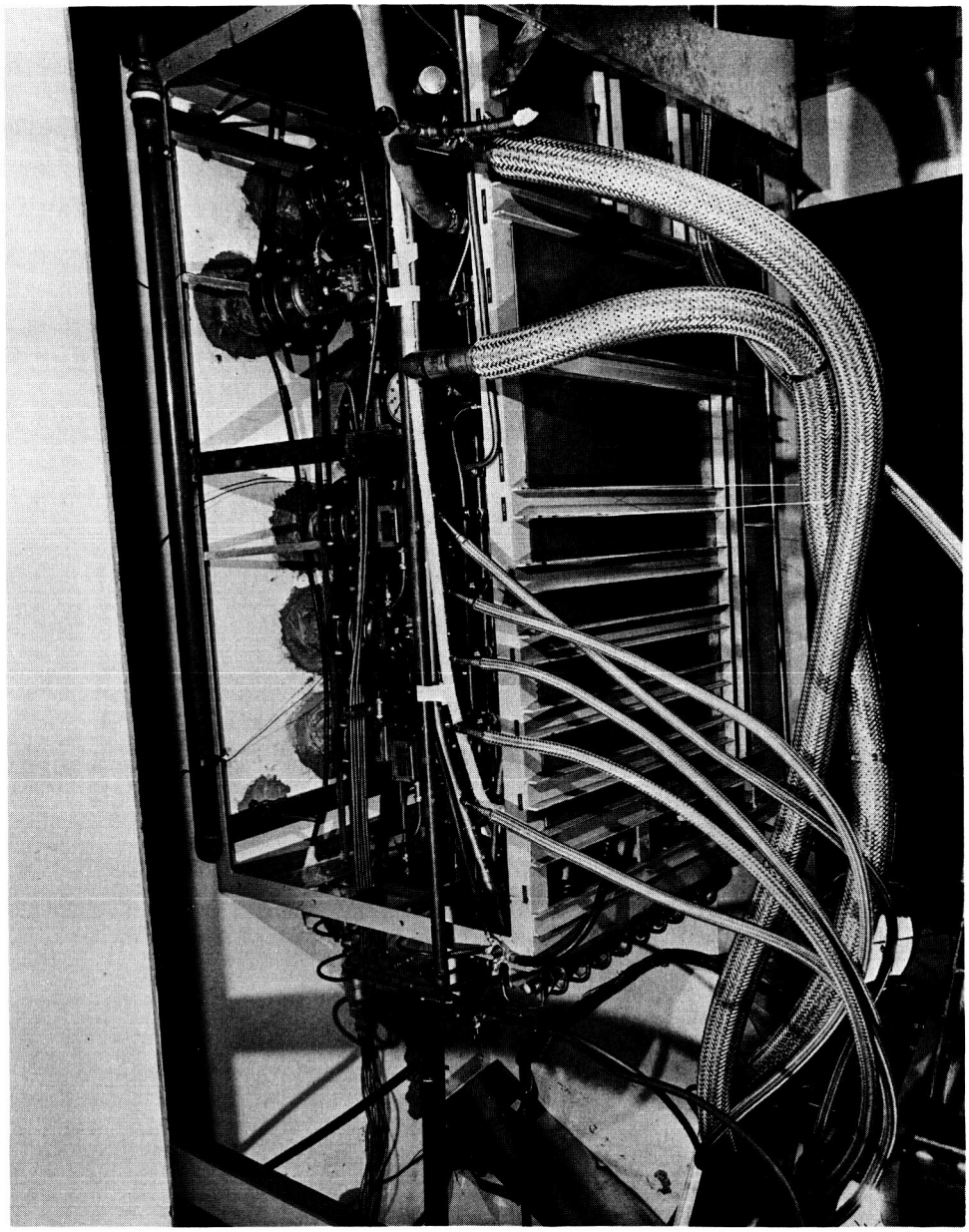

Fig. 20 -- Valve package and connections

always possible to evacuate the system to better than 5 mm of mercury; valving off the vacuum pump and observing the loss of vacuum over a period of time always indicated excellent integrity, with a loss of 0.2 mm of mercury in five minutes being about normal.

3.3. SYSTEM CONTROLS AND INSTRUMENTATION

Operation of the liquid hydrogen dewar required several systems of controls and instrumentation to provide the maximum efficiency and safety. Liquid temperature was monitored by three copper-constantan thermocouples located in chamber one and read out with sufficient accuracy by a Rubicon potentiometer. These were also used as additional level indicators. Additional copper-constantan thermocouples were placed on the outside of the vent lines at their point of exit from the dewar to indicate to the operator any tendency for the temperature of the vent lines to fall below the air liquefication temperature. Iron-constantan thermocouples were connected to a multipoint recorder, interlocked with the Linac control system, to indicate fires in many of the locations where fires would otherwise be impossible to detect. One set of thermocouples also monitored the temperature of the fast neutron source.

Except for the temperature readouts and light and ventilation blower switches, all system controls and condition indicators were located on the control console (Fig. 21) located in the data retrieval area. Two pressure gauges were used, an Ashcroft gauge covering

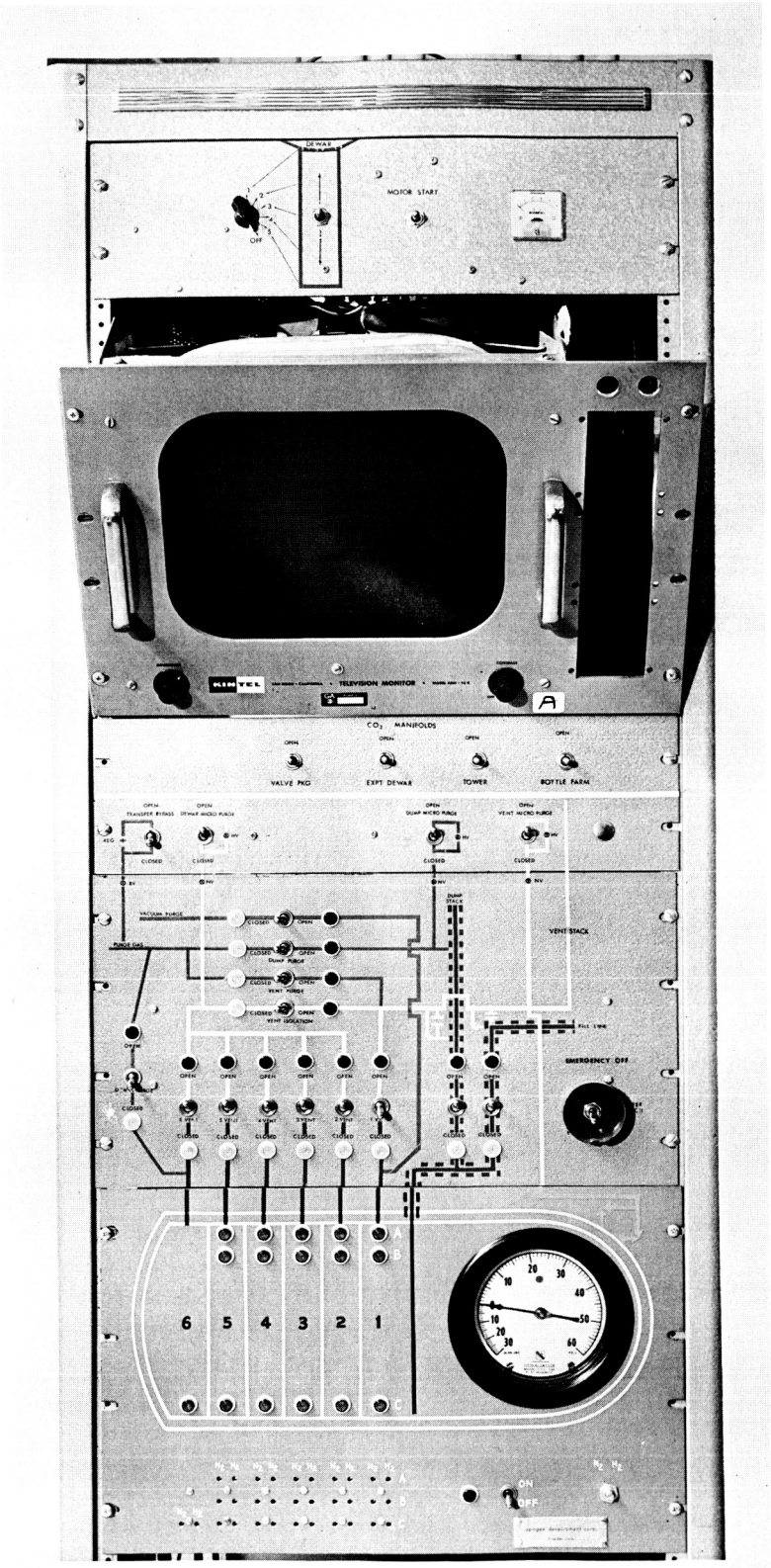

Fig. 21 -- Control console

the range from -30 inches of mercury to +60 psig, and a Barton gauge covering the range from 0 psig to 50 inches of water, or about 2 psig. The Barton gauge proved extremely useful in the liquid flow control operations, as most operations with the liquid hydrogen required pressures which fell within the range of this gauge. Additional pressure gauges for monitoring the dewar internal pressure and probe tube pressure, showing both negative and positive pressures, were installed in all areas where operating personnel could be expected to be during any of the experiments.

The liquid level readouts, discussed in Section 3.1.11, may also be seen in Fig. 21; they are located in the same panel with the Ashcroft pressure gauge. In the panel above, the piping and valve system is outlined with open or closed lights indicating the position of each remote operated valve. The operating switches for controlling these valves are also located on this panel. Immediately above these controls, the switches controlling the CO_2 fire extinguishing system solenoid valves are located on a small panel. The television monitor at the top of the console serves a camera located at the dewar and views the top of the dewar and the vent line connections to act as an additional emergency warning device and to observe liquid air being formed on the vent lines in order to minimize this effect.

A combustible gas sniffer system power supply is located at the bottom of the console (not shown in Fig. 21). The sniffers are located

at the valve package, inside the ventilation roof tunnel, at the experimental room roof, at the rear entrance, and halfway up the vent/dump stack tower. Buzzers in the readout unit operate if the sniffer unit detects a mixture of hydrogen gas and air as low as 10 per cent of the combustible level.

An intercom system provides communication from the data taking center to all parts of the liquid hydrogen facility. One master intercom is located at the side of the console to enable the system operator to quickly communicate with the tower area or the bottle farm. During operations, one member of the crew remains in the vicinity of the bottle farm and supply trailer to adjust the various purge flow rates at the direction of the operator and to monitor the rear areas for hydrogen leaks and low purge or pneumatic valve operator gas supplies. Once the flow rates are adjusted and the hand valves at the bottle farm are set in their operating positions, the experimental operator at the control console can handle all the required functions from the console. A complete discussion of the methods of operation is contained in the operating procedures in Appendix C.

3.4 FIRE AND HAZARDOUS CONDITION PREVENTION MEASURES

Great emphasis was placed upon the prevention of hazardous conditions which could possibly lead to fire or explosion. During the system design phase, each step was taken only after an evaluation of its effect upon the safety of operation. The considerable experience in the handling of liquid hydrogen of some of the Cryenco designers was called upon, as well as the experience of the General Dynamics Astronautics materials test lab personnel. After installation of the dewar and its piping system, safety men well acquainted with the handling problems and hazards associated with LH_2 were asked to inspect the area and make recommendations to improve the safety of the system. As a result, a large amount of labor was expended in providing better ventilation and leak tightness, removal of ignition sources, and addition of extra hazardous condition warning devices.

Of foremost importance was the elimination of any fuel to form a combustible mixture. To attain this condition, exhaustive leak tests and checks were performed. During construction the dewar was checked for leak tightness with a helium mass spectrometer; and upon arrival at General Atomic and installation of the piping system and dewar, the entire system was again checked by pressure and vacuum, and all leaks which were located were stopped until the entire system was helium leak tight. For further safety, the system was leak tested both for pressure and vacuum tightness before each experiment.

A second major area of fire prevention importance was the elimination of sparking sources which could provide ignition in a potentially dangerous atmosphere. While it is virtually impossible to operate an experiment on a Linac with all sparking sources eliminated--the electron beam traveling through the air obviously is an excellent ignition source--it is possible to turn off or disconnect AC outlets, room lights, experimental electronics used by other experimenters, and pumps, fans, and motors not connected with the LH_2 experiment. Even the Linac piping system's vacuum stations in the experimental room were turned off. All necessary lights were explosion-proofed and the room exhaust blower and intake blower were designed for use in explosive atmospheres. Magnets and amplifiers which were necessary for the piping and locating of the electron beam were shrouded and the shrouds purged with nitrogen. The electropneumatic valves and solenoid valves which were a part of the LH_2 transfer system were sealed and explosion-proofed, and all electrical connections of any kind to the dewar or its associated equipment were potted in silicone rubber. Since a static charge sufficient to cause an ignition spark may be built up by the passage of gaseous or liquid hydrogen through a transfer line, all lines and, indeed, everything in the vicinity of the LH_2 experiment, were connected to a good common ground and checked to ensure that their resistance to ground did not exceed one-fifth of an ohm. Even the floor was covered with metal in the vicinity of the dewar to conduct away static charges and to quickly vaporize liquid

air which could drip from the vent lines.

The third main area of fire and hazardous condition prevention consisted of providing good ventilation to remove any spilled or leaked hydrogen quickly. After making the ventilation modifications mentioned in Section 2.2, a curtain made of a conducting plastic film, called Velostat, was hung from the ceiling of the experimental room to completely enclose the dewar and valve package as shown in Figs. 8, 22, and 23. Tests of the air flow patterns in the experimental room required us to turn off an exhaust blower in the accelerator cell, after which the air flow was observed to be strongly into the experimental room at all cracks in the walls. With the intake duct directed into the curtained area, a complete change of air occurred in this area approximately once every thirty seconds.

A final safety precaution was the practice of sealing off the experimental room when LH_2 was present in the dewar, and severely limiting access to any area containing LH_2 experimental equipment or transfer lines at any time hydrogen was present on the site. Operating personnel were provided with antistatic clothes and "no smoking" signs were posted everywhere. Every crew member was made familiar with the complete system and the procedures to be followed in case of emergency.

3.5 FIRE CONTROL

Possible hydrogen fires at the supply trailer, the valve package, experimental dewar, or the outlets of the vent and dump stacks were

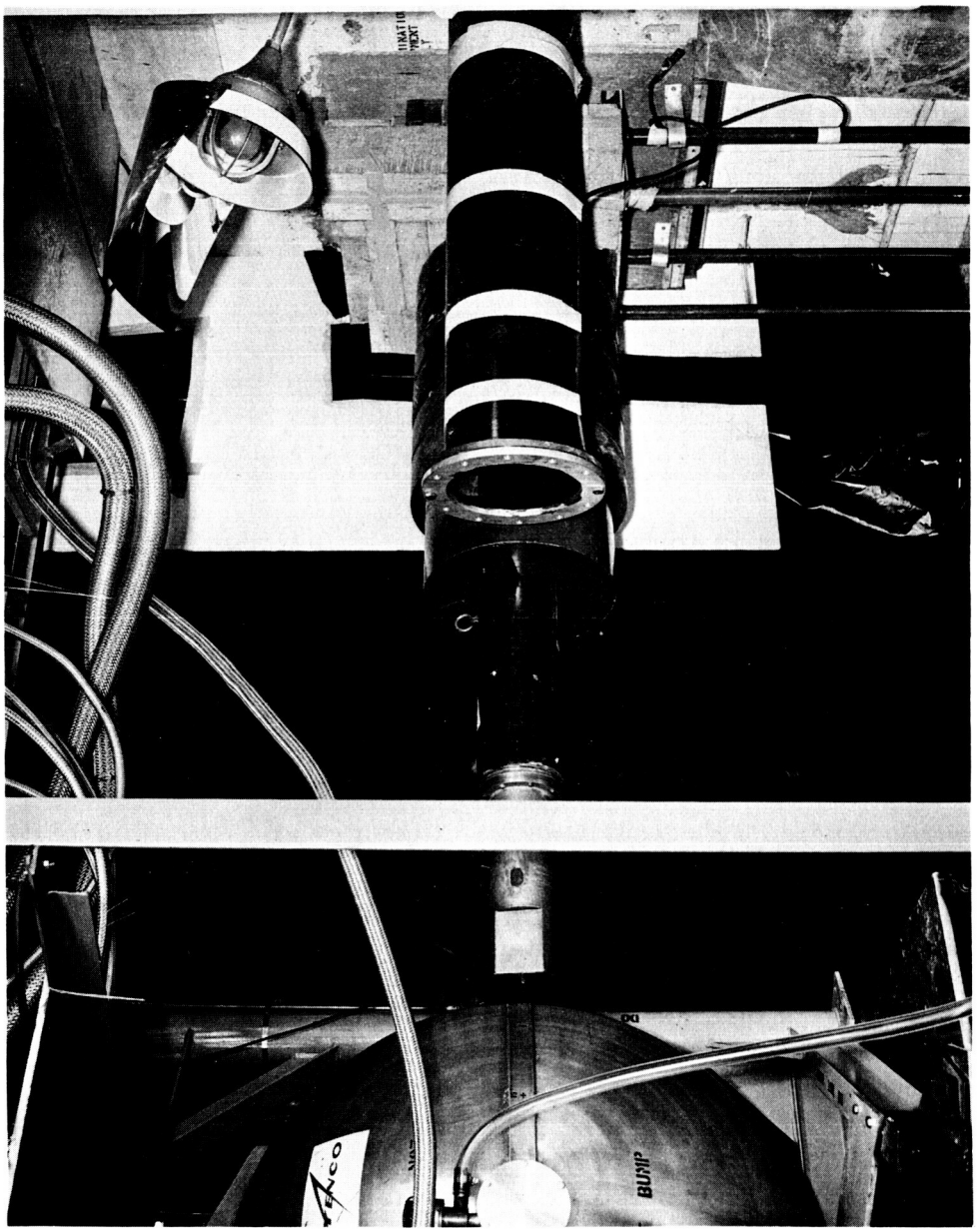

Fig. 22 -- LH_2 dewar velostat curtain and collimators

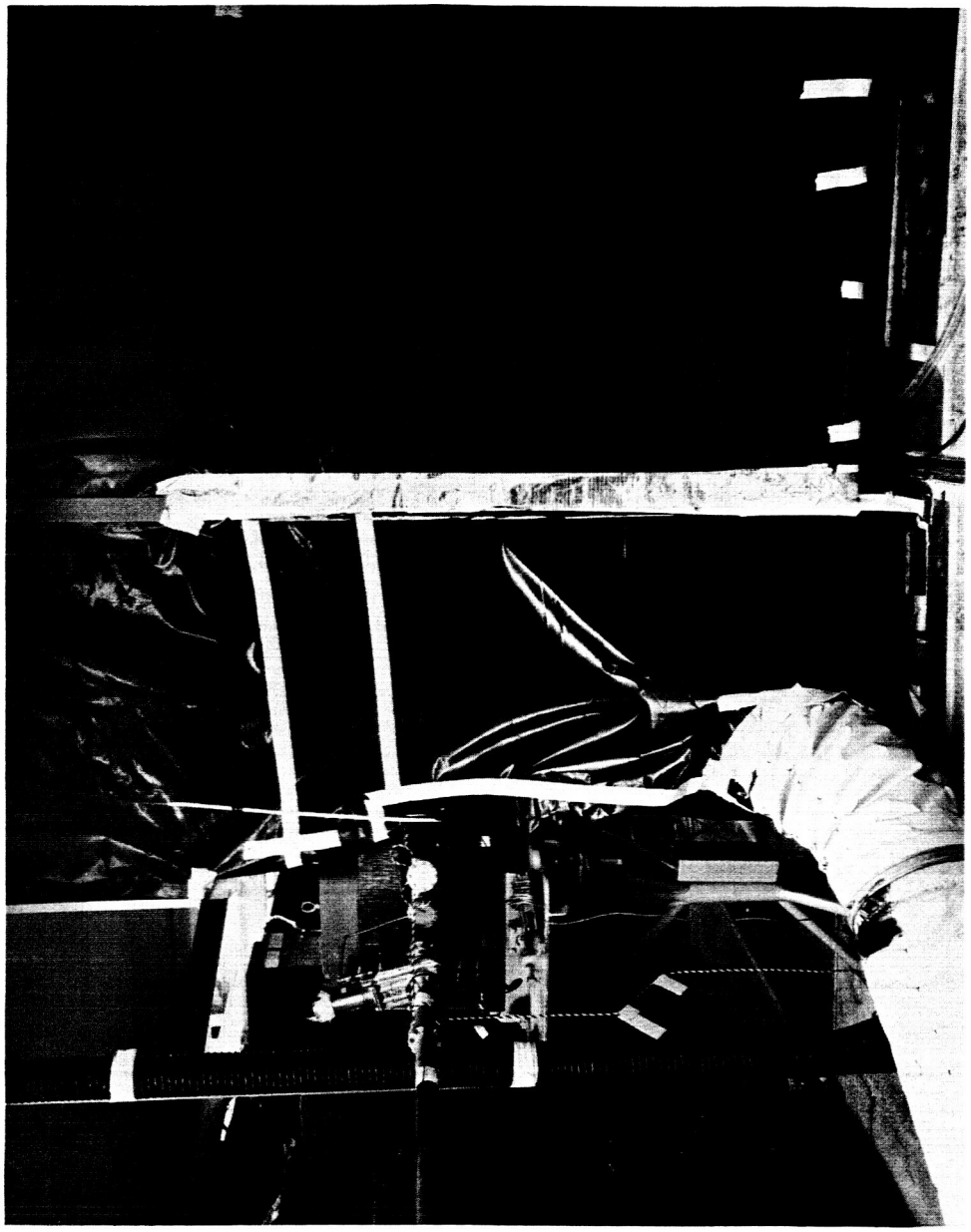

Fig. 23 -- Velostat curtain and ventilation ducts

detectable by the console operator by means of the neutron source observation television monitor, the dewar observation television monitor, or any of twelve iron-constantan and eight copper-constantan thermocouples. The console operator could have put out a fire at the dewar and valve package area by opening the solenoid valves controlling a high pressure CO_2 system located at the tower above. An automatic building water sprinkler system in the experimental room could have also aided in fire control in this area; operation of this system would have set off an alarm bell to provide an additional fire warning. Fires in the rear areas and at the base of the tower could have been controlled by the rear area watchman with fire hoses from the CO_2 tank and from the General Atomic emergency water supply. Solenoid valves operated by switches at the console controlled the CO_2 flow for the hoses. A fire at the outlet of either the vent or dump stack could have been controlled by the console operator by using a high flow rate helium purge system, incorporated in the dewar piping system, to blow out the fire and sweep the lines clear of hydrogen gas. For further fire control details refer to the emergency procedures in Appendix C.

3.6 LIQUID HYDROGEN FACILITY OPERATION

The dewar was filled as follows: liquid hydrogen flowed into the first chamber through the 3/4 inch diameter fill/dump line until the liquid level was at the level of the 1/2 inch diameter transfer tube connecting chamber one with chamber two; the LH_2 then flowed over into chamber two and filled chamber two to the level of the chamber-two-to chamber-three transfer tube. The same process was followed in the succeeding chambers until chamber six was reached. Since chamber six is a pressure equalizing chamber to allow the first hydrogen layer (in chamber five) to be a flat surface without requiring extremely thick baffle walls for bending resistance, chamber six is not filled with liquid (except at the start of an experiment it is partially filled to help cool down the metal and insulation in that end of the dewar). Flash gas resulting from the boiloff of the cold liquid on the warm dewar surfaces is routed out through the vent line. Each chamber had an individual vent line and vent valve, so close control of chamber pressure was possible. Initial cooldown was aided by passing as much cold boiloff gas as possible through unfilled chambers rather than directly out the vent stack. During the filling procedure, liquid level in the various chambers was monitored by lights on the control console activated by the carbon resistor liquid level indicators. When it was desired to change the hydrogen layer thickness between the inner window of the probe tube and the fast neutron source, helium gas was used to pressurize the empty

end of the dewar and force the LH_2 back through the transfer tubes from chamber to chamber. Excess liquid could then be dumped from chamber one, either through the dump line to the atmosphere outside the building or through the fill line to the supply dewar. Back transfer could be closely controlled, after some practice, and stopped when one chamber has just been emptied but the next chamber was still completely full. A complete operational procedure was written prior to the experiment to assist the operators of the LH_2 system in operation and control, and has been included in Appendix C.

Boiloff rates during operating conditions were carefully observed and indicated that the cryogenic design and effectiveness of the insulation were very good. A tendency for the dewar insulation space vacuum to deteriorate with age was noted, and it was necessary to re-evacuate this space twice since the dewar arrived at General Atomic. The loss of vacuum was small--perhaps one to fifteen microns over a period of weeks--but the insulation properties and boiloff rate appeared to be highly dependent upon this vacuum. Possibly vibration and thermal cycling released entrapped gas molecules from within the ninety layers of superinsulation; whatever the cause, a bad vacuum appears to be intolerable in terms of heat leak and provisions should be made for continual evacuation of the insulation space in vessels of this type.

After several months of operation of the LH_2 experimental dewar and its associate piping systems, described in this section, a few flaws

in the design were noted. While none of these flaws detracted from the experimental usefulness or adherence to the physics requirements set forth in the design parameters section, they did in most cases contribute to increasing the difficulty of operation of the system. Our major complaint was the insufficient number of locations of liquid level indication in the various chambers, especially in chamber six. The proximity of the upper and lower level indicators to the tops and bottoms of the chambers meant that only a very small volume in comparison to the chamber volume was contained between, say, the lower level indicator and the bottom of the chamber. Additional level indicators would help indicate the rate of transfer of fluid during fill and back-transfer operations and help ease precise level control. While transfer rates for LH_2 in the dewar are relatively high with only very moderate pressures being required, even for dumping out the fifty foot vertical dump line, the transfer rates for LN_2 are so low and the pressures involved in transferring LN_2 are so high that an increased knowledge of the conditions in the dewar would be an invaluable aid to the operator.

Contrary to normal cryogenic design practice, an extremely small ullage space was designed into the dewar. A few unexpected problems arose which are directly attributed to this fact, such as the entrainment of liquid droplets in the gas flowing out the vent lines during high gas flow conditions with the chambers nearly full, and a certain degree of difficulty in completely filling the chambers without running liquid up

into the vent lines. Entrainment of droplets of liquid in the vent gas or the running of liquid into the vent lines could cause a massive condensation of liquid air upon the unjacketed and uninsulated vent lines, leading to a possible hazardous condition. Either increased ullage space at the top of the dewar or baffling of the entrances to the vent lines might have helped this situation, while vacuum jacketing of the vent lines would probably have eliminated the liquid air formation altogether.

A few areas in the mechanical design of the experimental dewar either should be or must be improved upon in order to improve performance and ease of operation. Of major importance would be a more rigid dewar hanging system, with the single overhung support yoke being replaced by a double columnar support with the dewar hung from a crossbeam. While the large Timken tapered roller bearing which supports the dewar and provides for its rotation is adequate for the loads involved, the inner race tends to cock in the outer race and change alignment radically under the application of a heavy asymmetrical load such as is caused by loading LN_2 in chamber one only. Some modification of the bearing locating system will be required to provide adequate stability. A possible solution might be the addition of a second rotational guide at the bottom of the dewar, thus providing a trunion with a vertical centerline. Rotation of the dewar, given correct original alignment, has little tendency to disturb the alignment of the probe tube, so a motor-operated remotely controlled dewar rotation and angle indication device

would contribute greatly to increased experimental versatility and usefulness. At present, our safety procedures call for the dewar to be empty and purged well before rotation to a new angle of measurement. Although this does not create too much of a hardship on an experiment involving low counting rates in the detector, where fourteen to eighteen hours of experimental time are required at each angular position, a great deal of time would be wasted on any relatively high counting rate experiment merely in filling, emptying, stabilizing, and cooldown procedures.

Although these problems and numerous others were encountered during the initial checkout and operational phases of the experiment, many of the new concepts and ideas which were tried in the dewar proved to be of real value. Evacuation of the probe tube to shorten it for rotation--with pressurization to seat the tube on the window and eliminate any LH_2 layer between the probe and window--proved to be extremely useful. Exact location of the probe tube could be maintained because of the elimination of any torque producing drag forces. In practice, the integral layer thickness variations of the liquid hydrogen were both fast and accurate, given an experienced operator, with definite count rate indications of the thickness variations being provided by the fast neutron detector. The excellent over-all performance of the insulation and the stability of liquid levels and conditions in a cooled down dewar have been mentioned earlier, as well as the ease of maintenance of correct alignment of the dewar with the flight path.

IV. WATER MOCKUP FACILITY

4.1 WATER MOCKUP EXPERIMENT DESIGN CONSIDERATIONS

A water tank was designed to serve as a similar-medium mockup for the liquid hydrogen dewar and to verify the experimental techniques to be used for the liquid hydrogen spectral measurements. An attempt was made to apply many of the original LH_2 dewar design parameters to the water tank to provide an experiment similar in as many ways as possible to the LH_2 experiment. Because of the differences in hydrogen atom density between water and LH_2, the critical dimensions of the LH_2 dewar were reduced by the ratio of the hydrogen atom densities in liquid hydrogen to that in water which was a factor of 1:1.65. The resulting water tank was physically very similar to the LH_2 dewar except that many construction details were simplified for the sake of economy.

Our primary reason for constructing the water mockup was to provide a quick and simple experimental basis for obtaining a better feeling for any problems which might be encountered during the actual liquid hydrogen experiments. By carefully observing collimation effects, background ratios and other experimental factors, we felt that we would be able to produce much better results in the final liquid hydrogen experiments.

Fig. 24 illustrates the water tank design used in the mockup experiment; the physical similarity to the inner tank of the LH_2

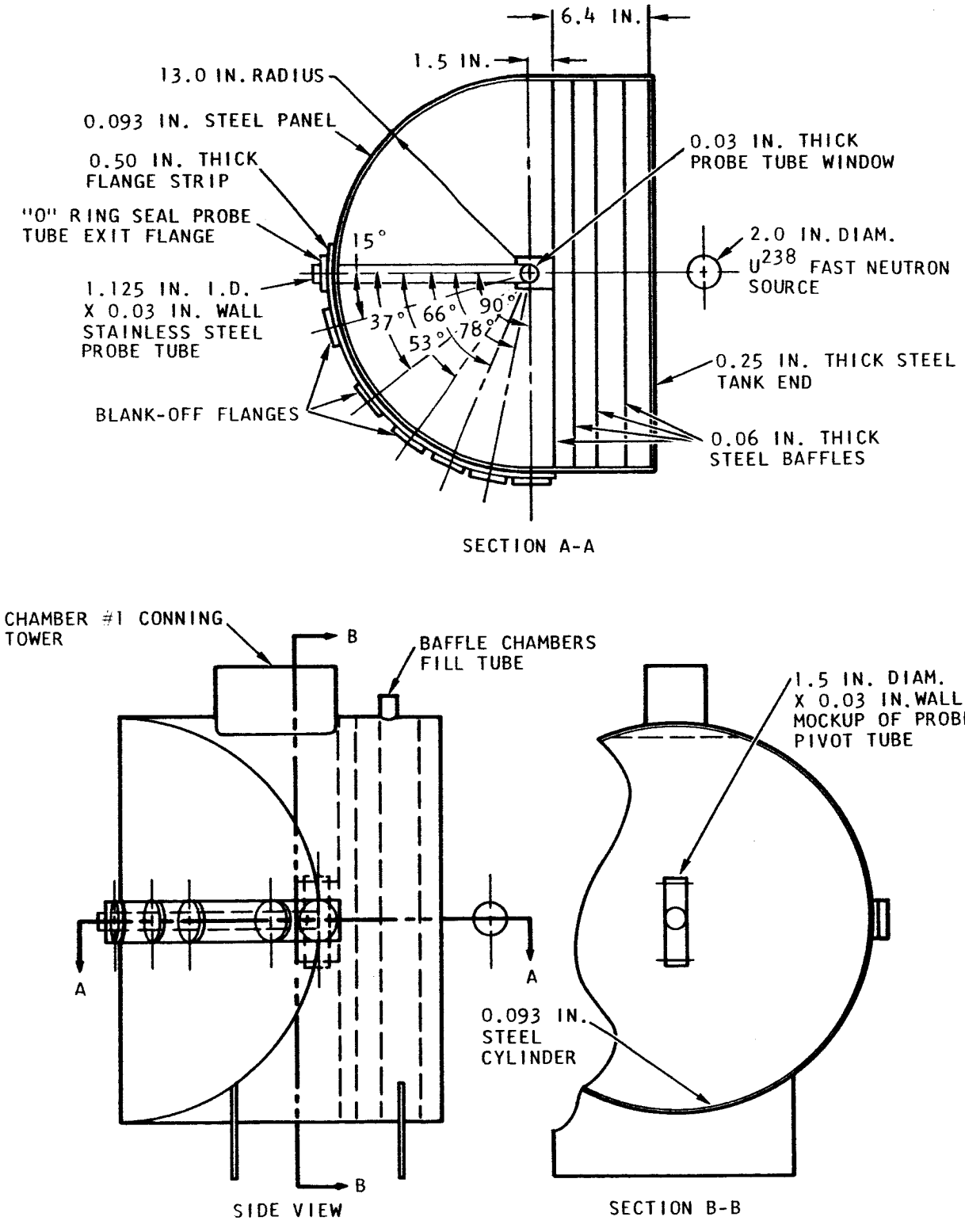

Fig. 24 -- Details of water mockup of liquid hydrogen dewar

experimental dewar is obvious. However, the detector end of the tank is made from two rolled pieces of flat steel plate rather than a hemispherical head. The source end has steel baffles with a thicker steel end plate to approximate the amount of steel in the LH_2 dewar. Probe tube dimensions were similar to allow the LH_2 experimental collimation system to be used.

No inexpensive method could be found to provide the infinite probe tube angular variation between 0^o and 90^o. Therefore, particular angles of interest were selected by the method indicated in Appendix A. Seven angles were chosen, and flanges were welded onto the outside of the dewar at these locations. The probe tube could be inserted through one of the flanges and seated in a mockup of the probe pivot tube in the center of the dewar; the remaining flanged holes would then be blanked off. We made no provision for rotation since the tank was light enough to be moved easily.

4.2 OPERATIONAL RESULTS OF THE WATER MOCKUP EXPERIMENTS

One result of the water mockup experiments stood out strongly as the problem most urgently needing a solution: at large angles and penetrations, the detector counting rates and signal-to-background ratios were low.

There were several methods to attack this problem:

1. Increase Linac power--however, this required that the fast neutron source's heat-removal capacity be increased also.

2. Increase the effectiveness of the collimating shielding, so that all neutrons except those that are scattered down the probe tube of the assembly are stopped or scattered out.
3. Decrease the ambient background of the detector.
4. Increase the efficiency of the detector.

At the time of the water mockup experiments, work on a power output upgrading program had already been started by the Linac operating crew. As indicated in Section 2.1, the available delivered power capability had been raised by a factor of ~1.6 by the time the LH_2 experiments started. However, considerable effort was necessary to perfect a fast neutron source capable of absorbing the new-found power with reliability. Air flow over the surface is obviously not the most ideal method of cooling a solid uranium ball, and a great deal more effort will be required to provide a really reliable high power source. The present source cannot safely handle the power the Linac will deliver, and future power increases will therefore be unusable. A more complete discussion of the source design may be found in Section 5.1.

The full collimation system was not completed at the time the water mockup experiments were run, but the collimator diameters were the sizes that were expected to be used with the LH_2 experiments. Shielding was expected to be somewhat inferior since many of the shielding portions of the collimation system had not been finished. It proved to be fortunate

that we had not completed the system, because we were able to revise the unfinished portions to provide probably twice as much shielding and much more restrictive collimation than was originally planned.

Originally, a 2 in. liquid scintillator was to be used as the fast neutron detector. However, due to the low counting rates, a 5 in. liquid scintillator was developed and used. This larger detector increased the efficiency by an order of magnitude.

Another problem area proved to be accurate monitoring of the fast neutron source strength from run-to-run and from day-to-day. Many difficulties arose during the water mockup experiment because of monitor sensitivity to scattered radiation pattern changes which were due to changes in material placement in the experimental room and albedo from the water tank. Monitoring by the activation method requires that the material to be activated be precisely located in exactly the same relation to the source at all times, while an electronic type monitor, such as a fission counter, must be carefully biased and shielded so that its results will be repeatable. A discussion of our final monitoring techniques will be found in section 5.4.

Accelerator tuning and steering operations for the water mockup experiments were so difficult and ambiguous that we were forced to attempt to develop standard operational techniques to try to save time. This program included additional Linac design upgrading with the object of providing a tighter electron energy spectrum and a complete analysis

of the interactions of the various steering and bending magnets. A visual final beam spot tuning technique was developed with some changes being made in the fast neutron source to ease beam spot locating. Our closed circuit television system was used to observe the effect of the electrons in the Linac beam upon a phosphorescent screen placed on the surface of the source, thus allowing the Linac operator to position the beam and control the size and shape of the beam spot with his focusing magnets to provide the heat distribution and isotropy production required.

Because of the hazardous nature of the experiment, a decision was made to design all parts of the experiment so that no room entrances would be required from the time LH_2 flowed into the dewar until the dewar was emptied and purged and the experiment shut down. It became obvious, from the water experiments, that considerable effort would have to be made, especially in monitoring, to evolve new remote monitoring techniques.

V. EXPERIMENTAL CONSIDERATIONS

5.1 ISOTROPIC FAST NEUTRON SOURCE DESIGN

One of the more important experimental considerations was the development of an isotropic fast neutron source to be used with the liquid hydrogen experiment. Sources used previously on fast and thermal neutron experiments at Linac had been designed only to provide neutrons without overheating and no effort had been made by the Linac scientific staff to develop an isotropic fast neutron source. Therefore, a study of the required characteristics of an isotropic fast neutron source was made with the result that the following parameters were set forth.

a. The source must have a high electron-to-neutron conversion efficiency since it was expected that source attenuation in the liquid hydrogen, especially at large scattering angles and deep penetrations, would be quite large. Since only a limited amount of Linac beam power is available at a pulse width of 20 nanoseconds (311 watts), the best and most efficient use possible must be made of this power, in terms of neutron production, in order to achieve a meaningful neutron flux intensity at the detector which will be located fifty meters from the liquid hydrogen assembly.

b. To further guarantee that maximum use can be made of the Linac's output, the fast neutron source must have sufficiently great heat dissipation properties to absorb all the available

Linac power without melting and contaminating the experimental area.

c. The source must have a high degree of over-all isotropy so that changes in the view of the source presented to the hydrogen in the experimental dewar do not appreciably change the intensity or energy spectrum of the neutrons bombarding the hydrogen.

An isotropic neutron target is required for two reasons: (1) in order to measure angular spectra it is necessary to rotate the liquid hydrogen dewar while the probe tube remains fixed. This means that the flat front surface of liquid hydrogen upon which the fast neutrons from the source impinge also rotates. The source is permanently mounted to the dewar in order to maintain a constant geometry. But in order for the electron beam to strike the same surface of the source for each angular measurement, the source must rotate about its axis. In doing so, the surface which is presented to the liquid hydrogen in the experimental dewar changes (see Fig. 25); and (2) even if the same surface of the source was presented to the first surface of liquid hydrogen for each angular spectrum measurement, this does not imply that each point on the surface of the source emits the same energy spectrum or gives the same intensity.

d. Because of the anticipated low detector counting rates and hence long experimental running times, and because of the complicated nature and difficulty of the liquid hydrogen experiments, the source must be designed to operate for long periods of irradiation time without fear of failure. Although the beam power to be dissipated in this source is somewhat less than that used on other sources at the Linac, the special requirements for this experiment place certain limitations on the type of cooling available. The source material to be used and the allowable source geometry made this one of our most difficult problems.

e. The size and mass of the source must be sufficient to remove all but a very small quantity ($\sim$10 watts) of the gamma power developed in the source. Gamma rays in the liquid hydrogen can conceivably produce violent boiling with a resultant density variation or void volume, and might even cause a potentially hazardous condition in the liquid hydrogen dewar.

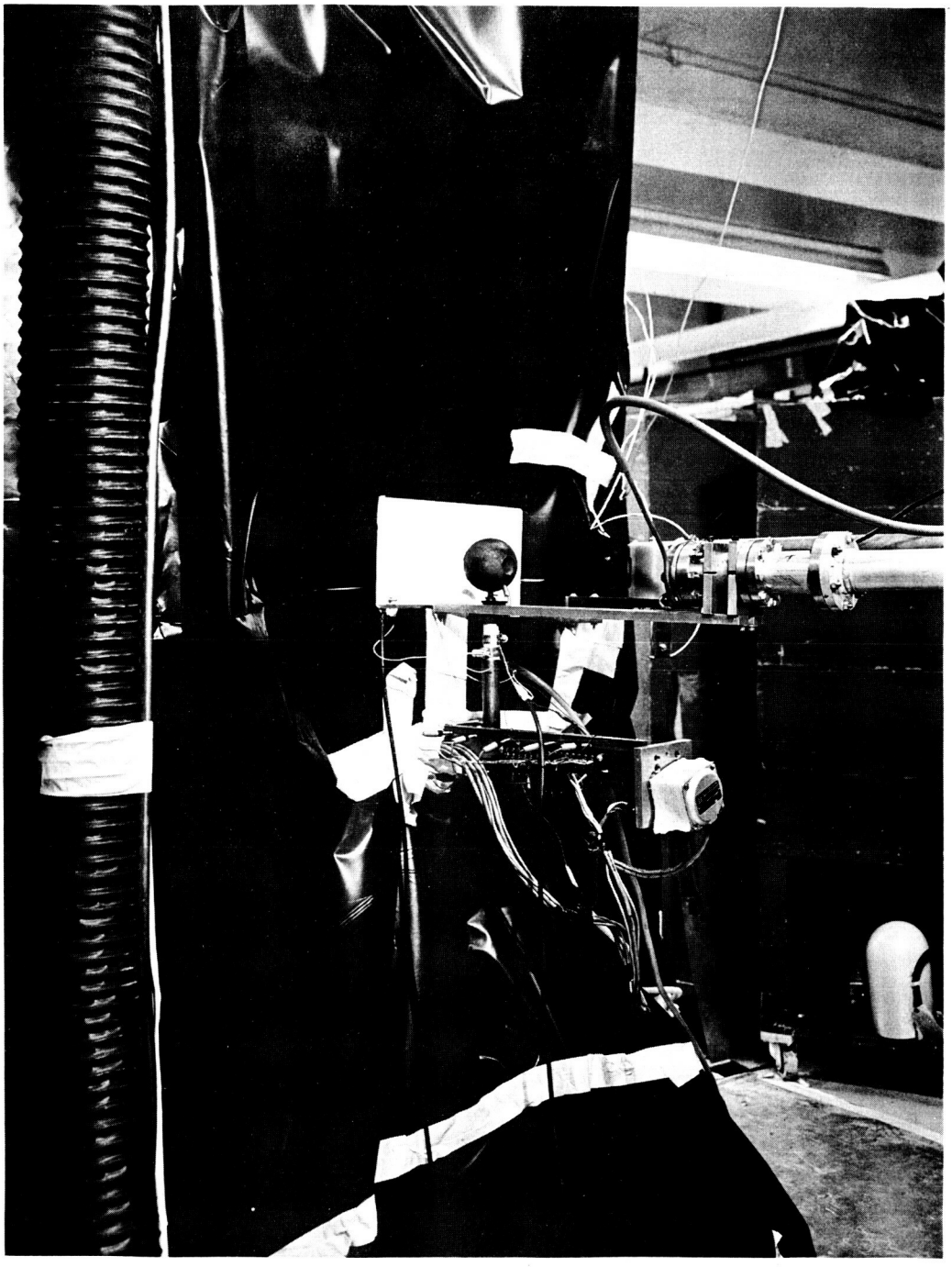

Fig. 25 -- Geometry for the 3-inch diameter uranium source

A discussion of the thinking and experimentation which went into satisfying these design parameters is included in the following two sections.

5.1.1 Isotropy Studies

Theoretically, an isotropic fast neutron source may be made by generating neutrons at the center of a homogeneous sphere. Since the center of neutron production and the center of the sphere are coincident, all neutrons will undergo the same average number of collisions with the material in the sphere and a neutron energy spectrum measured at one point on the surface will be the same as the spectrum at any other point. In addition, the sphere must be large enough in diameter and of a sufficiently efficient gamma absorbing material to attenuate the bremsstrahlung which might cause excessive heat input to the liquid hydrogen.

Experimentally, a cylindrical hole must be made in the source to allow the Linac electron beam to reach the inside of the source where it may be used to generate the neutrons. In order to keep the center of neutron production as small as possible to maintain a nearly point source of neutrons in relation to the over-all physical size of the source, these electrons must be stopped in a small distance of a high density material which also has a high efficiency (high atomic number) for conversion from electrons to gamma (bremsstrahlung) rays; the gamma rays then interact with the source material nuclei and produce neutrons by a (γ, n) reaction.

Here again, conversion efficiency from gamma rays to neutrons is important, so a high density, high atomic number, material must be used.

Our initial attempt at the production of an isotropic fast neutron source is shown in Fig. 26; here, the electron beam enters through a 1-1/2 inch diameter cylindrical hole, passes through a 0.010 inch thick copper window and 0.125 inch of cooling water, and strikes a hemispherical fansteel (89% tungsten, 7% nickel, 4% copper) cup which is 0.5 inch thick. The electrons are stopped in about one centimeter of fansteel; the resulting gamma rays produce the neutrons in about four radiation lengths (0.42 in.). Therefore, the fansteel cup acts both as the gamma and neutron converter. After four radiation lengths, the quality of the bremsstrahlung beam is such that there are very few gammas with energy near the giant resonance cross section for (γ, n) reactions in tungsten, but a large low energy gamma component remains and must be removed by the rest of the source to keep the energy input to the liquid hydrogen to a minimum. A 5-inch diameter lead sphere was therefore cast around the fansteel converter with additional cooling water lines cast in place. Fansteel was used in the converter in preference to lead because of its higher gamma and neutron conversion efficiency, superior thermal conduction, and higher melting temperature. The fansteel cup was positioned within the lead sphere so that our estimate of the center of neutron production was at the center of the sphere.

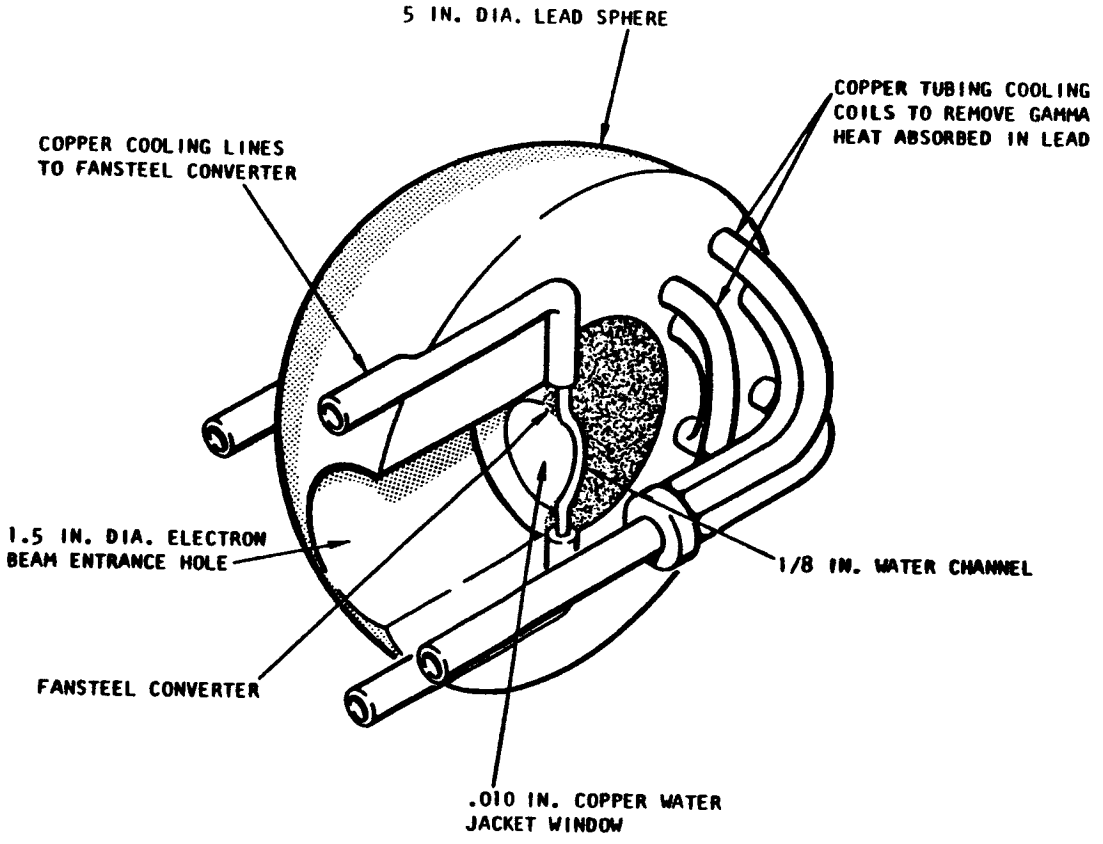

Fig. 26 -- Details of experimental isotropic neutron source assembly No. 1

A measurement of the isotropy of this design was made with a series of threshold detectors with a 3 MeV neutron threshold. The sulfur disks were placed at 30^{o} intervals around the periphery of a horizontal diametrical plane of the source, with the results shown in Fig. 27; here, the fast neutron flux is not isotropic but is asymmetrical and peaks in the direction of the electron beam. It was concluded from this simple approach that a more fundamental and detailed approach to the electron-to-neutron conversion process would have to be undertaken.

As a first step in understanding the electron-to-neutron conversion process in the fansteel converter, a series of measurements of the neutron distribution for only the converter, Source 2, was made using both large and small electron beam spots, with the results shown in Fig. 28. Obviously the neutron distribution is not isotropic but very much peaked in the direction of the electron travel, with a small beam spot tending to increase the asymmetry. Our explanation of this asymmetry is that a neutron traveling in a direction parallel to the direction of the electron beam will pass through less material than one traveling perpendicular to the electron beam; therefore the actual center of neutron production must differ from the "guessed" center of production. A large beam spot tends to smear out this effect because it broadens the neutron production region.

After analysis of these preliminary experiments, some conclusions about isotropic source design could be drawn: first, neutron distribution

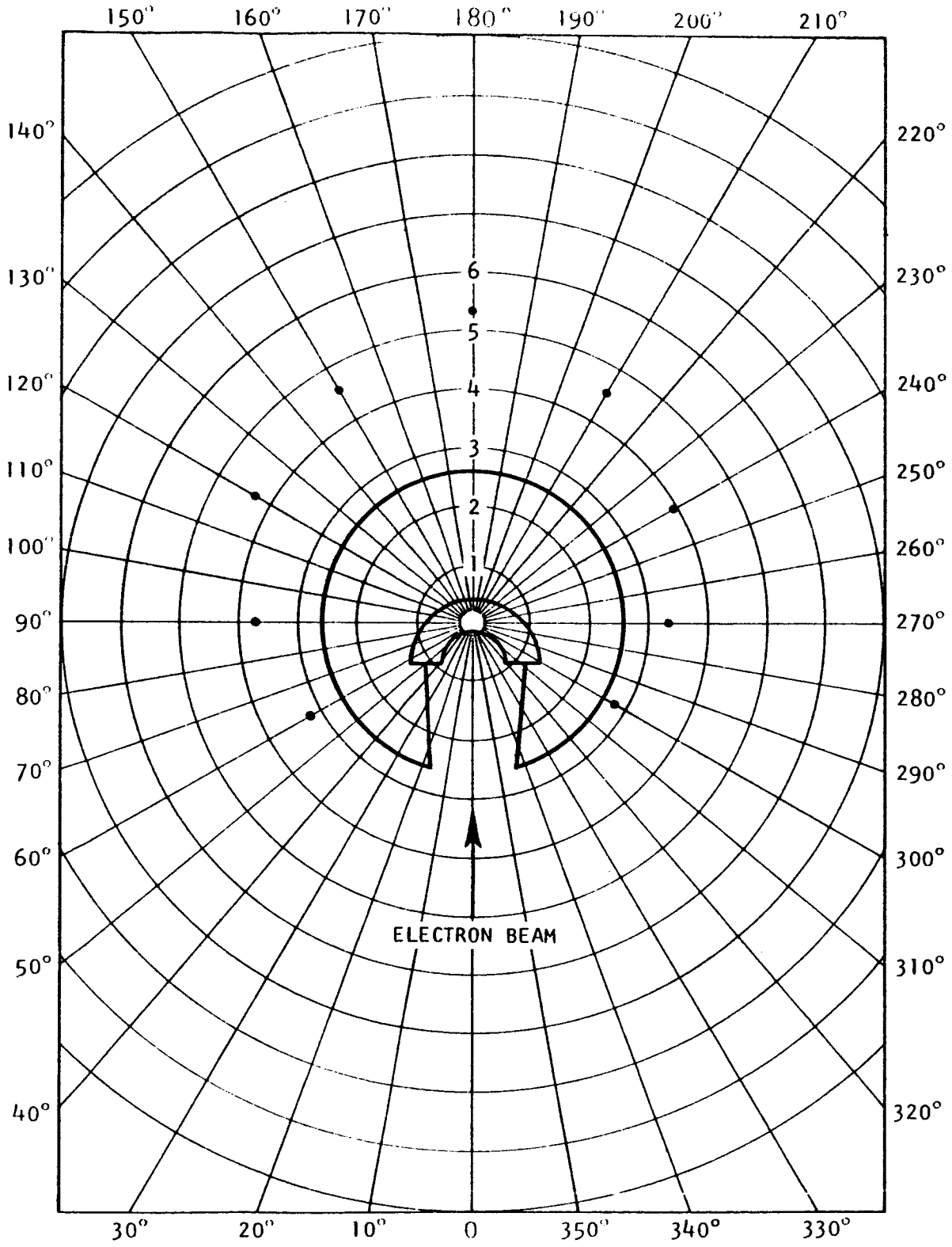

Fig. 27 -- Sulfur activation data for source No. 1

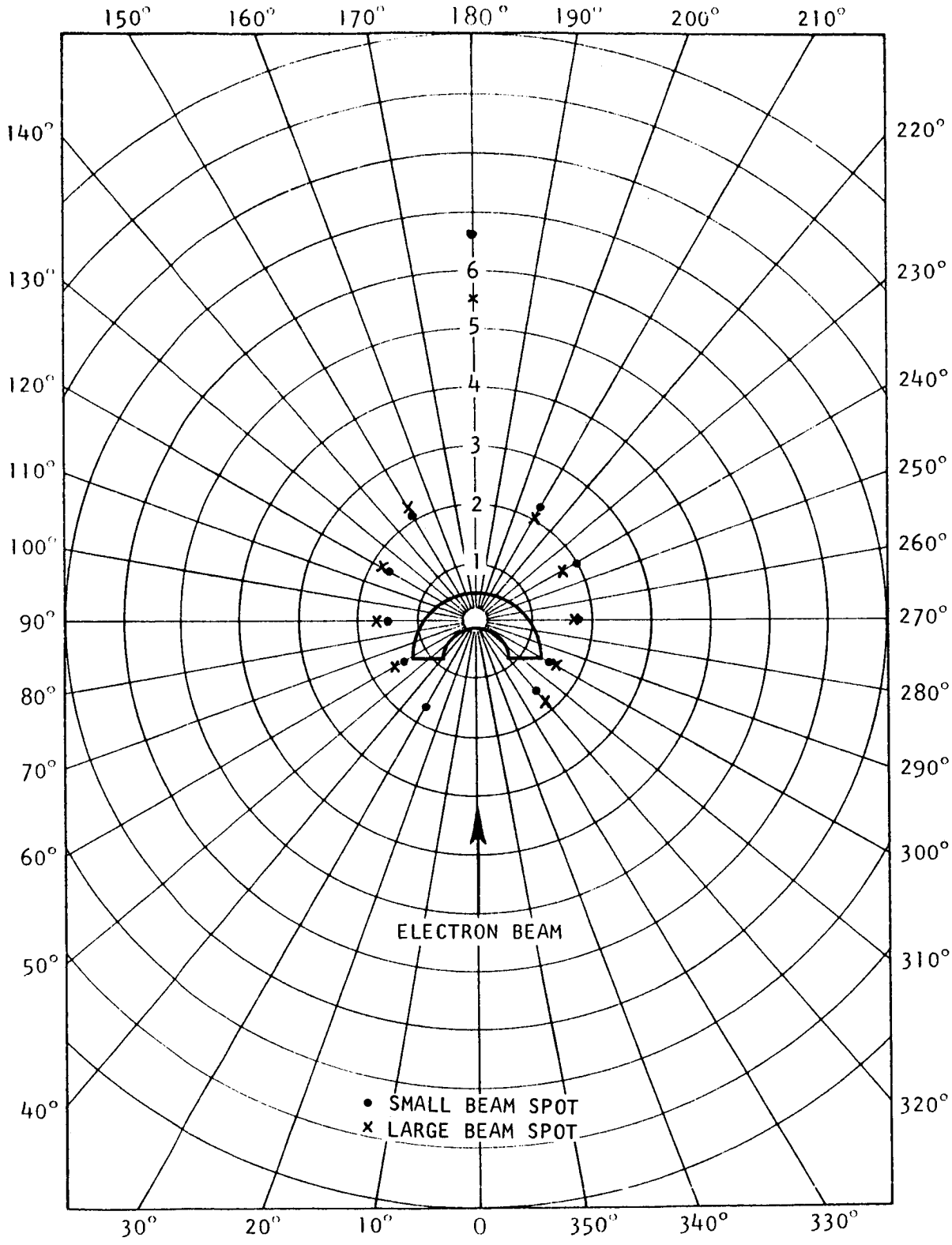

Fig. 28 -- Sulfur activation data for source No. 2

is fairly sensitive to a small error in the location of the center of neutron production with respect to the geometric center of the source. Second, an inhomogeneous sphere --such as our first lead and fansteel sphere--may tend to cause asymmetry because the type and density of the material through which a neutron may travel is dependent upon the direction of the neutron. Even though neutron distribution could possibly be isotropic with this type of design, neutron energy isotropy could not be guaranteed since the energy spectrum will be dependent upon the atomic number and path length of the material the neutrons travel through. Third, water cooling of the source will probably be unnecessary if the source is carefully designed to use air cooling. Water passages, and the water in them, could introduce a problem similar to that of the differing densities of lead and fansteel. Fourth, our original assumption that the (γ, n) process is isotropic could easily be mistaken.

Bearing these conclusions in mind, a second experiment was performed using a 1-inch diameter spherical fansteel source, source No. 3. The object of this measurement was to determine experimentally the centroid for neutron production in fansteel. This source, shown in Figs. 29, 30, and 31, together with the data from this experiment, has a 5/8-inch diameter cylindrical opening for electron beam entrance, with the bottom of the hole--the surface struck by the electrons--one radiation length or 0.14 inch before the geometrical center of the sphere. Again, we assumed that the centroid of neutron production was one

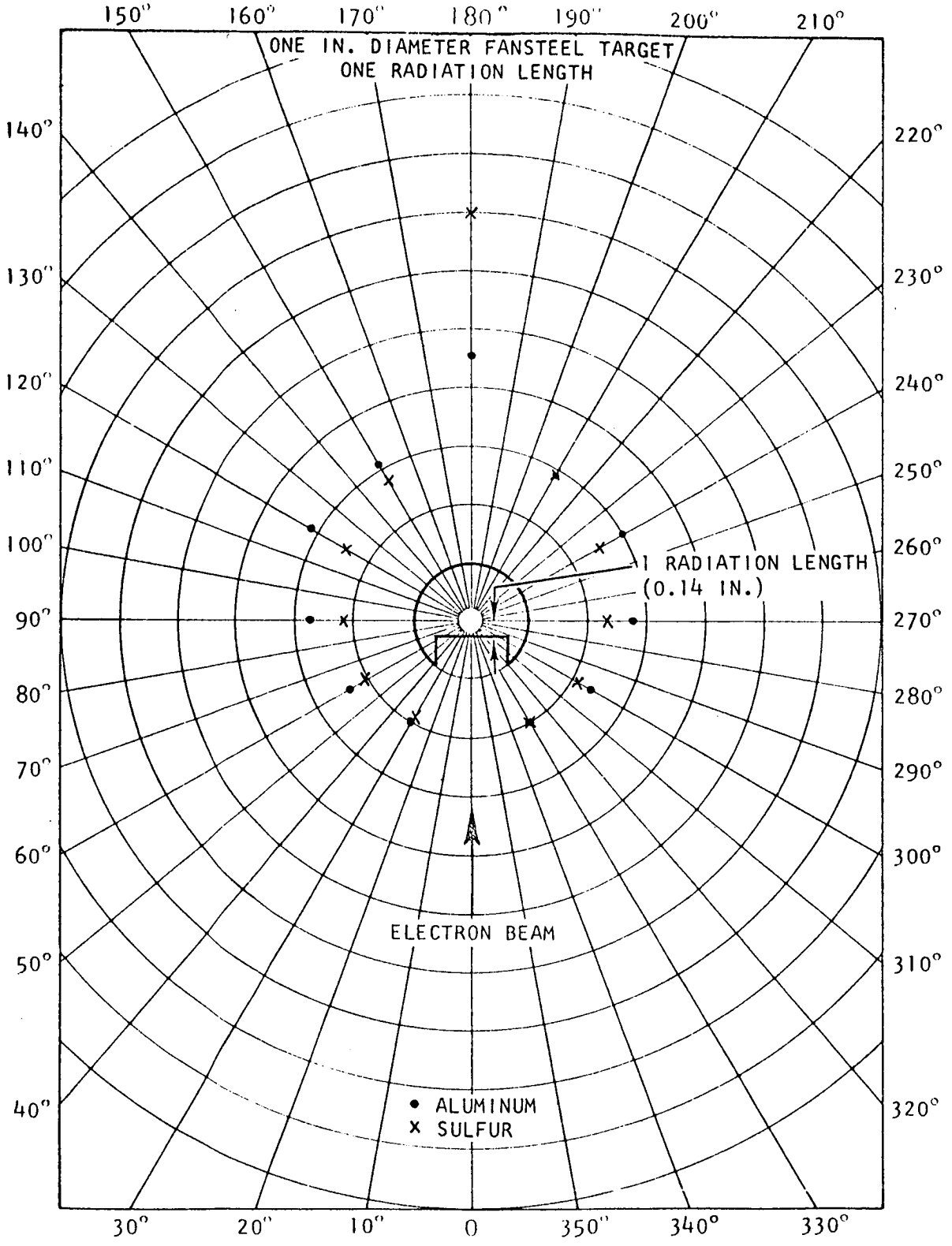

Fig. 29 -- Sulfur and aluminum activation data for source No. 3 with one radiation length

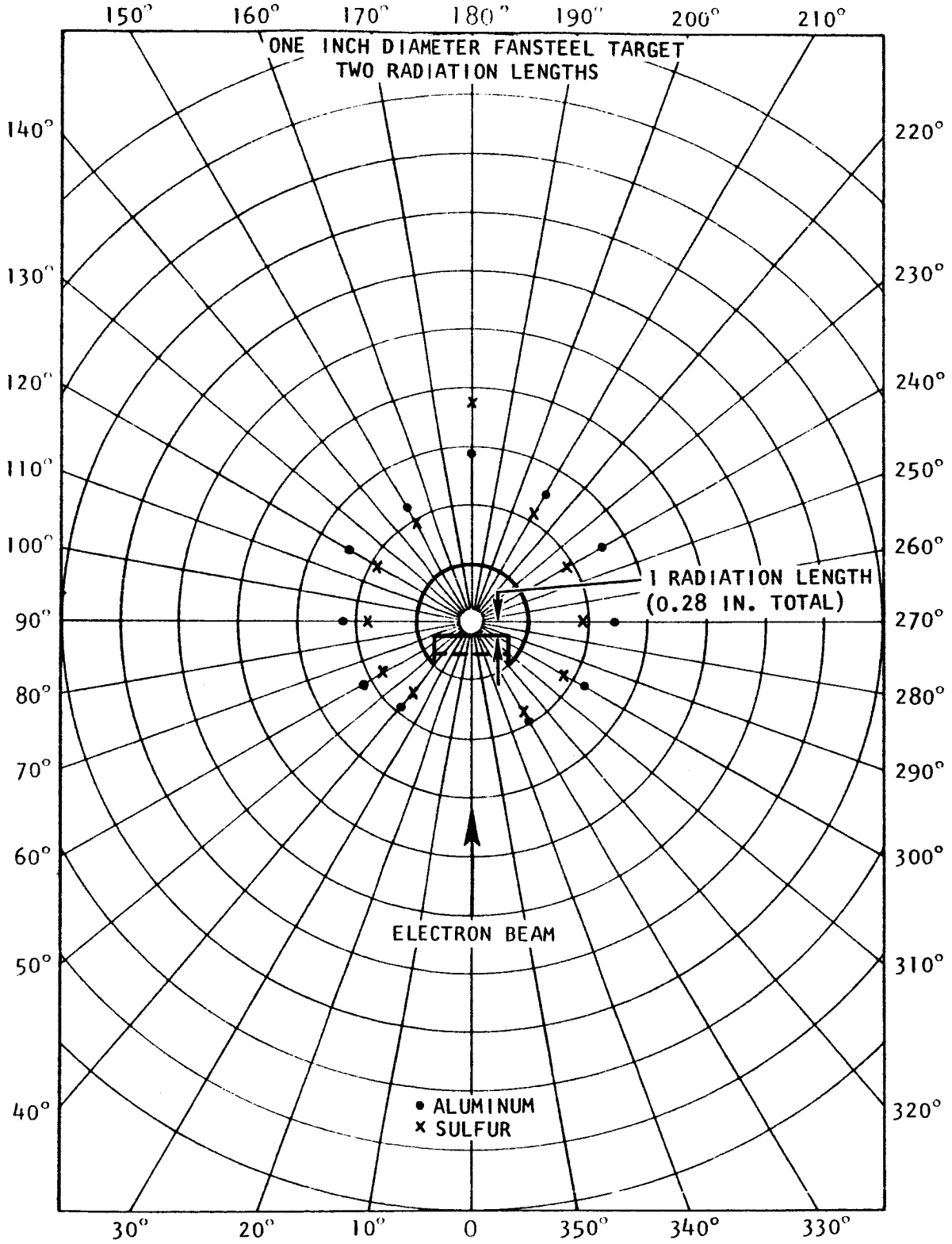

Fig. 30 -- Sulfur and aluminum activation data for source No. 3 with two radiation lengths

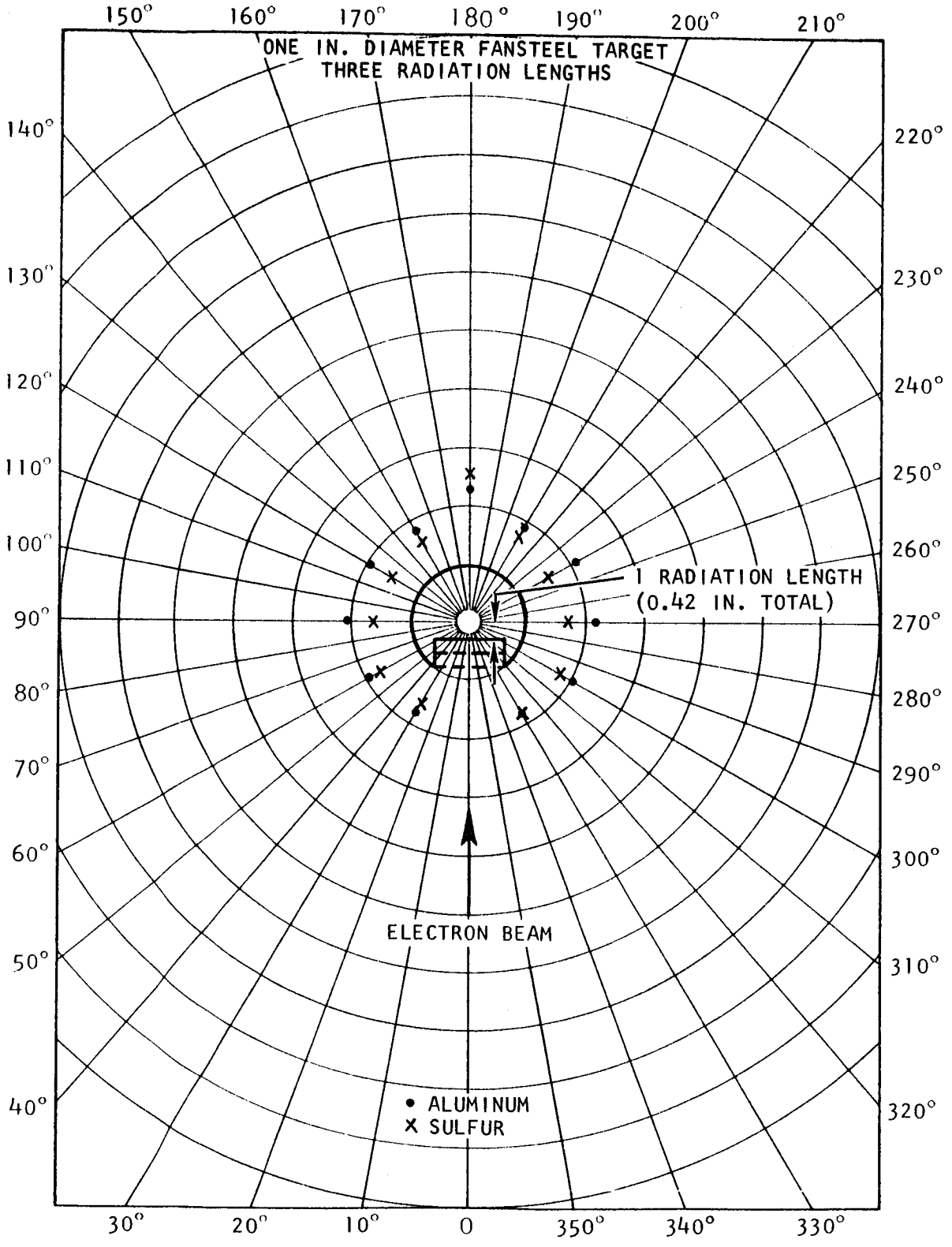

Fig. 31 -- Sulfur and aluminum activation data for source No. 3 with three radiation lengths

radiation length from the surface struck by the electrons and a neutron flux distribution was taken at 30^{o} intervals about the sphere. This time, both sulfur with a 3 MeV neutron activation threshold and aluminum, with a 7 MeV neutron activation threshold, were used to indicate the distribution; this allowed a somewhat better rough analysis of the energy isotropy of the source or spectral index. If one radiation length were truly the distance from the electron impingement surface to the centroid of neutron production, then the physical center and the center of neutron production would coincide and an isotropic neutron distribution could be expected, but as the data shows, this was certainly not the case.

A 5/8 inch diameter fansteel disk one radiation length thick was then inserted in the beam entrance hole in the source and the experiment repeated. Our new assumption was that the centroid of neutron production is two radiation lengths from the electron impingement surface, but again the resulting data does not support this assumption, with the distributions given by both the sulfur and aluminum showing a decided forward peaking with respect to the electron beam. An additional one-radiation-length fansteel disk was placed in the beam entrance hole making three-radiation lengths or 0.42 in. of fansteel, and the experiment was repeated again; this time except for the continued strong but narrow forward peak, the source appeared to be reasonably isotropic. While some anisotropy occurs at the back angles of 30^{o} and 330^{o}, the experiment

can be designed in a way the dewar never sees this side of the source so the anisotropy caused by the beam entrance hole may be discounted. An interesting fact pointed out by these experiments is that the sulfur detectors exhibited a greater degree of anisotropy in the forward direction than does the higher-threshold aluminum detectors.

In order to eliminate the ambiguity associated with threshold detectors, fast neutron energy distributions at 96^{o} and 162^{o} using pulsed source time-of-flight techniques were measured. Since the three-radiation length configuration showed the greatest degree of isotropy, this source was used for the measurements. These measurements were normalized by using sulfur monitors. The resulting neutron spectra are shown in Fig. 32 and can be used to show why the activation monitors showed a strong forward peak at 180^{o}; here, the ratio of these two spectra in the 3 to 7 MeV neutron range is about seven or eight to one, which would be seen only by the sulfur detectors. The ratio above 7 MeV, which would be seen by both detectors is only about four or five to one.

In an effort to smear out the forward peak seen with the one inch diameter spherical target, and to further establish that three radiation lengths gave the most isotropic neutron flux distribution, a three inch diameter spherical fansteel source, source No. 4, was constructed with three radiation lengths between the electron beam impingement surface and the geometrical center of the sphere and the beam entrance hole enlarged to one inch in diameter. Additional one radiation length thick

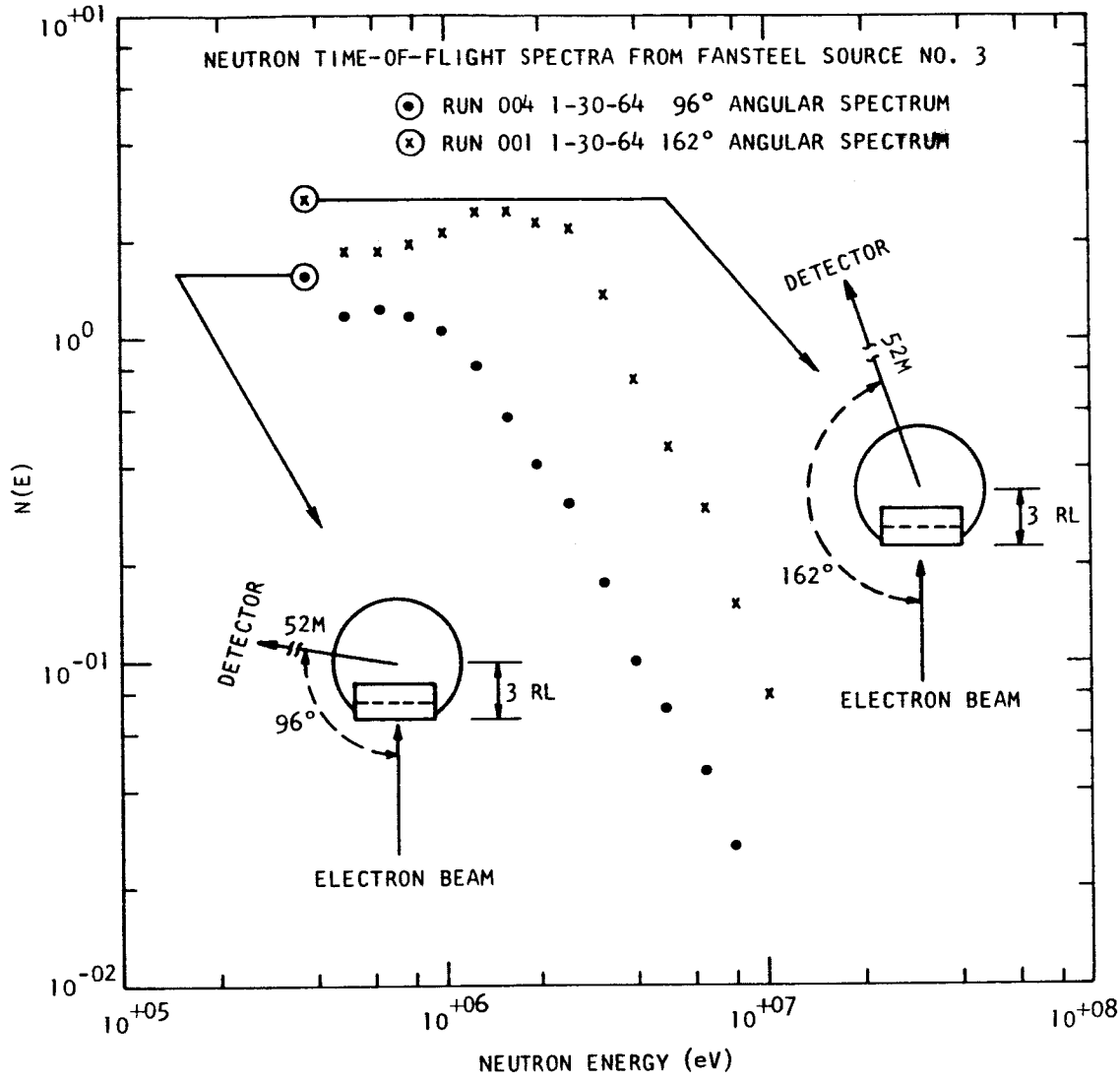

Fig. 32 -- Neutron time of flight spectra for source No. 3

disks were made so that four and five radiation length neutron flux distributions could be measured. Figures 33, 34, and 35 illustrate the results of these measurements, and demonstrate once again that three radiation lengths gives the most isotropic distribution. In Figs. 33 and 34, the sulfur and aluminum data have been normalized at 90^{o}. Only the aluminum threshold detector data is shown in Fig. 35. A forward peaking effect still may be seen in the sulfur detection data while none is present in the aluminum detector data.

For the 3 in. spherical fansteel source, fast neutron spectra at 103^{o} and 180^{o} were measured using time-of-flight techniques, with the results shown in Fig. 36. Now, the spectra may be seen to be much more isotropic than those seen with the one inch diameter spherical source. However, although the activation detectors indicated that the three inch diameter (three radiation lengths) spherical target was very nearly isotropic, the neutron spectra indicate otherwise; a definite enrichment in neutrons in the 2 to 6 MeV range of about thirty per cent is observed in the 180^{o} direction with respect to the 103^{o} direction. This accounts for the anisotropy seen by the sulfur detectors with their 3 MeV threshold and explains why the 7 MeV threshold aluminum detectors indicate an isotropic flux.

The two effects which produce neutrons in the fansteel target may be called direct and indirect. The direct process is caused by a gamma ray directly interacting with the tungsten nucleus and ejecting

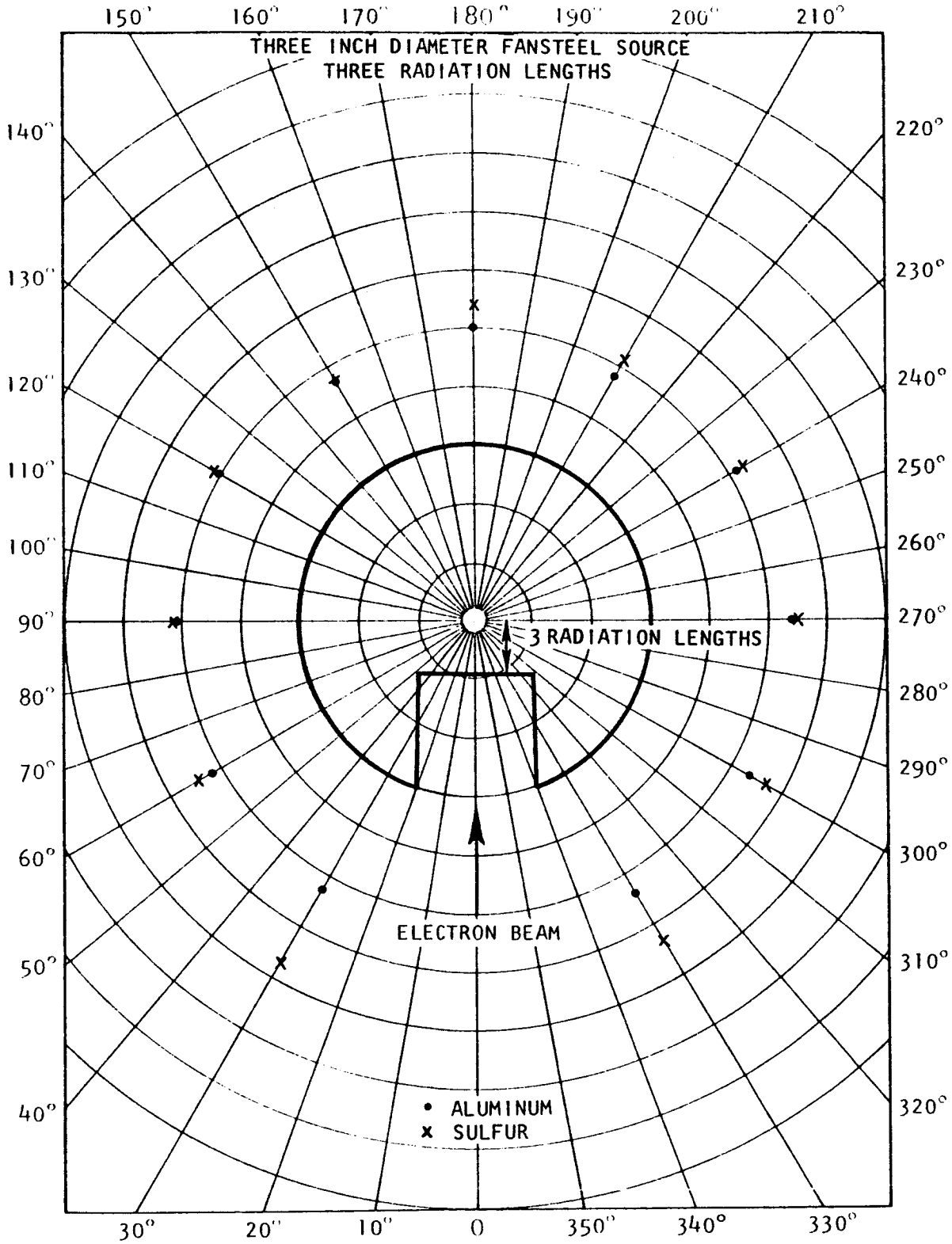

Fig. 33 -- Sulfur and aluminum activation data for source No. 4 with three radiation lengths

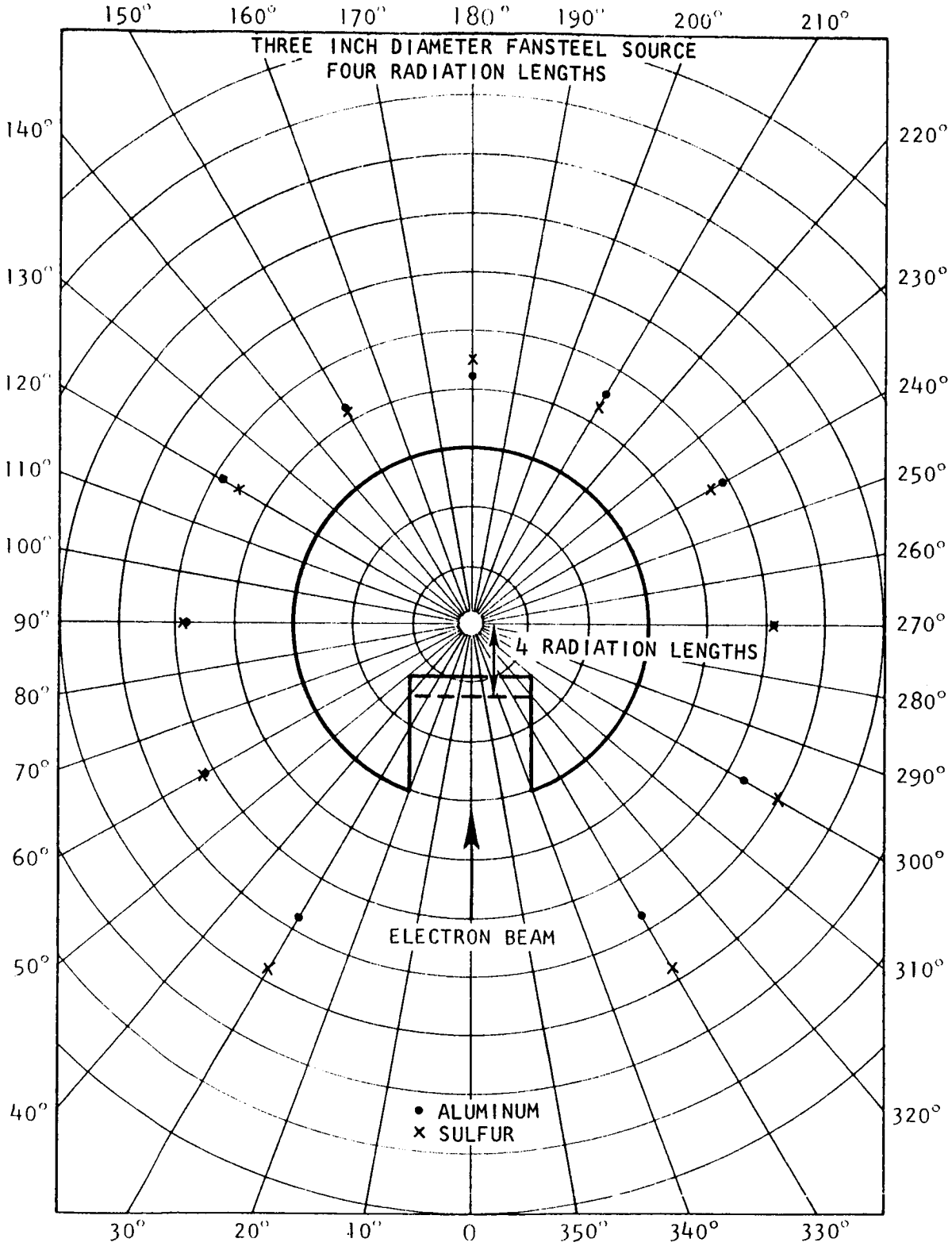

Fig. 34 -- Sulfur and aluminum activation data for source No. 4 with four radiation lengths

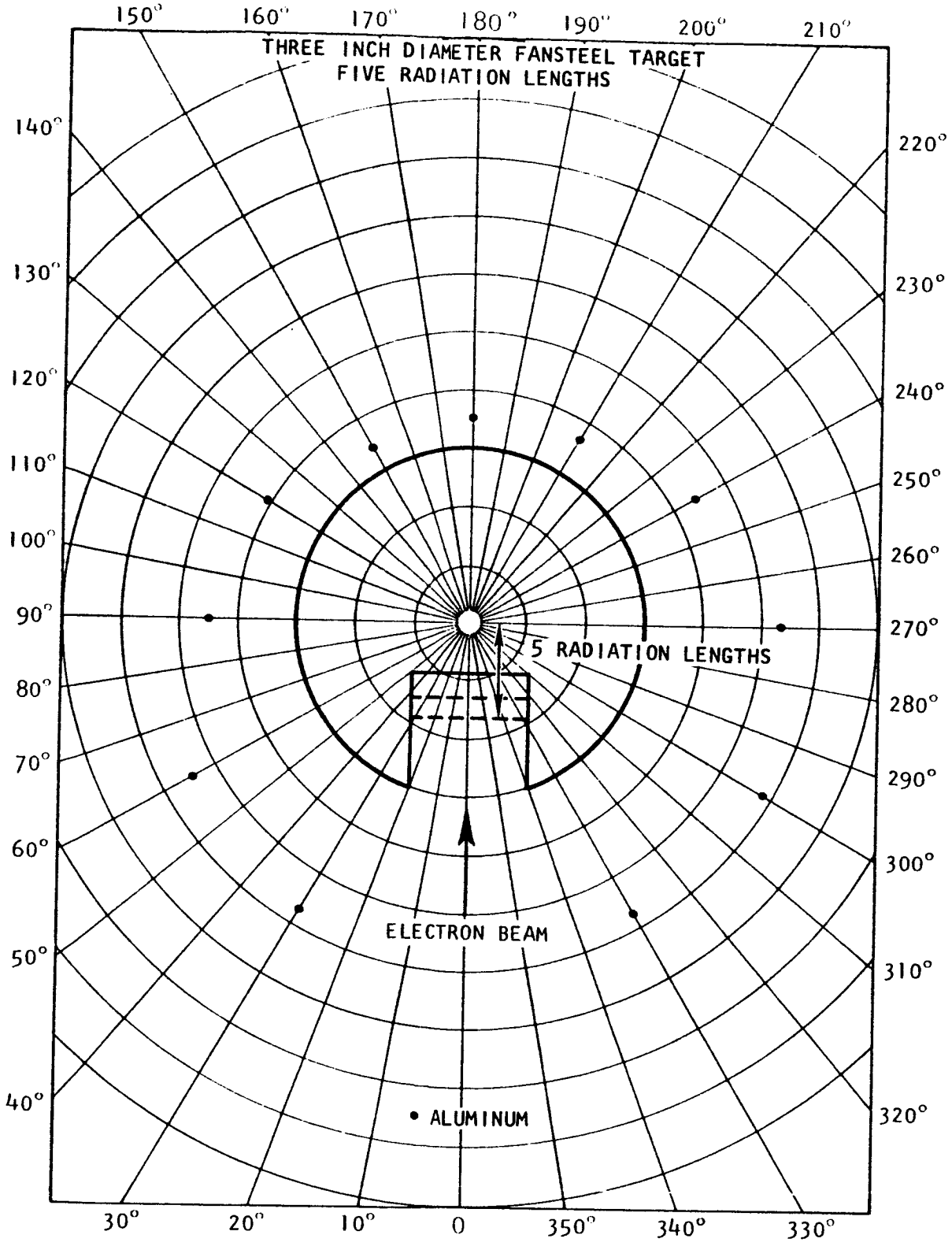

Fig. 35 -- Aluminum activation data for source No. 4 with five radiation lengths

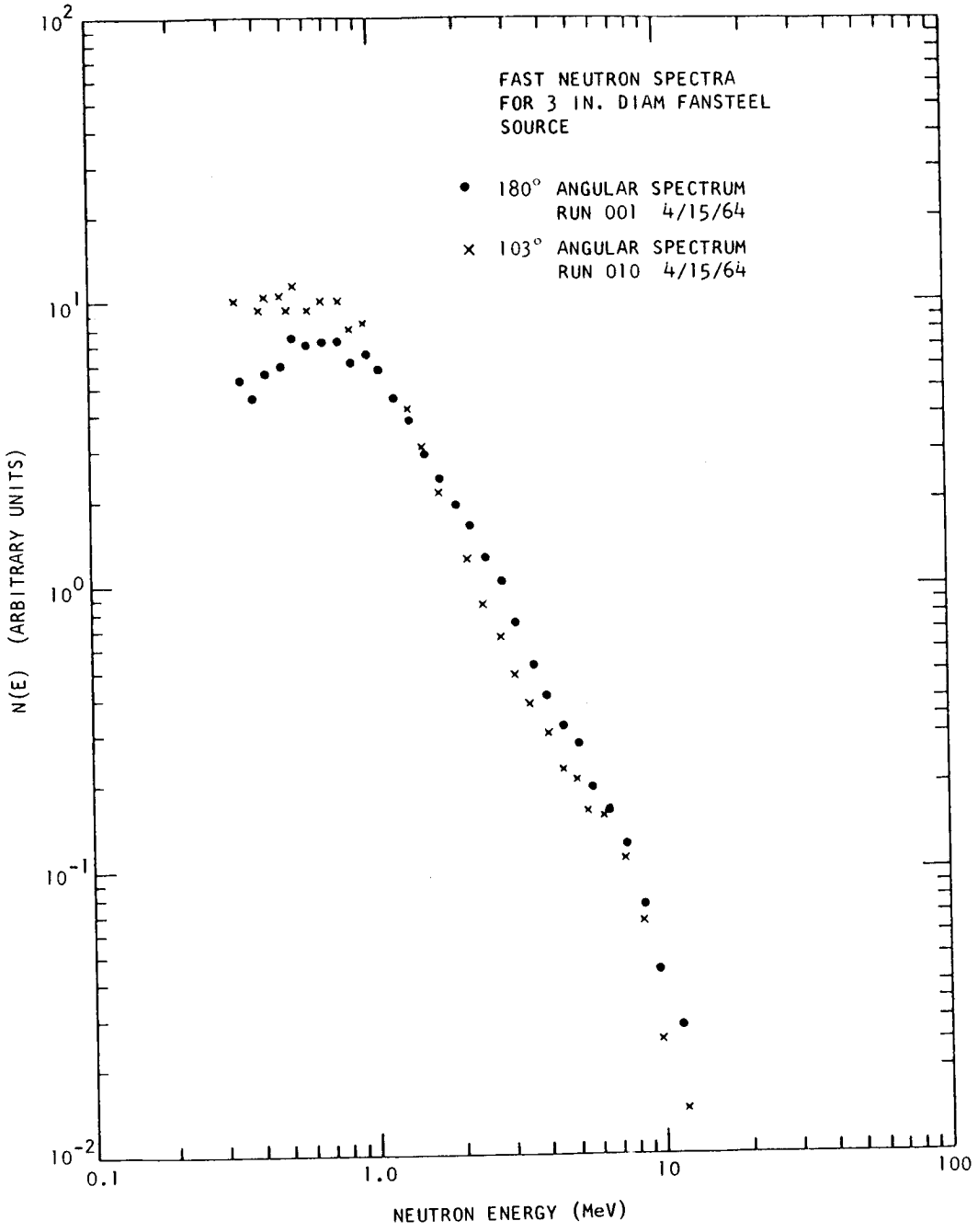

Fig. 36 -- Neutron time of flight spectra from source No. 4

a neutron, while the indirect process causes an evaporation or boil-off of a neutron from the tungsten nucleus. This indirect process tends to be isotropic, whereas the direct process can very probably be anisotropic.

Analysis of the three inch diameter tungsten sphere experiments led to two conclusions concerning improvement of isotropy: first, an increase in source diameter from three to four inches could smear out the effects of the direct interaction process; second, to use uranium as a source material rather than tungsten (fansteel) since uranium can produce neutrons by both a (γ, n) process and a (γ, f) process. As the (γ, f) process, which produces an isotropic distribution of neutrons, is strongly predominant, the anisotropic direct interaction part of the (γ, n) process would be masked and general isotropy improved.

A 3.78 inch diameter spherical fansteel source, source No. 5, was therefore constructed, using the three radiation length rule, to see if the smearing out of the direct interaction component would produce an isotropic source. Again the sulfur and aluminum activation detectors were located at 30° intervals around the source, with two additional positions, 15° either way off the 180° - 0° axis, to give more information about the anisotropy usually observed at 180°. Data resulting from these experiments is shown in Fig. 37, with the sulfur and aluminum data normalized using the average of the 90° and 270° angles. Now, the anisotropic effect is no longer present and the flux distribution flattens out slightly in the 180° direction.

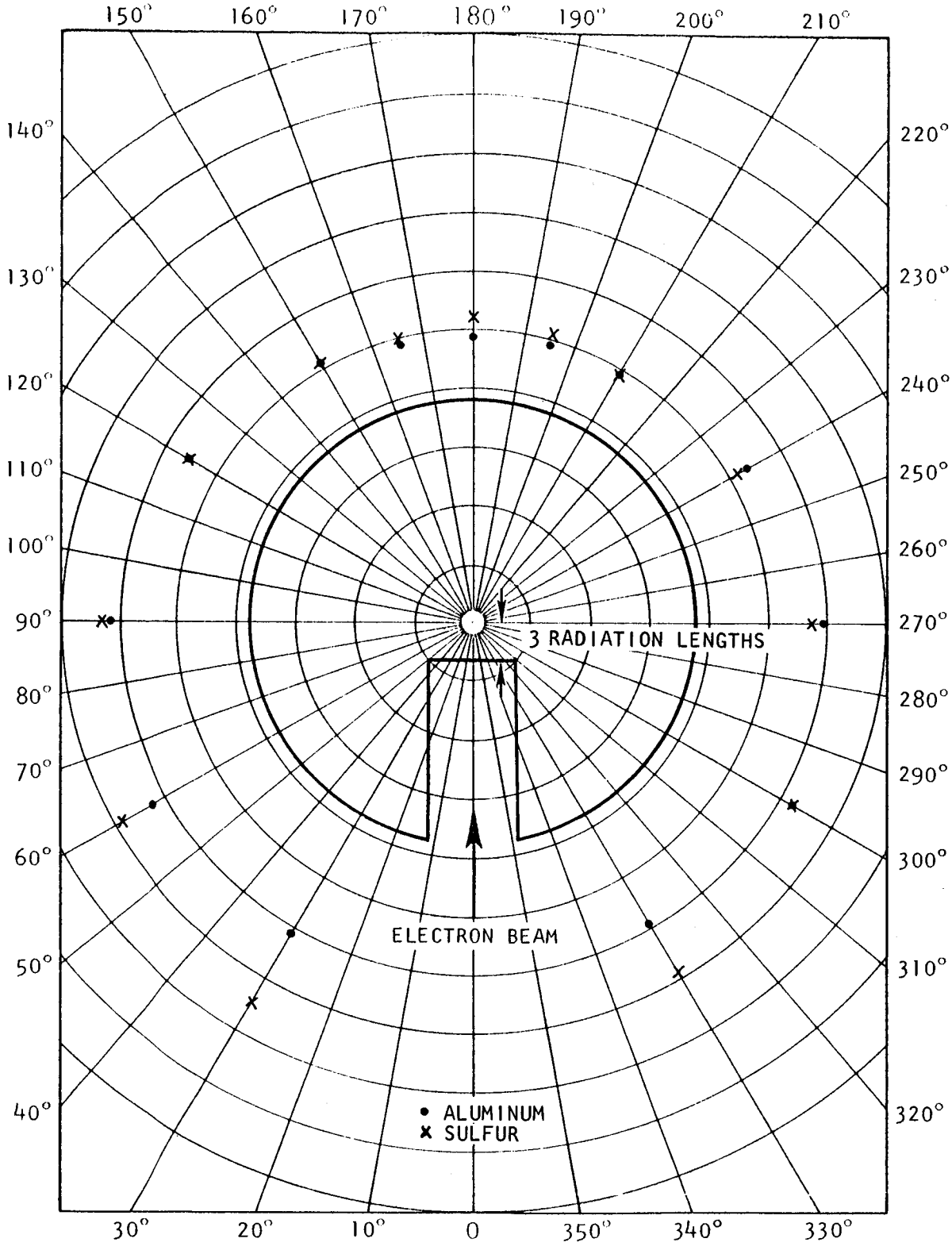

Fig. 37 -- Sulfur and aluminum activation data for source No. 5 with three radiation lengths

To check the alternate solution to the anisotropy problem, a spherical uranium source two inches in diameter, source No. 6, with a 3/4 inch diameter beam entrance hole, was constructed. The electron impingement surface was one radiation length or 0.11 inch from the geometrical center of the sphere, and two 3/4 inch diameter by 0.11 inch thick disks were made to allow a repeat of the fansteel sphere isotropy experiments in order to establish the center of neutron production. Because the uranium fission process generates several fission products which will badly contaminate the experimental area, any uranium target used in conjunction with the Linac must be contained in a sealed can or heavily plated to contain these fission products. A 0.015 inch thick coating of copper was therefore plated onto the uranium sphere and the two disks to seal in the fission products and to ensure that uranium atoms would not be evaporated from the source's surface due to heating by the electron beam; source cooling was by compressed air blowing into the beam entrance hole.

Neutron flux distributions given by the sulfur and aluminum activation monitors, located as in previous experiments, are shown in Figs. 38, 39, and 40 with the sulfur and aluminum data normalized at 90° for comparison. The skewed sulfur flux distribution in Fig. 39 is due to the electron beam striking the surface at a small angle to the normal rather than perpendicular. Once again three radiation lengths may be seen to produce the most isotropic flux, with the sulfur and

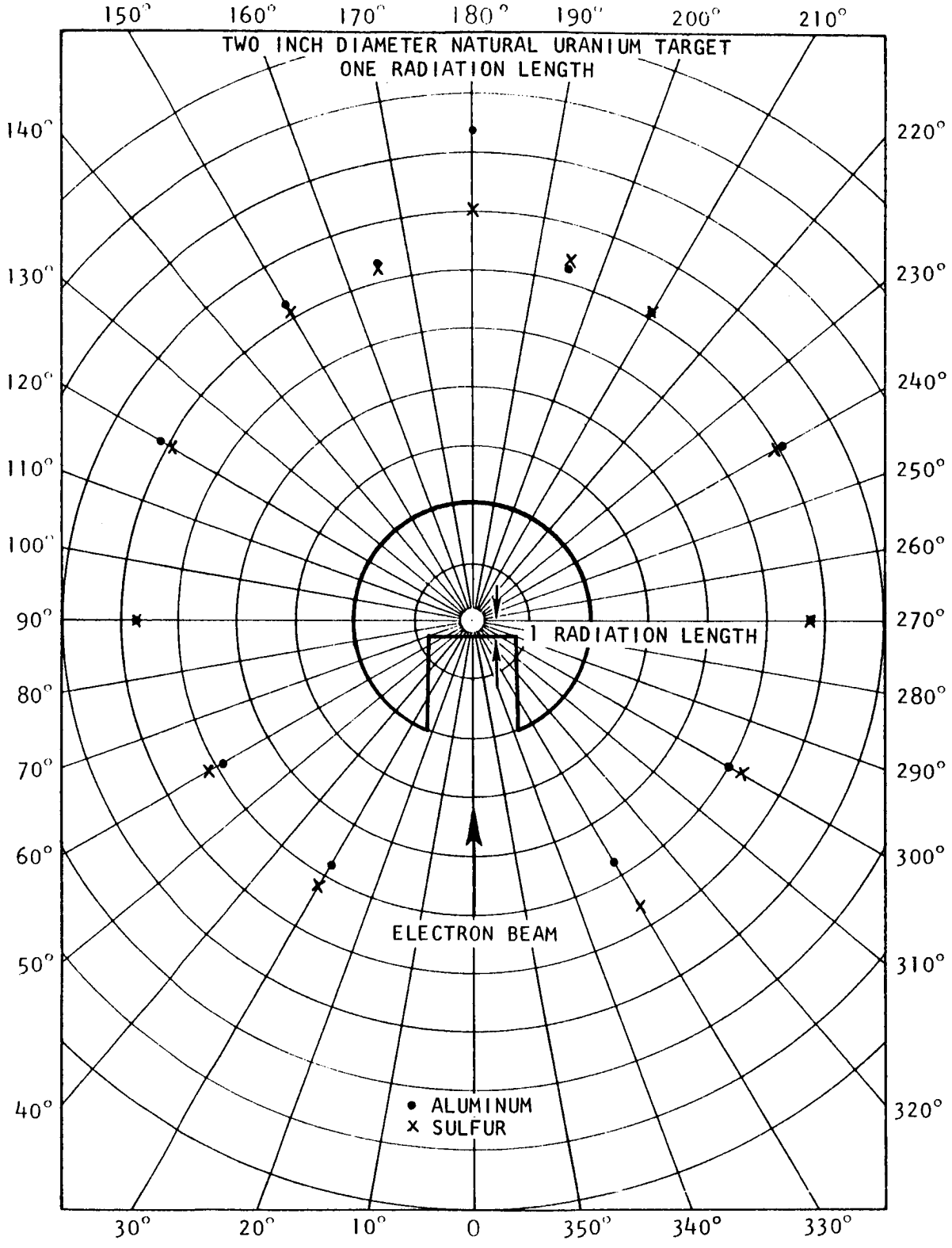

Fig. 38 -- Sulfur and aluminum activation data for source No. 6 with one radiation length

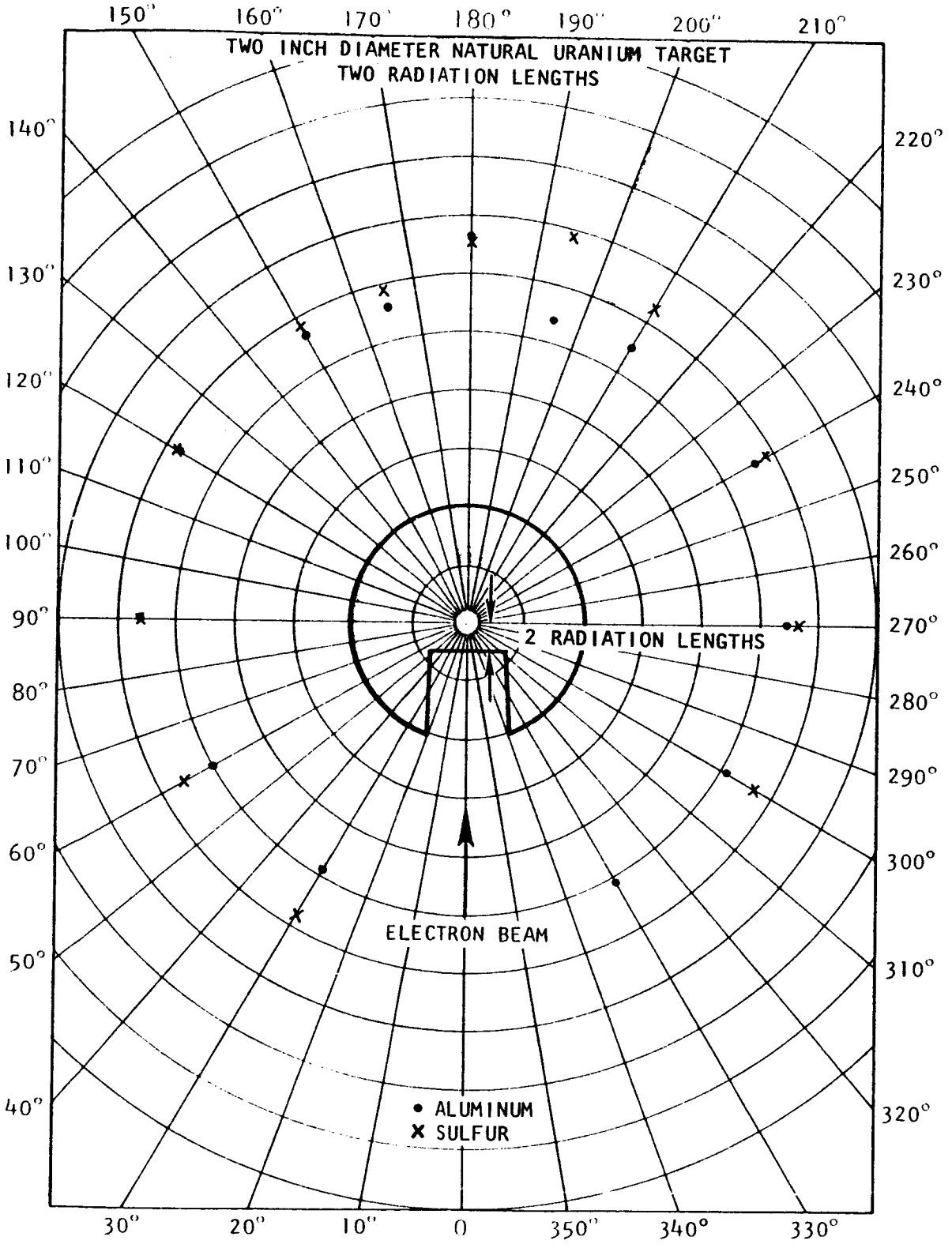

Fig. 39 -- Sulfur and aluminum activation data for source No. 6 with two radiation lengths

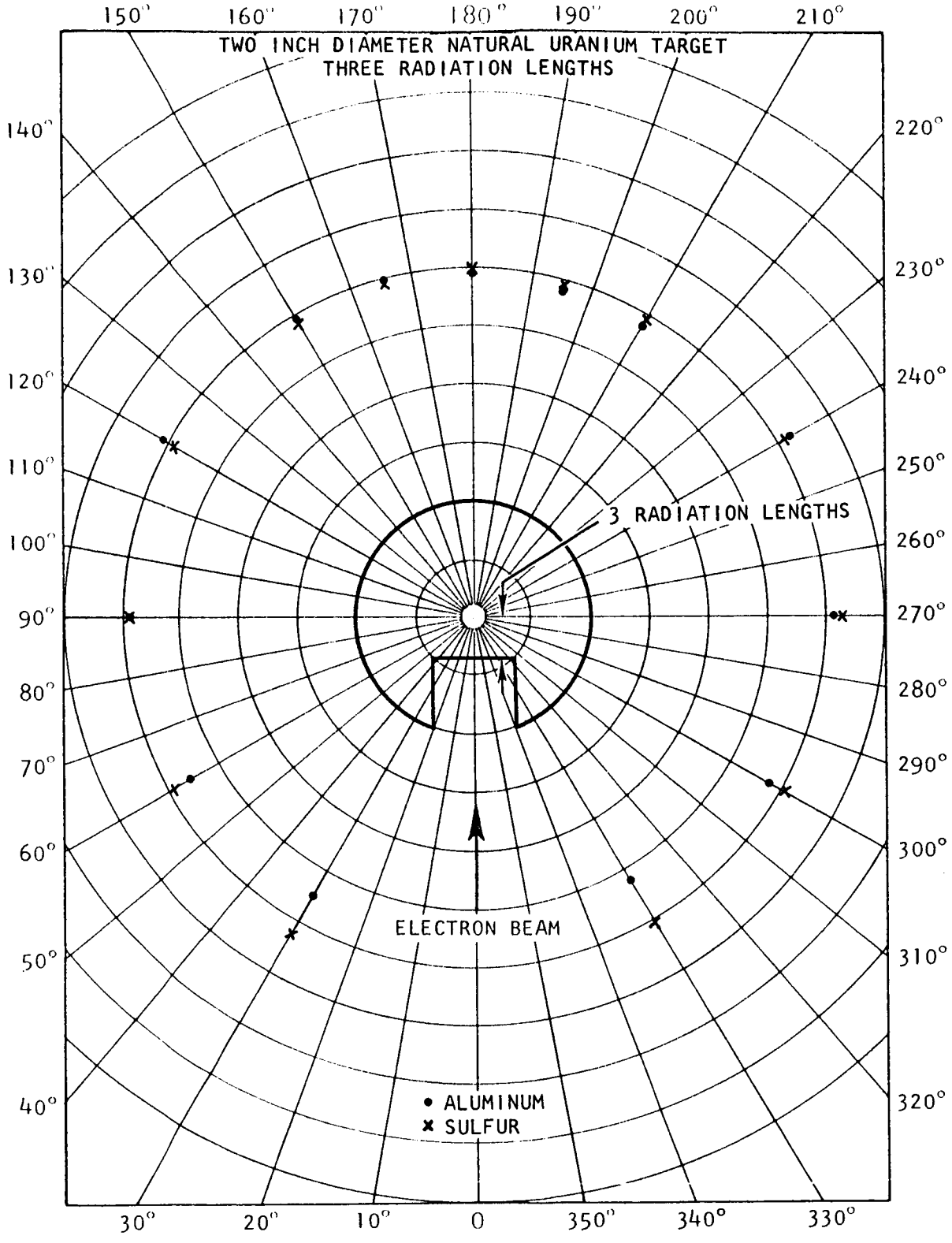

Fig. 40 -- Sulfur and aluminum activation data for source No. 6 with three radiation lengths

aluminum monitors both exhibiting a high degree of isotropy with no forward peaking effect. Figure 41 shows the neutron spectra at 103^{o} and 180^{o} taken by time-of-flight techniques. Once again the 180^{o} direction shows a fairly large degree of anisotropy above 2 MeV; however, this time the spectral shapes are very similar with only a 30 per cent absolute magnitude change being evident.

Since the time-of-flight results agreed well with the activation detector data, except as noted above, the 2 inch diameter uranium source was felt to be sufficiently isotropic to be used in the water mockup experiments as we were unable to obtain enough uranium to make a larger sphere in time to run the experiments on schedule. Therefore, the two one-radiation length disks were soft-soldered into the sphere and the source was used for the water mockup experiments using only air-blast cooling. A discussion of the cooling of this and other sources used in these source design experiments is found in Section 5.1.2.

After the completion of the water mockup experiments, a three inch diameter by three radiation length uranium sphere was machined and electroplated with 0.010 inch of copper and 0.005 inch of nickel. Details of this source, source No.7, which is the one used in the liquid hydrogen experiments, are shown in Fig. 42. Primarily, this larger source was built to reduce the bremsstrahlung radiation which could be absorbed in the liquid hydrogen and to smear out the small amount of anisotropy which was present with the two inch uranium sphere.

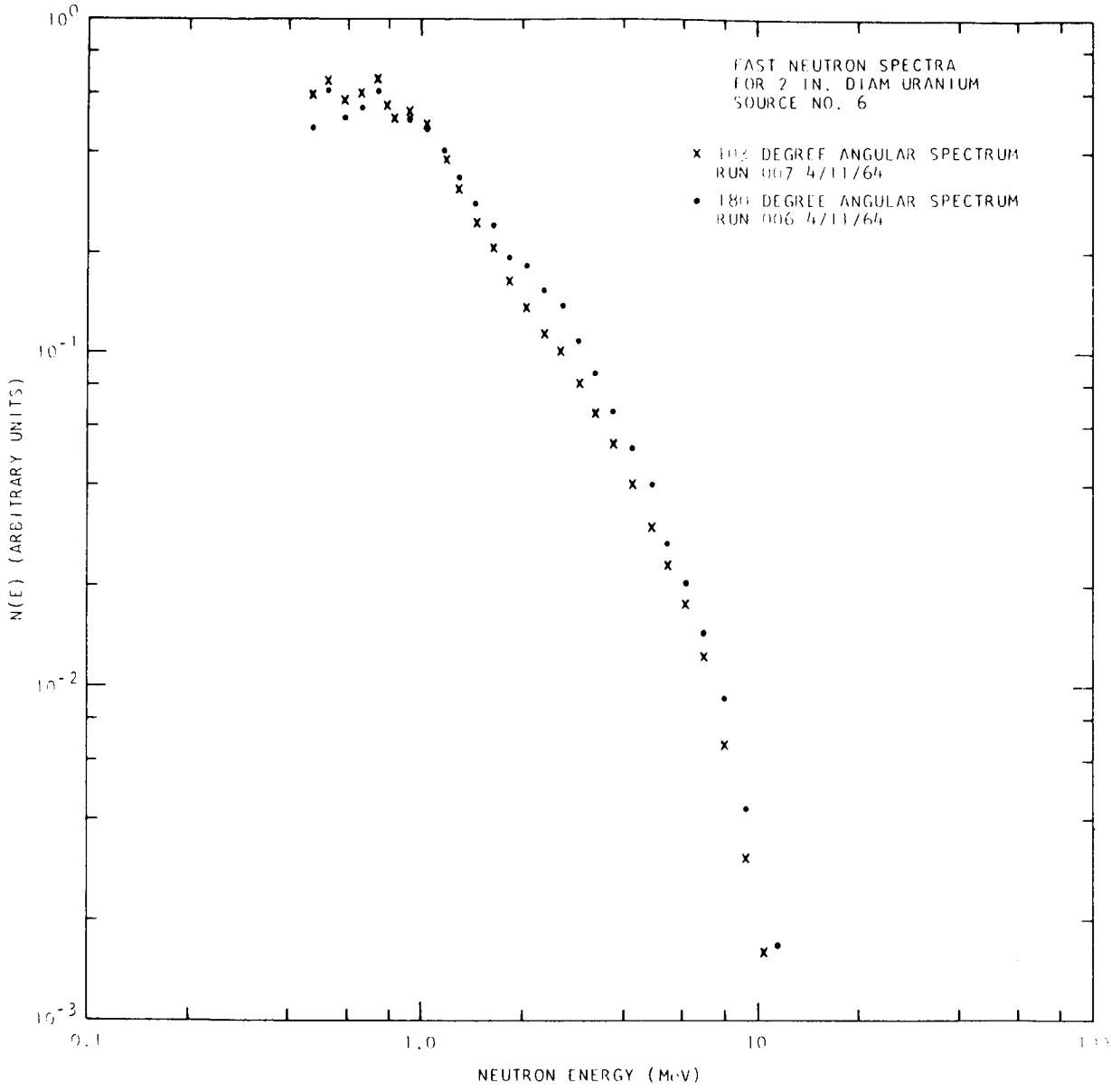

Fig. 41 -- Neutron time of flight spectra from source No. 6

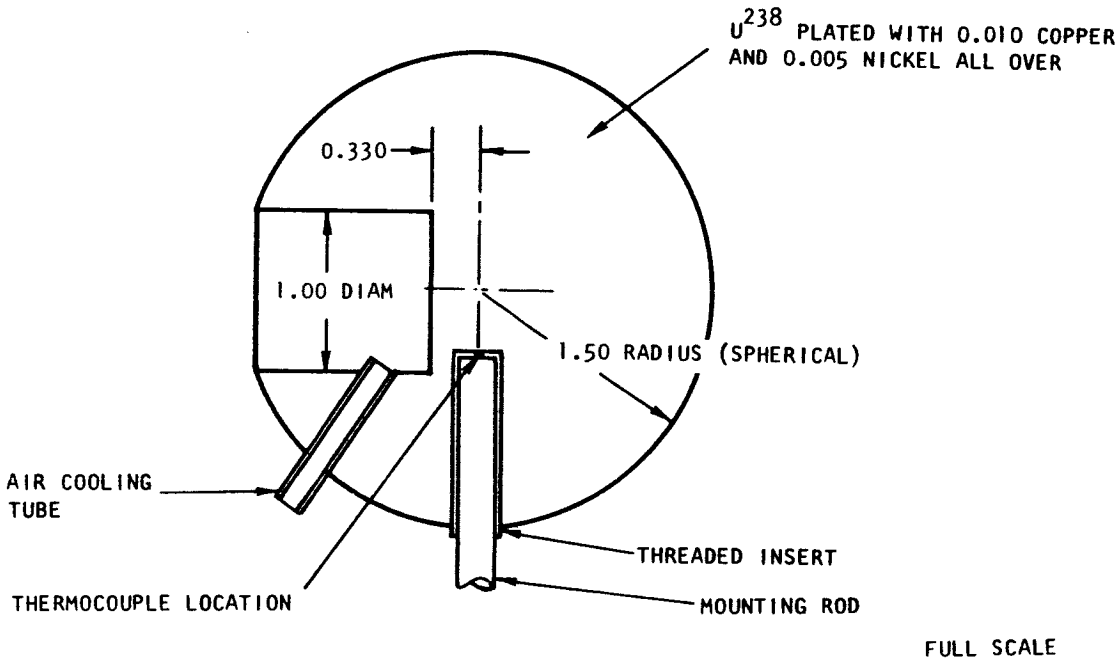

Fig. 42 -- Detail of 3 inch diameter uranium sphere, source No. 7

Neutron flux distribution measurements were made in the usual manner with sulfur and aluminum activation foils, with the results shown in Fig. 43; the data have been normalized at 90^{o} for comparison purposes. It can be seen that the flux indicated by both foils is now fairly isotropic, with a slight tendency to flatten out at 180^{o} and the ratio of sulfur to aluminum to change at the extreme back angles where the cylindrical opening perturbs the flux. However, these back angles cannot be seen by the liquid hydrogen dewar.

Fast neutron spectra for the 3 inch diameter uranium sphere was measured at angles of 70, 90, 130, 167, and 180^{o} and normalized using aluminum activation foils for monitoring. These spectra are shown in Fig. 44. Here, the 70, 90, and 130^{o} spectra are identical, as are the 167 and 180^{o} spectra. The 180^{o} and 70^{o} spectra agree fairly well up to a neutron energy of about 5 MeV, which is in good agreement with the activation foil data of Fig. 43, where anisotropy exists for about 15^{o} on either side of 180^{o} and the ratio of sulfur to aluminum foils is about 1.1, or 10% higher, for neutrons above 3 MeV. While the data in Fig. 44 shows that some anisotropy does occur above 5 MeV, and at $180^{o} \pm 15^{o}$, the over-all isotropy of the 3 inch diameter uranium is excellent. Therefore, this source was used exclusively in the liquid hydrogen experiments.

5.1.2 Heat Dissipation and Reliability of Fast Neutron Source

As previously noted, possible flux distribution perturbations

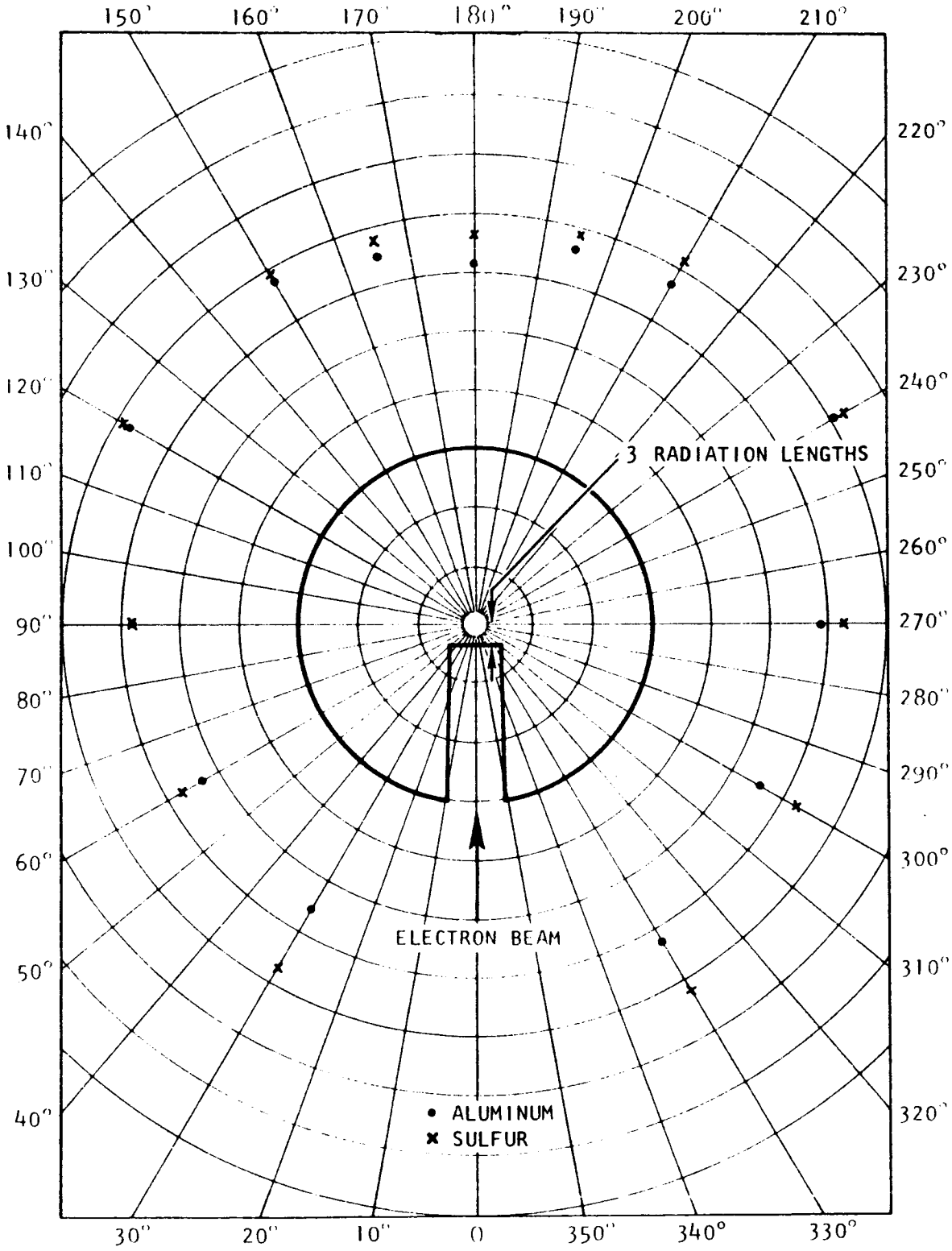

Fig. 43 -- Sulfur and aluminum activation data for source No. 7

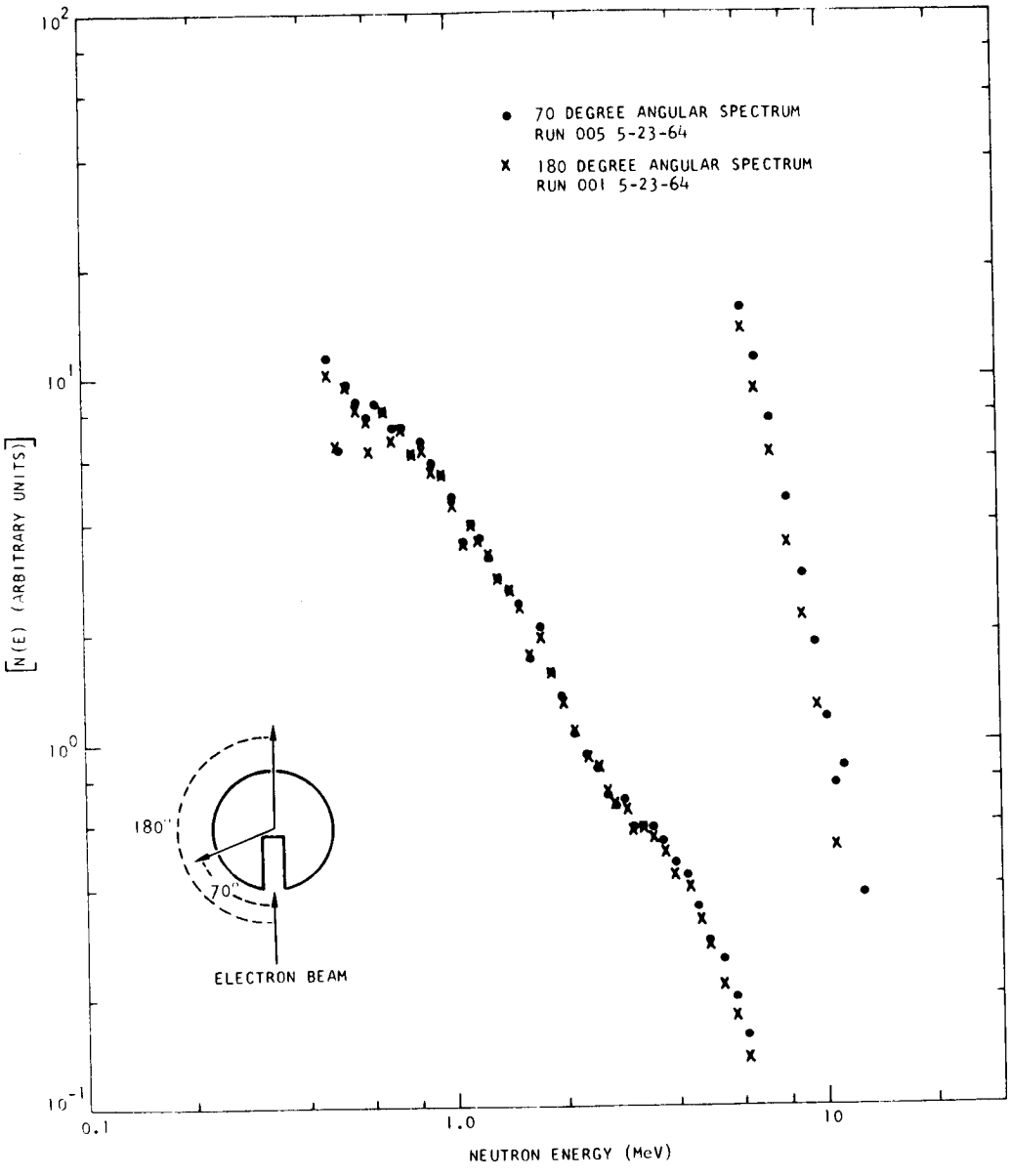

Fig. 44 -- Neutron time of flight spectra for source No. 7

ruled out the use of water as a cooling medium for the fast neutron source. Therefore, the only remaining method of cooling is gas flow over the source, and the most logical and desirable gas for this purpose is compressed air since the Linac has a relatively high-capacity compressor system and a distribution system has already been installed to provide Linac output window cooling.

Prior to the construction of the air-cooled test sources, some effort was put into power dissipation calculations to attempt to predict the thermal behavior of the source materials under consideration. An attempt was made to design the source to absorb one kilowatt of beam power--Linac conditions for this power output being a beam pulse current of 2.06 amps, at a pulse width of 0.05 microsecond and an electron energy of 27 MeV, with a pulse rate of 360 pulses per second--which would certainly be well above the actual delivered beam power that could be obtained during the experiments.

Of the two source materials considered, fansteel had by far the greater thermal conductivity--by a ratio of 3.5:1, in fact--and, in addition, permitted a much higher operating temperature since fansteel melts at above 1300°C while uranium undergoes a damaging phase change at only 600°C. A heat removal calculation was made for a three inch diameter uranium sphere, using a power input of 1 kilowatt, a central heat source temperature of 800°F (425°C), and a Linac beam spot size (heat source spherical diameter) of 0.55 inch. This calculation indicated

that it would be necessary to limit the outer surface temperature to 100°F, which did not seem to be possible with only air-blast cooling. However, the greater heat transfer rate of fansteel can make the dissipation of one kilowatt in this spherical source possible without the problem of approaching a failure temperature.

Since the heat dissipation properties of the source are of secondary importance to the isotropic neutron flux density requirements, the approximately two-to-one advantage in neutrons/electron and the markedly superior isotropy of a spherical uranium source forced us to choose uranium in spite of the increased cooling difficulty. In addition to poor heat transfer, uranium possesses other even more undesirable characteristics which must be taken into account in the source design. Uranium is a difficult material to machine, in that it is abrasive and pyrophoric, and special techniques and equipment must be used to produce an acceptable finished product. Furthermore, attachment of cooling tubes, source mounts, etc., is made difficult because these parts cannot be welded or soldered to the uranium but must be pressed into precision-bored holes.

Perhaps the most difficult problem associated with using uranium as a fast neutron source material is the elimination of the danger of contamination of the experimental area. Fission products formed during the fission process must be contained or removed to avoid contamination and personnel hazard, since these fission products in many cases have long radioactive half-lives. Also, direct impingement of the electron beam

on a metallic surface may knock-off or "boil off" atoms from the surface; uranium atoms boiled off a source would obviously be a definite hazard. Our attempt at control of these problems, copper/nickel electroplating, has been only partially successful, since the plating is subject to the same burning and "boil off" as the uranium, and only a 0.015 inch thick coating can successfully be plated onto uranium. The copper which is plated onto the uranium is held only by a mechanical bond in the imperfections found on the machined surface of the uranium, so it is subject to handling and thermal cycling damage. Nickel may be plated onto the copper to reduce copper "boil off" but cannot affect the lack of bond strength of the coating.

During the isotropy experiments with the 2 inch diameter uranium sphere, one of the one radiation length uranium disks sustained a plating failure due to inadequate cooling on one side. A great deal of time was lost in decontamination of the experimental room; therefore, the construction and plating of the 3 inch diameter sphere were very carefully checked and heating studies, using a thermocouple placed almost in the center of the sphere as a guide, were undertaken before allowing full allowable beam power to be used. The results of these studies are shown in Fig. 45.

One additional problem which could be associated with the use of a plated uranium source appears to have manifested itself during the liquid hydrogen experiments: internal overpressure of the plating by the

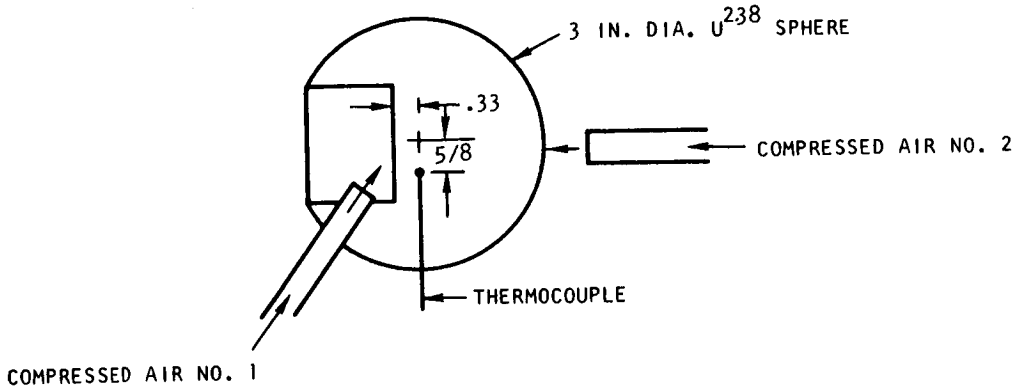

POWER (WATTS)	TEMPERATURE AT THERMOCOUPLE LOCATION	AIR FLOW AT POSITION NO. 1	AIR FLOW AT POSITION NO. 2
	TESTING		
120	127°F	LOW	HIGH
275	200°F	LOW	HIGH
400	240°F	HIGH	HIGH
	DURING LH_2 EXPERIMENTS		
0	75°F	HIGH	HIGH
50	80°F	HIGH	HIGH
320	185°F	HIGH	HIGH
500	270°F	HIGH	HIGH

Fig. 45 -- Heat dissipation properties of source No. 7

buildup of fission product gases, with the resulting plating failure or "blowout," occurred in the exact area upon which the Linac beam strikes, indicating that beam heating may have thinned and weakened the plating allowing the fission product gas pressure to crack the plating open. We were forced to discontinue the experiment in progress, decontaminate the experimental area, and replate the source before continuing the experiments. It appears that considerable additional study may be required to produce a really reliable uranium source.

Both the isotropy and heat dissipation experiments pointed out that careful control of the Linac electron beam size and location was very important to the consistent isotropic production of neutrons and distribution of the heat source. The centroid of neutron production--and thus the electron beam--must be in the geometric center of the source, while a too-small beam spot may affect the isotropy of neutron production and overheat the center of the source. An overlarge or unround spot may strike partially outside the beam entrance hole and completely destroy both the neutron isotropy and the ability of the experiment source strength monitors to function correctly. Because of these facts, great emphasis was placed on the correct quality electron energy spectrum and steering of the electron beam.

5.2 FAST NEUTRON DETECTOR

Two fast neutron detectors were used to take the time-of-flight data: the 5 in. detector for greater sensitivity and the 2 in. detector when reduced sensitivity to γ-flash was desired.

The 2 in. fast neutron detector consists of an RCA 6810A 14-stage photomultiplier viewing a 2 in. diameter by 2-1/2 in. long glass container painted white on the outside and filled with liquid scintillator (Nuclear Enterprises Inc. - NE 211). The 5 in. fast neutron detector consists of an Amperex XD1040 14-stage photomultiplier viewing a 5 in. diameter by 5 in. long glass container painted white on the outside and filled with liquid scintillator (NE 211).

Detection of a neutron occurs indirectly through the kinetic energy transferred to a proton in an elastic collision. A given neutron yields a continuous energy spectrum of "recoil" protons. The fraction of detected recoils is less for a low energy neutron than for a high one, since there is some minimum pulse height or bias which the electronic circuitry will accept.

5.3 TIME-OF-FLIGHT ELECTRONICS

A block diagram of the time-of-flight electronics is shown in Fig. 46. The injector trigger from the linear accelerator which occurs about one microsecond before the electron beam strikes the uranium target and produces the "γ-flash" is sent to an inverter and pulse shaper. The positive pulses are sent through a variable delay network and line driver to the photomultiplier gate generator and trigger the phototube of the detector. The photomultiplier tube of the detector is normally inoperative; it is not gated on until some time after the "γ-flash" has passed through the detector but before the highest energy neutron that is desired to be measured

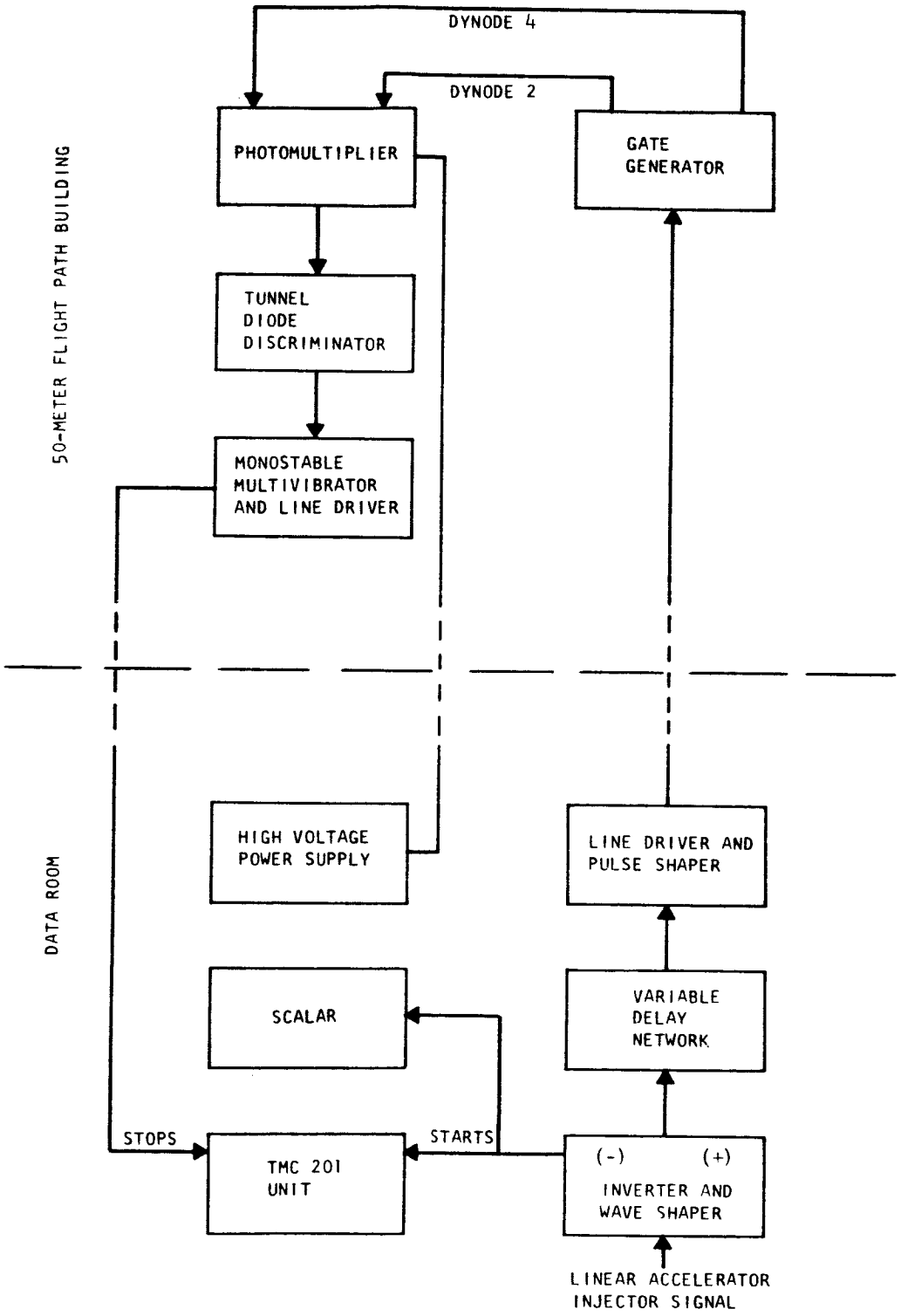

Fig. 46 -- Block diagram of time of flight electronics

reaches the detector. When the photomultiplier is gated the gain is reduced a factor of 10^3. This is done since it would otherwise be impossible to detect neutron pulses above the scattered γ-rays or to avoid paralysis of the phototube.

The photomultiplier is normally off due to a bias on dynodes 2 and 4. At a time dictated by the delay of the delay network, transit time of the cables, and electronics, a gated pulse is applied to dynodes 2 and 4; it takes about 250 nanoseconds for the phototube to reach full gain. The detector is on-gated for 50 microseconds.

The negative pulse from the inverter and wave shaper serve as the "starts" for the system trigger input of the TMC 201 unit. This negative pulse also triggers a scalar and is used to count the Linac beam pulses.

The output from the anode of the photomultiplier tube is fed to a tunnel diode discriminator then to a monostable multivibrator and line driver and serves as the signal input or "stops" for the TMC 201 unit.

In order to avoid ambiguity introduced by the several electronic delay times due to photomultipliers, etc., one measures the neutron arrival time relative to the arrival time of gamma rays scattered by the (γ, n) target. This time zero reference is determined by adjusting the variable delay until the γ-flash is recorded by the TMC 201 unit (time-of-flight module). This is usually channel 37. The interval between the γ-flash and the neutron arrival time represents the neutron flight time plus 171 nanoseconds, which is the flight time of the scattered gamma rays.

The bias or "threshold" energy for the fast neutron detectors was calibrated relative to the Compton edge of the pulse height distribution taken with a Cs^{137} source. In terms of the photon energy E_γ, the energy of the Compton peak or the maximum single-collision energy transfer E_c is given by $E_\gamma \ (1 + (m_o C^2)/2\ E_\gamma)^{-1}$, where $m_o C^2$ is the electron rest energy. For the 660 kev gamma-ray of Cs^{137}, E_c is 478 kev. E_c was chosen as the pulse height at which the intensity of pulses had fallen to approximately two-thirds of its value at the "Compton peak."

The experimental procedure is as follows. The linear output signals or pulse heights from dynode 9 of the phototube are amplified, delayed for proper coincidence timing and applied to the TMC in pulse height mode and a Cs^{137} spectrum recorded. From this data the intensity of the "Compton peak" can be determined and therefore the pulse height or channel corresponding to E_c or 478 kev. Another Cs^{137} pulse height distribution is taken with the discriminator signal serving as the coincidence signal. This coincidence spectrum shows a sharp discriminator bias level which can be recorded as a fraction of E_c, the 478 kev pulse height. This procedure gives the energy bias level in electron kev.

The tunnel diode discriminator is initially adjusted for some fixed voltage. The energy bias is adjusted on a day-by-day basis by means of the high voltage power supply until a bias of 48.7 electron kev is obtained. This is equivalent to a 220 kev neutron bias.[2] This is also checked by

[2] R. Batchelor, et al., "The Response of Organic Scintillators to Fast Neutrons," Nuclear Instruments and Methods, 13, pp 70-82 (1961).

observing which channel the neutron counts extrapolate into the average background.

All of the liquid hydrogen neutron spectrum measurements were made in a single series of runs covering eight days and all of the electronics for the fast neutron detector remained on during this time. Prior to each set of measurements the bias was checked according to the above procedure. An adjustment in the high voltage power supply of only 25v in 2550v was necessary for the 5 in. fast neutron detector in order to maintain the same bias. The 2 in. detector was used only for the 0^{o} measurements.

5.4 SOURCE MONITORS

5.4.1 Requirements for a Source Monitor

One of the most difficult problems facing the people using the Linac for fast neutron experiments has been the accurate run-to-run monitoring of the fast neutron sources. Many methods have been used: average Linac beam current or instantaneous beam pulse current monitoring, which unfortunately tells one nothing about variations in electron energy and hence neutron production and energy spectrum in the source; target temperature, which may be varied by many factors other than beam power and has little sensitivity to the neutron energy spectrum; electronic or counting type monitors, which utilize BF_3 thermal neutron detectors or U^{235} fission chambers and which must be located so as to integrate scattered and thermalized fast neutrons; activation monitors,

which must be placed in a particular geometrical location with respect to the source before an experimental run and removed after the run and the activation products analyzed.

The main requirement of an experiment monitor is accuracy, the ability to follow from run to run the changes of source strength and to indicate these changes in direct proportion to the actual source strength variation. It must indicate correctly flux variations over a wide range and must be insensitive to changes made in the experimental area, seeing only actual primary flux intensity changes. Sensitivity to the correct neutron energy range is important, since electron energy changes may cause a shift in the neutron energy spectrum. The monitor must be reliable, reasonably inexpensive, and fairly simple to set up or locate. Its results should be comparable on a day-to-day basis, so the setup, biasing, or locating procedures should be easily standardized and repeatable. For the LH_2 experiments, two types of monitors were used, an activation monitor and a U^{235} fission chamber.

5.4.2 SOURCE ACTIVATION MONITORS

The activation source monitors used with the LH_2 experiments were 1100 series aluminum slugs positioned in a nylon housing as shown in Fig. 47. Aluminum has a 7 MeV threshold for an (n, α) reaction.

Because of the high activation threshold an aluminum activation monitor is relatively insensitive to albedo from the dewar material, liquid hydrogen surface, and environmental surroundings. The nylon

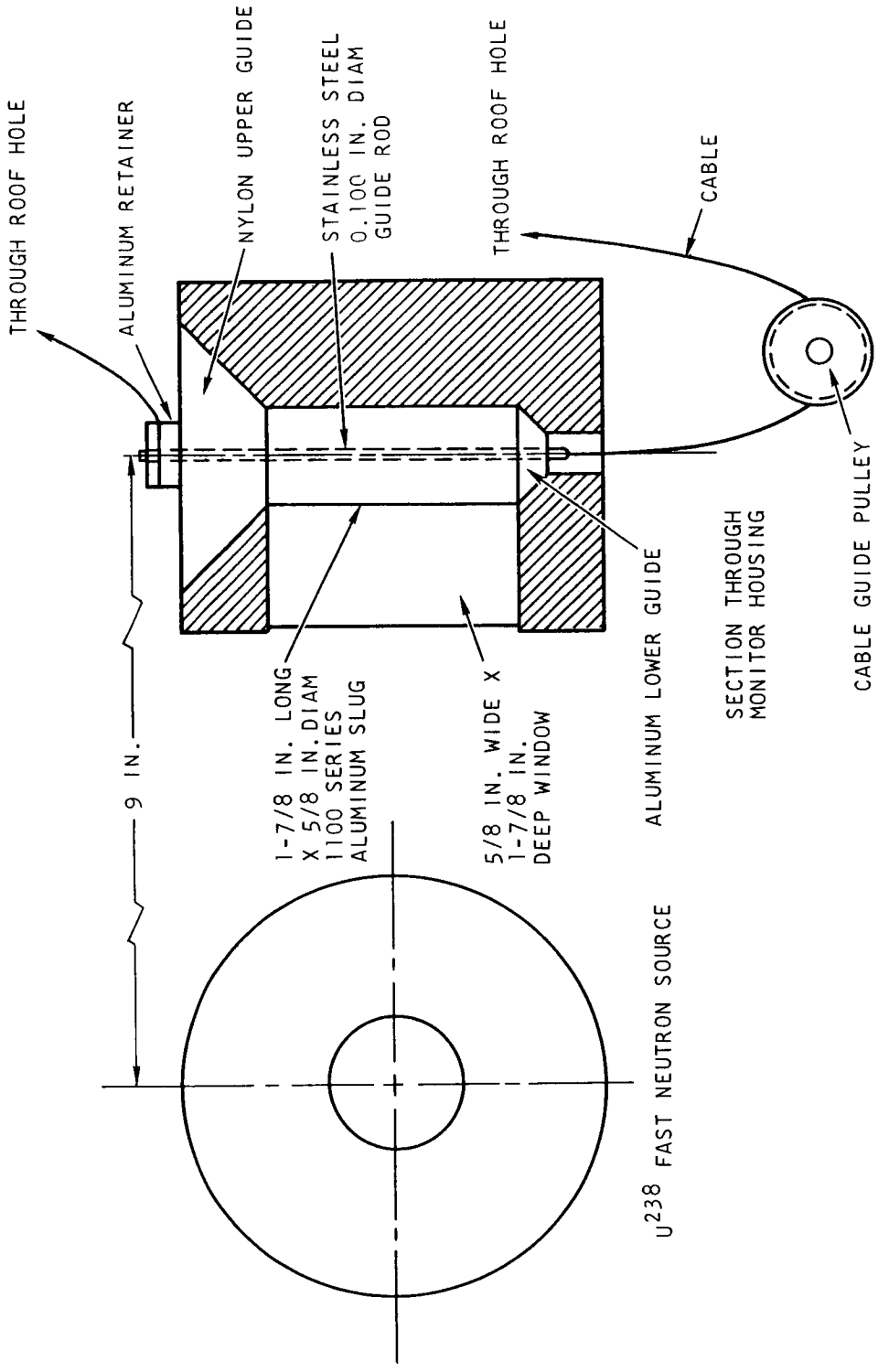

Fig. 47 -- Detail of baffle showing location of LH_2 level sensors

housing also provided some albedo shielding and guaranteed positive identical location of the aluminum slug for each run. The safety requirement of no entrances to the experimental room during the presence of liquid hydrogen in the dewar prompted us to design a remote monitor insertion system. A small passage through the roof of the experimental room provided an ideal transfer hole; a continuous cable run through the nylon housing and around the pulley under the housing was used to pull the aluminum slugs in and out of the experimental room and seat them in the housing, with a new slug being put into the housing for each run.

The Na^{24} activity from the Al(n, α) reaction was counted by using a NaI well counter and conventional electronics. Great care was taken to maintain the same bias for each day. This was accomplished by taking pulse height distributions for the signal in coincidence with the discriminator output. The discriminator was adjusted at the "valley" prior to the 1.37 MeV γ-peak to minimize any effect of electronics drift and to give a reproducible reference point. Each aluminum monitor was counted several times with at least 10% statistical accuracy in order to ensure that the bias was adjusted for only the Na^{24} 15 hr half-life activity. Some discrepancy in the die-away of the radiation from the activated aluminum monitors was observed when the slugs were counted soon after activation. This activity had a 2-1/2 hr half-life and was probably due to Mn^{56} which occurs in trace quantities in aluminum. However, the

cross section for the production of Mn^{56} by a (n, γ) reaction is much larger than for the production of Na^{24} by an (n, α) reaction. Since the half-life of the extraneous activity was 2-1/2 hours, the aluminum monitors were reliably counted twelve or so hours after irradiation.

The alternate monitor used on the LH_2 experiments consisted of a small U^{235} fission chamber and associated amplification electronics. This monitor was used as an instantaneous trouble-indicating monitor and as a backup for the activation monitor. Although the day-to-day agreement was rather poor, the run-to-run agreement with the activation monitor was excellent. The disagreement on a run-to-run basis between these two monitors was less than $\pm$ 10%.

5.5 BACKGROUND STUDIES

Two different types of backgrounds in the liquid scintillator detector were studied. The first was ambient background which is the natural radioactivity of the liquid scintillator and environment and cosmic radiation. The second background was due to source produced neutrons which do not come directly from the probe tube of the assembly but either leak around or through the collimation and shielding.

The ambient background was reduced a factor of three or four by shielding the 5 in. detector with a dolly mounted lead "housing" around the entire detector system, open at both ends to allow the highly collimated neutron beam to pass through without striking the walls of the "housing." The walls are 2 in. thick lead and the housing is 40 in. long.

The detector and its "housing" are shown in Fig. 48; the tape on the flight path window defines the outline of the collimated neutron beam at that point. The off-angle photograph gives the appearance that the detector is not centered from left to right. The vertical center of the liquid scintillator is marked in this photograph by a piece of black tape.

Following the measurement of differential fast neutron spectra in water, it became apparent that better shielding and collimation were necessary especially for large angle, large thickness measurements. At large angles where the neutron intensity is low, the fast neutron source views the precollimator directly. This is shown in Fig. 49. Therefore, the precollimator itself can act as a secondary source of neutrons if improperly designed. This situation is somewhat improved at the smaller angles or small thicknesses since the signal is much larger. Another reason is that the liquid hydrogen acts as a self shield. The probe tube extends 21 in. into the center of the hemispherical portion of the dewar and therefore any neutrons not travelling in the direction of the probe tube must penetrate an additional thickness of perhaps 10 or 20 in. of liquid hydrogen, depending on the angle, in order to strike the precollimator.

One source of background determined by measurements with a setup similar to that shown in Fig. 49, was due to leakage from the surface of the 55 in. long 0.87 in. diameter precollimator at the point where the precollimator is changed to a 1.5 diameter. This was

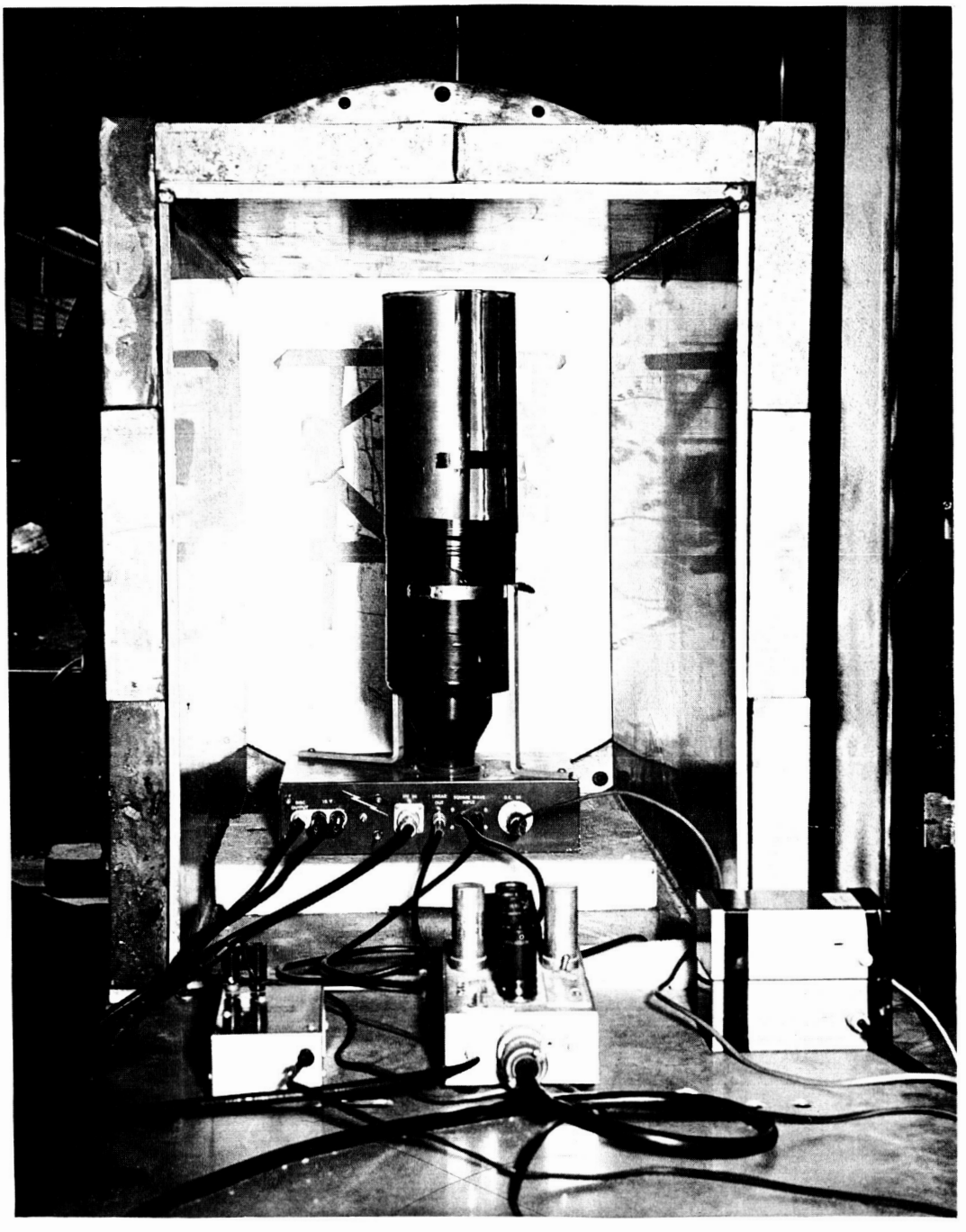

Fig. 48 -- Detector and lead housing

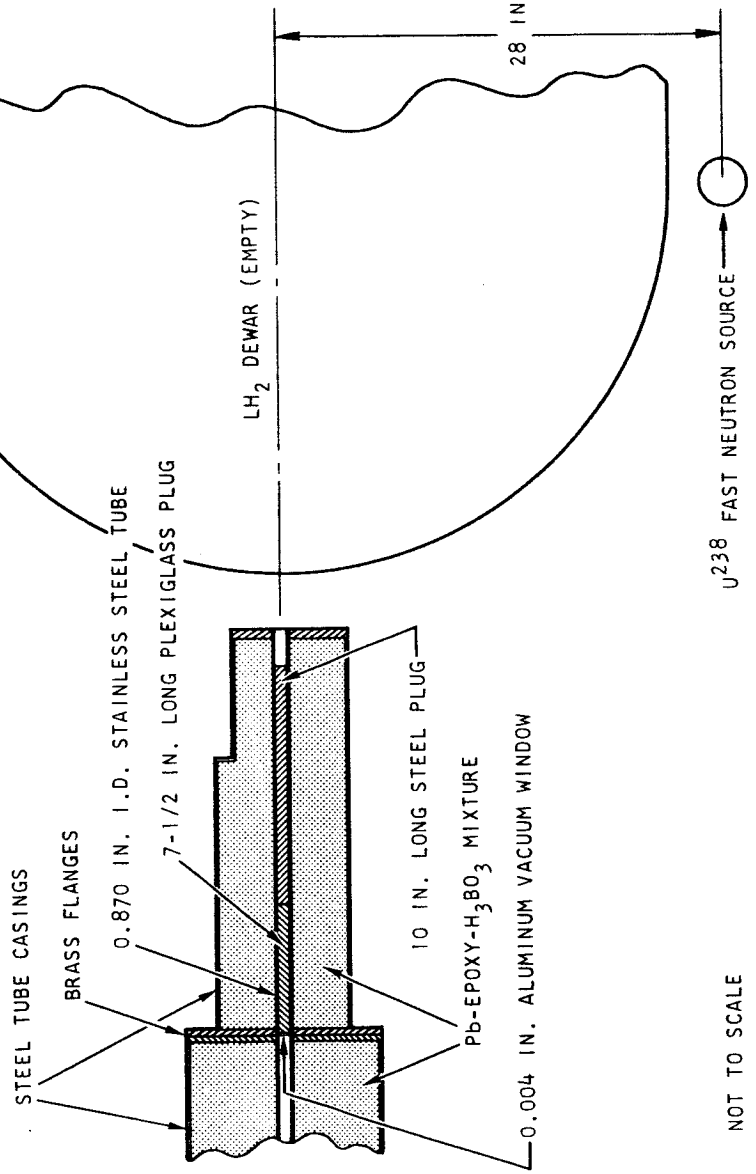

Fig. 49 -- Details of precollimator construction and shielding effectiveness experiment setup

corrected by increasing the shielding in this area by placing collars around the existing shielding as shown in Fig. 6.

In its final form, the effectiveness of the flight path shielding was tested by bombarding our U^{238} Linac target at a very high power level, approximately 2-1/2 feet off the flight path axis as shown in Fig. 49. The 0.870 inch precollimator was plugged at its assembly end with plexiglass and stainless steel rods to stop or scatter out all neutrons coming directly into the open portion of the flight path. Ambient background during this time was approximately 66 counts per minute; the transmitted plus ambient background was only 93 counts per minute so the difference of 27 counts per minute due to transmitted background was judged to be negligible. There was no real evidence of time dependence in this transmitted background, since it was evenly distributed in time. This setup also served to establish the lower limit of detection or background level of the 5 in. liquid scintillator. It was felt during the actual liquid hydrogen neutron spectrum measurements that this level had been reached at 78^{o} and 13 in. of liquid hydrogen and therefore data was taken for a relatively short time. However, by comparison with the results from the above experiment it was determined that this measurement was still 60% above the lower limit.

VI. TREATMENT OF THE DATA

6.1 DISCUSSION OF EXPERIMENTAL TECHNIQUE

The experimental technique adopted for this program made use of the time-of-flight principle with the Linear Accelerator providing a pulsed source of fast neutrons. Electrons from the linear accelerator with an energy of 27 $\pm$ 1 MeV impinge upon the 3 in. diameter depleted uranium sphere. The pulse width of the electron beam is 20 nanoseconds and the maximum current is 1.6 amps. These electrons are decelerated and stopped in the uranium target and in so doing produce bremsstrahlung radiation or, in other words, a continuous spectrum of radiation ranging from γ rays to x rays. The more energetic gamma rays, above about 5 MeV, interact with the uranium nuclei and produce neutrons either by a (γ, f) or a (γ, n) process, i.e., either by producing a fission or knocking out a neutron.

The time-of-flight technique sorts the neutrons by allowing them to travel a fixed distance (an evacuated flight path of 50 meters) and measuring their time of arrival after some time-zero reference. The time-zero reference is obtained by measuring, with the liquid scintillator located at the end of the flight path, the bremsstrahlung radiation burst produced by the electron beam pulse striking the target and adding the flight time of the γ rays which is 171 nanoseconds. The difference in

time between this fiducial point and the time of arrival of a neutron detection pulse produced by a proton recoil in the liquid scintillator is then a measure of the energy of the neutron since:

$$E = 1/2\ m\ v^2 = 1/2\ m \frac{x^2}{(t-t_o)^2}$$

$$t - t_o = g\ E^{-1/2} \text{ where } g = \sqrt{\frac{m\ x^2}{2}}$$

The "γ-flash" or bremsstrahlung burst is recorded in channel 37 of the Technical Measurements Corporation 201 time-of-flight unit. This fiducial point is recorded prior to running any neutron spectra since the TMC 201 time analyzer unit will only accept one pulse per electron beam pulse and since the γ flash occurs for each pulse, only the γ flash would be counted. During neutron spectrum measurements the fast neutron detector is not operative during the γ flash as explained in Section 5.3. The elapsed time spectrum is converted to a pulse height spectrum by the TMC 201 unit and analyzed into 512 intervals. The data for each burst of neutrons is accumulated in the memory of the TMC and although the linear accelerator is pulsed 360 times per second only about 1 neutron in several hundred bursts of neutrons for the angular measurements will be in such a direction and energy after its penetration through the liquid hydrogen that it will be detected. After many thousands of such bursts the number of neutrons for each time interval can be determined. The smallest time interval or time channel provided by the TMC 201 unit is 31.25 nanoseconds and this was used for all neutron spectrum measurements.

A typical resolution of the experiment with this flight path can be determined by considering that the uncertainty in the γ flash or fiducial point is one-half of the time channel or 15.625 nanoseconds and the uncertainty in the determination of a neutron pulse is also one-half a time channel for a total uncertainty of 31.25 nanoseconds. Since the flight time for a 10 MeV neutron is 970 nanoseconds and for a 1 MeV neutron it is 3500 nanoseconds and $\frac{\Delta E}{E} = \frac{2\Delta t}{t}$, then the energy resolution for a 10 MeV neutron is $\pm 6\%$ and for a 1 MeV neutron it is $\pm 2\%$.

The neutron bias for the fast neutron detector is 0.22 MeV or time channel 283. Therefore, only counts recorded up to channel 283 are time correlated to Linac neutrons pulses and the remaining 228 of the 512 time channels can be used to determine the background for each measurement since counts received in these channels are not time correlated to the Linac neutron pulses.

Neutron spectrum measurements were made for thicknesses of 0, 2.5, 4.5, 7, 10.5, and 13 in. of liquid hydrogen for angles of 0°, 15°, 37°, 53°, and 78°. All thicknesses for each angle were completed during one measurement period. This was done since considerable set-up time was required to change from one angle to another. For each measurement the fast neutron source was monitored by two different methods described in Section 5.4.

Details of the geometry for the angular neutron spectrum measurements are shown in Figs. 7, 15, and 50. As can be seen by these figures, every attempt has been made to minimize the mass of material near the center of the dewar. The fast neutron source remained in a fixed geometry for every measurement, i.e., as the thickness of liquid

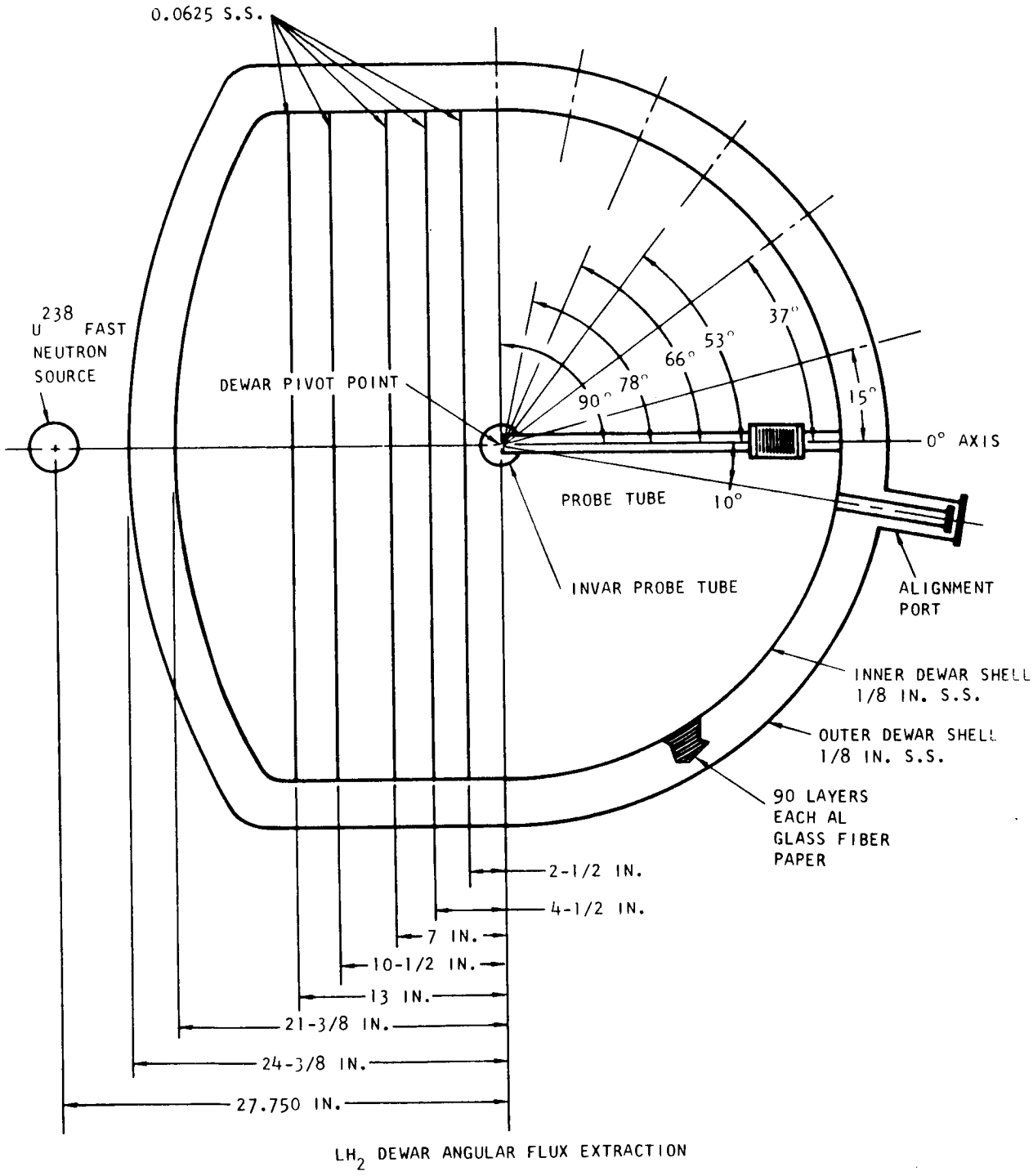

LH_2 DEWAR ANGULAR FLUX EXTRACTION

Fig. 50 -- LH_2 experimental dewar baffle spacings

hydrogen increased the distance between the first liquid hydrogen surface and the center of the fast neutron target decreased. The exact distances from the center of the fast neutron target to the first surface of liquid hydrogen is shown in Fig. 50 for each thickness. Also shown are the thicknesses of the inner and outer torispherical heads and the baffles. Located between the inner and outer heads is the multilayer insulation; It is composed of 90 layers of 0.0007 in. aluminum foil interspersed between 90 layers of 0.002 in. glass fiber paper (borosilicate glass). This amounts to a total of 0.063 in. of aluminum and 0.18 in. of glass fiber paper.

The baffles are 0.0625 in. 304 stainless steel. After each integral layer of liquid hydrogen there is a baffle, i.e., for 13 in. of liquid hydrogen the baffle would start at 13 in., for 2.5 in. of liquid hydrogen the baffle would start at 2.5 in., and so on.

6.2 DETECTOR SENSITIVITY

The detector sensitivity can be divided into two parts: the detector efficiency G(E), and the flight path transmission T(E). The product of these G(E) T(E) will be called S(E) the detector sensitivity.

6.2.1 Detector Efficiency

The detector efficiency for the 2-1/2 by 2 in. diameter NE 211 liquid scintillator fast neutron detector was taken from the experimental results of Batchelor, et al., for an identical liquid scintillator. The detector efficiency $G_2(E)$ is shown in Fig. 51. The data up to 3.5 MeV

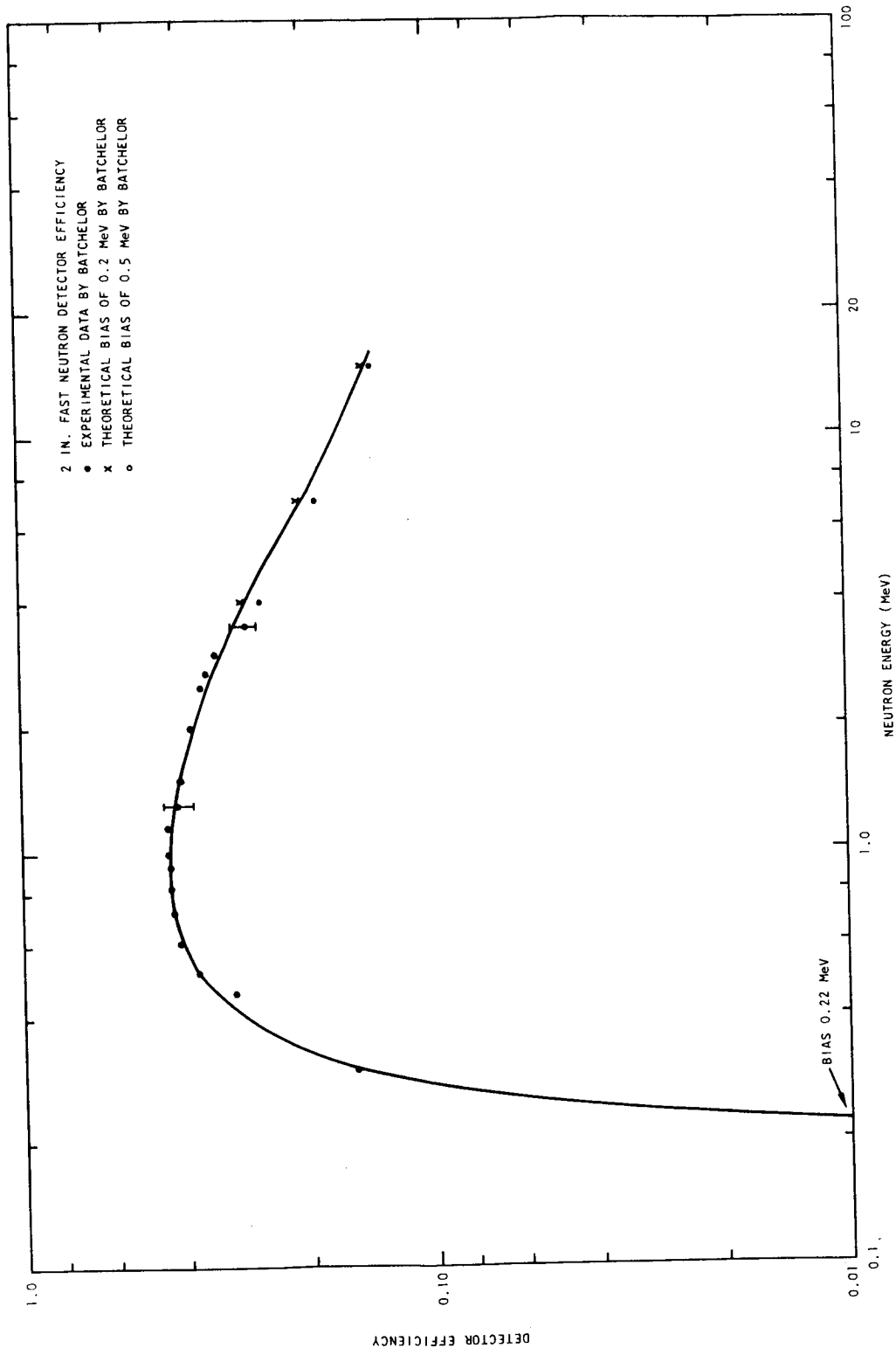

Fig. 51 -- Two inch liquid scintillator efficiency

are the experimental efficiency and the data from 3.5 MeV to 15 MeV are the theoretical efficiency also taken from the work of Batchelor, et al. The uncertainty in this data is less than 10%. One interesting thing to note about the efficiency curve is the relative insensitivity to a change of bias after about 4 MeV. The difference between the 0.2 and 0.5 MeV bias is 12% at 4 MeV and becomes less at the higher energies. This follows from the fact that a given energy neutron yields a continuous energy spectrum of "recoil" protons. However, the fraction of detected recoils is dependent upon the neutron bias energy and this fraction is less sensitive to the neutron bias as the value of the initial neutron energy increases.

The detector efficiency for the 5 in. fast neutron detector is determined by comparison with the 2 in. fast neutron detector. The method of calibration is as follows: a rather arbitrary neutron spectrum is measured with the 2 in. detector after the bias has been adjusted to 0.22 MeV using the technique described in Section 5.3. This arbitrary neutron spectrum could be obtained from a fast neutron source attenuated by 4 in. of lead since lead has a fairly smooth total cross section. This same arbitrary neutron spectrum is then measured using the 5 in. detector after this detector has been properly biased to 0.22 MeV. If

$N_2(E)$ = number of neutrons counted per unit energy for the 2 in. detector

$G_2(E)$ = detector efficiency of 2 in. detector

$N_5(E)$ = number of neutrons counted per unit energy interval for the 5 in. detector

$G_5(E)$ = detector efficiency of 5 in. detector

$N(E)$ = true number of neutrons per unit energy interval

$T(E)$ = transmission of the flight path

since $N_5(E) = G_5(E)T(E)N(E)$

and $N_2(E) = G_2(E)T(E)N(E)$

then $$G_5(E) = \frac{N_5(E)}{N_2(E)} G_2(E) .$$

Therefore, it is only necessary to take the ratio of the neutrons counted per unit energy interval for the two detectors and multiply this by the efficiency for the 2 in. detector.

The detector efficiency for the 5 in. detector $G_5(E)$ is shown in Fig. 52. It is desirable but not necessary that the 5 in. detector be biased at 0.22 MeV since the ratio of the 5 in. to the 2 in. detectors will still give the proper G(E) for that bias. What is important is that the same neutron bias for the 5 in. detector is used when the G(E) of the detector is measured as when the neutron spectra are measured.

6.2.2 Flight Path Transmission

Attenuation of the neutron flux over the flight path is calculated in a straightforward manner. If

$T(E)$ = transmission

N_i = atom density in units of atoms/cm^3 for the i^{th} element

$\sigma i\ (E)$ = cross section for element i

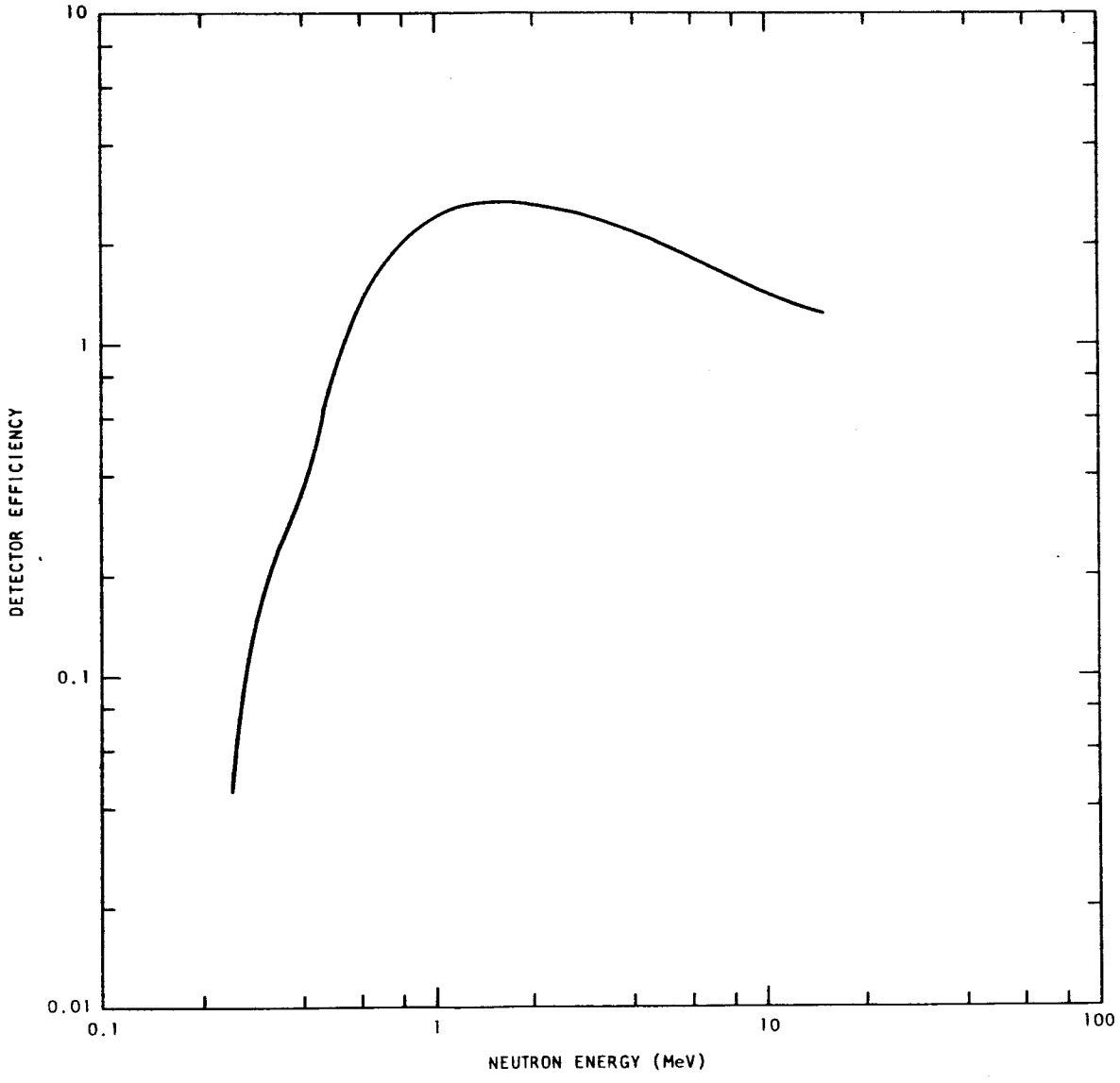

Fig. 52 -- Five-inch liquid scintillator efficiency

t_i = thickness for element i

then $T(E) = e^{-\sum_i N_i \sigma_i t_i}$

The thickness of material in the flight path is as follows:

Air: 126 in. of air gap between evacuated sections

Aluminum: 0.004 in. and 0.010 in. windows on first evacuated section, 0.025 in. on each window of the second evacuated section, and 0.040 in. on each window of the third evacuated section.

Helium: 21.1 in. in probe tube at 20°K and 5 psig.

304 Stainless Steel: 0.0726 in. average thickness of inner window in head, 0.0789 in. average thickness of outer window in head, 0.0312 inner cap on probe tube, and 0.035 outer cap on probe tube, a total of 0.2177 in.

Water: Assume 50% relative humidity for 126 in. of air at 72°F and standard atmospheric pressure.

$$\text{Then } \sum_i N_i \sigma_i t_i = (1.26 \times 10^{-2})\sigma_N + (3.50 \times 10^{-3})\sigma_O + (2.07 \times 10^{-4})\sigma_H + (2.21 \times 10^{-2})\sigma_{Al} + (2.64 \times 10^{-2})\sigma_{He} + (3.40 \times 10^{=2})\sigma_{Fe} + (.456 \times 10^{-3})\sigma_{Ni} + (9.79 \times 10^{-3})\sigma_{Cr}$$

The flight path transmission varies between 70 and 80% with energy.

6.3 REDUCTION OF DATA

Data was obtained from the TMC analyzer in the form of a printed tape and punched paper tape bearing counts versus channel number (address). The punched paper tape was used to convert to cards for use with the IBM 7040. The code used to reduce the data is called ECTOPLASM. Essentially ECTOPLASM converts neutron time-of-flight spectra into

energy spectra. ECTOPLASM performs the following functions:

1. Corrects for count rate losses
2. Subtracts the background
3. Normalizes each run by use of the monitor counts
4. Converts time into energy
5. Corrects for the energy dependent sensitivity, S(E), of the fast neutron detector
6. Groups the data for both a given energy and statistical error.

6.4 BACKGROUND AND AFTERGLOW CORRECTION

The observed time spectra are contained in the data tapes from the TMC. A typical time spectrum is plotted in Fig. 53 where the abscissa is shown for channel number and energy.

Each time spectrum contains a background which must be determined prior to reduction by ECTOPLASM. This background is composed of two parts: a steady state background and an afterglow background.

The steady state background is composed of the ambient background and a capture gamma background due to fast neutrons thermalizing and being captured in the vicinity of the fast neutron detector. This steady state background is determined by summing the time channel counts from channel 412 to 512 and dividing by 100 to obtain the average background. However, as mentioned previously, a count rate loss correction must be applied since the TMC 201 unit will only accept at most one neutron pulse for each Linac beam pulse. If

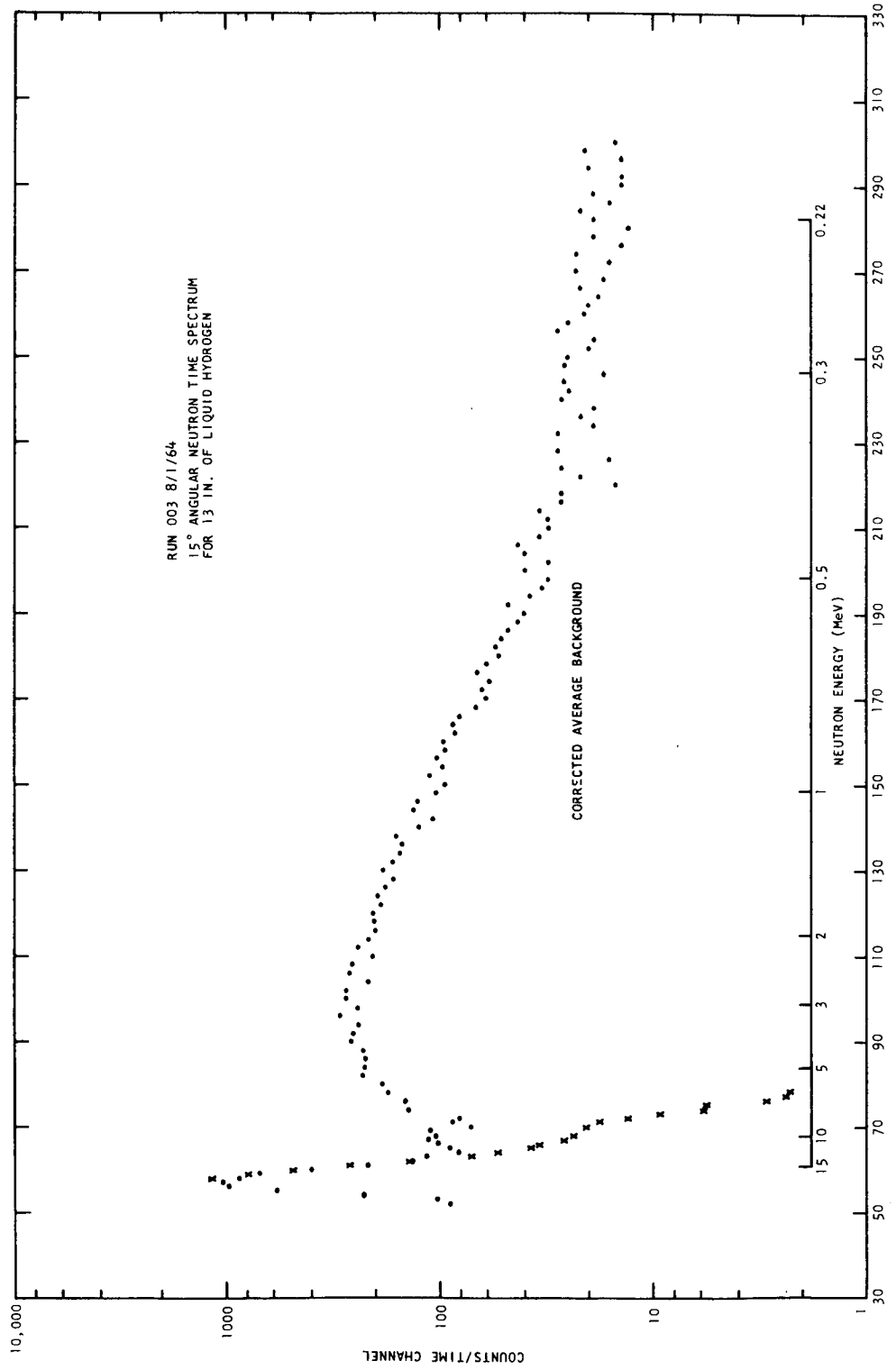

Fig. 53 -- Typical time vs. counts spectrum

n_i = number of counts for the ith time channel

ℓ = number of Linac beam pulses

$\sum_{j=f}^{i-1} n_j$ = summation of all counts from the first time channel which contains data up to the time channel of interest

then the corrected counts for time channel i are:

$$n_i(\text{corr}) = \frac{\ell n_i}{\ell - \sum_{j=f}^{i-1} n_j}$$

This method of correcting the background was important only for the 0^o angle and the empty dewar measurements where the ratio $\frac{\ell}{\sum_{j=f}^{i-1} n_j}$ was about 5. For all other measurements this ratio was 100 or more.

As mentioned previously, when the γ flash occurs the fast neutron detector gain is reduced a factor of 10^3 due to a reverse bias in dynodes 2 and 4 of the phototube. However, the γ flash is sufficiently intense to create an afterglow. The fast neutron pulses are amplified by a factor of 10^3 greater than the γ flash pulses. If the γ flash is sufficiently large, this gain increase catches the "tail-off" portion of the γ flash and produces what is called the "afterglow." This afterglow therefore constitutes the second source of background. It is possible to eliminate the afterglow at the sacrifice of one of two things. Either the neutron bias must be raised cutting off the low energy neutron response or the delay after the γ flash increased cutting off a portion of the high energy end of the neutron spectrum. The afterglow does not occur for each Linac beam pulse or only the afterglow

would be measured since the TMC 201 unit will accept only one count per Linac beam pulse. However, there is always a struggle between neutron intensity as seen by the fast neutron detector and the amount of afterglow. The usual procedure is to increase the Linac power on target until a small amount of afterglow occurs. This means essentially that the level of the afterglow is sometimes large enough to override the bias. The problem of the afterglow becomes greatly exaggerated with liquid hydrogen. This is so since the number of scattered gamma rays seen by the detector for a given Linac power remains essentially the same for all thicknesses of liquid hydrogen because of the poor γ-ray attenuation of hydrogen but the neutron attenuation increases rapidly. Therefore, the ratio of the afterglow peak counts to the neutron peak counts increases with increasing thicknesses of hydrogen.

The afterglow or die-away of the scintillations within the liquid scintillator has been measured. This was done by viewing a carbon target bombarded with a 17 MeV electron beam with the fast neutron detector. The maximum bremsstrahlung energy is therefore 17 MeV and lower than the (γ, n) threshold in carbon. To make sure that only bremsstrahlung was detected by the fast neutron detector, 8 in. of paraffin was placed at the 16-meter end of the 50-meter flight path. The afterglow is shown in Fig. 54. Here it can be seen that there is a fast component decaying by a series of jumps into a longer component. This measured afterglow was used to obtain the afterglow background. First

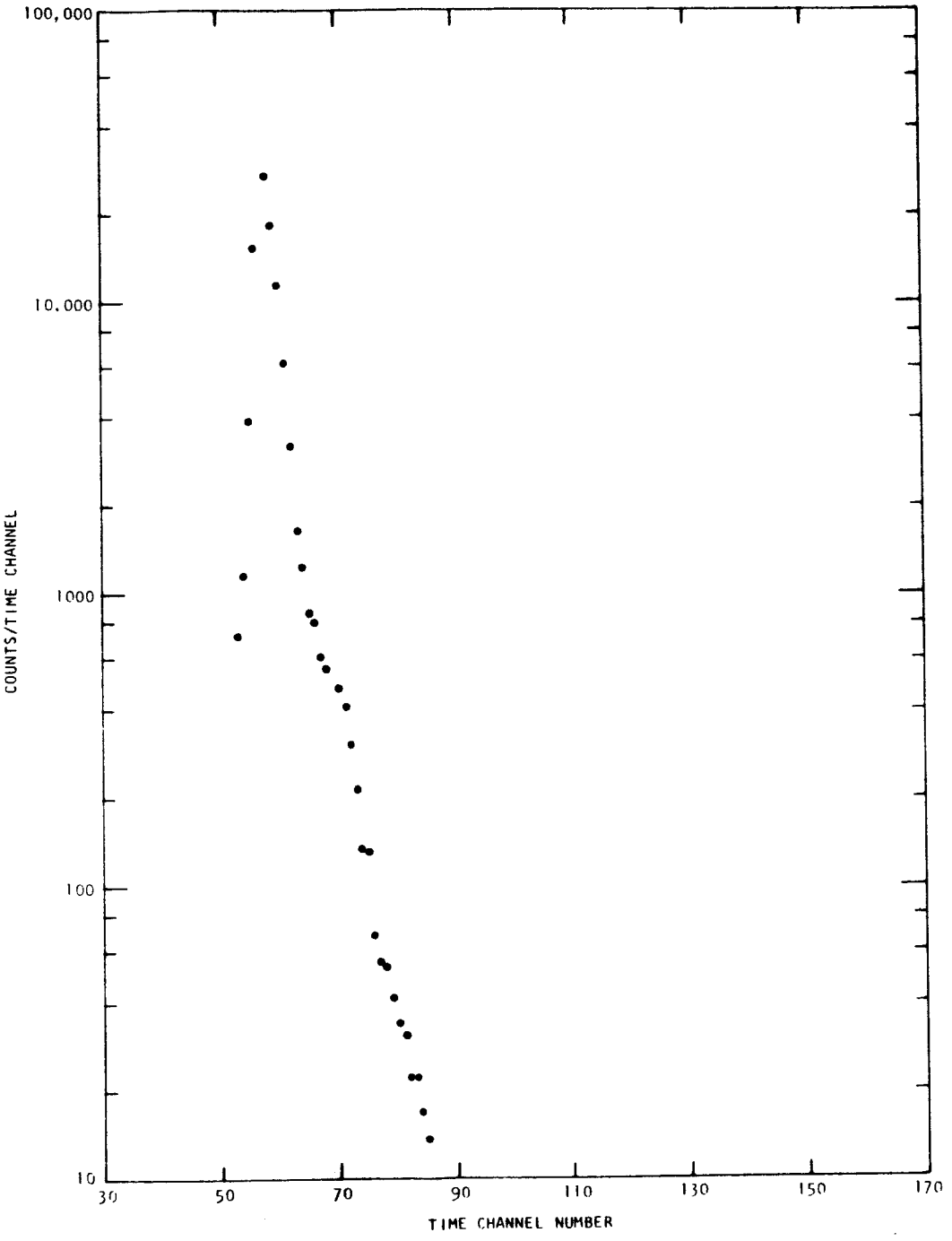

Fig. 54 -- Liquid scintillator afterglow

the steady state background is subtracted from the afterglow background and the data replotted, then the experimentally obtained afterglow, which is shown in Fig. 54, is used as an overlay and fitted to the afterglow portion of the fast neutron time spectrum. Both the steady state and afterglow background subtraction is shown in the time plot in Fig. 53, and the steady state background has already been subtracted from the afterglow background. This background then serves as the background input to the code ECTOPLASM. It can not be subtracted from the data prior to insertion into ECTOPLASM since a proper count rate loss would not be made.

6.5 ACTIVATION MONITORS

The aluminum activation monitors were used to normalize the intensity of the fast neutron source from one experiment to the other. A tabulation of the values for each experiment is shown in Table 1.

TABLE 1

Values of Activation Monitors for Normalizing Reduced Data

Angle (Degrees)	Thickness of Liquid Hydrogen (in.)	Corrected Count Rate C/M
0	13.0	2,222.0
0	10.5	2,073.3
0	7.0	1,413.0
0	4.5	916.7
0	2.5	1,178.2
0	0	905.7
15	13.0	23,293.4
15	10.5	32,164.2
15	7.0	23,793.5
15	4.5	14,151.5
15	2.5	11,545.5
15	0	6,462.2
37	13.0	71,846.6
37	10.5	62,630.9
37	7.0	52,344.3
37	4.5	55,442.6
37	2.5	42,377.8
37	0	25,825.5
53	13.0	58,969.1
53	10.5	33,682
53	7.0	49,942.1
53	4.5	35,054.5
53	2.5	36,415.5
53	0	11,175.7
78	13.0	7,963.9
78	10.5	53,234.6
78	7.0	70,166.6
78	4.5	47,345.4
78	2.5	48,178.9
78	0	15,086.9

VII. RESULTS

7.1 DIFFERENTIAL FAST NEUTRON SPECTRA IN WATER

Fast neutron spectrum measurements were made only for the 3.84 and 20 cm water thicknesses. These two thicknesses of water were chosen since they are equivalent (on a hydrogen number density basis) to the minimum and maximum amount of liquid hydrogen which were intended to be measured. Differential fast neutron spectra were measured at angles of 0, 15, 37, 53, 66, 78, and 90° for the 3.84 cm water thickness and at angles of 0, 53, and 90° for the 20 cm thickness. These measurements were made to verify the experimental techniques to be used with liquid hydrogen and no special attempt was made to obtain a high degree of statistical accuracy.

In these measurements a constant source-to-surface of the water slab geometry was maintained. In this respect they differed from the liquid hydrogen measurements since the source remained at a fixed position for the latter.

Differential fast neutron spectra for the 3.84 cm slab of water at 0, 15, 37, and 53° angles are shown in Fig. 55. The 66, 78, and 90° measurements are not shown since low intensities and inadequate collimation shielding, as explained in Section IV, make these measurements highly dubious.

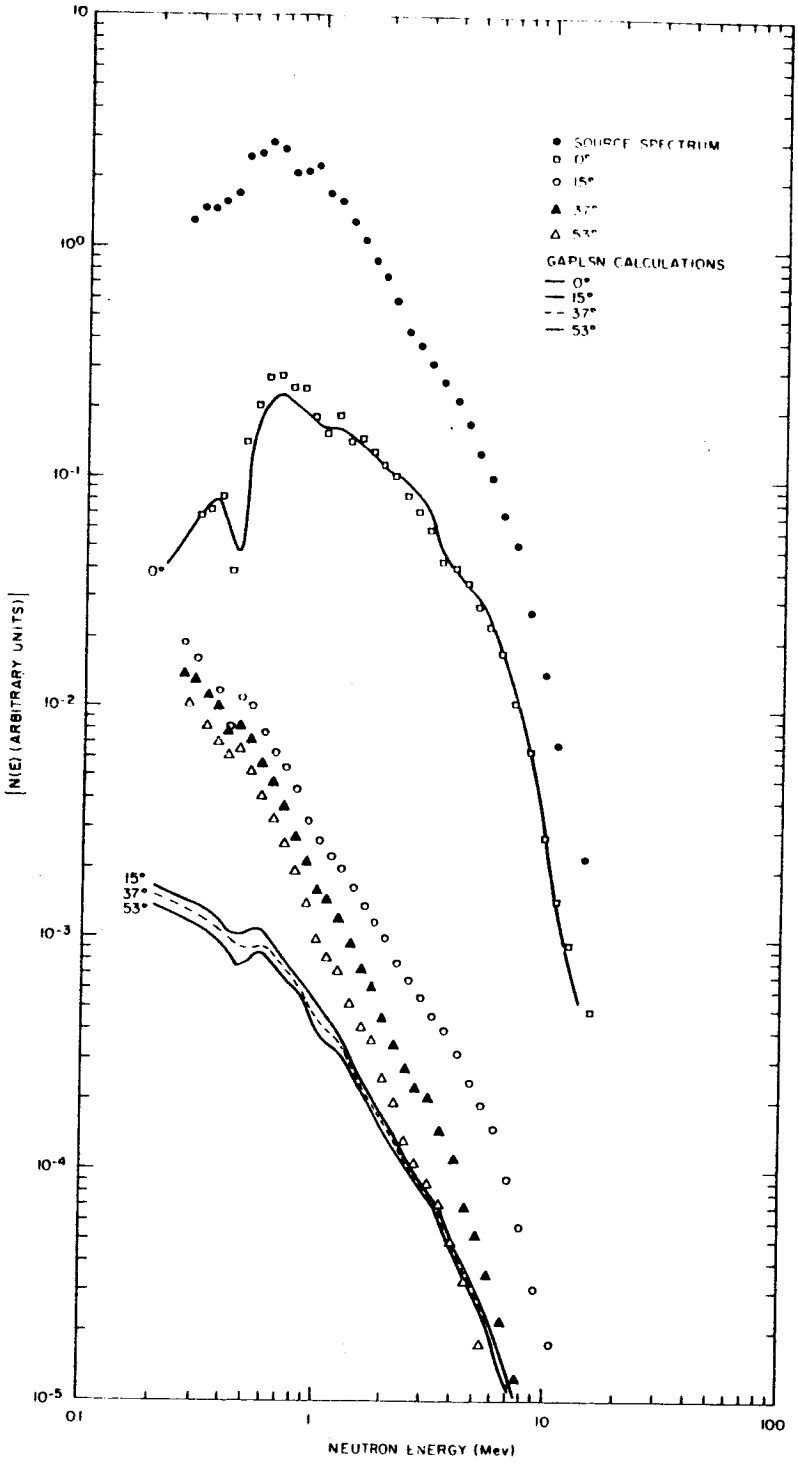

Fig. 55 -- Fast neutron spectra in 3.84 cm of water at 0^{o}, 15^{o}, 37^{o}, and 53^{o}

Theoretical calculations were performed using the one-dimensional transport theory code GAPLSN.[3] These calculations are also shown in Fig. 55. The source input to GAPLSN is shown in Fig. 56 and was treated as a surface source with normal incidence to the water slab. The 0.25 in. thick iron in the water tank surface was treated as a boundary and the iron baffles were homogenized over the space between this iron boundary and the surface of the water slab. The agreement between theory and experiment for the 0° direction is rather good. However, neither the shape nor the relative intensities for the 15, 37, or 53° angular spectra is in good agreement with the experimental measurements. A part of this disagreement is due to the fact that the source geometry has not been prescribed exactly. Experimentally, the source approximates an isotropic point source. Probably the best approximation within the framework of GAPLSN is an isotropic volume source in spherical geometry.

The source spectrum shown in Fig. 55 is not the true source spectrum but rather the empty water tank measurement and serves to correct the 0° angular spectrum measurement for those neutrons which are transmitted through the water slab and do not undergo a scattering collision. It differs from the true source spectrum shown in Fig. 56, inasmuch as the precollimator is not designed to view the entire fast neutron source and the source is viewed through approximately one centimeter of iron. In Fig. 56 a large precollimator opening was used

3. Alexander, H. H., G. W. Hinman, and J. R. Triplett, "GAPLSN - A Modified DSN Program for the Solution of the One-dimensional Anisotropic Transport Equation," GA-4972, March, 1964.

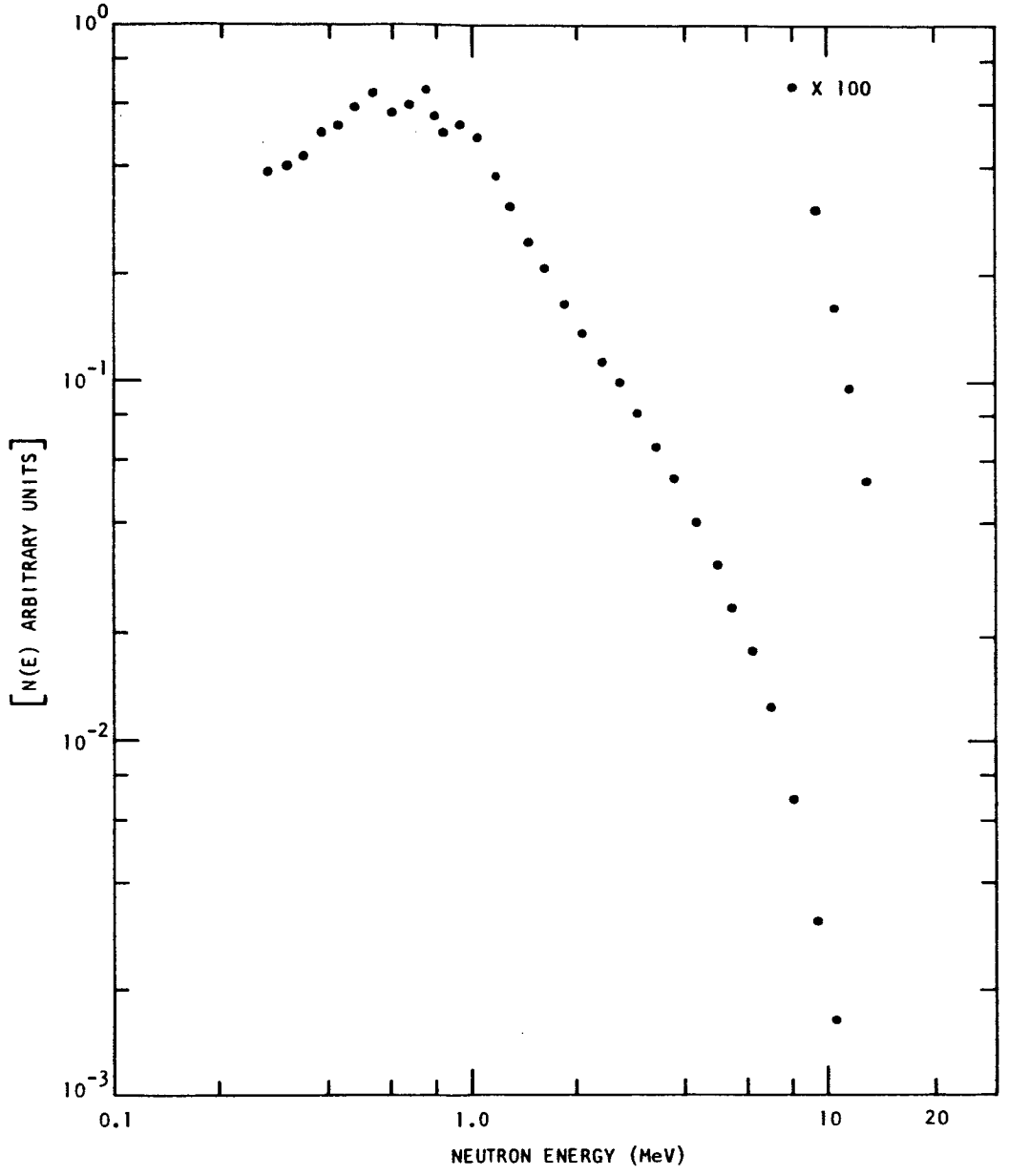

Fig. 56 -- Two inch uranium source spectrum

and the entire source spectrum can be viewed by the fast neutron detector. This spectrum was used as the source input for the GAPLSN calculations.

Figure 57 is a comparison of the fast neutron spectra for the 0^{o} direction for the 3.84 and 20 cm slabs of water. These data show quite vividly the effect of the oxygen resonances at 0.44, 0.98, 1.3, 1.8, and 3.5 MeV. This figure also illustrates the effect of increased hydrogen scattering at the lower neutron energies in producing an apparent shift of the peak energy to a higher value.

The 53 and 90^{o} angular spectra for the 20 cm slab of water hav not been shown. These data appear to be unreliable.

7.2 DIFFERENTIAL FAST NEUTRON SPECTRA IN LIQUID HYDROGEN

Differential fast neutron spectra were measured at angles of 0, 15, 37, 53, and 78^{o}. At each angle, measurements were made for 13, 10.5, 7, 4.5, and 2.5 in. of liquid hydrogen and for the empty dewar. The fast neutron source spectra for these measurements are shown in Fig. 44. A large precollimator opening was used and the entire source spectrum was viewed by the fast neutron detector. These spectra would serve as the source input for theoretical calculations and are tabulated in Table 2. (see page 157).

The differential neutron spectra in liquid hydrogen are shown in Figs. 58, 59, 60, 61, and 62 and are tabulated in Table 2. These spectra have been normalized by use of aluminum activation monitors discussed in Section 5.4 and tabulated in Table 1 of Section 6.5. The absolute

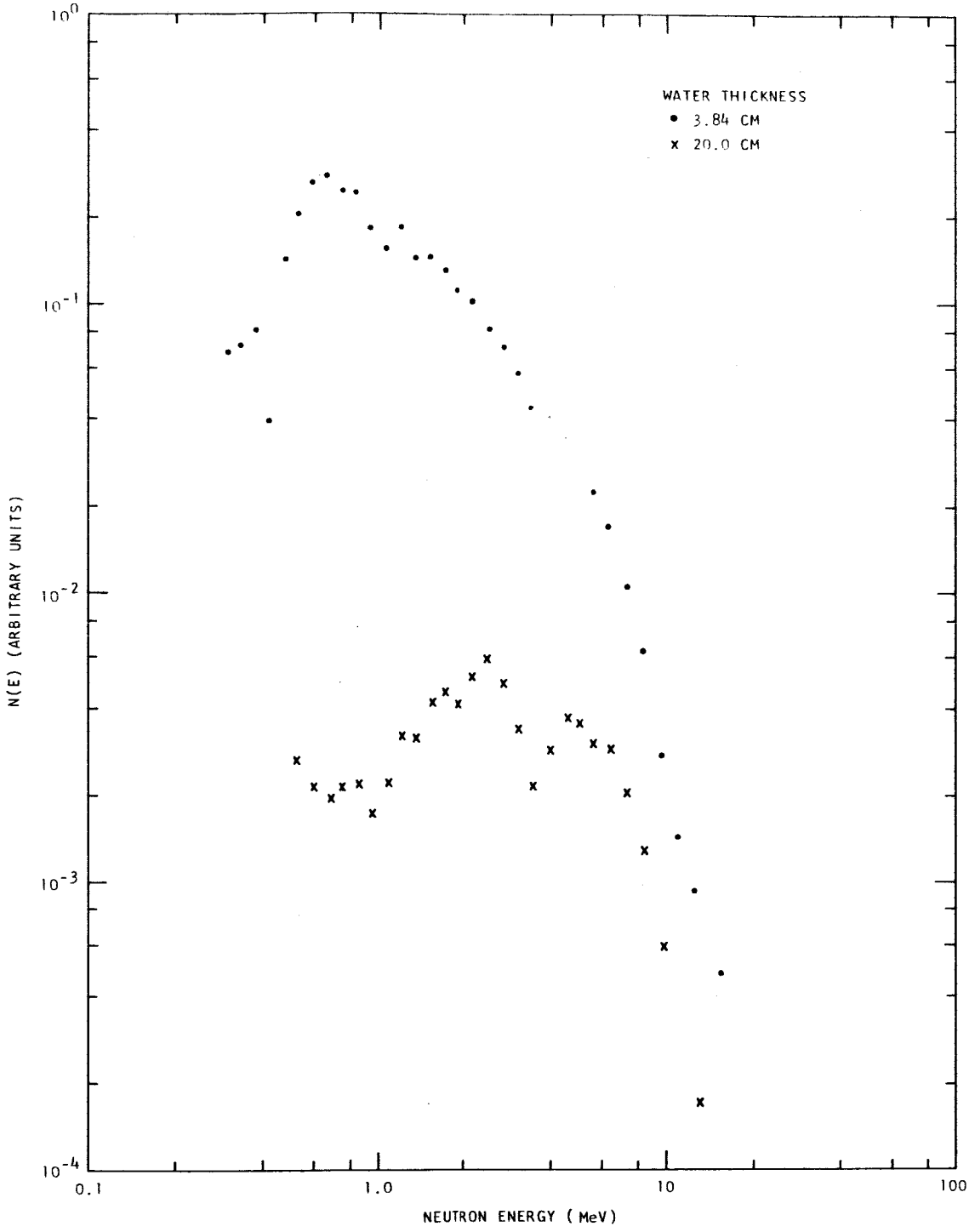

Fig. 57 -- Fast neutron spectra at 0^{o} for 3.84 cm and 20 cm of water

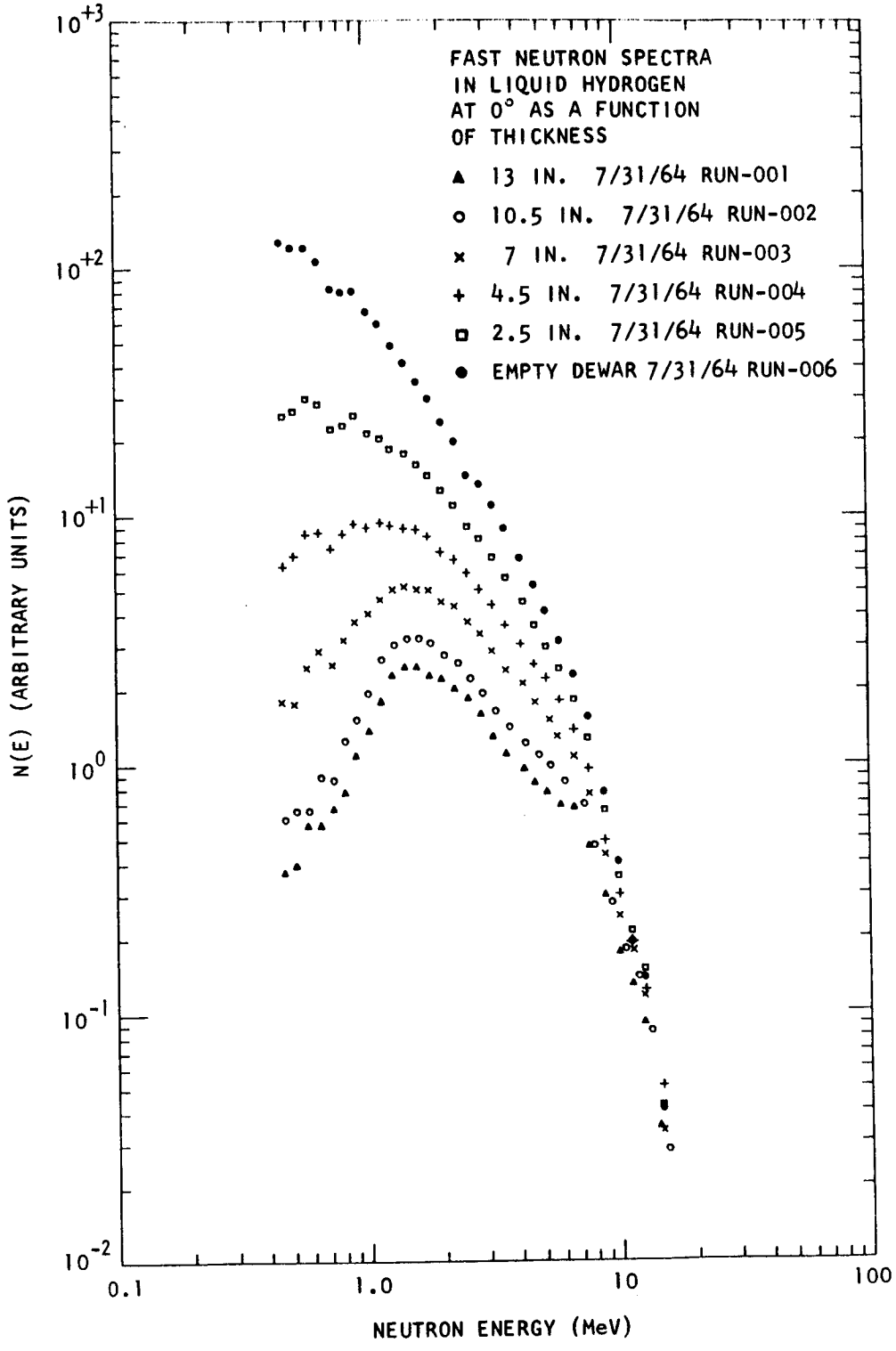

Fig. 58 -- Fast neutron spectra in LH_2 at 0^{o} as a function of thickness

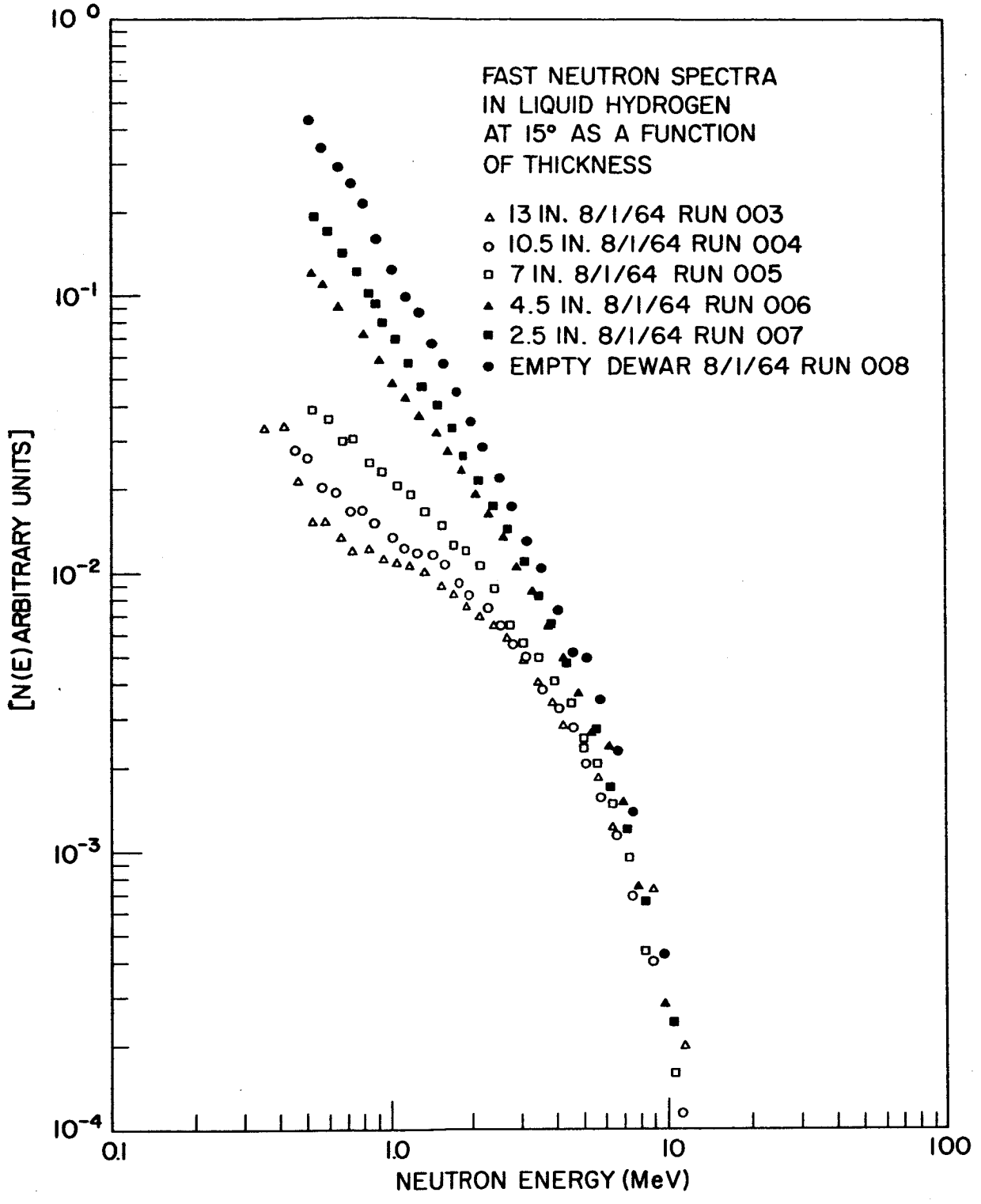

Fig. 59 -- Fast neutron spectra in LH_2 at 15° as a function of thickness

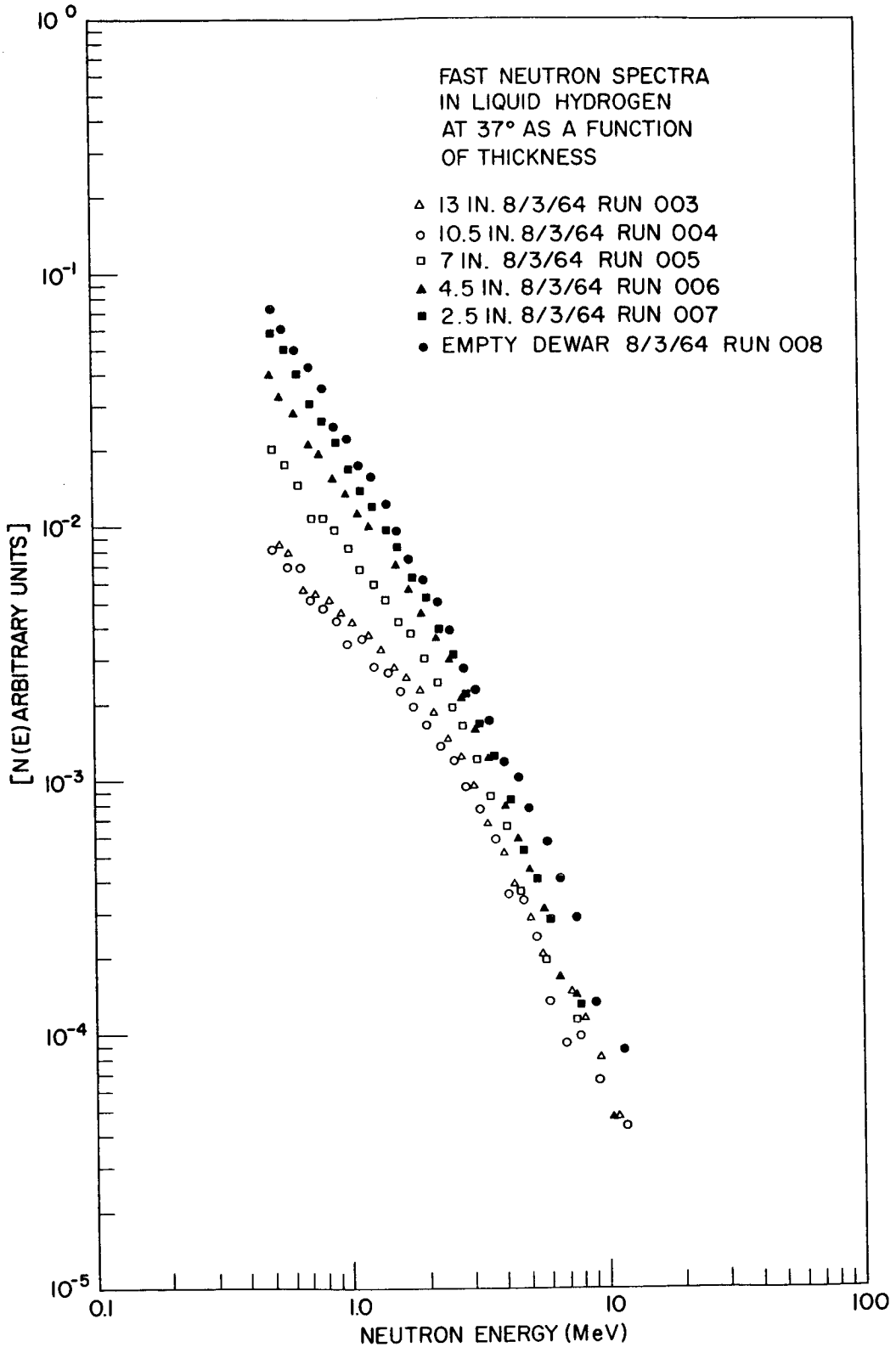

Fig. 60 -- Fast neutron spectra in LH_2 at 37^{o} as a function of thickness

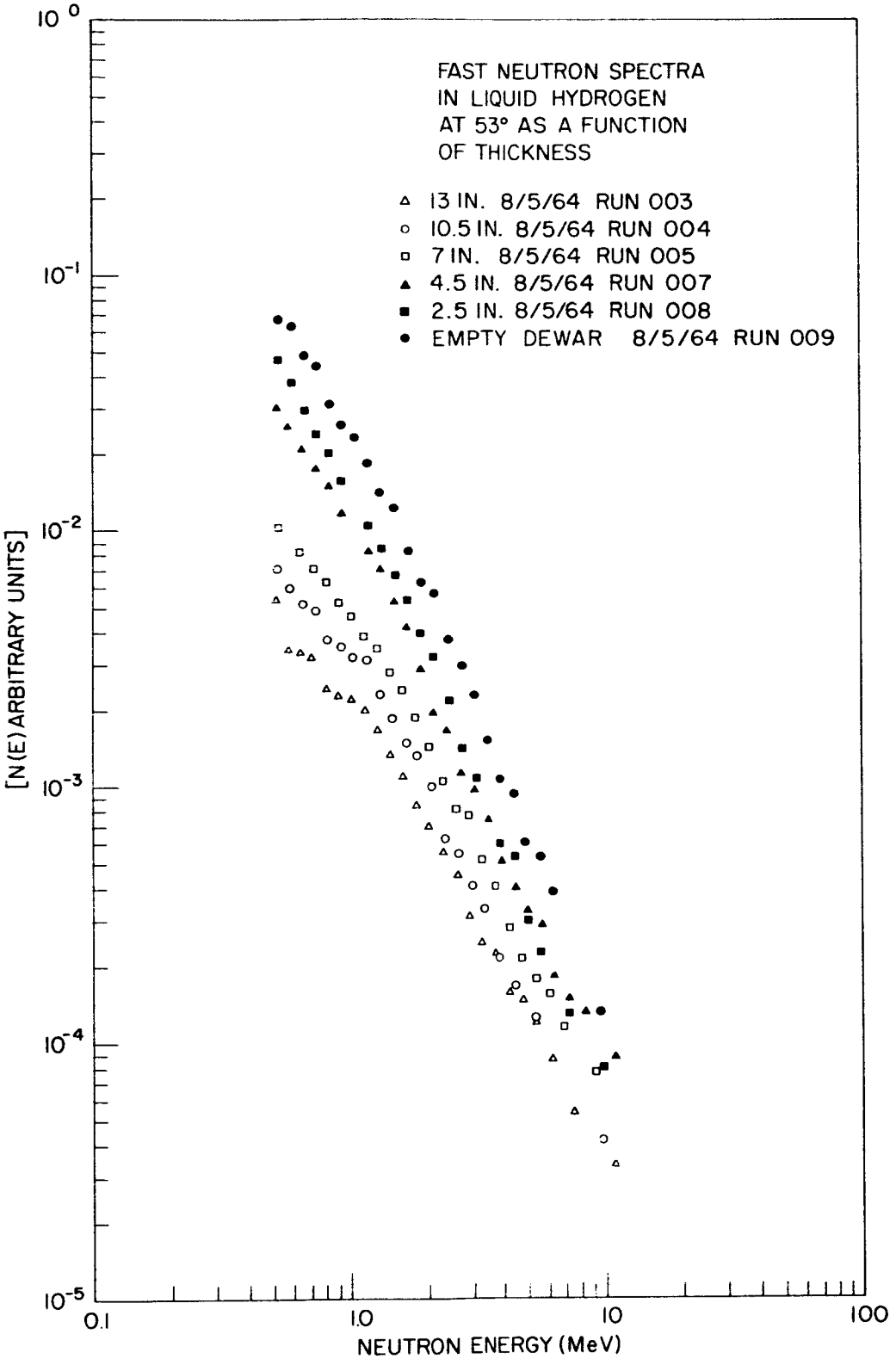

Fig. 61 -- Fast neutron spectra in LH_2 at 53^{o} as a function of thickness

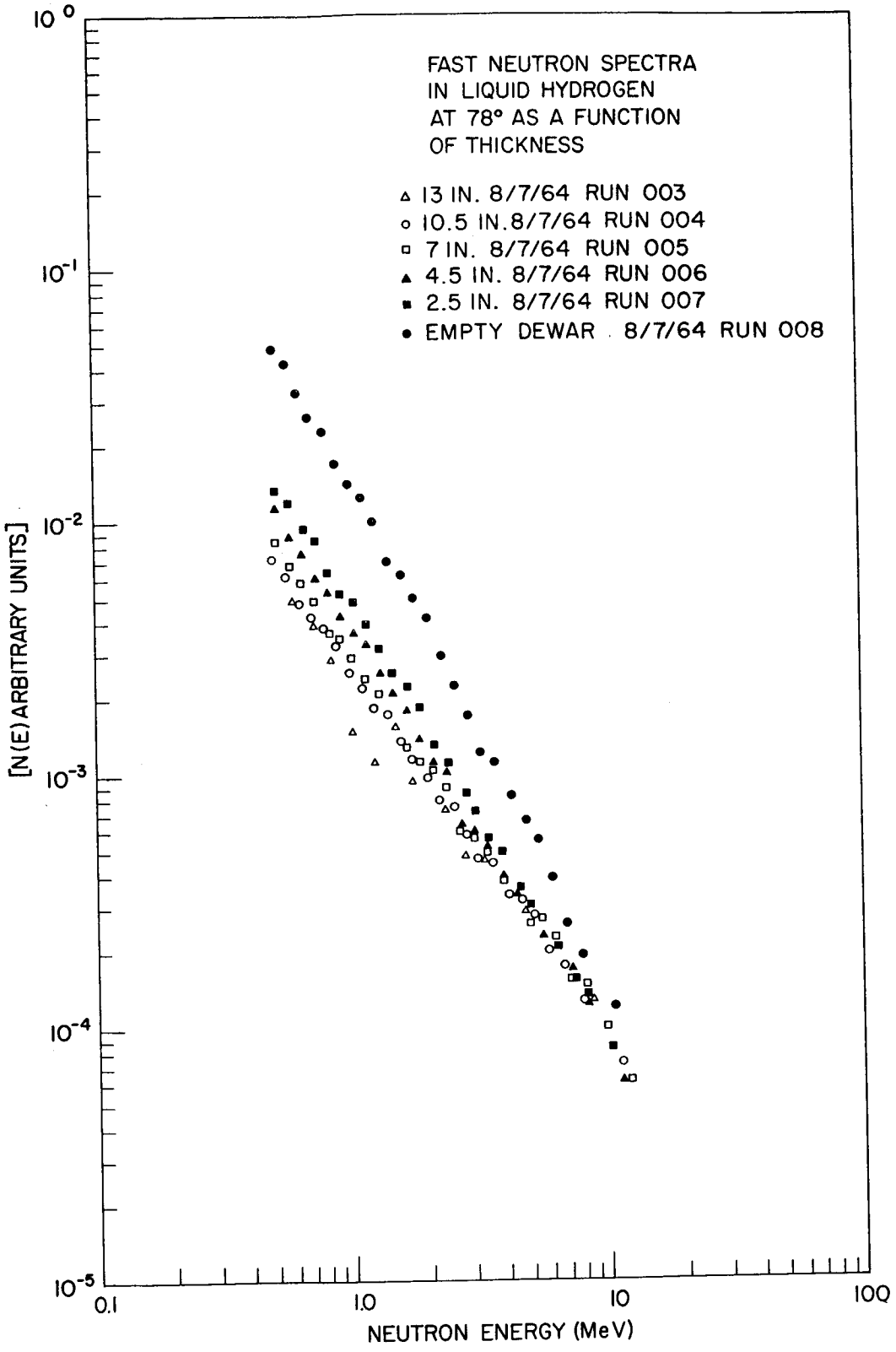

Fig. 62 -- Fast neutron spectra in LH_2 at 78° as a function of thickness

intensity of the source spectrum is arbitrary, i.e., it is not normalized with respect to the liquid hydrogen spectra. Also shown in Table 2 is the statistical error, $\Delta N/N$, for a fixed energy resolution, $\Delta E/E$, of 10%.

Referring to the graphs in Figs. 58 to 62, it may be seen that the data appear to converge at the higher energies and diverge at the lower energies. This can be attributed directly to the hydrogen cross section which is fairly large at low energies and very small at high energies.

In Fig. 60 for the 37^{o} angular spectra, it can be seen that the 10.5 and 13.0 in. thicknesses of liquid hydrogen are almost identical. For a given angle, measurements start at the largest thickness of 13.0 in. and proceed to the smallest thickness of 2.5 in. Therefore, the only plausible explanation for this result is that when compartment No. 4 was measured, which is the 10.5 in. thickness, chamber No. 5, which corresponds to the 13.0 in. thickness, was not completely empty.

The fast neutron source for all of the liquid hydrogen measurements remained at a fixed position. Therefore, the distance between the source and first liquid hydrogen surface changed as the thickness of liquid hydrogen changed. There were two possibilities in conducting the experiment: (1) the source could be moved for each measurement so that the distance from the source to the first liquid hydrogen layer was fixed, and (2) the source could remainfixed as mentioned above. In either of these cases, the same number of theoretical calculations must be performed. There are at least two advantages to keeping the source

position fixed. The first is an increase in the solid angle subtended by the first liquid layer as the thickness of this layer increases. This increases the counting rate as seen by the fast neutron detector. The second advantage lies in that only one measurement is required at each angle in order to obtain the empty dewar neutron spectrum. If the source to surface of the dewar was changed, an empty dewar neutron spectrum would be needed for each position of the source. Since the effect of the containment vessel is a very real part of any theoretical calculation, the empty dewar measurements serve as a methods test for just the containment vessel. The empty dewar measurements also enter indirectly into each measured spectrum since this is a secondary source viewed directly through the intervening thickness of liquid hydrogen. From the studies performed in this program one would expect generally the neutron scalar and angular fluxes in the first foot of liquid hydrogen to be influenced appreciably by (1) containment design, (2) intervening shields or structure between the source and the hydrogen tank, and (3) the general surroundings of the source dewar arrangement if they are not sufficiently distant. The third effect has been shown to be small in our case. The first two effects are at a bare minimum also in these experiments. However, they are present and would be expected to even play an even more important role in practical applications such as the determination of energy deposition in a hydrogen propellant exposed to fast leakage neutrons from a nuclear reactor.

Table 2

RUN 001
5-23-64

3.0 IN. DIAMETER URANIUM SOURCE AT 180°

E	N(E)	DELTA(N)/N
1.0743464+07	5.2407596-03	0.1025
9.6321895+06	1.2510146-02	0.1144
8.9216836+06	2.2175518-02	0.0636
8.0853443+06	3.5105180-02	0.0533
7.3613354+06	6.3506696-02	0.0431
6.7304034+06	9.2436377-02	0.0384
6.1772503+06	1.3527595-01	0.0336
5.6895964+06	1.7641432-01	0.0316
5.2574938+06	2.1616716-01	0.0308
4.8728137+06	2.7525037-01	0.0291
4.5288621+06	3.2328231-01	0.0285
4.2200852+06	4.0105976-01	0.0269
3.9418452+06	4.3733461-01	0.0267
3.6902438+06	5.0398247-01	0.0256
3.4619861+06	5.5303402-01	0.0248
3.2542707+06	5.7002785-01	0.0244
3.0647045+06	5.6354189-01	0.0250
2.8912331+06	6.5831652-01	0.0234
2.7320846+06	6.7479723-01	0.0224
2.5857244+06	7.3438882-01	0.0218
2.4508182+06	8.4682106-01	0.0212
2.2970023+06	9.0796906-01	0.0169
2.1302853+06	1.0662907+00	0.0162
1.9810831+06	1.2853286+00	0.0157
1.8470252+06	1.5619563+00	0.0146
1.7261292+06	1.9240120+00	0.0140
1.6167267+06	1.7393274+00	0.0150
1.5174056+06	2.3448429+00	0.0135
1.4269641+06	2.5646811+00	0.0135
1.3443744+06	2.8113680+00	0.0137
1.2687532+06	3.2533643+00	0.0131
1.1993379+06	3.5269183+00	0.0138
1.1354676+06	3.8742742+00	0.0131
1.0765670+06	3.4753810+00	0.0141
1.0135921+06	4.5549498+00	0.0113
9.4802250+05	5.4599993+00	0.0117
8.8861609+05	5.5440385+00	0.0115
8.3462395+05	6.3707066+00	0.0119
7.8540752+05	6.2611150+00	0.0134
7.4041971+05	7.1407215+00	0.0128
6.9918959+05	6.7373951+00	0.0133
6.6131001+05	8.2525972+00	0.0130
6.2642750+05	8.0720513+00	0.0136
5.9423400+05	7.5430964+00	0.0144
5.6094682+05	8.1444961+00	0.0133
5.2708662+05	9.2700502+00	0.0144
4.9620243+05	6.4498898+00	0.0153
4.6795542+05	1.0241570+01	0.0143

RUN 005
(5-23-64)

3.0 IN. DIAMETER URANIUM SOURCE AT 70°

E	N(E)	DELTA(N)/N
1.2778774+07	3.8149225-03	0.1024
1.1345829+07	8.5207106-03	0.1178
1.0727039+07	7.6453579-03	0.1290
1.0157525+07	1.1831465-02	0.1066
9.6321895+06	1.8757446-02	0.0870
8.9216836+06	2.8449579-02	0.0534
8.0853443+06	4.6562856-02	0.0440
7.3613354+06	7.6947154-02	0.0374
6.7304034+06	1.1150734-01	0.0334
6.1772503+06	1.5716363-01	0.0298
5.6895964+06	2.0059064-01	0.0284
5.2574938+06	2.5176953-01	0.0273
4.8728137+06	2.8497751-01	0.0274
4.5288621+06	3.5409094-01	0.0261
4.2200852+06	4.3286632-01	0.0249
3.9418452+06	4.6589224-01	0.0248
3.6902438+06	5.4069728-01	0.0237
3.4619861+06	5.8721408-01	0.0232
3.2542707+06	5.9389154-01	0.0230
3.0647045+06	5.9432767-01	0.0234
2.8912331+06	6.9491321-01	0.0220
2.7320846+06	6.7022480-01	0.0217
2.5857244+06	7.1638147-01	0.0213
2.4508182+06	8.5682055-01	0.0204
2.2970023+06	9.2855915-01	0.0161
2.1302853+06	1.0644088+00	0.0157
1.9810831+06	1.3339697+00	0.0149
1.8470252+06	1.5736407+00	0.0141
1.7261292+06	2.0705980+00	0.0132
1.6167267+06	1.7014529+00	0.0146
1.5174056+06	2.3806421+00	0.0131
1.4269641+06	2.6037741+00	0.0131
1.3443744+06	2.8286856+00	0.0134
1.2687532+06	3.2534195+00	0.0129
1.1993379+06	3.6023612+00	0.0134
1.1354676+06	3.9538130+00	0.0128
1.0765670+06	3.5503778+00	0.0238
1.0135921+06	4.7110255+00	0.0111
9.4802250+05	5.5648353+00	0.0115
8.8861609+05	5.8698164+00	0.0111
8.3462395+05	6.7612007+00	0.0116
7.8540752+05	6.2696435+00	0.0134
7.4041971+05	7.2711491+00	0.0128
6.9918959+05	7.2946519+00	0.0129
6.6131001+05	8.1723651+00	0.0132
6.2642750+05	8.4806404+00	0.0135
5.9423400+05	7.9091669+00	0.0143
5.6094682+05	8.5521441+00	0.0132
5.2708662+05	9.6445971+00	0.0144
4.9620243+05	6.3891251+00	0.0158
4.6795542+05	1.1137384+01	0.0140

RUN 001
(7-31-64)

13.0 IN. LIQUID HYDROGEN AT 0°

3 IN. DIAMETER URANIUM SOURCE

E	N(E)	DELTA(N)/N
1.4154101+07	3.4577006-02	0.1551
1.2512080+07	9.0495517-02	0.0651
1.1140114+07	1.3000946-01	0.0488
9.9820636+06	1.7287115-01	0.0412
8.7787807+06	2.8802598-01	0.0262
7.5945406+06	4.6527294-01	0.0217
6.6347784+06	6.2209943-01	0.0199
5.8461330+06	6.8321826-01	0.0202
5.1902095+06	7.6274789-01	0.0203
4.6388092+06	8.4618467-01	0.0204
4.1018782+06	9.5472332-01	0.0178
3.5929299+06	1.0874820+00	0.0179
3.1731699+06	1.2919234+00	0.0175
2.8229094+06	1.5890076+00	0.0168
2.5276084+06	1.8526960+00	0.0168
2.2484013+06	2.0214402+00	0.0154
1.9883956+06	2.2118134+00	0.0159
1.7710249+06	2.2877172+00	0.0170
1.5874510+06	2.4704701+00	0.0177
1.4170481+06	2.4470640+00	0.0178
1.2602870+06	2.2851779+00	0.0201
1.1281749+06	1.7940564+00	0.0247
1.0074391+06	1.3624367+00	0.0287
8.9765708+05	1.0697799+00	0.0351
8.0489240+05	7.7185788-01	0.0472
7.2074196+05	6.6770420-01	0.0516
6.4461080+05	5.6583034-01	0.0629
5.7632305+05	4.5657558-01	0.0775
5.1511106+05	3.9281347-01	0.1032
4.6057872+05	3.6963227-01	0.1333

RUN 002
(7-31-64)

10.5 IN. LIQUID HYDROGEN AT 0°

3 IN. DIAMETER URANIUM SOURCE

E	N(E)	DELTA(N)/N
1.5099097+07	2.8035724-02	0.1985
1.3295141+07	8.4686776-02	0.0708
1.1796230+07	1.3882843-01	0.0481
1.0537263+07	1.7822594-01	0.0414
9.2356794+06	2.7804312-01	0.0272
7.9611538+06	4.6787706-01	0.0220
6.9334167+06	7.3478467-01	0.0186
6.0926186+06	8.4120352-01	0.0184
5.3960150+06	9.9068379-01	0.0180
4.8124177+06	1.0792689+00	0.0183
4.2460272+06	1.2212639+00	0.0159
3.7108942+06	1.4259253+00	0.0158
3.2709278+06	1.6361308+00	0.0158
2.9048255+06	1.9416689+00	0.0154
2.5969295+06	2.2211719+00	0.0154
2.3065005+06	2.5837488+00	0.0137
2.0366558+06	2.7727855+00	0.0143
1.8115486+06	3.1000828+00	0.0147
1.6218075+06	3.2202387+00	0.0156
1.4460011+06	3.2123688+00	0.0156
1.2845487+06	3.0511889+00	0.0175
1.1487067+06	2.6585948+00	0.0204
1.0247533+06	1.9482727+00	0.0242
9.1220846+05	1.5122634+00	0.0298
8.1723902+05	1.2475432+00	0.0370
7.3119808+05	8.7708390-01	0.0464
6.5344917+05	8.9308675-01	0.0506
5.8379104+05	6.5503252-01	0.0660
5.2141782+05	6.4979434-01	0.0796
4.6590852+05	6.0793724-01	0.0989

RUN 003
(7-31-64)

7.0 IN. LIQUID HYDROGEN AT 0°

3 IN. DIAMETER URANIUM SOURCE

E	N(E)	DELTA(N)/N
1.4634224+07	3.6506344-02	0.1559
1.2512080+07	1.1739762-01	0.0663
1.1140114+07	1.7825022-01	0.0500
9.9820636+06	2.4639121-01	0.0422
8.7787807+06	4.3583447-01	0.0265
7.5945406+06	7.7440765-01	0.0210
6.6347784+06	1.0767714+00	0.0189
5.8461330+06	1.2932266+00	0.0183
5.1902095+06	1.5131919+00	0.0180
4.6388092+06	1.7769351+00	0.0175
4.1018782+06	2.1076609+00	0.0149
3.5929299+06	2.4045965+00	0.0150
3.1731699+06	2.8810506+00	0.0146
2.8229094+06	3.3243552+00	0.0145
2.5276084+06	3.7358011+00	0.0146
2.2484013+06	4.3166441+00	0.0130
1.9883956+06	4.4971943+00	0.0138
1.7710249+06	5.0229983+00	0.0141
1.5874510+06	5.0676885+00	0.0153
1.4170481+06	5.2385417+00	0.0150
1.2602870+06	5.0512640+00	0.0167
1.1281749+06	4.6899747+00	0.0188
1.0074391+06	4.0249690+00	0.0204
8.9765708+05	3.7661440+00	0.0227
8.0489240+05	3.1945367+00	0.0277
7.2074196+05	2.5270394+00	0.0315
6.4461080+05	2.7607113+00	0.0329
5.7632305+05	2.4552879+00	0.0372
5.1511106+05	1.7516370+00	0.0537
4.6057872+05	1.7921896+00	0.0627

RUN 004

(7-31-64)

4.5 IN. LIQUID HYDROGEN AT 0°

3 IN. DIAMETER URANIUM SOURCE

E	N(E)	DELTA(N)/N
1.4634224+07	5.0483717-02	0.1379
1.2512080+07	1.2321378-01	0.0781
1.1140114+07	1.9391908-01	0.0582
9.9820636+06	2.9510161-01	0.0468
8.7787807+06	4.9660245-01	0.0305
7.5945406+06	9.5571188-01	0.0234
6.6347784+06	1.3653463+00	0.0208
5.8461330+06	1.8038462+00	0.0192
5.1902095+06	2.2230082+00	0.0183
4.6388092+06	2.5129048+00	0.0183
4.1018782+06	3.0132865+00	0.0155
3.5929299+06	3.6137503+00	0.0152
3.1731699+06	4.3452971+00	0.0148
2.8229094+06	5.0151761+00	0.0147
2.5276084+06	5.4469447+00	0.0151
2.2484013+06	6.6255417+00	0.0132
1.9883956+06	7.1412978+00	0.0137
1.7710249+06	8.2870499+00	0.0138
1.5874510+06	8.8360534+00	0.0145
1.4170481+06	8.9822471+00	0.0144
1.2602870+06	9.1601503+00	0.0156
1.1281749+06	9.3757412+00	0.0167
1.0074391+06	8.9283674+00	0.0171
8.9765708+05	9.2721643+00	0.0180
8.0489240+05	8.5234638+00	0.0209
7.2074196+05	7.3803917+00	0.0225
6.4461080+05	8.6425194+00	0.0226
5.7632305+05	8.4159554+00	0.0240
5.1511106+05	6.9325356+00	0.0305
4.6057872+05	6.3491795+00	0.0364

RUN 005

(7-31-64)

2.5 IN. LIQUID HYDROGEN AT 0°

3 IN. DIAMETER URANIUM SOURCE

E	N(E)	DELTA(N)/N
1.4634224+07	4.2186346-02	0.1556
1.2512080+07	1.5040112-01	0.0626
1.1140114+07	2.1010888-01	0.0504
9.9820636+06	3.5083820-01	0.0382
8.7787807+06	6.5158540-01	0.0236
7.5945406+06	1.2860112+00	0.0178
6.6347784+06	1.8269977+00	0.0159
5.8461330+06	2.4127477+00	0.0147
5.1902095+06	2.9776833+00	0.0140
4.6388092+06	3.6526217+00	0.0134
4.1018782+06	4.5362933+00	0.0112
3.5929299+06	5.6542290+00	0.0108
3.1731699+06	6.8098878+00	0.0105
2.8229094+06	8.1378458+00	0.0103
2.5276084+06	9.0958334+00	0.0105
2.2484013+06	1.1129741+01	0.0091
1.9883956+06	1.2672879+01	0.0092
1.7710249+06	1.4561234+01	0.0094
1.5874510+06	1.6179001+01	0.0097
1.4170481+06	1.7992547+01	0.0092
1.2602870+06	1.8690797+01	0.0099
1.1281749+06	2.0824304+01	0.0102
1.0074391+06	2.1544247+01	0.0101
8.9765708+05	2.5338252+01	0.0100
8.0489240+05	2.3339095+01	0.0116
7.2074196+05	2.2375201+01	0.0119
6.4461080+05	2.8397051+01	0.0115
5.7632305+05	2.9848831+01	0.0117
5.1511106+05	2.6520122+01	0.0144
4.6057872+05	2.5289870+01	0.0167

RUN 006

(7-31-64)

DEWAR EMPTY AT 0°

3 IN. DIAMETER URANIUM SOURCE

E	N(E)	DELTA(N)/N
1.4634224+07	4.0690416-02	0.1783
1.2512080+07	1.3871343-01	0.0749
1.1140114+07	2.4606069-01	0.0521
9.9820636+06	4.0750521-01	0.0403
8.7787807+06	7.7819709-01	0.0246
7.5945406+06	1.5536794+00	0.0185
6.6347784+06	2.3344552+00	0.0160
5.8461330+06	3.1980964+00	0.0145
5.1902095+06	4.1944357+00	0.0134
4.6368092+06	5.3181727+00	0.0127
4.1018782+06	6.7074939+00	0.0104
3.5929299+06	8.9118226+00	0.0097
3.1731699+06	1.1039105+01	0.0093
2.8229094+06	1.3535010+01	0.0090
2.5276084+06	1.5837859+01	0.0089
2.2484013+06	2.0037344+01	0.0076
1.9883956+06	2.4238297+01	0.0075
1.7710249+06	2.9907673+01	0.0074
1.5874510+06	3.5007792+01	0.0074
1.4170481+06	4.1965325+01	0.0068
1.2692870+06	4.8375468+01	0.0069
1.1281749+06	5.9695681+01	0.0068
1.0074391+06	6.6838694+01	0.0065
8.9765708+05	8.1094210+01	0.0064
8.0489240+05	8.0785122+01	0.0071
7.2074196+05	8.3645177+01	0.0070
6.4461080+05	1.0864229+02	0.0068
5.7632305+05	1.2267562+02	0.0067
5.1511106+05	1.2091458+02	0.0078
4.6057872+05	1.2694360+02	0.0086

RUN 003
(8-1-64)

13.0 IN. LIQUID HYDROGEN AT 15°

3 IN. DIAMETER URANIUM SOURCE

E	N(E)	DELTA(N)/N
7.2526888+06	8.8680193-04	0.0633
6.3550326+06	1.1987778-03	0.0560
5.6143121+06	1.8289315-03	0.0466
4.9959602+06	2.3583869-03	0.0430
4.4744304+06	2.7682537-03	0.0421
3.9649496+06	3.3417535-03	0.0356
3.4805041+06	4.0155528-03	0.0350
3.0797311+06	4.9981225-03	0.0334
2.7444110+06	5.6651178-03	0.0337
2.4296664+06	6.3952978-03	0.0309
2.1386019+06	6.8177520-03	0.0330
1.8968837+06	7.5502970-03	0.0343
1.6939538+06	8.3190488-03	0.0358
1.5066349+06	8.9167808-03	0.0356
1.3352227+06	1.0016478-02	0.0374
1.1914886+06	1.0687489-02	0.0408
1.0607483+06	1.0837277-02	0.0426
9.4239341+05	1.1176309-02	0.0475
8.4280022+05	1.2134826-02	0.0536
7.5280483+05	1.1882328-02	0.0617
6.7168023+05	1.3285117-02	0.0695
5.9916927+05	1.4968115-02	0.0784
5.3438395+05	1.5151224-02	0.1114

RUN 004
(8-1-64)

10.5 IN. LIQUID HYDROGEN AT 15°

3 IN. DIAMETER URANIUM SOURCE

E	N(E)	DELTA(N)/N
1.1211419+07	1.1291162-04	0.1815
8.7787807+06	3.9964445-04	0.0852
7.5945406+06	6.8912427-04	0.0593
6.6347784+06	1.1400261-03	0.0466
5.8461330+06	1.5647172-03	0.0416
5.1902095+06	2.0660770-03	0.0380
4.6388092+06	2.7913188-03	0.0344
4.1018782+06	3.2717004-03	0.0295
3.5929299+06	3.8124979-03	0.0296
3.1731699+06	5.1050273-03	0.0272
2.8229094+06	5.5861359-03	0.0279
2.5276084+06	6.4476336-03	0.0281
2.2484013+06	7.4787912-03	0.0252
1.9883956+06	8.3930758-03	0.0260
1.7710249+06	9.2111253-03	0.0272
1.5874510+06	1.0836688-02	0.0276
1.4170481+06	1.1468625-02	0.0273
1.2602870+06	1.1693272-02	0.0304
1.1281749+06	1.2445684-02	0.0327
1.0074391+06	1.3572888-02	0.0325
8.9765708+05	1.5430549-02	0.0342
8.0489240+05	1.6829347-02	0.0391
7.2074196+05	1.6865721-02	0.0425
6.4461080+05	1.9503224-02	0.0475
5.7632305+05	2.0309705-02	0.0569
5.1511106+05	2.5734607-02	0.0677

RUN 005
(8-1-64)

7.0 IN. LIQUID HYDROGEN AT 15°

3 IN. DIAMETER URANIUM SOURCE

E	N(E)	DELTA(N)/N
1.0601038+07	1.5955457-04	0.1771
8.3549796+06	4.4109662-04	0.0985
7.2526888+06	9.5244139-04	0.0595
6.3550326+06	1.4893491-03	0.0485
5.6143121+06	2.0856818-03	0.0427
4.9959602+06	2.4975596-03	0.0411
4.4744304+06	3.3890352-03	0.0371
3.9649496+06	4.0894518-03	0.0313
3.4805041+06	4.9783131-03	0.0306
3.0797311+06	6.6466880-03	0.0282
2.7444110+06	7.5113326-03	0.0285
2.4296664+06	8.7720775-03	0.0256
2.1386019+06	1.0689913-02	0.0253
1.8968837+06	1.2139792-02	0.0259
1.6939538+06	1.3765950-02	0.0266
1.5066349+06	1.5182484-02	0.0260
1.3352227+06	1.6621277-02	0.0275
1.1914886+06	1.9081028-02	0.0287
1.0607483+06	2.0250695-02	0.0289
9.4239341+05	2.3319335-02	0.0299
8.4280022+05	2.5062735-02	0.0337
7.5280483+05	3.0237508-02	0.0334
6.7168023+05	3.0293726-02	0.0395
5.9916927+05	3.5991731-02	0.0421
5.3438395+05	3.9721642-02	0.0537

RUN 006
(8-1-64)

4.5 IN. LIQUID HYDROGEN AT 15°

3 IN. DIAMETER URANIUM SOURCE

E	N(E)	DELTA(N)/N
9.7563127+06	2.8222954-04	0.1587
7.9611538+06	7.4515994-04	0.0883
6.9334167+06	1.4938827-03	0.0597
6.0926186+06	2.3686957-03	0.0489
5.3960150+06	2.6375146-03	0.0492
4.8124177+06	3.6945062-03	0.0436
4.2460272+06	4.8909518-03	0.0350
3.7108942+06	6.5089008-03	0.0328
3.2709278+06	8.4756934-03	0.0308
2.9048255+06	1.0608912-02	0.0294
2.5969295+06	1.3399722-02	0.0282
2.3065005+06	1.6290904-02	0.0246
2.0366558+06	1.9352070-02	0.0247
1.8115486+06	2.3231274-02	0.0246
1.6218075+06	2.7588793-02	0.0247
1.4460011+06	3.1890507-02	0.0233
1.2845487+06	3.6818325-02	0.0241
1.1487067+06	4.2991812-02	0.0246
1.0247533+06	4.8156577-02	0.0240
9.1220846+05	5.7924680-02	0.0244
8.1723902+05	7.2247088-02	0.0253
7.3119808+05	7.8560215-02	0.0259
6.5344917+05	9.1196009-02	0.0283
5.8379104+05	1.0994885-01	0.0296
5.2141782+05	1.2049103-01	0.0369
4.6590852+05	1.5158701-01	0.0436
4.1646828+05	1.5794069-01	0.0614
3.7262365+05	1.7251311-01	0.0725
3.3367466+05	1.6819854-01	0.1033
2.9917829+05	2.6826130-01	0.1044
2.6077017+05	2.8794320-01	0.1948
1.9372136+05	1.8397825+00	0.1995

RUN 007
(8-1-64)

2.5 IN. LIQUID HYDROGEN AT 15°

3 IN. DIAMETER URANIUM SOURCE

E	N(E)	DELTA(N)/N
1.0601038+07	2.3697706-04	0.1751
8.3549796+06	6.5973990-04	0.1043
7.2526888+06	1.2050919-03	0.0721
6.3550326+06	1.6762981-03	0.0647
5.6143121+06	2.7283415-03	0.0523
4.9959602+06	3.4249474-03	0.0492
4.4744304+06	4.8262716-03	0.0438
3.9649496+06	6.4288811-03	0.0351
3.4805041+06	8.4167998-03	0.0330
3.0797311+06	1.1014323-02	0.0309
2.7444110+06	1.4607975-02	0.0286
2.4295664+06	1.7371547-02	0.0255
2.1386019+06	2.1665748-02	0.0250
1.8968837+06	2.6194101-02	0.0247
1.6939538+06	3.3328107-02	0.0239
1.5066349+06	3.9950611-02	0.0222
1.3352227+06	4.6347422-02	0.0228
1.1914886+06	5.6363026-02	0.0230
1.0607483+06	6.9390821-02	0.0213
9.4239341+05	8.0064873-02	0.0220
8.4280022+05	1.0273106-01	0.0223
7.5280483+05	1.2344550-01	0.0220
6.7168023+05	1.4127129-01	0.0237
5.9916927+05	1.7029710-01	0.0246
5.3438395+05	1.9331920-01	0.0297
4.7684956+05	2.4337590-01	0.0343
4.2570559+05	2.8327182-01	0.0451
3.8043458+05	2.3932398-01	0.0624
3.4028765+05	2.6950913-01	0.0765
3.0478848+05	3.1208034-01	0.0968
2.7332280+05	4.1651403-01	0.1273
2.4548647+05	7.4720626-01	0.1685
2.1742799+05	2.7174785+00	0.1946

RUN 008
(8-1-64)

DEWAR EMPTY AT 15°

3 IN. DIAMETER URANIUM SOURCE

E	N(E)	DELTA(N)/N
9.5210985+06	4.3488416-04	0.1543
7.5945406+06	1.3877260-03	0.0890
6.6347784+06	2.3125896-03	0.0704
5.8461330+06	3.4993498-03	0.0593
5.1902095+06	4.9900543-03	0.0523
4.6388092+06	5.1243486-03	0.0552
4.1018782+06	7.4040025-03	0.0425
3.5929299+06	1.0279061-02	0.0389
3.1731699+06	1.2977545-02	0.0371
2.8229094+06	1.7286979-02	0.0343
2.5276084+06	2.2345756-02	0.0326
2.2484013+06	2.8630833-02	0.0277
1.9883956+06	3.5104551-02	0.0274
1.7710249+06	4.4122445-02	0.0266
1.5874510+06	5.7184958-02	0.0257
1.4170481+06	6.6445999-02	0.0241
1.2602870+06	8.7517743-02	0.0233
1.1281749+06	1.0013994-01	0.0240
1.0074391+06	1.2568598-01	0.0220
8.9765708+05	1.5968120-01	0.0218
8.0489240+05	2.1445724-01	0.0219
7.2074196+05	2.5534216-01	0.0211
6.4461080+05	2.9207646-01	0.0233
5.7632305+05	3.4153240-01	0.0248
5.1511106+05	4.2802174-01	0.0285

RUN 003
(8-3-64)

13.0 IN. LIQUID HYDROGEN AT 37°

3 IN. DIAMETER URANIUM SOURCE

E	N(E)	DELTA(N)/N
1.0927433+07	4.6460292-05	0.1674
8.3549796+06	7.9964750-05	0.1637
7.2526888+06	1.1588241-04	0.1314
6.3550326+06	1.4391966-04	0.1216
5.6143121+06	2.0819690-04	0.1008
4.9959602+06	2.8754995-04	0.0865
4.4744304+06	3.7357377-04	0.0785
3.9649496+06	5.1458699-04	0.0602
3.4805041+06	6.6383828-04	0.0563
3.0797311+06	9.2983052-04	0.0493
2.7444110+06	1.2214160-03	0.0453
2.4296664+06	1.4604347-03	0.0401
2.1386019+06	1.8375756-03	0.0388
1.8968837+06	2.2086744-03	0.0384
1.6939538+06	2.4961344-03	0.0399
1.5066349+06	2.7587241-03	0.0392
1.3352227+06	3.2685446-03	0.0398
1.1914886+06	3.6087240-03	0.0428
1.0607483+06	4.0559516-03	0.0423
9.4239341+05	4.5212890-03	0.0448
8.4280022+05	4.9892685-03	0.0503
7.5280483+05	5.2502784-03	0.0558
6.7168023+05	6.4051857-03	0.0591
5.9916927+05	7.9276608-03	0.0629
5.3438395+05	8.2844945-03	0.0888

RUN 004
(8-3-64)

10.5 IN. LIQUID HYDROGEN AT 37°

3 IN. DIAMETER URANIUM SOURCE

E	N(E)	DELTA(N)/N
1.1876211+07	4.2886674-05	0.1806
9.2356794+06	6.5880537-05	0.1933
7.9611538+06	9.6945126-05	0.1473
6.9334167+06	9.1268523-05	0.1702
6.0926186+06	1.3332497-04	0.1399
5.3960150+06	2.3792505-04	0.0982
4.8124177+06	3.3505004-04	0.0945
4.2460272+06	3.5207820-04	0.0782
3.7108942+06	5.8564934-04	0.0615
3.2709278+06	7.6635020-04	0.0566
2.9048255+06	9.3129001-04	0.0545
2.5969295+06	1.1895924-03	0.0515
2.3065005+06	1.3600447-03	0.0465
2.0366558+06	1.6732475-03	0.0455
1.8115486+06	1.9302613-03	0.0466
1.6218075+06	2.2288878-03	0.0477
1.4460011+06	2.6454220-03	0.0443
1.2845487+06	2.7864012-03	0.0490
1.1487067+06	3.5306292-03	0.0478
1.0247533+06	3.4075751-03	0.0520
9.1220846+05	4.1993068-03	0.0523
8.1723902+05	4.7178220-03	0.0586
7.3119808+05	5.0718653-03	0.0629
6.5344917+05	6.8507456-03	0.0628
5.8379104+05	6.7770325-03	0.0796
5.2141782+05	8.2084291-03	0.1009

RUN 005
(8-3-64)

7.0 IN. LIQUID HYDROGEN AT 37°

3 IN. DIAMETER URANIUM SOURCE

E	N(E)	DELTA(N)/N
1.0089881+07	4.9468436-05	0.1764
7.5945406+06	1.1325548-04	0.1422
6.6347784+06	1.6136671-04	0.1182
5.8461330+06	1.9336516-04	0.1126
5.1902095+06	2.9365829-04	0.0909
4.6388092+06	3.5959425-04	0.0863
4.1018782+06	6.5031883-04	0.0561
3.5929299+06	8.7209626-04	0.0516
3.1731699+06	1.1991014-03	0.0463
2.8229094+06	1.6183130-03	0.0421
2.5276084+06	1.9262959-03	0.0417
2.2484013+06	2.4266563-03	0.0355
1.9883956+06	3.0137341-03	0.0348
1.7710249+06	3.8103658-03	0.0336
1.5874510+06	4.2056739-03	0.0353
1.4170481+06	5.1042271-03	0.0323
1.2602870+06	5.9738783-03	0.0333
1.1281749+06	6.8524656-03	0.0344
1.0074391+06	7.2316258-03	0.0348
8.9765708+05	8.6258975-03	0.0357
8.0489240+05	1.0873305-02	0.0372
7.2074196+05	1.0787746-02	0.0404
6.4461080+05	1.4697618-02	0.0406
5.7632305+05	1.7870089-02	0.0431
5.1511106+05	2.0502724-02	0.0540

RUN 006
(8-3-64)

4.5 IN. LIQUID HYDROGEN at 37°

3 IN. DIAMETER URANIUM SOURCE

E	N(E)	DELTA(N)/N
1.0400539+07	4.5940261-05	0.1748
7.5945406+06	1.4327374-04	0.1166
6.6347784+06	1.6541941-04	0.1131
5.8461330+06	3.0522077-04	0.0806
5.1902095+06	4.3592309-04	0.0688
4.6388092+06	5.7217090-04	0.0626
4.1018782+06	7.7688375-04	0.0492
3.5929299+06	1.2023641-03	0.0416
3.1731699+06	1.5493989-03	0.0390
2.8229094+06	2.0876338-03	0.0355
2.5276084+06	2.9307507-03	0.0321
2.2484013+06	3.5955149-03	0.0278
1.9883956+06	4.4382263-03	0.0273
1.7710249+06	5.5406830-03	0.0266
1.5874510+06	6.8678469-03	0.0262
1.4170481+06	8.1352885-03	0.0243
1.2602870+06	9.5039759-03	0.0250
1.1281749+06	1.1131524-02	0.0255
1.0074391+06	1.3219233-02	0.0241
8.9765708+05	1.5317331-02	0.0250
8.0489240+05	1.9291117-02	0.0260
7.2074196+05	2.1214555-02	0.0264
6.4461080+05	2.7911514-02	0.0271
5.7632305+05	3.2618409-02	0.0293
5.1511106+05	3.9760096-02	0.0349

RUN 007
(8-3-64)

2.5 IN. LIQUID HYDROGEN AT 37°

3 IN. DIAMETER URANIUM SOURCE

E	N(E)	DELTA(N)/N
1.2602098+07	4.9569557-05	0.2000
9.4888604+06	8.1049962-05	0.1674
7.9611538+06	1.2896485-04	0.1370
6.9334167+06	1.6909937-04	0.1222
6.0926186+06	2.7812745-04	0.0941
5.3960150+06	3.9774598-04	0.0803
4.8124177+06	5.1678125-04	0.0739
4.2460272+06	8.0539114-04	0.0534
3.7108942+06	1.2229801-03	0.0459
3.2709278+06	1.6510474-03	0.0420
2.9048255+06	2.0952130-03	0.0396
2.5969295+06	3.0275812-03	0.0351
2.3065005+06	3.8925586-03	0.0298
2.0366558+06	5.1227183-03	0.0283
1.8115486+06	6.2252348-03	0.0280
1.6218075+06	8.0340961-03	0.0269
1.4460011+06	9.6537247-03	0.0248
1.2845487+06	1.1875116-02	0.0249
1.1487067+06	1.3973195-02	0.0252
1.0247533+06	1.6862587-02	0.0236
9.1220846+05	2.1522848-02	0.0232
8.1723902+05	2.5768418-02	0.0247
7.3119808+05	3.0136188-02	0.0243
6.5344917+05	3.9626023-02	0.0248
5.8379104+05	4.9314979-02	0.0256
5.2141782+05	5.8079311-02	0.0307

RUN 008
(8-3-64)

DEWAR EMPTY AT 37°

3 IN. DIAMETER URANIUM SOURCE

E	N(E)	DELTA(N)/N
1.1510558+07	8.4822741-05	0.1877
9.0130164+06	1.3053093-04	0.1520
7.5945406+06	2.8625800-04	0.1018
6.6347784+06	4.0013866-04	0.0886
5.8461330+06	5.5234144-04	0.0783
5.1902095+06	7.4704060-04	0.0704
4.6388092+06	1.0007314-03	0.0641
4.1018782+06	1.1566673-03	0.0557
3.5929299+06	1.6961510-03	0.0493
3.1731699+06	2.2162765-03	0.0459
2.8229094+06	2.7222784-03	0.0442
2.5276084+06	3.8312722-03	0.0401
2.2484013+06	4.9299721-03	0.0339
1.9883956+06	6.0733010-03	0.0333
1.7710249+06	7.4763935-03	0.0327
1.5874510+06	9.4918169-03	0.0319
1.4170481+06	1.2206046-02	0.0283
1.2602870+06	1.5253907-02	0.0282
1.1281749+06	1.7399149-02	0.0291
1.0074391+06	2.2023828-02	0.0264
8.9765708+05	2.4738128-02	0.0279
8.0489240+05	3.4118987-02	0.0277
7.2074196+05	4.2015760-02	0.0262
6.4461080+05	4.9208177-02	0.0286
5.7632305+05	5.9462093-02	0.0301
5.1511106+05	7.1448267-02	0.0356

RUN 003
(8-4-64)

13.0 IN. LIQUID HYDROGEN AT 53°

3 IN. DIAMETER URANIUM SOURCE

E	N(E)	DELTA(N)/N
1.0396034+07	3.3278415-05	0.1833
7.6110422+06	5.3838685-05	0.1847
6.2265891+06	7.5746790-05	0.1821
5.3960150+06	1.1894701-04	0.1639
4.8124177+06	1.4161937-04	0.1569
4.2460272+06	1.5500807-04	0.1423
3.7108942+06	2.1318189-04	0.1265
3.2709278+06	2.4110689-04	0.1287
2.9048255+06	3.0764577-04	0.1180
2.5969295+06	4.4229066-04	0.1008
2.3065005+06	5.5191216-04	0.0861
2.0366558+06	6.9379405-04	0.0829
1.8115486+06	8.3478256-04	0.0825
1.6218075+06	1.0743032-03	0.0777
1.4460011+06	1.3126860-03	0.0717
1.2845487+06	1.6328377-03	0.0708
1.1487067+05	1.9618352-03	0.0714
1.0247533+06	2.1798512-03	0.0711
9.1220846+05	2.2527438-03	0.0811
8.1723902+05	2.3793014-03	0.0969
7.3119808+05	3.1620522-03	0.0880
6.5344917+05	3.2617431-03	0.1100
5.8379104+05	3.3837623-03	0.1375
5.2141782+05	5.2501457-03	0.1472

RUN 004
(8-5-64)

10.5 IN. LIQUID HYDROGEN AT 53°

3 IN. DIAMETER URANIUM SOURCE

E	N(E)	DELTA(N)/N
9.4826850+06	4.3692202-05	0.1901
5.4043406+06	1.2501307-04	0.1928
4.4801536+06	1.6334847-04	0.1857
3.8347669+06	2.1305648-04	0.1897
3.3732752+06	3.3124832-04	0.1516
2.9903605+06	4.1097566-04	0.1423
2.6691427+06	5.6809822-04	0.1237
2.3668818+06	6.2033429-04	0.1163
2.0866950+06	9.8982159-04	0.0941
1.8534795+06	1.3186666-03	0.0858
1.6572918+06	1.4716091-03	0.0904
1.4758509+06	1.8274598-03	0.0823
1.3095180+06	2.2721553-03	0.0808
1.1698042+06	3.1032958-03	0.0751
1.0425177+06	3.1829085-03	0.0795
9.2711665+05	3.4888388-03	0.0866
8.2987193+05	3.7488237-03	0.1013
7.4188345+05	4.8643700-03	0.0955
6.6247061+05	5.1085725-03	0.1164
5.9140517+05	5.9576614-03	0.1309
5.2784116+05	7.0561001-03	0.1680

RUN 005
(8-5-64)

7.0 IN. LIQUID HYDROGEN AT 53°

3 IN. DIAMETER URANIUM SOURCE

E	N(E)	DELTA(N)/N
9.0831281+06	7.6082202-05	0.1742
6.9334167+06	1.1526737-04	0.1892
6.0926186+06	1.5430067-04	0.1614
5.3960150+06	1.7894026-04	0.1567
4.8124177+06	2.1712608-04	0.1462
4.2460272+06	2.8193342-04	0.1151
3.7108942+06	4.0277586-04	0.0982
3.2709278+06	5.1995410-04	0.0904
2.9048255+06	7.7518223-04	0.0745
2.5969295+06	8.1575376-04	0.0798
2.3065005+06	1.0667108-03	0.0658
2.0366558+06	1.4525767-03	0.0599
1.8115486+06	1.8776029-03	0.0568
1.6218075+06	2.4109400-03	0.0541
1.4460011+06	2.8388291-03	0.0508
1.2845487+06	3.5243349-03	0.0503
1.1487067+06	3.8870704-03	0.0538
1.0247533+06	4.6518525-03	0.0508
9.1220846+05	5.3179313-03	0.0534
8.1723902+05	6.3662428-03	0.0578
7.3119808+05	7.1323448-03	0.0600
6.5344917+05	8.3590319-03	0.0672
5.8379104+05	1.0266166-02	0.0734
5.2141782+05	1.0213448-02	0.1081

RUN 007
(8-5-64)

4.5 IN. LIQUID HYDROGEN AT 53°

3 IN. DIAMETER URANIUM SOURCE

E	N(E)	DELTA(N)/N
1.0927433+07	8.8133574-05	0.1917
8.3549796+06	1.3014632-04	0.1920
7.2526888+06	1.4768328-04	0.1722
6.3550326+06	1.8354912-04	0.1573
5.6143121+06	2.8735469-04	0.1207
4.9959602+06	3.2877339-04	0.1186
4.4744304+06	3.9786894-04	0.1113
3.9649496+06	5.0815057-04	0.0899
3.4805041+06	7.4595583-04	0.0765
3.0797311+06	9.4550332-04	0.0717
2.7444110+06	1.1386518-03	0.0698
2.4296664+06	1.6484231-03	0.0545
2.1386019+06	2.4608501-03	0.0474
1.8968837+06	2.9021855-03	0.0475
1.6939538+06	4.2001896-03	0.0422
1.5066349+06	5.2662197-03	0.0383
1.3352227+06	7.0950935-03	0.0360
1.1914886+06	8.2504121-03	0.0373
1.0607483+06	1.0078850-02	0.0347
9.4239341+05	1.1845528-02	0.0356
8.4280022+05	1.4961037-02	0.0364
7.5280483+05	1.7814586-02	0.0364
6.7168023+05	2.1246264-02	0.0389
5.9916927+05	2.6236336-02	0.0406
5.3438395+05	3.1192794-02	0.0491

RUN 008
(8-5-64)

2.5 IN. LIQUID HYDROGEN AT 53°

3 IN. DIAMETER URANIUM SOURCE

E	N(E)	DELTA(N)/N
9.8523520+06	8.0835726-05	0.1885
7.2526888+06	1.3083463-04	0.1884
6.3550326+06	1.9346369-04	0.1468
5.6143121+06	2.3091331-04	0.1391
4.9959602+06	3.1077483-04	0.1200
4.4744304+06	5.2978856-04	0.0892
3.9649496+06	5.9748168-04	0.0781
3.4805041+06	7.4540199-04	0.0748
3.0797311+06	1.0769702-03	0.0642
2.7444110+06	1.4138272-03	0.0592
2.4296664+06	2.1562227-03	0.0450
2.1386019+06	3.1659883-03	0.0397
1.8968837+06	3.9847778-03	0.0383
1.6939538+06	5.3597930-03	0.0358
1.5066349+06	6.7147126-03	0.0325
1.3352227+06	8.6028872-03	0.0315
1.1914866+06	1.0600762-02	0.0316
1.0607483+06	1.3490866-02	0.0287
9.4239341+05	1.5917718-02	0.0292
8.4280022+05	2.0267539-02	0.0298
7.5280483+05	2.4325701-02	0.0296
6.7168023+05	2.9920930-02	0.0309
5.9916927+05	3.8335382-02	0.0313
5.3438395+05	4.7172077-02	0.0368

RUN 009
(8-5-64)

DEWAR EMPTY AT 53°

3 IN. DIAMETER URANIUM SOURCE

E	N(E)	DELTA(N)/N
9.4857720+06	1.3220086-04	0.1819
6.3550326+06	3.8840163-04	0.1515
5.6143121+06	5.3537114-04	0.1285
4.9959602+06	6.1177569-04	0.1285
4.4744304+06	9.0944098-04	0.1094
3.9649496+06	1.0940784-03	0.0921
3.4805041+06	1.5114940-03	0.0836
3.0797311+06	2.2713642-03	0.0718
2.7444110+06	2.9097241-03	0.0676
2.4296664+06	3.7200074-03	0.0577
2.1386019+06	5.6947604-03	0.0505
1.8968837+06	6.3531492-03	0.0520
1.6939538+06	8.3697815-03	0.0494
1.5066349+06	1.2474236-02	0.0409
1.3352227+06	1.4072704-02	0.0425
1.1914886+06	1.8573330-02	0.0411
1.0607483+06	2.3396683-02	0.0375
9.4239341+05	2.6137679-02	0.0394
8.4280022+05	3.1402215-02	0.0414
7.5280483+05	4.5358140-02	0.0371
6.7168023+05	4.9242332-02	0.0412
5.9916927+05	6.4633735-02	0.0411
5.3438395+05	6.8915548-02	0.0515

RUN 003
(8-7-64)

13.0 IN. LIQUID HYDROGEN AT 78°

3 IN. DIAMETER URANIUM SOURCE

E	N(E)	DELTA(N)/N
8.6463771+06	1.2506314-04	0.1973
4.7351953+06	2.8577777-04	0.1882
3.9014861+06	3.8178633-04	0.1955
3.3232828+06	4.5461185-04	0.1987
2.7878142+06	4.7347190-04	0.1891
2.3374705+06	7.0662335-04	0.1804
2.0366558+06	9.3274711-04	0.1867
1.7534083+06	9.3403427-04	0.1753
1.5066349+06	1.5414549-03	0.1692
1.2747913+06	1.1244223-03	0.1946
1.0270070+06	1.4711928-03	0.1984
8.5645169+05	2.8542158-03	0.1898
7.3706387+05	3.8778750-03	0.1803
6.1227387+05	4.8036374-03	0.1906
3.7147946+05	2.6496594-02	0.1981

RUN 004
(8-7-64)

10.5 IN. LIQUID HYDROGEN AT 78°

3 IN. DIAMETER URANIUM SOURCE

E	N(E)	DELTA(N)/N
1.1211419+07	7.2429524-05	0.1869
8.7787807+06	1.2636033-04	0.1461
7.5945406+06	1.6678707-04	0.1177
6.6347784+06	1.7535351-04	0.1225
5.8461330+06	2.0121721-04	0.1192
5.1902095+06	2.7908478-04	0.1013
4.6388092+06	3.2379018-04	0.0985
4.1018782+06	3.3693592-04	0.0914
3.5929299+06	4.4719897-04	0.0838
3.1731699+06	4.6360548-04	0.0899
2.8229094+06	5.8035801-04	0.0845
2.5276084+06	7.4031661-04	0.0795
2.2484013+06	7.8372941-04	0.0757
1.9883956+06	9.4478933-04	0.0753
1.7710249+06	1.1542822-03	0.0741
1.5874510+06	1.3653934-03	0.0746
1.4170481+06	1.7721801-03	0.0657
1.2602870+06	1.8526161-03	0.0739
1.1281749+06	2.2344443-03	0.0735
1.0074391+06	2.5901066-03	0.0711
8.9765708+05	3.2350520-03	0.0708
8.0489240+05	3.8110683-03	0.0781
7.2074196+05	4.2390836-03	0.0810
6.4461080+05	4.8853315-03	0.0933
5.7632305+05	6.1782618-03	0.0995
5.1511106+05	7.0877815-03	0.1335

RUN 005
(8-7-64)

7.0 IN. LIQUID HYDROGEN AT 78°

3 IN. DIAMETER URANIUM SOURCE

E	N(E)	DELTA(N)/N
5.4914051+07	6.4302627-05	0.1731
4.6002771+07	3.3301584-05	0.1379
3.7020316+07	4.2120733-05	0.1047
3.0434323+07	4.3337117-05	0.1064
2.5462038+07	4.7096283-05	0.1087
2.1616135+07	4.8054180-05	0.1186
1.8580318+07	7.1088801-05	0.0999
1.6142020+07	8.3608603-05	0.0988
1.4154101+07	8.5084802-05	0.1093
1.2512080+07	1.1029793-04	0.1004
1.1140114+07	1.4889009-04	0.0897
9.9820636+06	1.2361472-04	0.1125
8.7787807+06	1.8307131-04	0.0775
7.5945406+06	1.8999178-04	0.0852
6.6347784+06	2.7287436-04	0.0735
5.8461330+06	3.0278959-04	0.0752
5.1902095+06	3.6105087-04	0.0728
4.6388092+06	3.8512913-04	0.0756
4.1018782+06	4.3097240-04	0.0669
3.5929299+06	4.9790049-04	0.0680
3.1731699+06	6.0084236-04	0.0658
2.8229094+06	6.0158808-04	0.0724
2.5276084+06	8.1538472-04	0.0652
2.2484013+06	8.5423402-04	0.0624
1.9883956+06	1.0610516-03	0.0608
1.7710249+06	1.1384744-03	0.0654
1.5874510+06	1.4829877-03	0.0619
1.4170481+06	1.5118456-03	0.0642
1.2602870+06	1.6539409-03	0.0706
1.1281749+06	1.8927916-03	0.0730
1.0074391+06	2.1813147-03	0.0709
8.9765708+05	2.3069498-03	0.0795
8.0489240+05	2.4482085-03	0.0971
7.2074196+05	2.4290273-03	0.1104
6.4461080+05	3.1267442-03	0.1180
5.6922869+05	2.3148439-03	0.1971

RUN 006
(8-7-64)

4.5 IN. LIQUID HYDROGEN AT 78°

3 IN. DIAMETER URANIUM SOURCE

E	N(E)	DELTA(N)/N
1.1274564+07	6.1989502-05	0.1817
8.3549796+06	1.2730844-04	0.1479
7.2526868+06	1.7016653-04	0.1265
6.3550326+06	2.0322626-04	0.1213
5.6143121+06	2.2779824-04	0.1210
4.9959602+06	2.9047357-04	0.1086
4.4744304+06	3.4388583-04	0.1050
3.9649496+06	3.8252015-04	0.0929
3.4805041+06	5.1756874-04	0.0841
3.0797311+06	6.0572554-04	0.0831
2.7444110+06	6.3627952-04	0.0882
2.4296664+06	1.0439786-03	0.0627
2.1386019+06	1.1349105-03	0.0672
1.8968837+06	1.4377069-03	0.0638
1.6939538+06	1.8061306-03	0.0617
1.5066349+06	2.1360214-03	0.0584
1.3352227+06	2.5585304-03	0.0588
1.1914886+06	3.3558860-03	0.0566
1.0607483+06	3.6856133-03	0.0568
9.4239341+05	4.2963151-03	0.0584
8.4280022+05	5.3850526-03	0.0605
7.5280483+05	6.0490001-03	0.0639
6.7168023+05	7.5299714-03	0.0668
5.9916927+05	8.7976808-03	0.0736
5.3438395+05	1.1678806-02	0.0853

RUN 007
(8-7-64)

2.5 IN. LIQUID HYDROGEN AT 78°

3 IN. DIAMETER URANIUM SOURCE

E	N(E)	DELTA(N)/N
1.0293575+07	8.2582501-05	0.1663
8.3549796+06	1.3654119-04	0.1343
7.2526888+06	1.5656445-04	0.1284
6.3550326+06	2.0911670-04	0.1135
5.6143121+06	2.6640611-04	0.1019
4.9959602+06	3.1247926-04	0.0988
4.4744304+06	3.4693307-04	0.0998
3.9649496+06	4.9199805-04	0.0751
3.4805041+06	5.5279246-04	0.0772
3.0797311+06	7.0702871-04	0.0715
2.7444110+06	8.5287668-04	0.0696
2.4296664+06	1.1124928-03	0.0581
2.1386019+06	1.3119938-03	0.0586
1.8968837+06	1.8381631-03	0.0524
1.6939538+06	2.2472983-03	0.0517
1.5066349+06	2.5082917-03	0.0504
1.3352227+06	3.1390491-03	0.0496
1.1914886+06	3.9696948-03	0.0488
1.0607483+06	4.8296059-03	0.0457
9.4239341+05	5.0912481-03	0.0499
8.4280022+05	6.3249125-03	0.0521
7.5280483+05	8.5817036-03	0.0482
6.7168023+05	9.4989145-03	0.0540
5.9916927+05	1.1847934-02	0.0561
5.3438395+05	1.3476304-02	0.0732

RUN 008
(8-7-64)

DEWAR EMPTY AT 78°

3 IN. DIAMETER URANIUM SOURCE

E	N(E)	DELTA(N)/N
1.0657478+07	1.2274048-04	0.1812
7.9511538+06	1.9178816-04	0.1845
6.9334167+06	2.5649547-04	0.1578
6.0926186+06	3.8834451-04	0.1282
5.3960150+06	5.5003264-04	0.1088
4.8124177+06	6.4927980-04	0.1064
4.2460272+06	8.1586943-04	0.0876
3.7108942+06	1.1283710-03	0.0796
3.2709278+06	1.2471044-03	0.0817
2.9048255+06	1.6905734-03	0.0743
2.5969295+06	2.2216093-03	0.0694
2.3065005+06	2.9215414-03	0.0582
2.0366558+06	4.1667660-03	0.0526
1.8115486+06	4.9366147-03	0.0529
1.6218075+06	6.2344933-03	0.0513
1.4460011+06	6.9348220-03	0.0494
1.2845487+05	1.0059687-02	0.0452
1.1487067+06	1.2462756-02	0.0449
1.0247533+06	1.4052718-02	0.0435
9.1220846+05	1.6890561-02	0.0441
8.1723902+05	2.2809425-02	0.0442
7.3119808+05	2.6314512-02	0.0437
6.5344917+05	3.2835855-02	0.0459
5.8379104+05	4.2295768-02	0.0462
5.2141782+05	4.9195202-02	0.0559

APPENDIX A

NEUTRON HEATING CALCULATIONS

APPENDIX A

NEUTRON HEATING CALCULATIONS

At high energies neutrons lose energy in hydrogen by elastic scattering collisions. The volumetric heating H(x) due to these fast neutrons as a function of x (thickness) can be expressed as:

$$H(x) = q \sum_{g=0.5\ \text{Mev}}^{g_o=15\ \text{Mev}} \phi_g(x) N_H \sigma_H(\bar{E}_g)(0.5\ \bar{E}_g)\Delta E_g$$

where $\phi_g(x)$ = is the scalar flux at the position, x, for the energy group (g)

N_H = number density for hydrogen

$\sigma_H(\bar{E}_g)$ = hydrogen cross section at energy $\bar{E}_g$

$\bar{E}_g$ = average energy within the energy group (g)

q = conversion factor from energy (Mev) to heat units (BTU)

H(x) = heating (power)/unit volume

This formula assumes that for each scattering collision a neutron will lose on the average one-half of its initial energy.

$\phi_g(x)$ were obtained by a theoretical calculation using the transport theory code GAPLSN. These calculations were made assuming a fission neutron spectrum impinges on an 18 in. thick infinite (transverse) slab of liquid hydrogen. The GAPLSN calculations were made by dividing

the slab into 30 equal spatial intervals, i.e., 0.6 in., and dividing the energy interval (15 to 0.067 MeV) into 13 groups and doing an S_{32} (32 equal intervals of μ from μ=1 to μ=-1) calculation. The GAPLSN calculations above were used in the numerical integration of the above equation. These calculations are shown in Fig. A-1 as a graph of the fraction of the total heating, $H(x)_T$, which occurs in x thickness of liquid hydrogen versus the thickness of liquid hydrogen. This data is tabulated in Table 1. It can be seen from Fig. A-1 and Table 1 that 25% of the heating is obtained within the first 1.4 in., 50% within 3.5 in., and 75% within 7 in. It can also be seen that nearly all the fast neutron heating is over at about 13 in. However, $\phi_g(x)$ used in these calculations contains two components: the uncollided flux, $\phi_{go}(x)$, and the collided flux, $\phi_{gn}(x)$. Figure A-1 also shows the fraction of the total heating which occurs in x due to only the uncollided flux, $\phi_{go}(x)$. This data is also tabulated in Table 1 where it can be seen that about 50 to 60 percent (as was expected) of the total heating is due to the uncollided neutron flux. Since it is relatively simple to calculate the uncollided flux and hence the neutron heating due to this flux, the partitions which determine the fixed positions for measuring neutron spectra in the liquid hydrogen dewar should more appropriately be placed such that a proper sampling of the collided flux and the heating due to this flux is measured. The criterion which has therefore been chosen is to fix the partitions such that at each point of measurement the heating due to collided neutrons is 20% of the total heating due to collided neutrons.

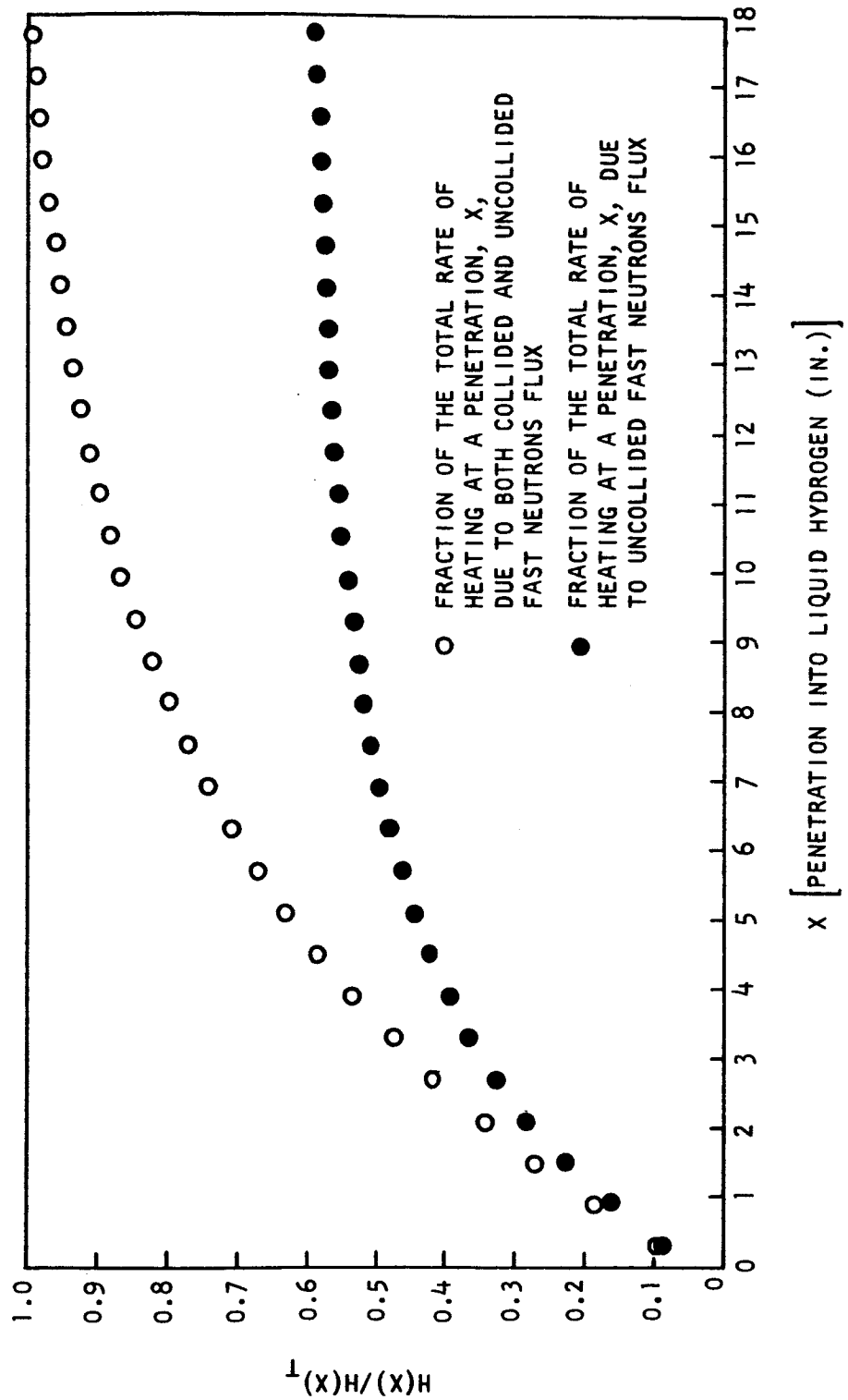
H(X)/H(X)⊥
1.0
0.9
0.8
0.7
0.6
0.5
0.4
0.3
0.2
0.1
0
0 1 2 3 4 5 6 7 8 9 10 11 12 13 14 15 16 17 18
X [PENETRATION INTO LIQUID HYDROGEN (IN.)]
FRACTION OF THE TOTAL RATE OF HEATING AT A PENETRATION, X, DUE TO BOTH COLLIDED AND UNCOLLIDED FAST NEUTRONS FLUX
FRACTION OF THE TOTAL RATE OF HEATING AT A PENETRATION, X, DUE TO UNCOLLIDED FAST NEUTRONS FLUX

Fig. A-1

Table 1

Depth of Penetration (in.)	Fraction of the Total Heating $H(x)/H(x)_T$	Fraction of the Total Heating Due to Uncollided Neutrons
0.3	0.097	0.092
0.9	0.187	0.168
1.5	0.270	0.232
2.1	0.346	0.285
2.7	0.416	0.329
3.3	0.478	0.367
3.9	0.535	0.398
4.5	0.589	0.425
5.1	0.632	0.448
5.7	0.673	0.468
6.3	0.710	0.485
6.9	0.744	0.500
7.5	0.774	0.512
8.1	0.801	0.523
8.7	0.825	0.533
9.3	0.847	0.541
9.9	0.867	0.548
10.5	0.885	0.555
11.1	0.901	0.560
11.7	0.915	0.565
12.3	0.928	0.570
12.9	0.939	0.573
13.5	0.945	0.577
14.1	0.959	0.580
14.7	0.968	0.582
15.3	0.976	0.584
15.9	0.983	0.587
16.5	0.989	0.588
17.1	0.995	0.590
17.7	1.000	0.592

Figure A-2 shows the fraction of the total heating which occurs in x due to collided neutrons only. Referring to this figure and using the criteria established above, partitions would be placed at 2.5, 4.5, 7.0, 10.5, and 13 in. from the end of the probe tube. Although these calculations are based on an 18 in. thick slab of liquid hydrogen, only a few percent of the heating occurs beyond this thickness (this can be seen by referring to Fig. A-2 and therefore the above discussion is also applicable to an infinite slab of liquid hydrogen.

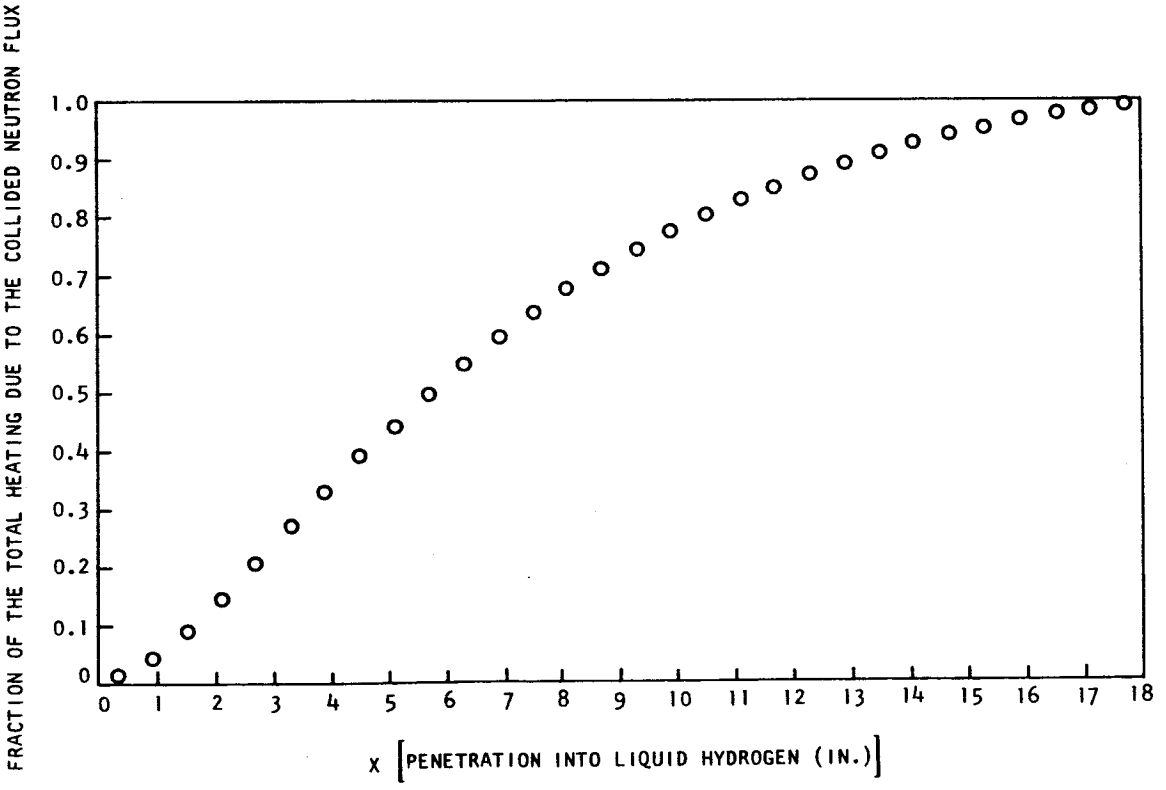

Fig. A-2

APPENDIX B

HEAT LEAKS IN THE GENERAL ATOMIC CRYOSTAT FOR THE LIQUID HYDROGEN NEUTRON EXPERIMENT

APPENDIX B

HEAT LEAKS IN THE GENERAL ATOMIC CRYOSTAT FOR THE LIQUID HYDROGEN NEUTRON EXPERIMENT

The purpose of this memoranda is to discuss and summarize our findings in regard to your requested investigation of the possibility of the presence of vapor bubbles in front of the probe tube of the cryostat to be used for the liquid hydrogen neutron experiment. We feel that vapor bubbles will not be present. Because vapor bubbles would be caused by boiling of the hydrogen, a literature search was made on this subject. A Nukiyama type boiling curve for hydrogen was found in Applied Cryogenic Engineering, by Vance and Duke, John Wiley and Sons, shown in Fig. B-1. This curve has been reproduced and is herein enclosed. It can be seen from the graph that a flux of at least 20 Btu/hr ft^2 would be required to cause nucleate boiling of hydrogen.

The following three heat sources were considered in investigating the possibility of the presence of vapor bubbles in front of the probe tube: (1) heat transferred through the insulation and the successive interior partitions to the interface between the innermost partition and the liquid hydrogen, (2) radiant heat transfer through the evacuated probe tube, and (3) radiant heat transfer through the evacuated hole in the bottom of the cryostat in the multi-layer insulation.

The evacuated multi-layer insulation will offer a very high

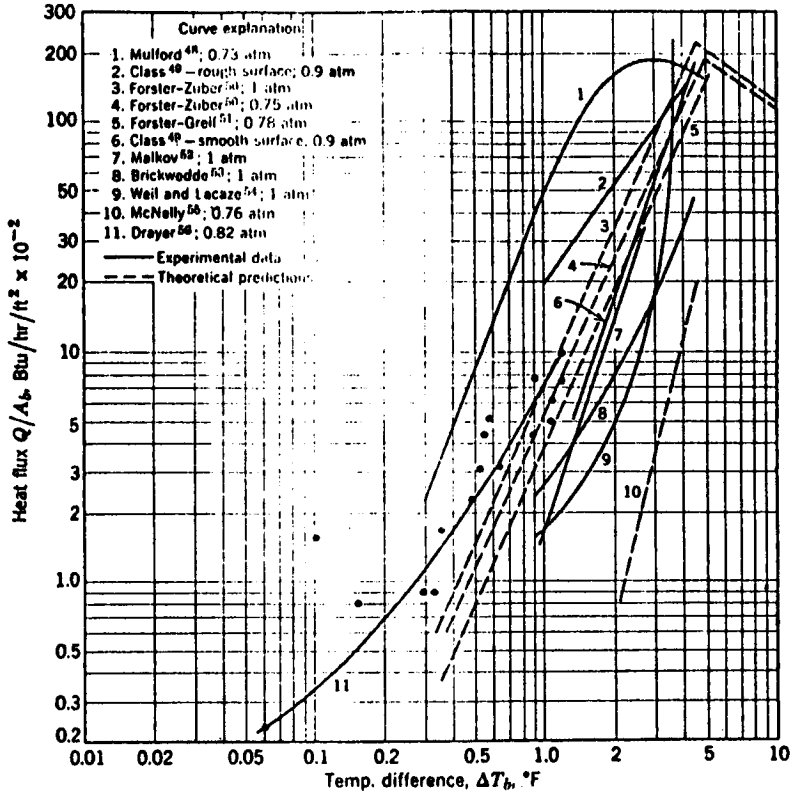

Fig. B-1 -- Experimental and calculated heat flux for nucleate boiling of liquid hydrogen

resistance to heat transmission from the surrounds to the interior of the cryostat. The thermal resistance of the interior partitions and their enclosed gaseous hydrogen will be very low compared to the resistance of the multi-layer insulation. As a consequence of this fact, the heat flow through the insulation and successive interior partitions will be controlled by the thermal resistance of the multi-layer insulation. By assuming an insulation thickness of 2.75 inches, an insulation thermal conductivity of 1.73×10^{-5} Btu ft/hr ft^2, ^oF, and a temperature difference of 493^oF, a heat flux of 3.74×10^{-2} Btu/hr ft^2 was determined. From the above discussion of nucleate boiling heat fluxes, it is apparent that the magnitude of the calculated heat flux is not large enough to cause nucleate boiling.

The remaining two heat sources both involve radiant heat transfer between two circular discs separated by a cylindrical space. Since the same material and temperature conditions exist in both cases, only the source which yields the maximum heat flux was considered, that is, the source having the largest shape factor. The radiation configuration associated with the source involving the hole in the bottom of the cryostat will have the largest shape factor. The heat flux from this source would be 5.29×10^{-2} Btu/hr ft^2 which would not produce nucleate boiling of hydrogen.

The foregoing analysis and discussion are based on the cryostat configuration and the multi-layer thermal insulation specified by

General Atomic. In the event that changes occur in the configuration of the system and in the effectiveness of the high resistance insulation, a re-evaluation of the gas generation problem would be required.

APPENDIX C

CHECK OFF LIST AND OPERATIONAL AND EMERGENCY PROCEDURES

EXPERIMENTAL SETUP CHECK SIGNED _____

(A) Dewar Positioning

1. _____ Open probe tube tower valve, probe tube helium valve, and vacuum relief valve. Set probe tube helium bottle at 5 psig. Then purge with helium. Close probe tube helium valve and vacuum relief valve.

2. _____ Turn on vacuum pump at electrical junction box.

3. _____ Open tower probe valve, make sure tower dewar valve is closed, and open valve package probe valve.

4. _____ Set dewar to angle to be measured and lock.

5. _____ Check probe alignment with room marks.

6. _____ Vacuum/Helium cycle four times. Leave probe tube at vacuum by closing probe tube tower valve, probe tube helium valve. Open vacuum relief valves and let vacuum pump up to helium, then close vacuum relief valve.

7. _____ Check dewar height and level.

8. _____ Check that proper beam tube/window has been installed.

(B) Source Positioning

1. _____ Check that source drive is in position nearest to dewar.

2. _____ Test monitor positioning and seating device.

3. _____ Mount 3 in. U^{238} source.

4. _____ Hook up air cooling line on beam tube window.

5. _____ Hook up air cooling lines on U^{238} source.

6. _____ Hook up target lead for U^{238} source.

7. _____ Check condition of phosphorescent screen.

8. _____ Check to see that source thermocouples (2) are hooked up with proper polarity.

(C) Interior Flight Path and Collimation

1. _____ Check that correct collimators are installed.

2. _____ Check that background plug is not inside collimator.

3. _____ Check that shielding is in place around collimators.

EXPERIMENTAL SETUP CHECK (continued) SIGNED _____

(D) TV System

1. _____ Give target viewing camera to operator.
2. _____ Set up and align mirrors to view U^{238} source and monitor seat.
3. _____ Observe and approve the operator's TV picture.

ELECTRICAL CHECK

SIGNED _____

1. _____ Turn on explosion proof lights and check

   _____ Experimental Room

   _____ Dewar

   _____ Tower

   _____ Rear Area

2. _____ Turn on back area outdoor lights.

   _____ HP door

   _____ Cooling Tower

   _____ Stairway

   _____ Bottle Farm

   _____ Boron Building

   _____ 70 Meter Building

   _____ Filling Station

   _____ 16 Meter Building

3. _____ Inspect velostat cover over α-magnet and steering magnets.

4. _____ Check all experimental room experimental areas to be sure no detectors, preamps, amplifiers, etc. have any power on.

5. _____ Tape all experimental room terminal board connections with signs saying "Do not use until LH_2 experiment is finished".

6. _____ Check to see that the boing amplifier is sealed up in a polyethylene bag and taped to the side of the dewar.

VENTILLATION CHECK

SIGNED _____

1. _____ Turn on 18 in. hole blower. Switch at panel by console.

2. _____ Turn on 6 in. hole blower and direct flow down 6 in. hole. Switch at panel by console.

3. _____ Turn on room pressurizing blower, switch at panel by console.

4. _____ Check to see that dewar area curtains are down with all high seams taped closed.

5. _____ Place flexible trunk for room pressurizing blower in position inside curtained area. Check that small trunks are in position.

6. _____ Check to see that valve package and dewar liquid air drip pans are in place.

7. _____ Check air flow patterns.

VALVE PACKAGE CHECK

SIGNED _____

1. _____ Visually inspect all gas and liquid lines, for damage.

2. _____ Visually inspect all welded and threaded gas and liquid lines connections for damage and tightness.

3. _____ Visually inspect pneumatic valves for damage.

4. _____ Check to see that all manual over-ride valves are closed and all manual bleed valves are open. Check to see that the stuffing box vent valves are open.

5. _____ Visually check liquid level cables at dewar.

6. _____ System leak check.

   (a) _____ Close the following valves; dump, vent No. 1, vent isolation.

   (b) _____ Open dewar purge valve and pressurize to 20 psig.

   (c) _____ "Snoop" test all soldered joints and fittings.

   (d) _____ Record pressure at the end of 1/2 hour _____.

   (e) _____ Open all gauge valves and check agreement of all pressure gauges.

   (f) _____ Drop pressure in dewar to 2 psig by opening vent No. 1 and vent isolation valves, then closing valves.

TOWER AREA CHECK

SIGNED _____

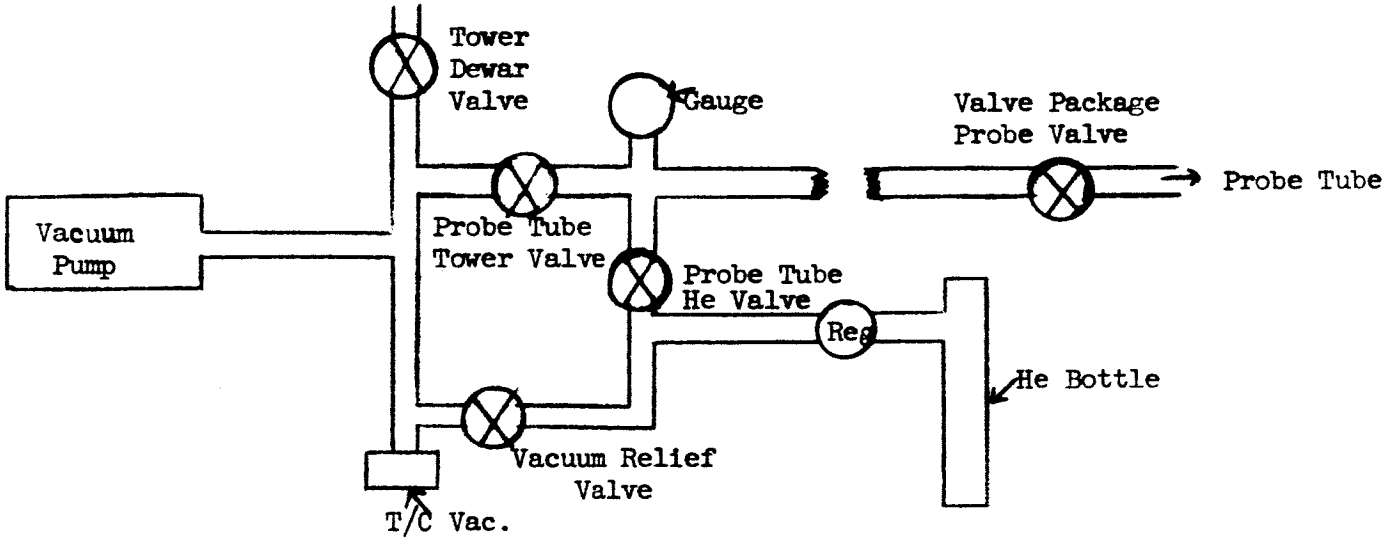

1. _____ Check that probe tube bottle is helium, and regulator is set at 5 psig.

2. _____ Open dewar micropurge ball valve.

3. _____ Check aluminum monitor operation.

TRAILER AREA CHECK

SIGNED _____

1. _____ Attach grounding cable to trailer.

2. _____ Post "No Smoking" signs at trailer.

3. _____ Check level of LH_2 in trailer. _____ Gals.

4. _____ Attach 110 vac. extension cord for supply trailer vacuum pump. (Do not disconnect until after shut down.) Check vacuum.

5. _____ Put Lox drip pan under supply trailer.

6. _____ Check that pressure on supply trailer is between 19 and 22 psia.

7. _____ Close transfer bypass and open dewar purge valve. Then open fill valve and leave open so as to purge transfer line while making connection to supply trailer.

8. _____ Connect transfer line to trailer and tighten with spanner wrench.

9. _____ Close fill valve.

CONSOLE FOR LIQUID HYDROGEN SIGNED _____

1. _____ Turn on valve package control panel power and check operation of all valve package valves, position indicator lights, and control switches. This check must be done simultaneously by one man at the control panel and one man at the valve package.

Control Panel	Valve Package	Valve
_____	_____	Fill valve
_____	_____	Dump valve
_____	_____	No. 1 vent valve
_____	_____	No. 2 vent valve
_____	_____	No. 3 vent valve
_____	_____	No. 4 vent valve
_____	_____	No. 5 vent valve
_____	_____	No. 6 vent valve
_____	_____	Vent isolation valve
_____	_____	Vacuum purge valve

ON NEXT FOUR VALVES LISTEN FOR GAS FLOW

_____	_____	Transfer bypass
_____	_____	Dewar emergency purge
_____	_____	Vent emergency purge
_____	_____	Dump emergency purge

2. _____ Check fail-safe position of all valves by turning off the valve package control panel master switch. Valve position indicator lights should indicate the normal position of each valve. Turn master switch back on.

BOTTLE FARM CHECK

SIGNED _____

1. _____ Check bottle supplies at bottle farm and tower to see that bottles are full; all bottle except the first one in the micropurge system should be wide open.

2. _____ Gas Bottle Check.

   _____ Bottles helium on emergency purge.

   _____ Bottles helium on micropurge.

   _____ Bottles nitrogen on magnet purge.

   _____ Bottles nitrogen on valve operators.

3. _____ Set pressure regulators.

   _____ Dewar micropurge at 20 psig.

   _____ Vent/Dump line micropurge at 20 psig.

   _____ Emergency purge at 35 psig.

   _____ Transfer regulator at 5 psig.

   _____ Valve operators at 68 psig.

4. _____ Check that all manual by-pass valves are closed.

5. _____ Adjust helium flow on micropurges with needlevalves.

   _____ Dewar micropurge - make sure all valves are closed except dewar micropurge and vent isolation valve, then adjust dewar micropurge to _____ ft^3/hr. Then close dewar micropurge and vent isolation valve.

   _____ Vent micropurge - open vent micropurge valve and adjust flow to _____ ft^3/hr.

   _____ Dump micropurge - open dump micropurge valve and adjust flow to _____ ft^3/hr.

6. _____ Vent line flapper valve operation.

EMERGENCY PROCEDURES

There are three categories under which an emergency condition may exist. These are: (1) a hydrogen fire, (2) loss of vacuum either between the inner and outer dewar shell or in the transfer lines, and (3) overheating the uranium target.

I. Hydrogen Fire

These fires are determined mainly by Fe/Con thermocouples placed in the following places:

(1) Experimental dewar.

(2) Valve package - three thermocouples.

(3) Supply trailer.

(4) Vent stack on supply trailer.

(5) Vent stack for the experimental dewar.

(6) Dump stack for the experimental dewar.

However, there are very many local places where hydrogen fires could occur such as the transfer lines from the supply trailer to the experimental dewar and the bottle farm.

In case of fire, the Linac will be automatically shut off which will be indicated by a red light. The location of the fire can be determined by scanning the chart recorder for the number of the Fe/Con thermocouple which has caused this.

The following procedures are to be followed when a hydrogen fire occurs at the following discrete places and will in general cover most areas where a fire could happen.

A. Fire at the exhaust of the vent stack

(1) Do not use the emergency dump.

(2) Open the vent and dump purge valves and continue the purge until the Fe/Con T/C recorder indicates the temperature is normal.

(3) Close vent 1 and the vent isolation valve. These may be closed temporarily or for a longer period of time depending upon the operation which is in process at the time of the fire. Make sure dewar micropurge is closed.

(4) Make sure the dump valve is closed.

(5) Since a pure hydrogen fire can not be visually observed, continue to purge the dump and vent lines for a period of time after the fire has been extinquished.

(6) Alert all intercom areas to the location of the fire.

NOTE: There is a CO_2 manifold connected to a flexible hose at the tower in case a fire should occur in the area of the tower.

(7) Close the fill valve.

B. Fire at the Dump Stack

(1) Close the dump valve.

(2) Close the fill valve.

(3) Open the vent and dump purge valves and continue the purge until the Fe/Con T/C recorder indicates the temperature is normal.

(4) Since a hydrogen fire cannot be visually observed, continue to purge the dump and vent lines for a period of time after the fire has been extinquished.

(5) Close vent 1 and the vent isolation valve. These valves may be closed temporarily or for a longer period of time depending upon the operation which is in process at the time of the fire. Make sure the dewar micropurge is closed.

NOTE: There is a CO_2 manifold connected to a flexible hose at the tower in case a fire should occur in the area of the tower.

C. Fire at the top or connectors to the experimental dewar.

(1) Open the experimental dewar CO_2 manifold.and the valve package CO_2 manifold.

(2) Shut off the air intake motor switch located on the electrical junction box behind the control console. Shut off the exhaust fan motor located on the same electrical junction box.

(3) After the fire is out continue the CO_2 purge and USE THE EMERGENCY DUMP.

(4) After "1C" light goes out turn the valve panel console on and open the dump purge valve and purge for a few minutes.

(5) Alert all intercom areas of this emergency dump.

(6) After the flow of hydrogen has been stopped and the dewar is empty turn on the air intake and exhaust motors at the electrical junction box and purge the experimental room (velostat enclosure).

D. Fire at the valve package.

(1) Turn on the valve package and experimental dewar CO_2 manifold.

(2) Close the fire and dump valves.

(3) Refer to the Fe/Con T/C.recorder to determine which of the three areas in the valve package the fire is located.

(4) Close the vent isolation valve and vent 1 valve. This may be temporary or permanent depending upon the operation.

(5) If the fire is not in the area of the dump line, then dump the liquid hydrogen.

(6) Shut off the air intake motor and the exhaust fan at the electrical junction box.

(7) After the liquid hydrogen has been dumped completely purge the experimental room (velostat enclosure) by turning on the intake and exhaust motors.

E. Fire at the supply trailer vent stack.

(1) Shut off the vent valve on the supply trailer.

(2) Use CO_2 manifold which is connected to a flexible hose at the bottle farm to extinquish the fire.

(3) If the vent valve on the supply trailer cannot be shut off because of the heat use CO_2 to extinquish the fire. Then close supply trailer vent valve.

(4) Close the experimental dewar fill valve.

F. Fire at the supply trailer.

(1) If the fire is small try to extinquish with CO_2.

(2) Close the experimental dewar fill valve.

(3) If the fire is large, evacuate the rear entrance area and notify the General Atomic Fire Department.

II. Loss of Vacuum

A. Between inner and outer shell.

(1) The existence of such a failure will be noticed by a sudden large pressure rise within the experimental dewar.

(2) USE THE EMERGENCY DUMP.

(3) After the "1C" light goes out on the liquid level panel, turn the valve console on and open the dump purge valve and purge for a few minutes and open all the vent valves.

B. Vacuum loss in the transfer lines

(1) This will be obvious due to frosting on the main body of the transfer lines.

(2) Open the valves on the 12 ft. transfer line which is nearest supply trailer.

(3) Evacuate personnel from this area during warm-up of the transfer lines.

III. Overheating Uranium Target

(1) The existence of target failure or overheating will be noticed by a sudden or rapid rise in the air monitor. In some cases the air monitor may rise to a high value. In this case shut off the Linac and observe if the air monitor shows a decrease. If so, the target has not failed. If not the target has failed and normal procedures for transferring of the liquid hydrogen to the supply trailer will be necessary.

(2) The Fe/Con T/C will also detect overheating. The target thermocouples are # 1 and 2. Should these thermcouples show a temperature rise above 350°F, shut off the Linac. Follow the normal procedures for transferring the liquid hydrogen to the supply trailer.

IV. Maximum Credible Accident

(1) The maximum credible accident would be caused by a fire or minor explosion at the connection of the vent #1 line to the experimental dewar or at the valve package resulting in the inability to pressurize the dewar to the extent the liquid hydrogen could be transferred out of the experimental dewar.

(2) In this case the only method which can be used is to evaporate the liquid hydrogen. The procedure to be used is as follows:

(a) Open the dewar purge, dump purge and vent purge valves to minimize cryopumping.

(b) Open the experimental and dewar CO_2 manifolds. Shut off the intake and exhaust blowers.

(c) Open the alignment window pump out valve and pressurize with helium.

(d) Purge the experimental dewar with helium gas to evaporate the liquid hydrogen.

HEALTH PHYSICS CHECKOUT LIST SIGNED _____

1. Start each series of liquid hydrogen experiments with a clean filter in the Constant Air Monitor.

2. Check the Constant Air Monitor every one-half hour and in case of a suspected uranium target failure notify the experimenters: Bob Beyster, George Houghton, Jerry Trimble.

3. The experimental room will not be opened during the liquid hydrogen runs. It should not be necessary to enter the experimental room after these runs. If it is deemed absolutely necessary for wipe samples these may be taken prior to the liquid hydrogen experiments and then only by J. Audas, Bob Beyster, Jerry Trimble or George Houghton.

4. No health physics monitoring equipment of any kind will be allowed in the "C" or "D" area throughout the liquid hydrogen experiment.

ELECTRONICS SETUP CHECK

SIGNED _____

1. _____ Hose up 2 in. or 5 in. scintillator system for bias setting.
2. _____ Set 2 in. or 5 in. scintillator system bias-keep TMC tapes and plots.
3. _____ Rehose 5 in. scintillator system for time-of-flight.
4. _____ Hose up and turn on fission monitor electronics.
5. _____ Check discriminator level on fission monitor.
6. _____ Check location and shielding of fission monitor.
7. _____ Check HV setting on fission monitor.
8. _____ Check bias setting on aluminum monitor counter.
9. _____ Check all scalers and TMC for proper operation.
10. _____ Check position of movable flight tubes.
11. _____ Check position of movable post collimators.
12. _____ Check vacuum in 16 meter, 32 meter, and 50 meter flight tubes.
13. _____ Check condition of all flight path vacuum pumps.
14. _____ Check position of detector.
15. _____ Check position of background shield around detector.
16. _____ Check to see that gamma-flash suppressing lead is in position dictated by the experiment.
17. _____ Check to see that 3 in. dia. water collimator is filled.
18. _____ Check to see that 8 in. dia. collimator is filled.
19. _____ Remove all extraneous material from 50 meter building.
20. _____ Remove thin window shield from all flight tubes.

WARNING AND SAFETY SYSTEM CHECK SIGNED _____

1. _____ Turn on H_2 sensor panel at least 24 hours before start of experiment.
2. _____ Check out all H_2 sensors with lecture bottle.

_____ Rear Area _____ Tower

_____ 18 in. hole _____ Roof Cavity

_____ Valve package

3. _____ Hook up 12 meter flight path TV camera in drift tube.
4. _____ Attach plexiglass window to drift tube.
5. _____ Check adjustments so that TV camera views the dewar and vent lines.
6. _____ Observe operator's TV picture and approve.
7. _____ Vacuum Checks.

_____ Dewar Insulation Space.

_____ Dewar Alignment Port.

_____ Storage Dewar Insulation Space.

8. _____ Thermocouples

_____ Position chart in place at recorders.

_____ Calibration chart at recorders.

_____ Cu/Con reference dewar filled with LN_2.

_____ Rubicon Cu/Con reader hooked up.

_____ Thermocouple operation.

Cu/Con		Fe/Con	
_____ 1	_____ 7	_____ 1	_____ 7
_____ 2	_____ 8	_____ 2	_____ 8
_____ 3	_____ 9	_____ 3	_____ 9
_____ 4	_____ 10	_____ 4	_____ 10
_____ 5	_____ 11	_____ 5	_____ 11
_____ 6	_____ 12	_____ 6	_____ 12

WARNING AND SAFETY SYSTEM CHECK (continued) SIGNED _____

9. _____ Check operation of the Fe/Con T/C Linac interlock.

10. _____ Turn on liquid level indicators and visually check panel for damage.

11. _____ Check all intercom elements for operation.

_____ 50 meter flight path.

_____ 16 meter flight path.

_____ 12 meter flight path.

_____ Gas bottle area.

_____ Rear entrance area

_____ Tower area

_____ Linac Operator

_____ Boing Amplifier

12. _____ Disconnect CHP intercom and dewar area intercom.

13. _____ Thermocouple resistors (record resistance).

_____ 1C	_____ 3C	_____ 5C
_____ 1B	_____ 3B	_____ 5B
_____ 1A	_____ 3A	_____ 5A
_____ 2C	_____ 4C	_____ 6C
_____ 2B	_____ 4B	
_____ 2A	_____ 4A	

OPERATOR'S CHECKOFF LIST

1. _____ Put on the beam tube and window required for the experiment.
2. _____ Check vacuum system in cave area; valve off C3, put thick window on C4, and blank-off on thick window on C3. Fix any leaks in the system.
3. _____ Turn off P.S. #3, except for the ring, and observe any vacuum change. Vacuum after 4 hours off _____.
4. _____ Check that ring signal power for ring #3 is run in from the VVL area.
5. _____ Completely turn off P.S. #4 and all associated devices.
6. _____ Unplug or disconnect:
   - _____ Russell's magnet power supply.
   - _____ Whittemore's magnet power supply.
   - _____ Graphite magnet power supply.
7. _____ Check that straight-ahead beam stopper is open.
8. _____ Check the LH_2 experiment magnets for operation and polarity.
9. _____ Set up and adjust the HTGR TV system to the satisfaction of G. D. Trimble.
10. _____ Adjust the Mowry-Beyster tube TV system to the satisfaction of G. D. Trimble.
11. _____ Remove the portable emergency lights from the experimental room.
12. _____ Deactivate the wired-in emergency lights in the experimental room.
13. _____ Close the rear door.
14. _____ Turn off all the experimental area wall plugs at the junction box except those in the VVL area.
15. _____ Turn off all lights in the experimental area at the switch in the VVL area.
16. _____ Check the target lead.
17. _____ Turn the area switch into position #3.
18. _____ Turn Jerry's interlock key.
19. _____ Carefully check over the Linac so that the fewest entries possible will have to be made.
20. _____ Close and lock the Red Door.

Turn this completed list into G. D. Trimble

LH_2 FILLING PROCEDURE

1. (a) Have storage dewar operator build up transfer pressure to _____ psig.
   (b) Have rear area man evacuate the probe tube and shut off vacuum pump.
   (c) Record Dewar temp thermocouple (bottom) _____.
2. Start with valves in the following positions:

Closed	Open
Dump Purge	Vent Line Micropurge
Vent Purge	Dump Line Micropurge
Dewar Purge	Vent Isolation
Vacuum Purge	Fill
All Vents	Alpha Magnet
Dump	
Transfer Bypass	
Dewar Micropurge	

The dewar should be at ~ 2 psig He_2.

3. Have the storage dewar operator crack his liquid transfer valve to cool the line, then open the valve slowly to the wide open position to permit liquid flow. Continually watch the dewar pressure gauge; when it rises above ____ psig, begin opening vent valves, starting from chamber #6 and working back to #1, to lower the dewar pressure and control it to between _____ psig and _____ psig. As the LH_2 flows into the first compartment, much of it will flash into gas; try to keep as many vent valves closed as possible so that this cold gas may be used to cool the other compartments, but keep the dewar pressure within the stated limits to allow a good flow rate without excessive back pressure. The temperature of the open vent line nearest chamber #1 should be monitored continuously, and the vent valve for that line should be closed if the line's temperature approaches the oxygen liquification point (indicated on the thermocouple calibration curve). The H_2 gas warning monitors should be observed during all operations where liquid or gaseous hydrogen gas is present in the dewar.

Time filling started _____.

4. Monitor the filling rate in chamber #1 by observing the liquid level indicators and thermocouples in that chamber. The thermocouple/liquid level reader should keep a record of the liquid level resistor resistance as a function of time to obtain an approximate depth calibration as a function of resistance in all chambers. The chamber #1 indicator levels are as follows:

1/2" liquid - level indicator "C" light Time _____
5-1/2" liquid - thermocouple #3 Time _____
21" liquid - thermocouple #2 Time _____
36" liquid - thermocouple #1 Time _____
39" liquid - level indicator "B" light Time _____
40" liquid - level indicator "A" light Time _____

The vent #1 valve must remain closed once the liquid level is above the #1 thermocouple to prevent entrained liquid in the flash gas from entering the vent line.

5. Immediately after the "1A" liquid level indicator is reached the LH_2 will overflow into chamber #2 causing a sudden small pressure rise. If the #2 vent valve is not already closed, close this valve now.

ΔT in chamber #1 _____

6. Continue to fill the dewar making sure that each chamber's vent valve is closed when the chamber starts to fill and continuously observing the vent line temperatures; to keep liquid air from forming, it may be necessary to reduce the LH_2 flow as well as closing most of the vent valves.

ΔT in chamber #2 _____

ΔT in chamber #3 _____

ΔT in chamber #4 _____

ΔT in chamber #5 _____

7. When chamber #6 begins to fill, leave the #6 vent valve open and closely observe the #6 vent line temperature. At a vent line temperature of 125°K (200 on scale) close the fill valve.

ΔT in chamber #6 _____

8. When the initial fill is completed, allow the dewar to complete its cool-down. While monitoring the vent line temperatures, open the vent valves one at a time, starting with #5 and working back to #1. This will reduce the pressure in the dewar and assist in the cooldown. Keep the vent lines above the air liquification temperature, if possible, by closing the vent valve on any line which rapidly approaches the liquid air temperature. When the dewar liquid

level indicators appear relatively stable and all the vent valves may be left open with a small positive pressure of ~ 1 inch of water indicated, the dewar is cooled down.

9. To adjust the liquid levels in the dewar so that chamber six is essentially empty and the five main chambers are full, excess liquid must be transferred out of chamber six. Close the #6 vent valve and the transfer bypass valve, and open the dewar purge valve. Chamber five will fill first; as its "5A" light goes on, the #5 vent valve should be closed. As each subsequent chamber fills, the corresponding vent valve should be closed until chamber #1 is reached. Now observe the resistance of the "6C" liquid level indicator and the "5A" indicator light. (a) If "6C" indicates that the chamber #6 liquid-gas interface is near the bottom, and/or if the "5A" light is blinking, close the dewar purge valve and quickly open all the vent valves; after the pressure relieves, reclose the chamber #6 vent valve and leave it closed. (b) If the liquid level in chamber #6 still appears to be well above the "6C" indicator with all the upper-level indicators in all chambers lit, close the #1 vent valve and open the dump valve. Allow the LH_2 to dump until the level in chamber #6 approaches "6C" and the upper light in chamber #5 are blinking. Then, close the dewar purge valve and the dump valve, and begin opening the vent valves, starting with chamber #6 and working slowly back to chamber #1 to keep from dripping liquid air from the vent lines; when the dewar pressure is down to 35 inches of H_2O or less, the #1 vent valve may be opened and left open and the #1 vent line will not be likely to drip liquid air. Now repeat the back-transfer process from chamber #6 to top off all the chambers. (c) If the liquid in chamber #6 is insufficient to top off all the chambers without emptying chamber #6 and going down into chamber #5 well below the "5B" indicator, close the dewar purge valve and quickly open all the vent valves. Then, open the dump valve, close the #1 vent valve, and open the fill valve. When a good flow of cold gas comes from the dump stack, close the dump valve and again transfer liquid into the dewar. Fill as before, closing the vent valve for each chamber as it indicates full, until chamber #6 begins to fill. Attempt to fill chamber #6 to about 6" from the bottom. Then close the fill valve and open all the vents as quickly as possible without over-cooling the vent lines. When the dewar has once more reached a steady condition, top back as before from chamber #6 to reach an "all full" condition.

Time finished and topped off _____

Total elapsed fill time _____

10. Have the rear area man let the probe tube up to +5 psig helium. The dewar is now ready for the experiment.

Confirmed By _____

VENT LINE TEMP AT MID RUN

CHAMBER	RUN	RUN	RUN	RUN	RUN	RUN	RUN
6							
5							
4							
3							
2							
2 mid							
1							
1 mid							

BOIL OFF

LIGHT	RUN	CHAMBER 5	CHAMBER 4	CHAMBER 3	CHAMBER 2	CHAMBER 1	
Light A							
Light B							
Light A							
Light B							
Light A							
Light B							
Light A							
Light B							
Light A							
Light B							
Light A							
Light B							
Light A							
Light B							
Light A							
Light B							
Light A							
Light B							

BETWEEN-RUNS PURGING PROCEDURE

1. After transferring the LH_2 back into the storage dewar, open the dewar purge valve and the dump valve and purge the dewar with warm helium until the temperature has risen to 30°K at the #3 thermocouple in chamber #1. Watch the pressure gauges carefully and make sure the dewar is always at a positive pressure. If necessary, increase the gas flow by opening the transfer bypass valve.

2. Close the dewar purge valve and dump valve simultaneously and turn on the vacuum pump. Have the rear area man open the tower dewar evacuation valve, and drop the dewar pressure to 2 psig by momentarily opening the dump valve. Open the vacuum purge valve and evacuate the dewar to 30 inches Hg.

3. Close the vacuum purge valve and open the dewar purge valve and pressurize the dewar to 15 psig. Turn off the vacuum pump and let the line up to helium. The valves should be left in the following positions:

Closed	Open
Vent Purge	Vent Line Micropurge
Dump Purge	Dump Line Micropurge
Dewar Purge	Fill
Transfer Bypass	
All vents	
Dump	
Dewar Micropurge	
Vacuum Purge	

4. Check the babysitter's list with him.

LH_2 EMPTYING PROCEDURE

1. Reduce storage dewar pressure to + 4 psig and have operator stand by to continually vent storage dewar during back-transfer to keep the back pressure between +4 and +5 psig.

2. Close all vent valves and dump valve, and open dewar purge valve and transfer bypass valve. Pressurize dewar to _____ psig.

3. Open fill valve and begin transfer of LH_2 back into storage dewar. Continually monitor chamber #1 thermocouples and level indicators, and check H_2 sniffer devices. Have rear area man carefully observe the transfer lines and storage dewar while the storage dewar operator controls the back pressure. When the liquid level in the dewar reaches the "1C" indicator, close the dewar purge valve, the fill valve, and the transfer bypass valve

4. Have the storage dewar operator close his liquid transfer valve; then open the fill valve. The dewar is now ready for purging.

LH_2 CHAMBER CHANGE PROCEDURE

Close the vent valves for all compartments which are "empty" (defining empty as being filled with only a few inches of LH_2) and for the last "full" compartment, leaving all the other full-compartment vents open. Open the dewar purge valve and watch the indicator lights closely. When the upper indicator light in the next-to-last "full" compartment goes on, close that compartment's vent valve; continue this process for each subsequent compartment until all the upper level indicator lights in the "full" compartments are lit.

(a) If the low-level indicator resistor in the compartment being emptied shows that the vapor-liquid interface is close to the bottom, and the upper indicators in the first full compartment are blinking, close the dewar purge valve, do not close the #1 vent valve, and open all the vent valves in the "full" compartments quickly to reduce their pressures. Keep the vent valves on the "empty" chambers closed; the pressure generated will help keep the "full" chambers topped off.

(b) If the low indicator in the compartment being emptied does not show that the vapor-liquid interface is close to the bottom and the upper lights in the first "full" compartment are not blinking, close the #1 vent valve and open the dump valve. Watch for the blinking lights and the low level indication in the chamber being emptied; when they come, close the dump valve and the dewar purge valve simultaneously and open the vent valves in the "full" compartments as quickly as possible to reduce the pressure. The #1 vent valve will have to be operated carefully to avoid over-cooling the vent line. If any of the "full" chambers appear to be a little low, top off with the liquid in the chamber just emptied.

(c) If the low-level indicator in the chamber being emptied and the upper level indicators in the first full chamber go out before the "full" chambers all indicate completely full, close the dewar purge valve and open all the vent valves to reduce the pressure. Then close the #1 vent valve, open the dump valve, and open the fill valve. When a good flow of very cold gas is coming from the dump stack, close the dump valve and transfer liquid into the dewar. As the chambers fill close their vent valves; when the first "empty" chamber has filled to a depth of 4-6" close the fill valve and open the vent valves as quickly as possible without overcooling the vent lines. Allow the dewar to settle down, then transfer back from the first "empty" compartment to top off any low compartments; leave the vent valves on the "empty" compartments closed to help keep the full chambers topped off. The dewar is now ready for the experiment.

APPENDIX D

CALCULATION OF SLOW NEUTRON SCATTERING CROSS SECTIONS OF MOLECULAR AND HYDROGEN AND DEUTERIUM

Editor's Note: Appendix D ("Calculation of Slow Neutron Scattering Cross Sections of Molecular and Hydrogen and Deuterium") is enclosed in only those copies of the report submitted to the contracting agency.

REPORT DISTRIBUTION LIST FOR CONTRACT NAS 3-4214

NASA
Washington, D. C. 20546
Attention: RNN/David J. Miller

NASA
Washington, D. C. 20546
Attention: NPO/Harold B. Finger

NASA
Washington, D. C. 20546
Attention: RNN/David Novik

NASA Ames Research Center
Moffet Field, California 94035
Attention: Librarian

NASA Goddard Space Flight Center
Greenbelt, Maryland 20771
Attention: Librarian

NASA Langley Research Center
Hampton, Virginia 23365
Attention: Librarian

NASA Lewis Research Center (3)
21000 Brookpark Road
Cleveland, Ohio 44135
Attention: Librarian

NASA Lewis Research Center
21000 Brookpark Road
Cleveland, Ohio 44135
Attention: Hugh M. Henneberry,
MS 54-1

NASA Lewis Research Center
21000 Brookpark Road
Cleveland, Ohio 44135
Attention: Herman H. Ellerbrock,
MS 54-1

NASA Lewis Research Center
21000 Brookpark Road
Cleveland, Ohio 44135
Attention: Donald J. Connolley,
MS 21-8

NASA Lewis Research Center (30)
21000 Brookpark Road
Cleveland, Ohio 44135
Attention: Michael J. Kolar,
MS 21-8

NASA Lewis Research Center
21000 Brookpark Road
Cleveland, Ohio 44135
Attention: AD&E Procurement
Section, MS 54-1

NASA Lewis Research Center
21000 Brookpark Road
Cleveland, Ohio 44135
Attention: Norman T. Musial,
Patent Counsel, MS 77-1

NASA Lewis Research Center
21000 Brookpark Road
Cleveland, Ohio 44135
Attention: Millard L. Wohl, MS 49-2

NASA Lewis Research Center
21000 Brookpark Road
Cleveland, Ohio 44135
Attention: I. M. Karp, MS 54-1

NASA Lewis Research Center
21000 Brookpark Road
Cleveland, Ohio 44135
Attention: Leonard Soffer,
MS 500-201)

NASA Lewis Research Center
21000 Brookpark Road
Cleveland, Ohio 44135
Attention: Solomon Weiss, MS 54-1

NASA Lewis Research Center
21000 Brookpark Road
Cleveland, Ohio 44135
Attention: Dr. John Liwosz,
MS 54-1

NASA Manned Spacecraft Center
Houston, Texas 77001
Attention: Librarian

NASA Marshall Space Flight Center
Huntsville, Alabama 35812
Attention: Librarian

NASA Marshall Space Flight Center
Huntsville, Alabama 35812
Attention: R. D. Shelton,
Research Project
Laboratory

NASA Lewis Research Center (3)
Space Nuclear Propulsion Office
21000 Brookpark Road
Cleveland, Ohio 44135
Attention: L. C. Corrington

NASA Marshall Space Flight Center
Huntsville, Alabama 35812
Attention: M. O. Burrell

U. S. Atomic Energy Commission (3)
Technical Information Service
Extension
Post Office Box 62
Oak Ridge, Tennessee

NASA Scientific and Technical
Information Facility (6 + 1 repro)
Box 5700
Bethesda 14, Maryland
Attention: NASA Representative

Los Alamos Scientific Laboratory
Post Office Box 1663
Los Alamos, New Mexico
Attention: Glen Graves

General Dynamics
Fort Worth, Texas
Attention: Wilburn A. Hehs
Nuclear Radiation
Shielding

ERRATA

NASA CR-54230

(GA-5750)

MEASUREMENT OF NEUTRON SPECTRA IN LIQUID HYDROGEN

by

G. D. Trimble, G. K. Houghton, and J. H. Audas

The following erratum should be noted in Report NASA CR-54230 (GA-5750):

Page B-1--

Change the fifth sentence in the first paragraph to read

This curve has been reproduced with the permission of the publishers; it was originally presented by D. E. Drayer in his Ph. D. thesis in chemical engineering at the University of Colorado in 1961.